

**Fibre Length Distribution and Dispersion during the  
Injection Moulding Process**

**M-J. GILSON**

**PHD**

**2018**

# **Fibre Length Distribution and Dispersion during the Injection Moulding Process**

An experimental study evaluating fibre length attrition and dispersion during processing of long glass fibre reinforced polymer composites in injection moulding including an evaluation of long glass fibre measurement techniques.

Millan-John GILSON

Submitted for the Degree of  
Doctor of Philosophy

Faculty of Engineering and Informatics  
University of Bradford

2018

## **Abstract**

### **Fibre Length Distribution and Dispersion during the Injection Moulding Process:**

An experimental study evaluating fibre length attrition and dispersion during processing of long glass fibre reinforced polymer composites in injection moulding including an evaluation of long glass fibre measurement techniques.

**Millan-John Gilson**

This project evaluates fibre length dispersion and distribution within the injection moulding process of long glass fibre reinforced polypropylene, sponsored by Autodesk Simulation.

The primary material used in this investigation was a 15 mm long glass fibre reinforced polypropylene consisting of two fibre content levels, 20 wt. % and 40 wt. %.

A review of previous research was compiled in this study to evaluate various glass fibre measurement methods and fibre breakage studies to establish where along the injection moulding process fibre breakage predominantly occurs and which process parameters have the greatest influence on fibre length distribution along the screw.

Based on literature findings, a manual fibre length measurement method was developed and applied in this study and benchmarked against existing commercially available automated software programs and found to be more accurate in obtaining a reliable fibre length distribution within a glass fibre reinforced sample.

Fibre length measurements from the nozzle confirmed that the majority of fibre breakage had already occurred in the screw. Measurements taken along the screw showed a drastic decrease in weighted average glass fibre length from initial pellet form to the end of the metering zone with sudden transitions to lower weighted average values seen at the beginning of the feeding zone and along the compression zone.

Fibre dispersion results from the nozzle and along the screw through the use of a  $\mu$ -CT scanner showed a complex fibre flow and orientation of fibres with the preservation of fibre clusters being seen all along the injection moulding process but chiefly in the feeding and compression zones of the screw.

**Keywords: Fibre, Length, Long, Glass, Injection Moulding, Moldflow, Dispersion, Breakage, Measurement.**

## Publications and Conferences

Gilson, M-J., Caton-Rose, P., Whiteside, B., Kelly, A., 2016. Fibre Dispersion and Fibre Length Distribution in long Glass Fibre Reinforced PP Injection Mouldings. *32<sup>nd</sup> International Conference of the Polymer Processing Society* (Lyon, France).

Caton-Rose, P., Gilson, M-J., Hine, P., 2017. Orientation, Dispersion and Length Reduction of Fibres in Long Glass Fibre Reinforced Injection Moulding. *21st International Conference on Composite Materials* (Xi'an, China).

Gilson, M-J., Caton-Rose, P., Whiteside, B., Kelly, A., 2017. Prediction of fibre length reduction during injection moulding of long fibre reinforced composites *Polymer Processing Engineering 17* (University of Bradford, UK).

Caton-Rose, P., Gilson, M-J., 2017. Fibre dispersion and breakage in long glass fibre reinforced injection moulding. *Connect - European Moldflow User Conference* (Frankfurt, Germany)

Caton-Rose, P., Gilson, M-J., 2018. Fibre dispersion and breakage during injection moulding of long fibre reinforced composites. *Connect - European Moldflow User Conference* (Frankfurt, Germany)

Gilson, M-J., Caton-Rose, P., Whiteside, B., Kelly, A., Costa, F., 2018. Fibre Dispersion and Fibre Length Distribution in Long Glass Fibre Reinforced PP Injection Mouldings. *Polymer Engineering International* (University of Bradford, UK).

Caton-Rose, P., Gilson, M-J., 2018. Fibre dispersion and breakage during injection moulding of long fibre reinforced composites. *Volume Graphics User Conference* (Heidelberg, Germany)

## **Acknowledgments**

It is a pleasure to acknowledge the many people who made this thesis possible.

Chiefly, I would like to express my gratitude to my supervisors Dr. Fin Caton-Rose, Prof. Ben Whiteside and Prof. Adrian Kelly for their continuous support throughout my PhD study who have offered invaluable assistance, encouragement and guidance.

The work carried out in this project was funded by Autodesk Inc, I would like to offer a special thanks to Dr. Franco Costa and other members of the Autodesk team, for their efforts in coordinating the programme and providing me with this great opportunity. I would also like to express my gratitude to Prof. Frederik Desplentere and his team at KU Leuven for their research and involvement in the project.

Special thanks go to Mr. Glen Thompson, and other members of the technical staff team at the University of Bradford who have given me invaluable technical support.

I would like to thank Professor Phillip Coates, colleagues and friends at the Polymer IRC who have kept me going over the past four years and have contributed immensely to my personal and professional time at Bradford.

Finally, but by no means least, I would like to say a heartfelt thank you to Lucy, my Mum, Dad and Sister for always believing in me and encouraging me to follow my dreams. They are the most important people in my world and I dedicate this thesis to them.

## Table of Contents

Abstract.....	i
Publications and Conferences .....	iii
Acknowledgments.....	iv
Table of Contents.....	v
List of Figures .....	ix
List of Tables.....	xvi
Nomenclature.....	xviii
<b>1. Introduction .....</b>	<b>1</b>
1.1. Project Aim .....	11
1.2. Project Objective.....	11
<b>2. Literature Review .....</b>	<b>12</b>
2.1. Fibre Dispersion.....	12
2.2. Effect of Fibre Length.....	14
2.3. Fibre Measurement Methods .....	17
2.4. Fibre Breakage Studies .....	25
2.5. Fibre Breakage Mechanisms .....	33
2.6. Fibre Breakage Models.....	37
2.7. Conclusions from Literature Review .....	39
<b>3. Experimental .....</b>	<b>45</b>
3.1. Injection Moulding.....	45
3.1.1. Material.....	45
3.1.2. Injection Moulding Apparatus and Settings .....	46
3.1.3. Nozzle Geometry - Battenfeld BA750/315 CDK .....	51
3.1.4. Injection Moulded Tensile Bar - Arburg Allrounder 270C.....	52
3.1.5. Nozzle Geometry - Arburg Allrounder 270C .....	53
3.1.6. Screw Geometry - Arburg Allrounder 270C.....	54

3.2. Fibre Dispersion.....	55
3.2.1. $\mu$ -CT of Long Glass Fibre Filled Samples.....	55
3.3. Fibre Length Measurement.....	59
3.3.1. Matrix Removal.....	59
3.3.2. Dispersion of Long Glass Fibres .....	60
3.3.3. Capturing of Long Glass Fibres .....	61
3.3.4. Measurement of Long Glass Fibres .. ..	63
3.3.5. Analysis of Data.....	67
3.4. Sample Extraction.....	69
3.4.1. Nozzle – Battenfeld BA750/315 CDK.....	69
3.4.2. Nozzle and Screw – Arburg Allrounder 270C .....	70
<b>4. Fibre Length Measurement – Evaluation of methods.....</b>	<b>75</b>
4.1. Image Pro Premier.....	76
4.2. Fibre Shape .....	79
4.3. CT-FIRE.....	82
4.4. FASEP .....	87
4.5. FASEP (ii).....	89
4.6. Others.....	94
4.7. Conclusion of Trialled Fibre Length Measurement Methods .....	95
4.8. Fibre Length Measurement through the use of Micro-CT.....	95
<b>5. Long Glass Fibre Distribution Results.....</b>	<b>100</b>
5.1. Nozzle Extraction Tests Numerical Results - Battenfeld BA750/315 CDK.....	101
5.1.1. Fibre Length Distribution Results - Battenfeld BA750/315 CDK.....	102
5.2. Screw Pull Out Test Numerical Results - Arburg Allrounder 270C .....	103
5.3. Summary of Screw Pull Out Test Results – 20YM240. 20 mm Screw Test (Low Back Pressure / High RPM) - Arburg Allrounder 270C .....	104



5.3.1. Fibre Length Distribution Results: Pellet – F2 .....	107
5.3.2. Fibre Length Distribution Results: F2 – F3 .....	108
5.3.3. Fibre Length Distribution Results: F3 – C1 .....	109
5.3.4. Fibre Length Distribution Results: C1 – C2 .....	110
5.3.5. Fibre Length Distribution Results: C2 – C3 .....	111
5.3.6. Fibre Length Distribution Results: C3 – M1 .....	112
5.3.7. Fibre Length Distribution Results: M1 – M2 .....	113
5.3.8. Fibre Length Distribution Results: M2 – Sprue .....	114
5.4. Summary of All Screw Pull Out Test Results - Arburg Allrounder 270C .....	115
5.4.1. Effect of Fibre Content .....	115
5.4.2. Effect of Screw Speed .....	118
5.4.3. Effect of Back Pressure .....	121
<b>6. Discussion.....</b>	<b>124</b>
6.1 Experimental Technique .....	124
6.1.1. Compensation for Cut Sample Size .....	125
6.1.2. 1D Correction for Cut Sample Size .....	126
6.1.3. 2D Correction for Cut Sample Size .....	130
6.1.4. Proposed Correction Method for Cut Sample Size .....	138
6.1.5. Review of Correction Methods for Cut Sample Size.....	139
6.2. Experimental Results .....	146
6.3. Fibre Length Distribution & Dispersion.....	151
<b>7. Conclusions .....</b>	<b>157</b>
<b>8. Further Work .....</b>	<b>165</b>
<b>9. References.....</b>	<b>170</b>
<b>Appendix 1: Injection Moulding Settings and Fibre Length Distribution Results for Screw Pull Out Tests Performed on an Arburg Allrounder 270C .....</b>	<b>180</b>
<b>Appendix 2: Compensation for Cut Sample Size.....</b>	<b>246</b>
Appendix 2.1: Manual Orientation Data Results .....	246

Appendix 2.2: Comparison of Original, 1D and 2D corrected fibre length  
distribution results for all other sample locations for screw test 4.....249

## List of Figures

Figure 1.1. - Market demand for long fibre thermoplastic materials in Europe (LFT: Long fibre thermoplastic, D-LFT: Direct-Long fibre thermoplastic, LFG: Long fibre granules, GMT: Glass mat thermoplastic).....	2
Figure 1.2. - Principle components of an injection moulding machine .....	5
Figure 1.3. – Example of a measured fibre length distribution plot of a sample area in a 2 mm thick centre gated plate .....	9
Figure 1.4. – Simulation and prediction of fibre length distribution in a 2 mm thick centre gated plate using Autodesk Moldflow .....	9
Figure 2.1. – Fibre distribution in the skin, shell and core layers of an injection moulded plate .....	12
Figure 2.2. - Tensile strength versus fibre content (♦ LF19, ■ SF19, ▲ SF14) .....	15
Figure 2.3. - Normalised mechanical properties versus fibre content .....	16
Figure 2.4. - Stress-Strain curves of single glass fibres after different thermal treatments .....	19
Figure 2.5. - Fibre degradation at various stages of the injection moulding process using a 40 wt. % long glass filled PP .....	27
Figure 2.6. - Measurement locations along the screw.....	28
Figure 2.7. - Average fibre lengths along the screw .....	29
Figure 2.8. - (Left) Schematic diagrams of a standard three-zone screw and a Maxi Melt screw. The dimensions shown (mm) indicate the distance from the hopper and the different sampling zones. (Right) Process parameters used during plastication of 30 wt. % reinforced long glass fibre polypropylene .....	30
Figure 2.9. - Average length of reinforcement as measured along each screw during the four sets of experiments.....	31
Figure 2.10. - Designs of the five tested screws .....	31
Figure 2.11. - Effect of screw diameter on fibre length during plasticization .....	32
Figure 2.12. – Initial fibre breakage mechanisms.....	34
Figure 2.13. - Various fibre breakage mechanisms.....	36

Figure 2.14. – Image J manual measurement: Pellet sample (Material: 20YM240) .....	41
Figure 2.15. - Weighted average comparison of a different number of fibre length measurements .....	43
Figure 3.1. - Battenfeld BA750/315 CDK injection moulding machine .....	46
Figure 3.2. - Arburg Allrounder 270C injection moulding machine .....	48
Figure 3.3 - Technical drawing of 3 mm Battenfeld BA750/315 CDK injection moulding machine nozzle .....	51
Figure 3.4 - Technical drawing of 6 mm Battenfeld BA750/315 CDK injection moulding machine nozzle .....	52
Figure 3.5. – 2D drawing of injection moulded tensile bar .....	53
Figure 3.6. Technical drawing of Arburg Allrounder 270C injection moulding machine nozzle .....	54
Figure 3.7. - 2D Drawing of Arburg Allrounder 270C 20 mm injection moulding screw .....	54
Figure 3.8. - Example of sample locations along Arburg Allrounder 270C injection moulding machine 20 mm screw .....	55
Figure 3.9. - XT H 225 ST Industrial CT scanner .....	55
Figure 3.10. - Example of an injection moulded sample positioned in micro-CT scanner .....	56
Figure 3.11. - Example of an image slice from the entry of a 3D reconstructed 3 mm nozzle manufactured using a Battenfeld BA750/315 CDK injection moulding machine .....	58
Figure 3.12. – Example of a long glass fibre reinforced screw sample scanned using the XT H 225 $\mu$ -CT machine.....	59
Figure 3.13. - Example of isolated sample placed in ceramic dish (left) and furnace (right).....	60
Figure 3.14. - A3 Epson Expression 10000XL Pro Scanner (left), Settings used to scan glass fibres (right) .....	62
Figure 3.15. - Example of scanned fibre length image.....	62

Figure 3.16. - Example of improved scanned fibre length image .....	63
Figure 3.17. - Example of a random area of measured fibres .....	64
Figure 3.18. – Example of a curved fibre .....	65
Figure 3.19. – Example of a measured curved fibre .....	66
Figure 3.20. – Comparison of measurements using a different number of straight line segments .....	67
Figure 3.21. – Images showcasing various stages of the screw pull out method .....	74
Figure 4.1. - Image J manual measurement vs Image Pro Premier automated measurement - Ticona sample. Material: 20 wt. %. 15 mm LGFRPP (Scanned image 1002) .....	77
Figure 4.2. - Image Pro Premier automated measurement - Ticona sample. Material: 20 wt. %. 15 mm LGFRPP (Scanned image 1002) .....	78
Figure 4.3. - Image J manual measurement vs Fibre Shape automated measurement - Feeding zone sample. Material: 20YM240 (Scanned image 1001).....	79
Figure 4.4. – Sample Fibre Shape automated measurement - Feeding zone sample. Material: 20YM240 (Scanned image 1001) .....	81
Figure 4.5. – Sample Fibre Shape automated measurement – An example of fibre branches being computed.....	82
Figure 4.6. - Image J manual measurement vs CT-FIRE automated measurement - Feeding zone sample. Material: 20YM240 (Scanned image 1001).....	83
Figure 4.7. – Sample CT-FIRE automated measurement: Parameters defined in-house .....	84
Figure 4.8. - Sample CT-FIRE automated measurement: Parameters defined by Giusti et al. (2015).....	86
Figure 4.9. - Image J manual measurement vs FASEP automated measurement - Feeding zone sample. Material: 20YM240 (Scanned image 1001) .....	87
Figure 4.10. – Temperature profile for fibre ashing suggested by FASEP .....	90

Figure 4.11. - Fibre length manual measurement protocol vs FASEP automated measurement protocol - Pellet Sample. Material: 20YM240 .....	91
Figure 4.12. - Fibre length manual measurement protocol vs FASEP automated measurement protocol - Sample F1 vs Sample F1b. Material: 20YM240 .....	93
Figure 4.13. - CT scan of a long glass reinforced polymer sample .....	97
Figure 5.1. – Example of extracted sample locations from a 20 mm Arburg Allrounder 270C injection moulding screw .....	100
Figure 5.2. - Fibre length distribution results from nozzle extraction tests .....	102
Figure 5.3. – Number and weighted average distribution of each 24 mm cut taken from various locations along the injection moulding process.....	104
Figure 5.4. - Summary of fibre length distribution results.....	106
Figure 5.5. - Pellet and F2 fibre length distribution results from screw pull out test .....	107
Figure 5.6. – F2 and F3 fibre length distribution results from screw pull out test .....	108
Figure 5.7. – F3 and C1 fibre length distribution results from screw pull out test .....	109
Figure 5.8. – C1 and C2 fibre length distribution results from screw pull out test .....	110
Figure 5.9. – C2 and C3 fibre length distribution results from screw pull out test .....	111
Figure 5.10. – C3 and M1 fibre length distribution results from screw pull out test .....	112
Figure 5.11. – M1 and M2 fibre length distribution results from screw pull out test.....	113
Figure 5.12. – M2 and Sprue fibre length distribution results from screw pull out test.....	114
Figure 5.13. – Effect of fibre content at low RPM (150 RPM) and low back pressure (2.5 bar) .....	115

Figure 5.14. – Effect of fibre content at low RPM (150 RPM) and medium back pressure (5 bar) .....	116
Figure 5.15. – Effect of fibre content at low RPM (150 RPM) and high back pressure (7.5 bar) .....	117
Figure 5.16. – Effect of screw speed at low back pressure (2.5 bar): 20YM240 .....	118
Figure 5.17. – Effect of screw speed at medium back pressure (5 bar): 20YM240 .....	119
Figure 5.18. – Effect of screw speed at high back pressure (7.5 bar): 20YM240 .....	120
Figure 5.19. – Effect of back pressure at low RPM (150 RPM): 20YM240 .....	122
Figure 5.20. – Effect of back pressure at high RPM (300 RPM): 20YM240 .....	123
Figure 6.1. – Helical direction and direction of the screw parallel to the axis of rotation.....	126
Figure 6.2. – Example of glass fibres falling within and across the sample cut boundary.....	126
Figure 6.3. – Example of glass fibres falling within and across the sample cut boundary creating two fragments.....	129
Figure 6.4. – Example $\mu$ -CT of fibres appearing parallel and transverse to the helical direction of the screw.....	131
Figure 6.5. – CAD cylinder wire positioned around glass fibre reinforced screw sample. ....	132
Figure 6.6. – Example of a CAD cylinder fitted to a glass fibre reinforced screw sample. ....	132
Figure 6.7. - Example of a CAD cylinder fitted to a glass fibre reinforced screw sample before unrolling (left) and after unrolling (right).....	133
Figure 6.8. – Idealised CAD model imported into VG Studio Max.....	133
Figure 6.9. – Axis of fibre orientation .....	136
Figure 6.10. – Definition of the orientation angles from the fibres elliptical footprint.....	136

Figure 6.10 - Image slice imported into LabView VA pre particle analysis (top). Image slice post particle analysis (bottom) .....	137
Figure 6.11. - Comparison of Original, 1D and 2D corrected fibre length distribution results (F2 Screw Test 4).....	140
Figure 6.12. – Example of clusters found in various samples aligned perpendicular to the helical direction.....	141
Figure 6.13. – Example of dispersed clusters in the latter stages of the injection moulding process.....	142
Figure 6.14. - Basic model of natural inclination of pellets along an injection moulding screw .....	143
Figure 6.15. - Overlaid lines showcasing example of pellets inclination along an injection moulding screw .....	143
Figure 6.16. - Example of clusters from slice data .....	144
Figure 6.17. - $\mu$ -CT top cross section from the entry a 3mm nozzle (top left) & 6mm nozzle (top right) (20YM240) and $\mu$ - CT top cross section from the entry of a 3 mm nozzle (bottom left) & 6 mm nozzle (bottom right) (40YM240) .....	147
Figure 6.18. - $\mu$ -CT results showing the random nature of the dispersion of clusters along the injection moulding process.....	149
Figure 6.19. - $\mu$ -CT evidence of pellet and screw flight interaction at hopper exit .....	150
Figure 6.20. - $\mu$ -CT evidence of pellet and screw flight interaction along injection moulding screw .....	150
Figure 6.21. - $\mu$ -CT results showing the effect of fibre content on the dispersion of fibres in the compression and metering zones at low back pressures .....	152
Figure 6.22. - $\mu$ -CT results showing the effect of fibre content on the dispersion of fibres at end of each zone at medium back pressures .....	153
Figure 6.23. - $\mu$ -CT results showing the effect of back pressure on the dispersion of fibres at end of the screw at sample location M2.....	156
Figure 8.1. - Example of iterative pattern matching of fibre clusters taken from a slice view .....	168



Figure 8.2. - Example of a frayed fibre clusters along the injection moulding process .....	168
Figure 8.3. - Example of curved fibres within an injection moulded screw sample .....	169

## List of Tables

Table 1.1. – Forecast revenue demand for automotive composites suppliers by material .....	1
Table 2.1. - Summary of results for a 20YM240 pellet .....	42
Table 3.1. - Battenfeld BA750/315 CDK machine specifications .....	47
Table 3.2. - Battenfeld BA750/315 CDK injection moulding settings for all nozzle samples .....	48
Table 3.3. - Arburg Allrounder 270C machine specifications .....	49
Table 3.4. - Arburg Allrounder 270C injection moulding settings for all screw pull out tests .....	50
Table 3.5. - Example of a fibre length data sample .....	69
Table 4.1. – Summary of comparison results between Image J manual measurements against automated Image Pro Premier measurements .....	77
Table 4.2. – Summary of comparison results between Image J manual measurements against automated Fibre Shape measurements.....	80
Table 4.3. – Summary of comparison results between Image J manual measurements against automated CT-FIRE measurements .....	83
Table 4.4. – CT-FIRE automated measurement: Settings used in-house.....	85
Table 4.5. – CT-FIRE automated measurement: Settings used by Giusti et al. (2015) .....	86
Table 4.6. – Summary of comparison results between Image J manual measurements against automated FASEP measurements .....	88
Table 4.7. – Summary of comparison results of a 20YM240 pellet between Image J manual preparation and measurements against automated FASEP preparation and automated measurements .....	91
Table 4.8. – Summary of comparison results between Image J manual preparation and measurements against automated FASEP preparation and automated measurements of an injection moulded screw sample.....	93
Table 5.1. - Summary of results (Battenfeld BA750/315 CDK) .....	101
Table 5.2. – Summary of results (Arburg Allrounder 270C) .....	103

Table 6.1. – Results comparing diameter of imported CAD cylindrical geometry during unrolling .....	134
Table 6.2. – Comparison of orientation data .....	145

## Nomenclature

<b><math>\Theta</math></b>	Angle theta ( $^{\circ}$ )	<b>RPM</b>	Revolutions per minute
<b>SGFRPP</b>	Short glass fibre reinforced polypropylene	<b>BP</b>	Back pressure
<b>LGFRPP</b>	Long glass fibre reinforced polypropylene	<b>PP</b>	Polypropylene
<b>CT</b>	Computed Tomography	$L_0$	Initial fibre length
<b>wt. %</b>	Weighted (%)	$L_{crit}$	Final average fibre length
<b>MFD</b>	Mould Flow Direction	$K$	Generalised fibre breakage dynamic constant
<b>AR</b>	Aspect Ratio	$f$	Percentage of location along the screw
<b>ELV</b>	End of life vehicle	$L_f$	Average fibre length at location $f$ .
<b>LFT</b>	Long fibre thermoplastic	$L_n$	Number average fibre length
<b>LGF</b>	Long glass fibre	$L_w$	Weighted Average fibre length
<b>D-LFT</b>	Direct-Long Fibre Thermoplastic	$L_i$	Measured length of fibre
<b>LFG</b>	Long Fibre Granules	$n$	Number of fibre length measurements
<b>GMT</b>	Glass Mat Thermoplastic	$L$	Length of extracted sample
<b>LF</b>	Long Fibre	$l_l$	Length of fibre where the centroid of the fibre is located within the sample region
<b>SF</b>	Short fibre	$P_l$	Probability of a fibre of length $l_l$ being sliced during sample extraction and having only some fragment of the fibre present in the removed sample
<b>FLD</b>	Fibre length distribution	$M_l$	Number of fibres which were measured to have a length $l_l$
<b>FOD</b>	Fibre orientation distribution	$N_l$	True number of fibres of length $l_l$ which had their centroids within the cut sample region before sample cutting
<b>UV</b>	Ultra-violet		
<b>CAE</b>	Computer Aided Engineering		
<b>CAD</b>	Computer Aided Design		
<b>LOCI</b>	Laboratory for Optical and Computational Instrumentation		
<b>RAM</b>	Random Access Memory		
<b>VA</b>	Vision assistant		
<b>2D/3D</b>	2 dimensional / 3 dimensional		

## 1. Introduction

Combining fibrous materials and polymeric matrices has been an established process for several decades and has expanded the use of thermoplastics into various high grade applications such as the aerospace, automotive and wind industries. By integrating reinforcing fibres into a thermoplastic it is possible to obtain a new and enhanced composite which can be tailored to its application. This has led to high and rising production demands of fibre reinforced plastic composite materials for its substitution of a number of traditional materials (Shuaib and Mativenga 2016; Wollan 2017). Marsh (2014) described such instances in the designs of relatively new aeroplanes for example the Airbus A350XWB and Boeing 787 Dreamliner. Such substitutions specifically in aeroplane structures has led to vast improvements in efficiency with up to 25% of CO<sub>2</sub> reduction being reported by Timmis et al. (2015) albeit from carbon fibre reinforced polymers.

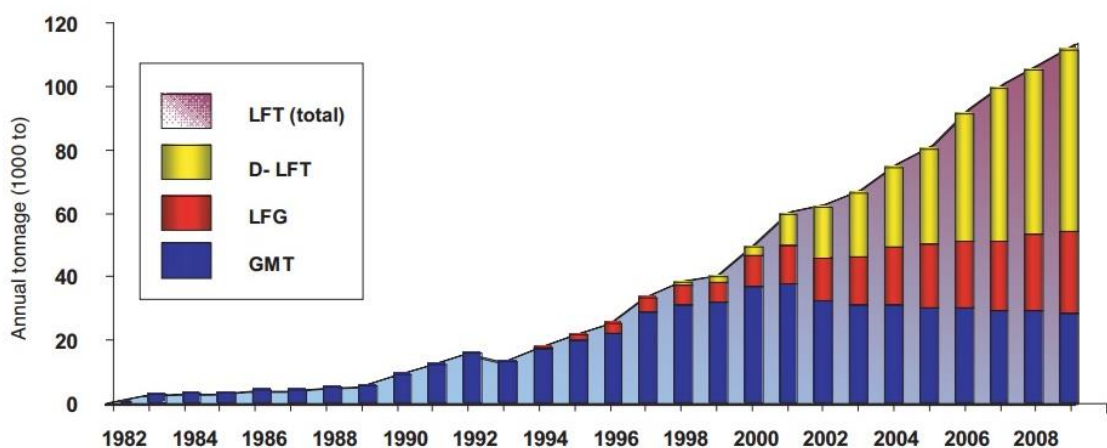
Regarding the UK market, a report compiled by Ernst & Young (2010) estimated the UK composites industry to be worth between £1.1 billion and £1.6 billion in 2010, with the monetary value for glass fibre composites assessed to be at £453 million in the same year.

	Demand (£m)		
	2010	2015	2020
Carbon Fibre Composites	19	39	59
Glass Fibre Composites	44	63	65
Total	63	102	124

**Table 1.1. – Forecast revenue demand for automotive composites suppliers by material. (Ernst & Young 2010)**

The production growth rates of vehicles built by volume manufacturers is the key driver for glass fibre applications. As seen from Table 1.1, growth in glass fibre composite demand is expected to continue broadly in line with overall UK vehicle production rates (Ernst & Young 2010).

Long fibre reinforced thermoplastics (LFT) have been predominantly used as high performance engineering materials for structural applications in the automotive industry. They have several advantages which include high performance in terms of stiffness, strength, heat resistance, warpage, mechanical behaviour under impact load, recyclability, low density, low material costs and high potential for integration. Their main benefit however lies in their high level of productivity in processing, which is a consequence of short cycle times achievable with thermoplastic polymer matrices (Schemme 2003). Such desirable properties have led to developments in the field of new materials and processing technologies over the past couple of decades. This has led to a continued market demand growth of LFT and GMT as seen in Figure 1.1, specifically in Europe. The volume of material manufactured in Europe has continued to grow at an above average rate of over 6% in 2014 as reported by Kraus et al. (2014).



**Figure 1.1. - Market demand for long fibre thermoplastic materials in Europe (LFT: Long fibre thermoplastic, D-LFT: Direct-Long fibre thermoplastic, LFG: Long fibre granules, GMT: Glass mat thermoplastic) (Schemme 2008).**

In accordance with the European Union “ratified end-of-life vehicle (ELV) directive”, the ease of recyclability for long fibre thermoplastics is also becoming an important factor as the recycling of glass reinforced plastic can be a problem. Thermoplastics (such as polypropylene or polyethylene) are easily recyclable because the polymer chain does not degrade when melted down and can be converted back to its original monomer (Correia et al. 2011). However, contaminated thermoplastics (e.g. black bin bags) are very expensive to recycle and are usually incinerated leading to harmful emissions or landfilled (El Haggag and El Hatow 2009). Furthermore, thermosets are also difficult to recycle as they cannot be re-melted because they contain polymers that are cross-linked together during the curing process to create an irreversible chemical bond (Pickering 2006).

Nevertheless, the European Composites Industry Association states that glass reinforced plastic is recyclable and compliant with EU legislation. Facilities to recycle predominately exist in Germany whereas in the UK, the recycling of glass reinforced polymers is excessively expensive coupled with the carbon footprint from transport leading to many companies resorting to landfill. Nevertheless, landfill bans in some countries and increasing landfill taxes in others support the need to recycle be it through established processes such as mechanical grinding or new developments in thermal and chemical recycling processes (Job 2013).

The European ELV Directive (2000/53/EC) 2015 states that 95% of the ELV should be reused or recovered. This legislation combined with global environmental concern and the potential for composites to reduce greenhouse gas emissions has led to considerable research into composite recycling technology and potential recycle applications, in not only the automotive industry but in the construction and aerospace industries as well (Cunliffe and Williams 2003; Palmer et al. 2009; Correia et al. 2011; Ahmad et al. 2012; Shuaib and Mativenga 2016).

Requirements for the automotive industry to reduce emissions to meet increasingly regulatory targets and increase fuel economy has been attainable

through the use of long glass fibre composites. A reduction in cost and weight of the vehicle, without endangering or abandoning passenger safety can only be reached by the use of new material and manufacturing technologies. The automotive industry has been rather reluctant toward the design, construction and selection of modern lightweight materials, however long fibre polymers are able to meet such demands through costs and mass production due to their competitive prices and cycle times (Schemme 2008).

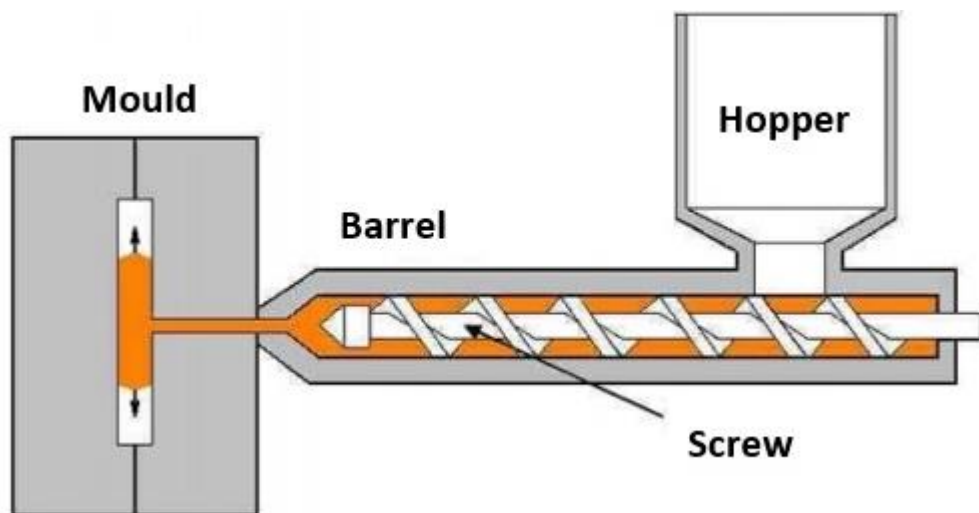
Injection moulding is the most commonly used method for producing thermoplastic polymers. It is a recurring process of quick mould filling and subsequent cooling and ejection. The main advantage of injection moulding is its ability to mass produce high quality structural parts with minimal tolerances in one step continuously in a highly economical process. Also, instead of producing multiple components which would be more expensive, the injection moulding process is able to produce a part with several integrated functions (Brydson 1990; Goodship 2004). Thus automotive applications such as frontends, dashboard carriers, door modules and underbody structures based on these polymers dictate this section of the market (Bürkle et al. 2003; Martin 2005).

Long fibre composite pellets are generally prepared by either co-extrusion or pultrusion of continuous fibres which are enveloped by the polymer matrix. The fibre melt strands are then sectioned into defined pellet lengths (8 mm, 12 mm or over 20 mm) with the fibre length equivalent to that of the pellet length. Short fibre granules are made by incorporating short fibres as staple fibres during compounding, with subsequent lengths being produced from 300 to 1000  $\mu\text{m}$ . Longer glass fibres and subsequently improved mechanical properties are expected for components manufactured with long glass fibres as opposed to short glass fibres (Rohde et al. 2011).

Figure 1.2 shows the principle components of an injection moulding machine. Initially, a plastic material (generally pre-formed thermoplastic pellets) is fed into a chamber (hopper) which is in turn fed into the barrel where a rotating tapered screw is located which is able to move forward and backwards along the barrel



under the force of electric or hydraulic mechanisms. The plastic pellets are initially fed and begin to flow inside the screw channels along the feeding zone. In the subsequent compression zone, the material is gradually compressed creating friction between the material and barrel wall leading to shear forces acting upon the material. Shear causes the material's viscosity to change which is described as shear thinning. The melt is then homogenized along the metering zone as it flows along the increasingly thin screw flights to the front end of the screw. As the screw rotates, mechanical energy is converted into heat, which melts the plastic material, however heat is also provided by the heater bands located along the barrel. Once enough molten material has accumulated in front of the screw, the injection process begins. The screw is then pushed forward injecting the molten material through a nozzle and then along a sprue into the mould cavity for a specific amount of time maintaining the pressure (packing) on the injected melt. A 'back flow stop valve' is sometimes employed to ensure material does not leak back into the screw flights during injection. Pressure is maintained for a short time to prevent shrinkage of the final part. The moulding is left to cool before being ejected from the mould (Rubin 1974; Huilier and Patterson 1991).



**Figure 1.2. – Principle components of an injection moulding machine (Phelps 2009).**

Reinforcement of a composite polymeric matrix with a stiffer fibre additive leads to an increase in its elastic modulus which is proportional to the fibre content. The material's strength is also increased as the higher aspect ratio of longer fibres

means a larger surface area is in contact with the polymer. The added length allows for the transfer of stress forces from the polymeric matrix to the stronger fibre reinforcement improving the materials ability to carry an applied load. Durability is also increased from the dissipation of impact forces throughout the component instead of being localised in one area by the intertwining of longer fibres developing an internal structural skeleton within the part (Wollan 2017).

Polypropylene is one of the most commonly used thermoplastics which this investigation is centred on (McCrum et al. 1997; Bush et al. 2000; Gleissle and Curry 2003) . It is tough, strong and abrasion resistant. It is used in various engineering applications reinforced with either glass (Von Turkovich and Erwin 1983; Bijsterbosch and Gaymans 1995; Thomason 2002), carbon (Creasy et al. 1996; Selzer and Friedrich 1997; Ning et al. 2015), or natural fibres (Wambua et al. 2003; Holbery and Houston 2006; Ku et al. 2011) . Other matrix materials include polyamide 6,6 (Cattanach et al. 1986; Lafranche et al. 2005; Lafranche et al. 2007), polyphthalamide (Pechulis and Vautour 1998; Skourlis et al. 1998; Stokes et al. 2000) and polycarbonate (Carneiro et al. 1998; Pechulis and Vautour 1998; Stokes et al. 2000) to name a few.

This study focuses on glass as a fibre reinforcing material. Glass is generally a popular choice as a fibre reinforcement material as it can be easily drawn into high strength fibres from its molten state. Also glass is readily available and can be manufactured efficiently into a glass fibre reinforced plastic. Glass as a fibre is relatively strong, and when it is implanted in a plastic matrix it creates a composite which yields a greater specific strength. When combined with different plastics, due to its inability to react with other elements it allows the composite to be used in a range of corrosive environments (Callister Jr and Rethwisch 2008).

The Young's Modulus, tensile strength and impact strength of a component is heavily connected to the average glass fibre length within as shown in reports by Thomason (2002) and (2007). To maximise the potential of fibre strength in the component, it is vital that fibres are longer than the critical fibre length which are presented to be in between 1.3 mm and 3.1 mm for glass fibre reinforced

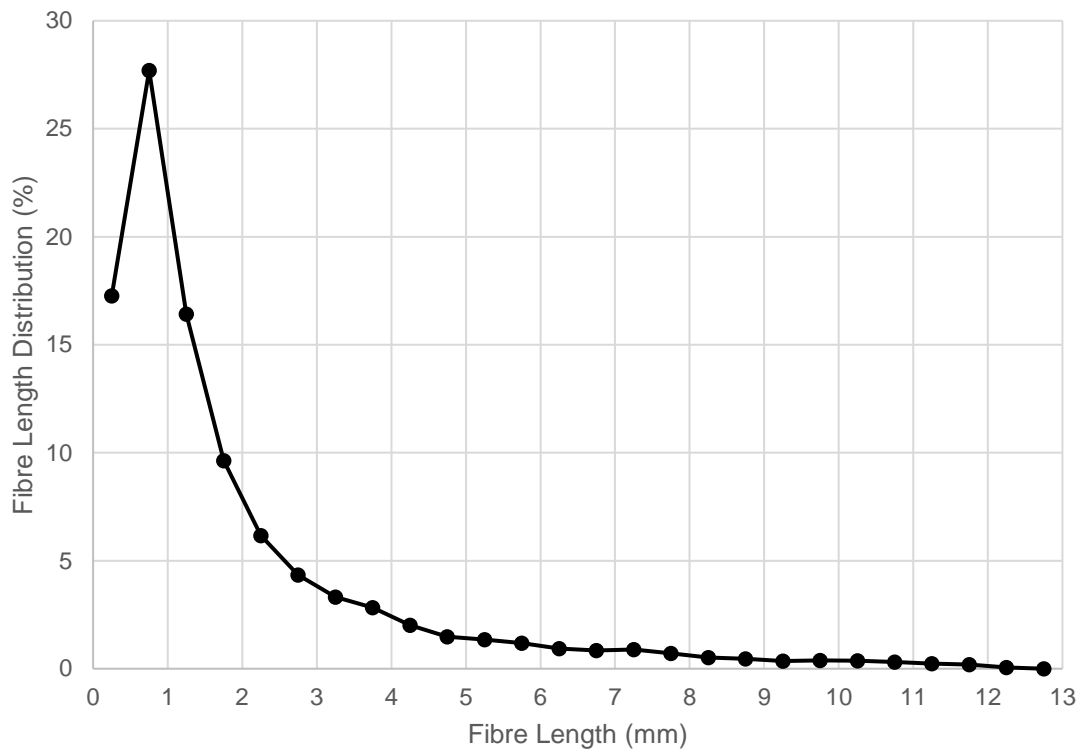
polypropylene (Metten and Cremer 2000). The Kelly and Tyson (1965) theory assumes the critical fibre length is the length required for the fibre to attain the maximum stress condition within the polymer matrix if the composite is loaded in tension which can differ from the grade or length of the raw material and the process parameters. Fibre breakage in processing is inevitable which has led to research attempting to identify where fibre attrition is at its highest in the injection moulding process and how it can be prevented. In general, mechanical properties of the moulded component decrease with decreasing fibre length (Fu et al. 2000). During the injection moulding process, fibres are exposed to high shear stresses during the plasticization process reducing the length of the fibres (Ogawa et al. 1995; Berton et al. 2010). Also, other parameters are shown to directly affect fibre length such as injection speed, revolution speed of the screw, back pressure and barrel temperature (Singh et al. 1998; Ho et al. 2011).

To be able to predict and modify mechanical properties of a structural component made from a polymer, information regarding certain parameters has to be known. For long and short glass filled polymers, fibre orientation, fibre length distribution and fibre content are the most influential of parameters with regards to the mechanical performance of the composite material (Matsuoka 1995; Von Bradsky et al. 1997). A number of methods have been established for investigating fibre length distribution in glass fibre reinforced polymer samples. In most procedures, fibres must be separated from the polymer matrix and this can either be done by burning off the polymer at a high temperature or by dissolving it in an appropriate solvent. Fibres are then manually scattered onto thin plastic sheets or placed in a diluted suspension and are scanned or photographed. The length distribution is then determined by manually measuring the fibres or by a semiautomatic or automatic image analysis system generated by computer software (Lee 1992; Huq and Azaiez (2005); Jin et al. (2016)). The disadvantages of using such destructive methods is that the sample under investigation cannot be further evaluated. Obtaining fibre length distributions can be time consuming especially semi-automatic and manual measurement methods. Also, different methods have to be applied when measuring fibre length or fibre orientation distributions. Lately however, non-destructive methods have been introduced in the form of X-ray computed tomography systems, however these are relatively

expensive, evaluate very small sample sizes and the availability of them restricts development of such methods (Salaberger et al. 2013).

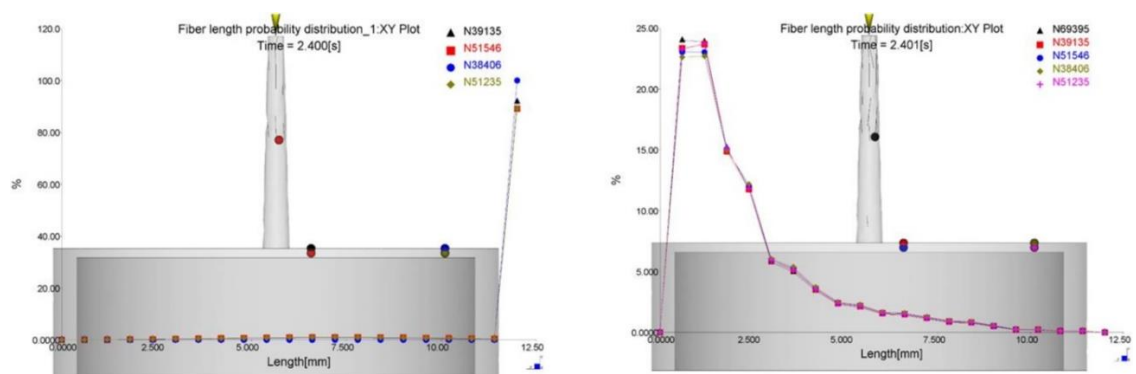
Moldflow, a plastic injection moulding simulation software package owned by Autodesk, whom sponsors this project, is aimed at improving plastic part designs, injection mould designs and manufacturing methods within the injection moulding process. An accurate simulation of the injection moulding process offers many advantages over costly physical prototypes and trial and error methods including plastic part design optimisation, moulding and process validation eradicating the occurrence of production errors (mould / part defects) and process inefficiencies (wasted material). If a manufacturer does not understand the causes of fibre length attrition and cannot minimize fibre length attrition, then they are forced to design thicker and thus heavier parts in order to achieve the same overall impact performance. Likewise, if the properties of a manufactured part cannot be predicted accurately, then a part designer is forced to design with large factors of safety. This is why understanding and predicting fibre length attrition is important in automotive and aerospace applications.

Below in Figure 1.4, are 2 outputs of predicted average fibre length through the part when a fill and pack analysis is ran on an injection moulded 2 mm thick centre gated plate using Autodesk Moldflow. The material selected for this particular analysis was a 12 mm long glass fibre reinforced polypropylene (30 wt. %).



**Figure 1.3. – Example of a measured fibre length distribution plot of a sample area in a 2 mm thick centre gated plate.**

Figure 1.3 shows a standard measured fibre length distribution plot within the main disk section of an injection moulded 2 mm thick centre gated plate showcasing considerable fibre length attrition taking into account the long glass fibres were originally 12 mm in length.



**Figure 1.4. – Simulation and prediction of fibre length distribution in a 2 mm thick centre gated plate using Autodesk Moldflow (Caton-Rose et al. 2017).**

The left hand side of Figure 1.4 shows the output results of an analysis using the software's default inlet conditions. Moldflow assumes that all fibres that enter the top of the sprue are the same size as the pellet they are encased within before processing. In this case, all fibres entering the sprue are assumed to have lengths of 12 mm. This is inaccurate as fibres will have inevitably been subject to mechanical work and shear forces along the injection moulding process, reducing greatly in length. On the right of Figure 1.4 is the same fill and pack analysis, however this time measured fibre length distribution taken from an air shot is applied as an inlet condition at the top of the sprue to achieve a more real representation of average fibre length distribution of the final part. The results highlight the importance of input distribution parameters and signify that with more data, more accurate simulations of injection mouldings can be created (Caton-Rose et al. 2017).

## **1.1. Project Aim**

The aim of this project is to understand how the injection moulding process directly affects the properties of long glass fibre reinforced polypropylene, specifically the fibres. The project will attempt to evaluate the influence of the screw and nozzle of an injection moulding machine on fibre length distribution and fibre length dispersion, predominantly through experimental methods.

## **1.2. Project Objective**

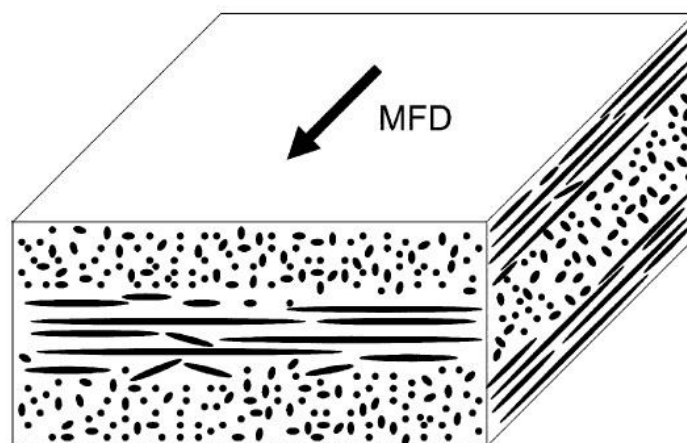
1. The development of a lab based test apparatus which offers removable sections along the length of a typical extrusion or injection moulding screw or the removal of an entire screw which would allow glass fibre reinforced samples to be collected. Through this method the fibre length distribution at stages during plasticization can be measured. Alternate screw geometries will also be considered alongside Objective 2.
2. Injection mouldings of test samples such as centre gated disc, centre gated plates and end gated plaques at a range of process settings; melt temperature, back pressure, etc. will be used for fibre length measurements.
3. Fibre length measurements will be evaluated against their corresponding fibre length dispersion results obtained through the use of micro-CT.
4. A phenomenological model linking screw geometry, process control and local flow to fibre degradation along the screw will be developed.
5. Application of fibre length distributions, from Objectives 1, 2 and 3, within Autodesk Moldflow will be considered and compared with experimental data.

## 2. Literature Review

The purpose of this chapter is to provide background information relevant to the research completed for this investigation. An initial overview of fibre dispersion and fibre length highlight the importance these factors play in the final mechanical properties of an injection moulded part before various techniques are introduced in quantifying residual fibre length. Theorised breakage mechanisms of long glass fibres along the injection moulding process are identified and explained in detail, previous to which these mechanisms are numerically modelled with the purpose of implementing a long glass fibre breakage model necessitated for the evaluation of fibre dispersion and fibre breakage along the injection moulding screw and consequently the prediction of properties of long glass fibre reinforced polypropylene components.

### 2.1. Fibre Dispersion

Mechanical properties are heavily influenced by the skin, shell and core layered structure usually seen in all injection moulded parts, not just composites. During the injection moulding process, the components shape, thickness, position and type of injection gate all have a significant effect on fibre orientation and fibre distribution.



**Figure 2.1. – Fibre distribution in the skin, shell and core layers of an injection moulded plate (Bernasconi et al. 2007).**



It can be seen from Figure 2.1 the separate orientations of short glass fibres in different layers of an injection moulded plate. During the melt flow of short glass fibre reinforced polymer, fibres experience internal shear and elongation stresses that disperse and orient them in preferential directions. Due to the plates shape and thickness, fibres are orientated in a particular direction and various conclusions can be drawn from this. During the injection of a short glass fibre reinforced polypropylene (SGFRP) into the mould, at the mould walls, the fibres tend to orientate parallel to the mould flow direction (MFD). However fibres are also aligned perpendicular to the MFD, this occurs in the core zones of the plate as there are no shear stresses present and extensional flow exists. At the surface of the plate, a very thin skin coating does not have any orientation effect on the SGFRP's, leaving them to orientate randomly due to the liquid polymer freezing when it contacts the cooler mould walls. These features of the polymer layered structure heavily rely on processing conditions (Bernasconi et al. 2007).

In the case of long glass fibre reinforced thermoplastic injection moulding, even if long fibres occasionally can be perceived to behave as short fibres would, the fibre interactions are more complex because of higher fibre length and the reinforcement clustering. This consequently can impede their desired orientation. Even if the skin/core/skin structure is kept, an increase of the core layer thickness with increasing fibre length is observed in a study conducted by Lafranche et al. (2005).

Fibre dispersion is suggested to be non-uniform where strong fibre interaction between fibres and the surrounding molten polymer hinders fibre movement. As a result, mechanical properties are decreased due to fibres clustering and void spaces within the material developing. These characteristics are also considered signs of an instability in the injection-moulding process (Gupta et al. 1989b) (Lafranche et al. 2007).

To minimise fibre degradation, injection moulding of long fibre materials must be done with minimum work. Fibre degradation can also be further reduced if the flow is in clusters of locally aligned fibres. However, these clusters of fibres split

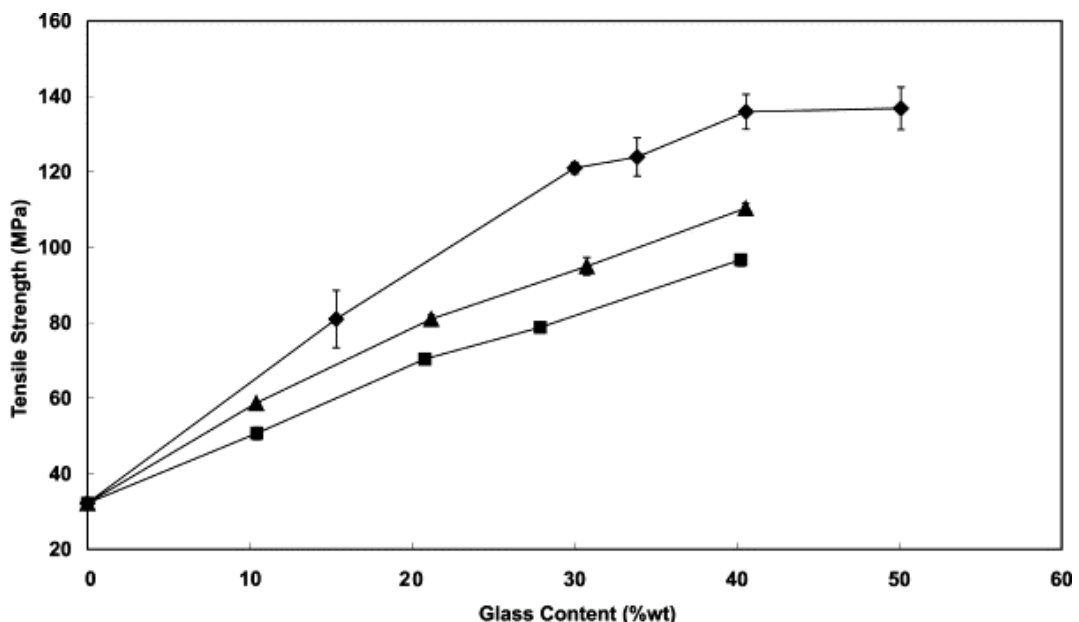
in high shear-stress regions, e.g., during plasticization or flow through small openings (Bijsterbosch and Gaymans 1995).

Fibre dispersion is an important factor in the processing of glass fibre reinforced polypropylene, without which many fibre clusters would be formed after the injection within the manufactured part. The collection of fibres reduces the surface quality and disturbs the mechanical properties of the product. Inoue et al. (2015) confirmed that processing parameters advantageous to minimise fibre degradation or enabling good fibre dispersion are in conflict. High shear stress regions increased fibre dispersion, however it decreased residual fibre length, thus making the simultaneous improvement of both properties challenging.

## **2.2. Effect of Fibre Length**

The mechanical properties of a fibre glass reinforced composite depend on a number of factors including: the properties of the reinforcing fibres themselves, the adhesion between the fibres and the surrounding polymer matrix, the orientation, dispersion, fibre content and length of the fibres. Desirable mechanical properties is restricted with the use of short glass fibre reinforced polymer within the plastics industry due the overall low fibre length distribution within the final part. A demand for higher mechanical performances in injection moulded components has led to the development of high aspect ratio glass fibres. The aspect ratio (AR) is a length/diameter ratio in which long glass fibres, which this study is centred on, exhibit a high aspect ratio. Long glass fibres will typically fall in the fibre diameter range of 16–20  $\mu\text{m}$  with a typical aspect ratio routinely above 600, whereas the standard fibre diameter for short glass fibres is in the 10–16  $\mu\text{m}$  range with an AR below 100. Retaining fibre length in the final component is paramount to attain strong mechanical properties in a long glass fibre reinforced composite to such a degree that long fibre thermoplastics are able to replace metals or more costly engineered polymers in certain applications. Nevertheless, long glass fibres are very susceptible to breakage in the manufacturing process of a component and thus their length is greatly reduced which influences final mechanical properties (Lafranche et al. 2007; Inceoglu et al. 2010).

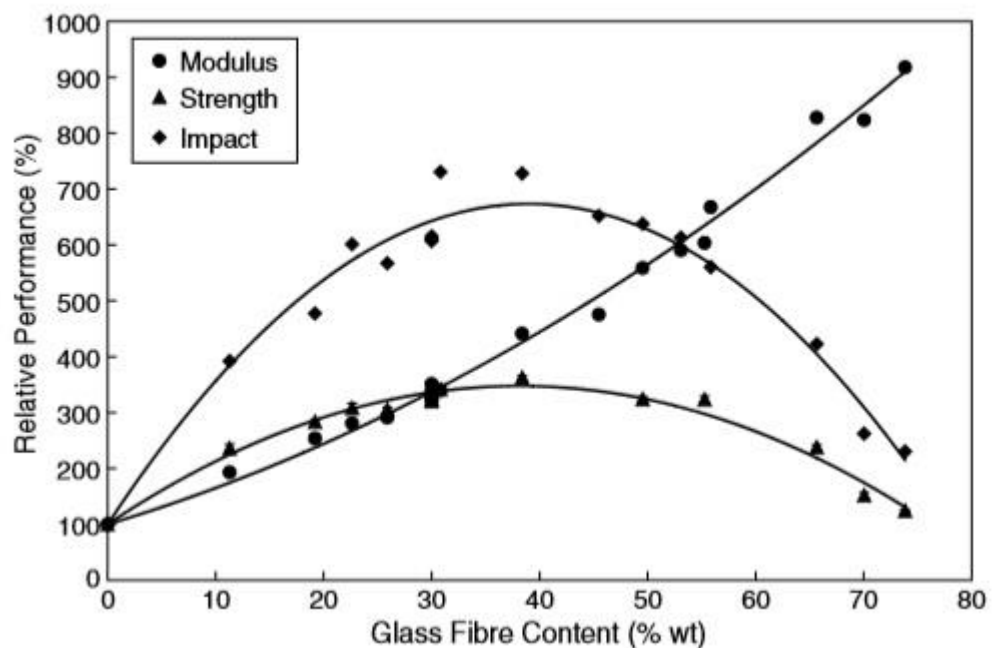
Schijve (2000) suggests good mechanical properties can be attained at relatively low fibre lengths of 5 – 10 mm but is dependent on good fibre matrix adhesion. The author argues that impact strength is the most important factor in terms of fibre length as many underbody shields of cars are produced due to the superior impact strength provided by long glass fibres. Thomason has completed several studies on the effect on fibre length and fibre content on mechanical properties of glass reinforced polypropylene composites. Thomason and Vlug (1996) found that the stiffness of a compression moulded polypropylene laminate was almost independent of fibre length above 0.5 mm. It was also found that the laminate tensile strength and impact strength increased with increasing fibre length before levelling out at higher fibre lengths between 3 – 6 mm and above 6 mm respectively (Thomason et al. 1996; Thomason and Vlug 1997). Thomason (2002) goes further to make a direct comparison of mechanical performance of an injection moulded long fibre reinforced polypropylene test bar against one reinforced with short fibres. The investigation found that at the same fibre diameter for both reinforcements over a range of fibre contents, long glass fibres showed increased tensile and flexural strength, impact resistance as well as a higher modulus as the strain increased.



**Figure 2.2. - Tensile strength versus fibre content (♦ LF19, ■ SF19, ▲ SF14) (Thomason 2005).**

Figure 2.2 displays one of the results published by Thomason (2005), revealing the long fibre composite (LF19) clearly exhibits a higher tensile performance in the same polymer matrix compared to the shorter fibre compounds (SF19 and SF14). The results show the magnitude of strength reduction as a function of fibre length which is a vital parameter for final part strength and the prediction of it.

Additionally, mechanical properties were seen to reach a maximum value between 40 – 50 wt. % glass fibre content as seen in Figure 2.3, apart from the composites modulus which increases linearly with fibre content. Strength and impact resistance decrease instead, reaching performance levels akin to unreinforced polypropylene at glass fibre glass fibre content levels of 73 wt. % (Thomason 2005; Thomason 2007). Çuvalci et al. (2014) suggest this is because at a high fibre content, there is insufficient matrix material and fibres are not dispersed homogenously within the polymer matrix, but as isolated clusters of glass fibres.



**Figure 2.3. - Normalised mechanical properties versus fibre content (Thomason 2007).**

### 2.3. Fibre Measurement Methods

Fibre length is one of the most significant factors in terms of glass fibre reinforced composites. Being able to reliably and accurately evaluate the residual fibre length distribution of a sample is the key to understanding the mechanisms of fibre breakage through experimental investigations, permitting the development of numerical models and the prediction of properties for long glass fibre reinforced components.

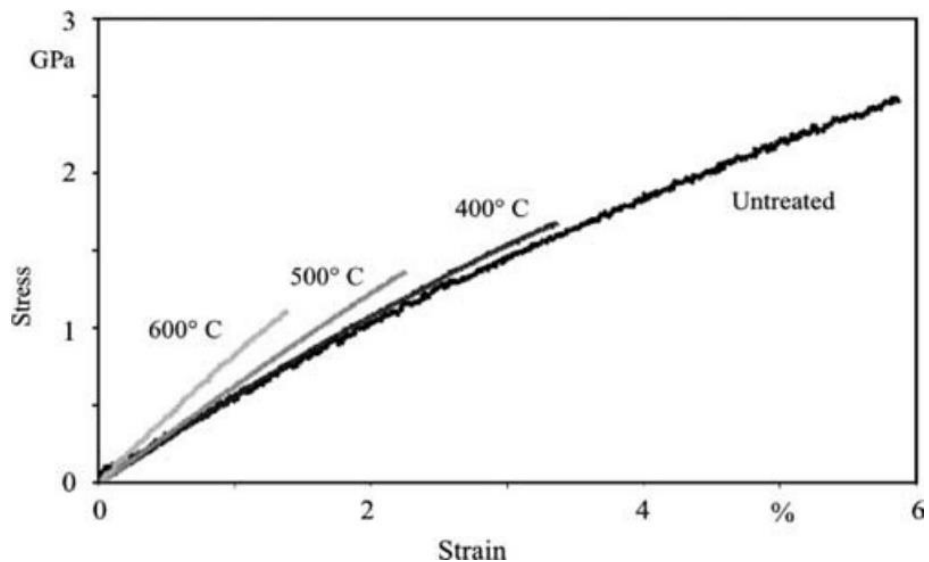
There is an international standard (ISO 22314:2006) which specifies a method of determining the length of fibres present in a fibre reinforced product, however it is limited to thermoplastics reinforced with short glass fibres. This applies to fibres less than 1 mm long or less than or equal to 7.5 mm prior to incorporation in the moulding material and moulding. The standard states that matrix removal should be accomplished via a muffle furnace, which is able to maintain a temperature of  $625^{\circ}\text{C} \pm 25^{\circ}\text{C}$  for 1.5 hours to burn off the polymer matrix. The short fibres should then be mixed in water in a basic ultrasound bath allowing for dispersion of fibres and negating the need for any mechanical action. After the diluted suspension is dried, a random selection of  $300 \pm 60$  short fibres should be measured manually for an accurate fibre length distribution using an optical microscope or stereoscope with fixed or variable magnification factors. These should be equipped with a video camera providing at least x50 magnification. This method is stated to be applicable to moulding materials and to moulded parts. (*International Organization for Standardization: ISO 22314: Plastics - Glass-fibre-reinforced products - Determination of fibre length, Switzerland (2006)*). There is currently no standardized fibre length measurement technique for long glass fibre reinforced thermoplastics, however the majority of recent studies that contain long glass fibre measurement analysis are linked to ISO 22314:2006 in some form.

First and foremost, the polymer matrix has to be separated from the glass fibres in order for long glass fibre lengths to be measured unless using micro-CT. In literature this is accomplished via two methods, most commonly via pyrolysis or very rarely chemical degradation of the matrix.

A few examples over the years of where the polymer matrix has been separated by chemical digestion is apparent. In one case, Schmid (1989), describes how polymer matrix is dissolved with sulphuric acid. In another investigation, Sawyer (1979) removes the matrix with a plasma oxidation process due to less debris leftover on the fibres themselves. Another case, reported by Von Turkovich and Erwin (1983), involves the use of soxhlet solvent extraction. The methods provide very gentle thermal treatment of the glass fibres avoiding the possibility of embrittlement, however sample size is strongly restricted ( $<1\text{cm}^2$ ), can be time consuming, a suitable solvent for the matrix polymer is required and chemical waste would have to be disposed of which is why this is not a popular polymer matrix removal process.

Thermal degradation of the polymer matrix is the generally accepted method for glass fibre separation due to time efficiency, sample size not being restricted and being relatively easy. On the other hand, degradation temperature and times vary across all literature. It was stated by Von Bradsky et al. (1997) that it was largely recognised that below  $600^\circ\text{C}$ , fibres are not embrittled during the polymer matrix removal process. However, Rohde et al. (2011) suggests a lower temperature of  $500^\circ\text{C}$  for 1 hour is sufficient enough. Higher pyrolysis temperatures have been reported by Yilmazer and Cansever (2002) removing the polymer matrix in a muffle furnace at  $650^\circ\text{C}$  for 30 minutes, Teixeira et al. (2015) also at  $650^\circ\text{C}$  and Inceoglu et al. (2011) separating short glass fibres at  $800^\circ\text{C}$  for 1 hour.

Rohde et al. (2011) compiled a report which included the effects of different thermal temperatures on glass fibres for one hour with results shown below in Figure 2.4.



**Figure 2.4. - Stress-Strain curves of single glass fibres after different thermal treatments (Rohde et al. 2011).**

It is seen on the stress-strain curve that a linear elastic trend is present for the glass fibres up until failure. A clear difference is seen between the virgin glass fibre and the one subjected to 600 °C for 1 hour. It was also reported that fibres exposed to 400°C retained 85% of their original strength as opposed to 42% for fibres exposed at 600°C. Therefore 500°C was suggested as an appropriate matrix removal temperature to ensure complete removal of the polymer and the loss of mechanical properties is not as a drastic compared to the higher temperature. Scanning electron microscope scans showed complete fibre recovery.

The next step in the fibre measurement process is the dispersion of fibres leftover from pyrolysis. Fibre dispersion methods vary from study to study, with one method involving fibres being directly dispersed onto glass slides/films before measurement. Another method involves glass fibres being dispersed in a liquid solution, either manually or with the use of ultrasound, before the fibres are transferred for fibre length analysis where they are measured manually, semi automatically or automatically. Good fibre dispersion is critical in enabling a successful fibre length measurement process as clusters or crossing fibres can be difficult to measure especially for semi and automatic fibre length measurement analysis.

Thomason et al. (1996), Wang et al. (2011) and Bumm et al. (2012) to name a few all employed manual fibre dispersion techniques before being transferred to glass slides for fibre length evaluation. Multiple authors have presented a study with the use of a solution to aid in the dispersion of fibres before measurement with the addition of glycerine or a detergent added to the solution to reduce surface tension and promote fibre dispersion before the fibres are mixed manually. O'Regan and Akay (1996) and Inoue et al. (2015) both used untreated water whereas studies conducted by Gupta et al. (1989b), Kumar et al. (2007a) added glycerine to the mixture. Bijsterbosch and Gaymans (1995) dispersed fibres in a 1 wt. % solution of carboxy-methyl-cellulose in water, Lunt and Shortall (1979) dispersed fibres in iso-propyl alcohol solution, Zhuang et al. (2008) used a silicone-water suspension and Priebe and Schledjewski (2011) exercised propanol as the fibre dispersion solution. Mixtures are stirred mechanically which could lead to further fibre attrition as would manual dispersion of fibres. A few authors including Lafranche et al. (2005) and Teixeira et al. (2015) have placed the diluted suspension in an ultrasonic bath to encourage fibre dispersion instead of the mechanical action required in stirring and avoiding further breakage.

A compromise has to be met also on the stirring speed since shorter fibres will sink to the bottom if the mixture is not stirred quickly enough when portions of the mixture are poured onto glass slides or Petri dishes for fibre length analysis. In the case of manual dispersion, a collection of fibres are selected at random from the sample with the use of tweezers before being dispersed manually with a brush. Both dispersion methods can lead to further unwanted fibre attrition. Other methods of dispersion involve the use of a hand held air pump (Parveen 2014) whereas Goris et al. (2017) take this one step further with the use of an enclosed chamber system. The glass fibres are exposed to small compressed air bursts within the chamber with less than 1% of glass fibres being reported lost in the dispersion process.

The majority of investigations mentioned above and in literature in general all extract a random group of fibres from either the dry or diluted suspension before being scanned. This could possibly lead to a preference of sampling longer fibres thus producing a biased fibre length distribution measurement (Phelps et al.



2013). This down sampling, where a sample of fibres is randomly selected from the burnt off sample means the researcher is able to measure a few hundred or thousand fibres instead of the whole sample where the fibre count would be in the millions. The need for a down sampling process has been alluded to in multiple publications, but the actual practice of down sampling varies from researcher to researcher with no official standardized process in place.

Kunc et al. (2007) attempt to address this problem with the publication of a sampling bias correction method for fibre length measurements following the down sampling step. The process involves depositing an epoxy resin through the centre of a sample (post pyrolysis) with a needle forming a cylindrical sampling region through the thickness of the sample. The epoxy is cured and fibres not in the vicinity of the epoxy are carefully pulled away. The epoxy is then placed in a muffle furnace again, burnt off and the remaining fibres are dispersed and measured. The argument for this down sampling procedure is the application of a geometrical equation developed by the author to account for the perceived bias. This eliminates the bias caused by the preferential capture of long fibres compared with short fibres due to the small down sampling area captured with the use of the epoxy. This method is supported by a more recent study by Goris et al. (2017), who argues that this down sampling method also allows for the controlled collection and accurate representation of the length distribution of fibres from the intended sample whereas before, fibres at the edges of a sample which have been cut, may be counted. Further to this, the author goes on to adapt the method described above by using a UV (ultra-violet) curable epoxy which is less viscous and has a drastically lower curing time.

Some problems could arise from this method with the insertion of the needle leading to further fibre damage. Discarding fibres not attached to the epoxy may lead to the unintentional breakage of fibres that are attached. Also, the bias correction method relies on a uniform cylindrical epoxy plug to be deposited which would be quite challenging.

Another approach to down sampling seen in literature is that of a fairly recent fibre length measurement system developed by Hartwich et al. (2009) known as FASEP. A set of dilutions steps are performed after fibre dispersion to the water, glycerine and hydrochloric acid fibre mixture. Half of the original solution is poured into a second beaker which is then topped back up to its original level with distilled water. This process is repeated 7 times whilst the mixture is continuously mechanically stirred before the final diluted suspension is poured in to several Petri dishes ready to be scanned for fibre length analysis.

The dilution process publicised by this method is still time consuming and will suffer the same problem as mentioned before as shorter fibres will settle to the bottom of the beaker first thus the intended randomization of glass fibres in the final dilution may not be so accurate. Also, the need for constant mechanical action to stir the mixture could result in further unwanted fibre degradation.

Following dispersion, fibre detection is the next step in obtaining a fibre length distribution. Fibres are detected either through the use of an optical microscope with an attached video camera (Huq and Azaiez 2005; Patcharaphun and Opaskornkul 2008) or projected onto a digitized board with a high magnification projector (Kumar et al. 2007b) which relays the image over to the fibre length analysis software. Nevertheless, accurate stitching of images can be time consuming and inaccurate with the creation of artificial fibre ends. Scanning a larger area is far more practical and accurate and is utilized by several authors with a flatbed scanner at high resolution (Rohde et al. 2011; Parveen 2014; Giusti et al. 2015; Goris et al. 2017).

Fibre measurement is the final step in fibre length evaluation. Throughout literature, several image analysis systems have been mentioned that allow for manual, semi-automatic, or automatic measurement of glass fibres. Ideally, an accurate, reliable and fully automatic detection system for the measurement of long glass fibres would be best suited to obtaining fibre length distributions. However, most if not all systems suffer the same problem in that they are unable to analyse touching, intersecting and curved fibres, instead splitting them up into

smaller shorter segments. Digitised image files of the fibres are uploaded to an image processing program alike to ImageJ or OVM Pro where manual measurements can take place. Although very time consuming and laborious, it simply involves the user overlaying a straight or segmented line over the end points of a scanned glass fibre which is appropriately scaled computed to give a real measurement. This method is present in numerous studies including investigations by Arroyo and Avalos (1989), Nguyen et al. (2008) Thomason (2009) and Jin et al. (2016). This method is heavily subject to human error as results can vary from one researcher to the next. Also, there will be a degree of error present when selecting the end points of fibres.

Early on, sieving of glass fibres samples was a step introduced to separate fibres into different length intervals, simplifying fibre length measurements. A weighed fibre sample is dispersed and passed through a sieve stack of different mesh sizes under a constant stream of liquid from above. This allowed for the fibres to be filtered and a number of fibres would be measured for each distribution dependant on the sieve size (Lunt and Shortall 1979; Bailey and Kraft 1987; Truckenmüller and Fritz 1991; Akay and Barkley 1992). Image analysing systems nowadays have no problems generating fibre length distributions thus rendering the sieve method useless.

Semi-automatic fibre measurement programs have relatively recently become available and have been employed in various literature findings. Although they are able to measure short and straight fibres automatically and fairly accurately, they struggle to deal with long, curved, intersecting fibres which are central to this study. Media Cybernetics have created two image analysis software packages; Image-Pro Plus and Image Pro Premier which have been adopted by several researchers including Kumar et al. (2009) and Ren and Dai (2014) to name a few. Parveen (2014) outlined a semi-automatic method in which ImageJ was combined with in-house algorithms to measure short fibres but long, curved and intersecting fibres would need user input.

Progression in this field has led to fibre length measurement software being developed. FASEP, which has been gaining more and more attention in recent literature, utilizes a customized module of the image analysing software Image-Pro Plus, and can detect single and independent fibres. In spite of this, any crossing fibres again require user input rendering the process semi-automatic (Rohde et al. 2011; Lohr et al. 2017).

Giusti et al. (2015) adapted an open source software program, CT-FIRE, originally intended for extracting collagen fibre data from an image for the use of obtaining fully automated fibre length measurement results. The standalone MATLAB package based on curvelet transforms 'CT' and a fibre extraction 'FIRE' algorithm was reported to give successful analysis of long glass fibres. Images were split up to allow for a quick and efficient analysis. Consequently, a mask was placed on the screen before manual dispersion of the fibres to avoid them crossing the boundaries of the analysed image slice so their true length is captured.

Goris et al. (2017) also propose a fully automated fibre length measurement program based on the work of Wang (2007) where even bent and intersecting fibres are detected and measured with a relatively quick processing time of ~ 60 – 90 minutes for fibre sample populations ranging between 15,000 – 50,000 fibres. This program was developed onsite at the Polymer Engineering Centre at the University of Wisconsin-Madison.

To assure justification of computed statistical results, it is crucial that a sufficiently large number of fibres are measured to obtain a representative value for fibre length distribution within the sample. It is arguable if anything less than a 1000 fibres measured is statistically representative however the number of fibre measurements across the years in literature vary from 100 fibres measured (Bajracharya et al. 2016), to 500 fibres (Jin et al. 2016), to 1000 fibres (Inoue et al. 2015), and up to 2000 (Denault et al. 1989) and 3000 fibres (Hartwich et al. 2009). Surprisingly, Giusti et al. (2015) measured only 1000 fibres even with the use of a fully automated fibre length measurement program. This is in contrast to

Goris et al. (2017) who reported to be able to measure between 15,000 and 50,000 fibres automatically. A full fibre length analysis of a samples entire glass fibre population was reported, consisting of 350,000 – 750,000 measurements for a single sample although there is limited information available due to it being an industrial case study sponsored by SABIC (Krasteva 2009).

An assessment of fibre length distribution measurements with the use of  $\mu$ -CT is alluded to later in Chapter 4.8 following an evaluation of various fibre length measurement systems. It is introduced as a potential alternative to future fibre length studies due to the disadvantages of current measurement methods, which primarily involve the removal of the polymer matrix. However, research within this field is relatively new and suffers from limitations primarily due to sample size and is not adequate considering the scope of this study.

## **2.4. Fibre Breakage Studies**

Research into the breakage of fibres has been investigated significantly over the recent years. The majority of fibre attrition is related to the plastication (conversion of plastic pellets to flow-able melt) phase and various studies have focused on fibre breakage along different zones of the screw and the influence of injection moulding process parameters.

A study conducted by Kelleher (1993) explains that fibre degradation present in the injection moulding process is predominantly due to the mechanical work and shear forces imposed on the polymer by the screw as well as breakage during flow through restrictive gates. Phelps (2009) also explains that in both his literature review and experimental data, the majority of fibre length breakage happens in the earlier stages of injection moulding most notably in the screw, nozzle, runners and gates.

Von Turkovich and Erwin (1983) summarised that although some fibre breakage occurs in the mould and runners, most of the fibre length reduction occurs in the injection unit, specifically the melting (compression) zone with relatively minor

fibre breakage occurring beforehand in the feeding zone. It was also noted that various volume fractions (1 – 20 wt. %) of the 3.2 mm short glass fibre filled polypropylene processed all showed similar fibre length distributions.

Generally, machine settings recommended by the raw material supplier along with some researchers (Metten and Cremer (2000) and Gérard (1998)) advised a low screw rotation speed and low back pressure for the processing of long glass fibre filled materials. Hafellner et al. (2000) however, proposed in their study that short plasticisation times with high screw rotation speeds, low back pressures and pellet pre-heating before plasticisation reduces fibre breakage.

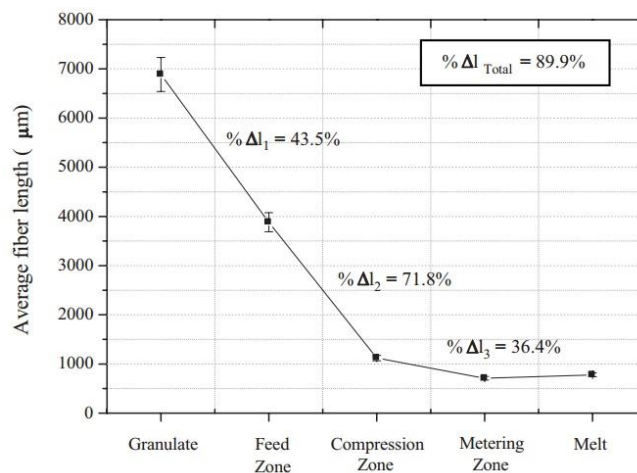
Kelleher (1993) went further to describe an assessment made on long glass fibre (10 mm) compositions of nylon 6-6 from which it was concluded that the greatest length reduction took place in the compression zone of the screw. This is supported by Lafranche et al. (2005) who measured fibre length degradation along the whole injection moulding process for a 10 mm long glass fibre reinforced polyamide 6. The study showed fibre attrition occurred mainly in the compression section where the number average fibre length had fallen by 70% and that remaining fibre lengths found at the nozzle were less than 50% of the initial length. It was also stated by Kelleher (1993) fibre degradation was not a gradual process but a localised sudden transition which was heavily dependent on the design of the screw which is an important factor in retaining fibre length.

Rohde et al. (2011) investigated the influence of process parameters on the impact behaviour of long fibre reinforced compounds where fibre length is a key factor (the original length of the glass fibres in the raw virgin pellet was 11 mm). Results showed a strong negative influence of the back pressure during injection on both impact energy and fibre length. This is in contrast to results published by Schmid (1989), Lafranche et al. (2005) and Kumar et al. (2007b) who found screw rotational speed had a stronger effect on fibre length degradation than back pressure. Furthermore, neither injection speed, screw speed nor holding pressure were seen to have a significant influence on fibre length.

Rohde et al. (2011) describes that at increasing back pressure during plasticization of the polymer, where fibres are pressed against each other and against the screw flights, fibre-melt and fibre-fibre interactions occur, the melt will apply higher forces on the fibres leading to increased bending and axial forces. This attrition is intensified in the initial zones of the screw in the solid to melt phase as the screw has to overcome the back pressure to reach the metering stroke. Lafranche et al. (2005) suggests however fibre-wall interactions due to screw movement are more significant than fibre-melt interactions caused by back pressure.

Yilmazer and Cansever (2002) described how the increase of the screw rotation speed produces high shear stress regions in the melt, increasing fibre breakage. This fibre degradation then becomes stable due to the shear thinning nature of the melt which in turn increases the melt temperature, decreasing its viscosity.

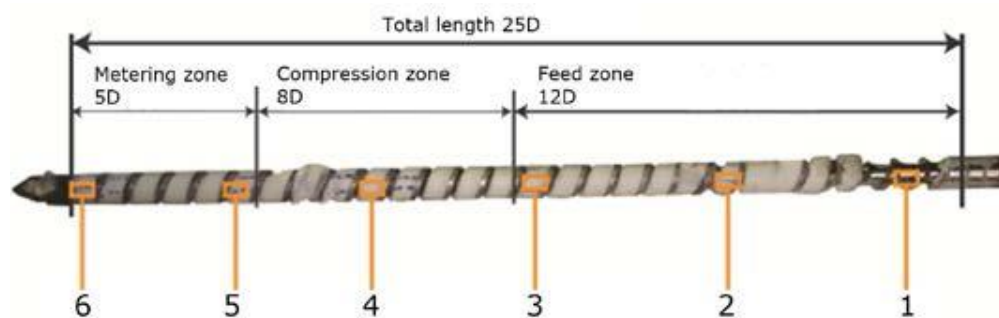
Patcharaphun and Opaskornkul (2008) conducted a study measuring the reduction in fibre length of 40 wt. % long glass (7 mm) fibre filled polypropylene along the screw channels and after the molten composite was injected through a nozzle of an injection moulding machine



**Figure 2.5. - Fibre degradation at various stages of the injection moulding process using a 40 wt. % long glass filled PP (Patcharaphun and Opaskornkul 2008).**

The results displayed above in Figure 2.5 show the percent difference between each stage of the injection moulding process. It was noted that extensive fibre degradation occurred specifically in the compression zone where the beginning of the melting process occurs. A 43.5% decrease in average fibre length is shown in the feed zone and the reduction is continued in the compression zone with a further 71.8% fibre length decrease due the increased fibre-fibre and fibre-wall interaction in the more viscous melt. Total reduction of fibre length is shown to be at nearly 90% for the material during plasticizing in an injection moulding machine. However, the polymer matrix was burnt off at a relatively high temperature of 650°C possibly leading further fibre attrition due to embrittlement of the fibres but the results are in agreement with other findings.

Desplentere et al. (2012) presented a paper on fibre breakage in the screw considering different processing properties including screw rotation speed and back pressure albeit centred on short glass fibres. The 20 mm screw was detached from its motor drive and pushed out using small iron rods. Fibre distribution results were measured in 8 locations, 6 of them shown in Figure 2.6 (7 being just in front of the non-return valve, and 8 being a sample from the extrudate). The material used was a 30 wt. % short glass fibre filled polypropylene.

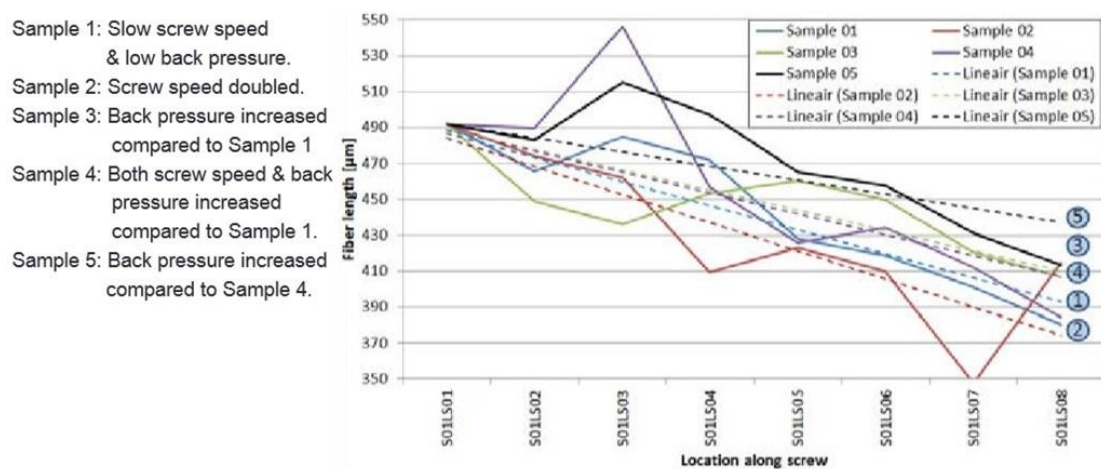


**Figure 2.6. - Measurement locations along the screw (Desplentere et al. 2012).**

The results presented in Figure 2.7 seem to display a few irregularities in that average fibre length is shown to increase in certain locations along the injection



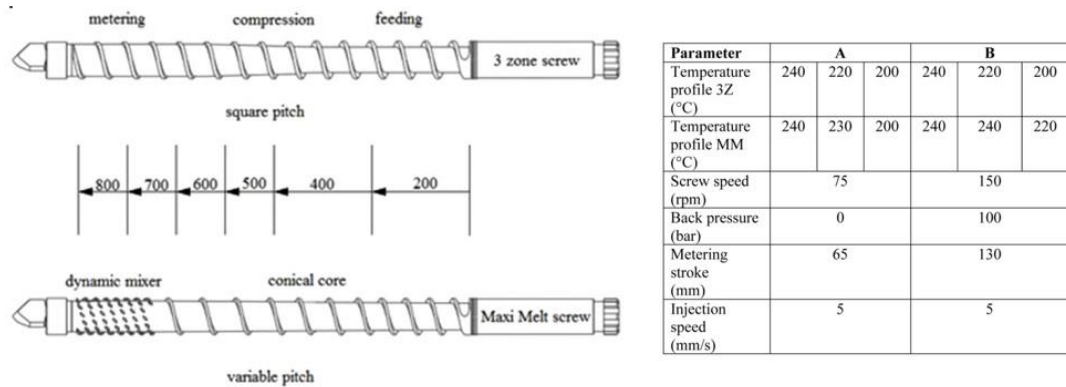
moulding process but this is probably due to the randomness of the sampling method. Still, there appears to be a decreasing linear trend in average fibre length suggesting the fibre breakage remains constant and the proportion of broken fibres increases. It was also concluded from the investigation, as seen from the graph in Figure 2.7 that whilst evaluating different process parameters, each one did not appear to have a significant effect on fibre length along the injection moulding process. However, this may be attributed to the report being centred on short glass fibre filled material where fibres are significantly shorter and not as susceptible to breakage compared to longer fibres.



**Figure 2.7. - Average fibre lengths along the screw (Desplentere et al. 2012).**

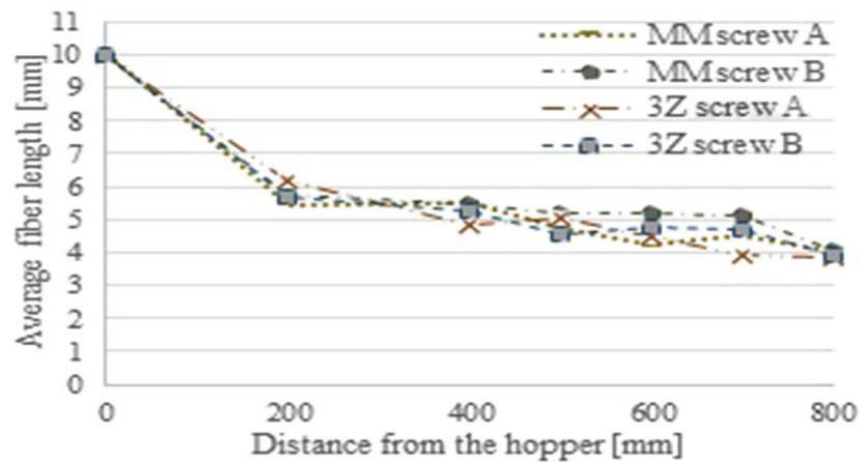
Fibre breakage studies have also centred on screw geometries as well as process parameters. Giusti et al. (2015) revealed an analysis of the plasticating performance of two different screws with regards to fibre length breakage. A standard three-zone screw and a 'Maxi Melt' were used both with a diameter of 40 mm. The main feature of the Maxi Melt screw includes a completely conical core, variable pitch, and the presence of a dynamic mixer in the metering zone. Again both screws were extracted from the barrel and samples were taken along the screw at different distances from the hopper. A 10 mm long glass fibre reinforced polypropylene (30 wt. %) was used. The extracted samples measured 20 mm in length, twice the length of the pellet size and were subsequently evaluated for fibre length distribution. Two sets of conditions were conducted for

each screw at different processing parameters (A and B), displayed in Figure 2.8. The three temperatures in each profile shown below in Figure 2.8 relate to the barrel temperature profile for each zone of the standard three zone screw and the Maxi Melt screw.



**Figure 2.8. - (Left) Schematic diagrams of a standard three-zone screw and a Maxi Melt screw. The dimensions shown (mm) indicate the distance from the hopper and the different sampling zones. (Right) Process parameters used during plastication of 30 wt. % reinforced long glass fibre polypropylene. (Giusti et al. 2015).**

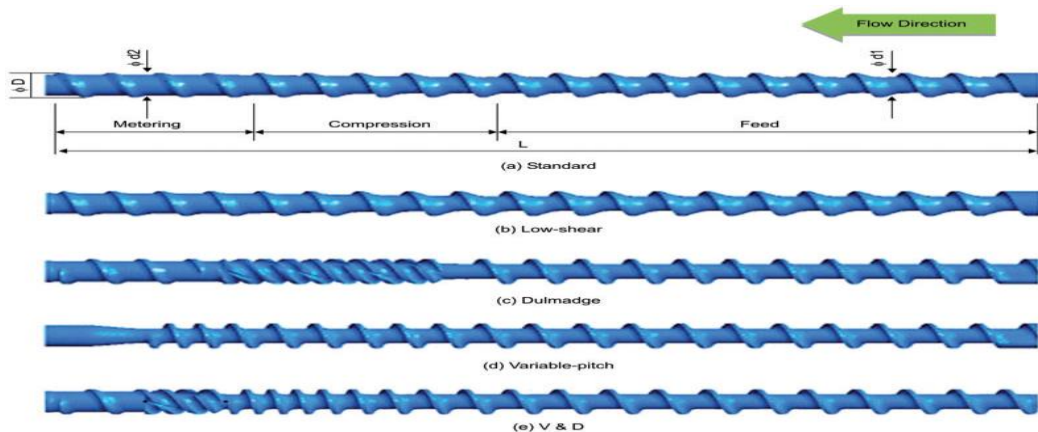
The results from the research carried out are displayed below in Figure 2.9. The 'Maxi-Melt' screw and the three zone screw results are fairly similar and are evaluated together. The data shows quite a sharp decrease in average fibre length during the feeding zone, signifying that the majority of long glass fibres suffered significant attrition in the initial stages of the injection moulding process. Average fibre length decreased by 40%, 200 mm from the hopper and 60% in total from the hopper to the non-return valve.



**Figure 2.9. - Average length of reinforcement as measured along each screw during the four sets of experiments (Giusti et al. 2015).**

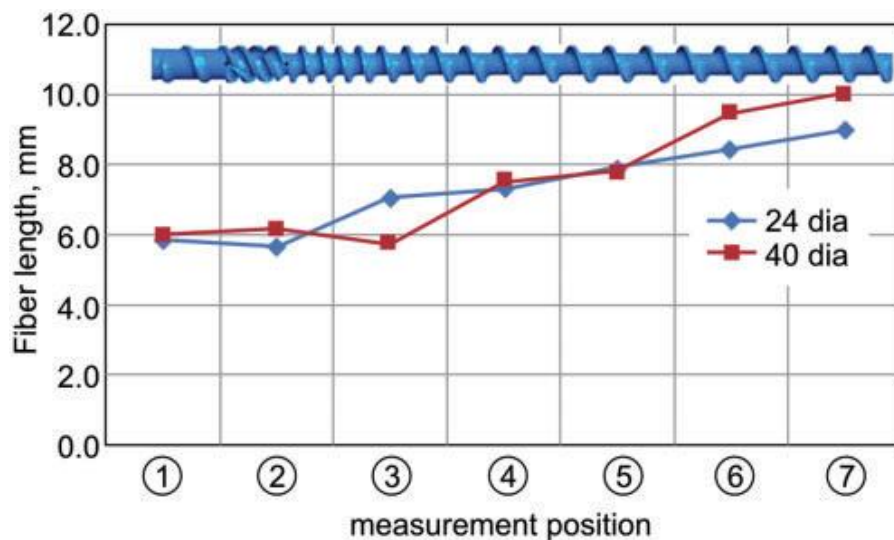
This showed that altering the screw in favour of higher productivity and better melt homogeneity did not lead to further fibre attrition compared to using a standard injection moulding screw.

Inoue et al. (2015) evaluated 5 different screw geometries presented in Figure 2.10 for improving fibre dispersion and reducing fibre length reduction along the injection moulding process. A 10 mm long glass fibre reinforced polypropylene (20 wt. %) was used. The first part of the report found that fibre length distribution was heavily dependent on screw geometry in the compression zone as mentioned in previous studies.



**Figure 2.10. - Designs of the five tested screws (Inoue et al. 2015).**

A negative relationship was observed for screws (a), (b), (c) and (d) between residual fibre length and fibre dispersion as expected, however the optimised screw design of (e) (Variable-pitch and Dulmage screw) overcomes this and improves both properties at the same time. The variable flight pitch and constant flight depth part prevented fibre breakage due to a low shear stress distribution and the complex flow of the Dulmage part improved fibre dispersion. The original 24 mm 'V & D' screw was evaluated as well as a proportionally larger 40 mm 'V & D' screw for fibre length attrition along the injection moulding process. It can be noted that from the data shown in Figure 2.11 that fibre degradation in the metering zone, from location 2 to location 1, is particularly small. However, fibre breakage is seen to predominantly occur beforehand in the feed and compressions zones where the pellets are not entirely melted. These average fibre length measurements are supported by the previous investigation conducted by Giusti et al. (2015). It was also concluded that the screw size and screw diameter has a minimal effect on average fibre length as indicated in Figure 2.11. However, screws with increased flight depths appear to reduce shear stresses acting on the fibres along the screw, increasing residual fibre length in the moulded component (Ramani et al. 1995; Shon and White 1999).



**Figure 2.11. - Effect of screw diameter on fibre length during plasticization (Inoue et al. 2015).**

## 2.5. Fibre Breakage Mechanisms

It is generally acknowledged that isolating the mechanisms that bring about fibre length attrition is challenging due to the complex phase change and shear history that is existent in the injection moulding process.

Fibre – fibre interaction, fibre – wall interaction and fibre – polymer matrix interaction were identified by Von Turkovich and Erwin (1983) as the three most significant fibre breakage mechanisms that lead to fibre degradation.

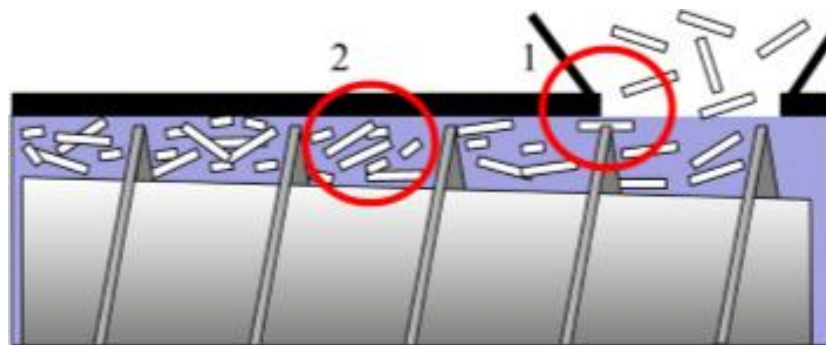
Fibre-fibre interaction describes a mechanism where fibres can overlap with one another leading to bending stresses induced on the fibres themselves. Stress concentrations are then produced due to abrasion between fibres causing a decrease in fibre strength. An increase in fibre concentration can lead to improved mechanical properties to a certain degree but will also inevitably lead to increased fibre – fibre interactions promoting fibre breakage which is why most industrial grades ranged from between 20 wt. % glass filled polypropylene to a maximum of 60 wt. % (Servais et al. 1999).

Fibre – wall interaction deals with fibre attrition as a result of fibres coming into contact with the machinery, specifically the inner barrel and screw surfaces which are gradually damaged over time. Ren and Dai (2014) found that the roughness of inner surface of the barrel compared with the relatively smoother screw surface lead to a weaker interaction between fibre and screw.

Finally, the fibre – polymer matrix breakage mechanism explains how shear stresses produced during the injection moulding process act on the polymer matrix and as a result affect the embedded glass fibres, causing them to break (Hernandez et al. 2002). Zhang and Thompson (2005) expressed that the polymer viscosity also influences the amount of fibre degradation. By raising the melt temperature, the viscosity of the thermoplastic matrix is decreased reducing fibre breakage, however this can lead to polymer degradation and increased cycle times if raised too high.

Wolf (1994) published a report investigating fibre breakage along a single screw extruder and suggested several breakage mechanisms along the screw channels from the ensuing results which can be applicable to an injection moulding screw.

Results suggested right from the beginning of the injection moulding process, before the polymer matrix reaches a molten state and as the raw virgin material flows through the hopper exit and the pellets are compacted into the screw channels, a small percentage of pellets are fractured between the edge of the hopper exit and screw flights as shown below in Figure 2.12 below, circled in red and labelled 1.



**Figure 2.12. – Initial fibre breakage mechanisms (Wolf 1994).**

Also, the pellets are damaged by interacting with one another along the flights of the screw of the feeding and compression zones similar to the fibre – fibre interaction mechanism leading to abrasion and fracture of the pellets before they are completely melted. This mechanism was described as pellet – pellet interaction and is circled in red in Figure 2.12 above, labelled as 2.

Additionally there is a clearance gap between the top of the screw flight and the inside diameter of the barrel shown in Figure 2.13, circled in red and labelled as 1. This mechanism is also accountable for fibre attrition as fibres touching or passing through will be damaged due to being exposed to shear and frictional forces.

Wolf (1994) explains another mechanism taking place at the solid - melt interface during melting, in that as the barrel is heated, thin molten layers of the polymer matrix will form at the barrels inner surface and along the outer surface of the screw whilst a solid bed of glass fibres is located in between. The thin molten layer is formed from some of the polymer reinforced pellets melting due to shear and conduction from the external barrel heaters. Any glass fibres, individual or clusters, protruding from the solid bed into the thin molten layer would be exposed to the machinery and high shear flows. The ends of the fibres would be subsequently sheared off subject to the drag forces exerting a bending moment large enough to cause flexural failure of the glass fibres at the point of anchor highlighted in Figure 2.13 as label 2 and 3. This was also examined previously by Gupta et al. (1989a) who suggested that this fibre breakage mechanism taking place at the solid – melt interface was the main reason for the degradation of glass fibre length along the screw.

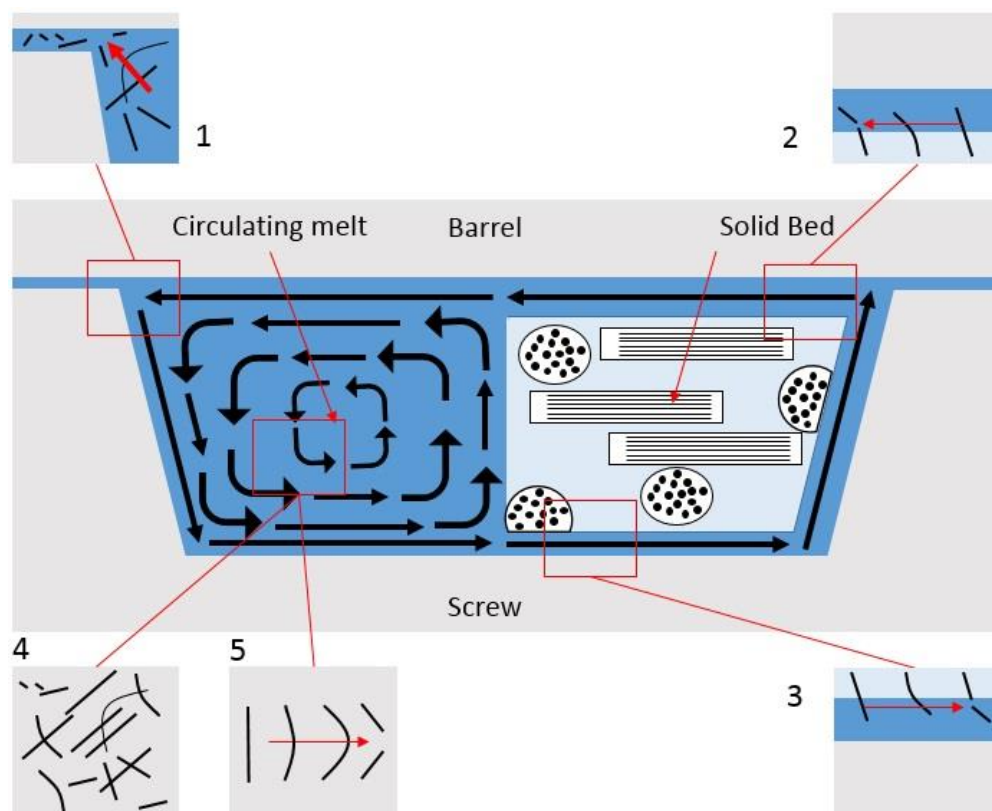
Alongside this solid bed of pellets within the screw channel, Wolf (1994) goes on to describe a separate pool of melt flowing in a circulatory manner due to the forward and rotational movement of the screw flights continuously scraping off the thin molten polymer layers.

As the glass fibre reinforced polymer material travels down the length of the screw, the polymer matrix begins to melt further, increasing the size of the molten layers and melt pool until finally, the solid bed of glass fibre pellets breaks up and disperses within a complete pool of molten polymer by the end of the screw (Gupta et al. 1989b).

With an ever increasing melt pool, individual fibres or clusters of fibres not anchored in the solid bed are free to move in the molten polymer as shown in Figure 2.13 in label 4. These fibres would be subject to bending and breaking from the shear and friction produced from the circulatory melt flow and also along the barrels inner surface and screws outer surface, which all leads to further fibre degradation. Forgacs and Mason (1959), concluded that fibre breakage is the result of buckling and bending in a laminar shear flow based on Euler's theory of



buckling, asserted also by Salinas and Pittman (1981). Forgacs and Mason (1959) calculated a critical shear stress value above which buckling of a single straight fibre transpires. Also the shear stress that leads to this buckling and bending of a fibre is inversely proportional to the fibres length meaning longer glass fibres have a lower buckling stress thus they are more susceptible to breakage. However, the work published focused on individual fibres and not bundles. These fibre structures protect themselves from the shear forces present during the moulding process however such clusters are not desirable and they can result in poor homogeneity in the final part leading to a decrease in mechanical properties and poor surface finish (Mittal et al. 1988). Clusters formed could be glass fibres not yet dispersed from their original pellet structure. Or additionally, Rohde-Tibitzl (2015) states that bundles are created by fibres aligning in the circulating flow of the melt pool and beginning to interact with one another entangling themselves in a super-lattice of glass fibres, again protecting individual fibres being vulnerable to breakage. The degree of entanglement is suggested to increase with fibre length and circular motion. Thus, the ability of a fibre to follow the melt without breaking will be governed by its length.



**Figure 2.13. - Various fibre breakage mechanisms (Wolf 1994).**



Further to this, the breakage of an original long 'parent' fibre/cluster will lead to the creation of 2 smaller 'children' fibres/clusters, with the shorter fibre being less susceptible to fibre breakage compared with its previous parent fibre. This is shown in Figure 2.13 in label 5. With longer fibres and higher concentrations of glass, there inevitably will be more fibre - fibre and fibre – surface interactions.

## **2.6. Fibre Breakage Models**

Ideally, it would be advantageous to assess fibre dispersion and breakage and the mechanisms concerned along the injection moulding process whilst evaluating the influence of different process parameters through the use of computer aided engineering (CAE) to determine the performance of a moulded part. This would allow for the optimization of geometric and processing settings within the injection moulding process and subsequently the improvement of mechanical properties in the manufactured component without the need of time consuming and expensive research, prototype geometries, material waste or trial and error based methods (Kim and Turng 2004).

Some authors have attempted modelling individual glass fibre breakage mechanisms along the injection moulding process. Mittal et al. (1988) described a model for the fibre breakage mechanism that takes place at the solid-melt interface by which the bending moment of a single fibre, anchored within the solid bed of material at one end, is governed by the drag forces produced from the surrounding flow of molten polymer at the other end. Bereaux et al. (2008) expanded their calculation of which it considered the molten polymer as a Newtonian fluid to a power-law fluid, a type of generalised form of a Newtonian fluid but which allows for the approximation of the behaviour of a real non-Newtonian fluid.

Both models showcase the effects of the thickness of the molten polymer and its viscosity, and the fibre orientation relative to the flow direction where breakage of a single fibre transpires when the bending load is higher than the failure load. Mittal et al. (1988) do consider the effect of fibre bundles, assuming that all fibres within the bundle behave independently of each other and naturally the minimum

thickness of a layer of molten polymer in which fibre breakage occurs is greater for a fibre cluster compared with an individual fibre.

Based on the work conducted by Von Turkovich and Erwin (1983) which concluded fibre interaction with the polymer matrix as the most significant mechanism of fibre degradation during processing, Yamamoto and Matsuoka (1995) developed a model simulating the dynamic behaviour of a flexible fibre, specifically the bending and twisting motions in a shear flow field which was implemented as well by Bereaux et al. (2008) with a few differences. This was determined by solving a group of translational and rotational equations for individual spheres where a chain of them bonded together would represent a single isolated fibre, located in the later stages of processing where the screw channel is completely filled with melt

With regards to fibre orientation, the Folgar-Tucker model (Folgar and Tucker III 1984) , which is based on the equation developed by Jeffery (1922) describing particle motion in a dilute suspension, has been widely recognised as a method to predict fibre orientation in injection moulded components which however is not applicable to fibre fracture and deformation.

Fibre breakage models on the other hand have been addressed relatively recently, significantly by Phelps et al. (2013) who developed a phenomenological fibre attrition model to predict fibre length distributions specifically within the moulding process which has been adopted by various software simulation companies such as Moldex3D and Moldflow.

Shon et al. (2005) were the first to develop a theoretical model to predict the evolution of average fibre length along different continuous processes such as the co-rotating twin screw, counter-rotating twin screw extruder, and Buss Kneader. Durin et al. (2013) developed a model similar to the one developed by Phelps et al. (2013) where the fibre length distribution was predicted along a twin-screw extruder however both models assume that fibre breakage due to buckling

under hydrodynamic forces that load the fibre in compression is the sole mechanism attributed to fibre attrition.

Based on experimental data and the Euler buckling theory, Bumm et al. (2012) developed an empirical model to describe average fibre length along the screw length of a co-rotating twin screw extruder with reasonable agreement shown between experimental and simulation results. Chen et al. (2015) recently modified this equation for their own model of fibre breakage along the injection moulding process in the form shown below in Equation 2.1:

$$\frac{L(f) - L_{crit}}{L_0 - L_{crit}} = -e^{-K*f}$$

**Equation 2.1**

$L_{crit}$  is taken to be the final average fibre length coming out from the end of the extruder as the critical fibre length can be fairly ambiguous with the presence of fibre bundles and  $L_0$  is initial fibre length.  $K$  is a generalised fibre breakage dynamic constant controlled by multiple factors and  $f$  is the percentage of location along the screw with  $f=0$  at the screw intake and  $f=1$  at the end of the screw.

A single screw extruder was first used to evaluate fibre breakage along the screw before the empirical model was tested on a larger screw within an injection moulding machine. The material used in the investigation was a 13 mm long glass fibre reinforced polypropylene (30 wt. %), provided by SABIC. A predicted final average fibre length value of 5.302 mm at the end of the screw was shown to be fairly similar to the measured experimental value of 4.52 mm taken from the nozzle material of the same injection moulding machine.

## 2.7 Conclusions from Literature Review

It can be concluded in this literature review that as expected, fibre degradation occurs early on in the injection moulding process. From the literature view, it can be ascertained that fibre breakage will chiefly occur during the feeding and compression zones of the screw. Fibre breakage will begin to level out along the compression zone of the screw as the bulk of long fibres will have broken down into smaller fibres.

From this study's literature findings, the contemporary method to examine fibre length degradation along the screw, involves pushing the whole screw out of the barrel from the injection moulding machine. Apparatus to allow for removable sections along the length of screw from the barrel of an injection moulding machine as mentioned in the project objectives does not exist at this time but instead has to be done manually. In all cases for fibre breakage analysis along the screw, the screw was pulled out of its position exposing the polymer to external conditions. This exposure forces the polymer to expand, as before the fibres had the confining geometry of the barrel keeping them from straightening out. However, out of the barrel due to the elasticity of the fibres, they would naturally try to recover to their original straight shape forcing the polymer outwards possibly breaking the fibres further which would affect the results. Also, removing the material from the screw for fibre length analysis may lead to further degradation of the fibres before the investigation has even started. The melt is either peeled off the screw before samples are prepared for evaluation or samples are taken directly off the screw by cutting at specified locations.

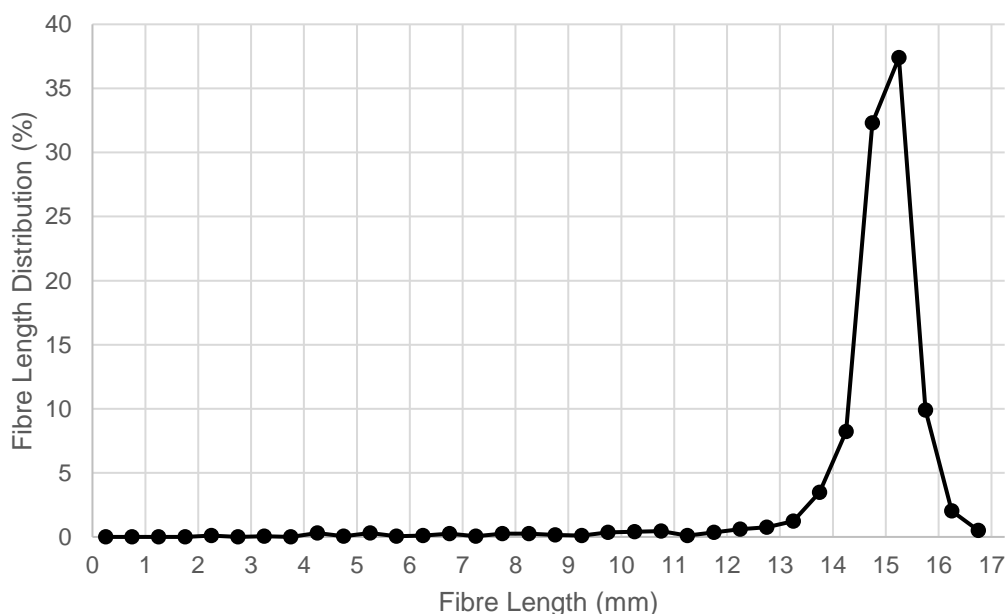
The majority of research regarding the effect of process parameters on fibre breakage along the screw concluded melt temperature, back pressure and screw speed to have the biggest influence on fibre length along the screw, keeping in line with the projects objectives.

Semi-automatic and automatic fibre measurement programs mentioned previously such as FASEP and Image Pro (which are further evaluated in Chapter 4) are relatively expensive and therefore difficult to justify for research work,

especially since they're shown to be relatively inaccurate. Thus an approach to conduct fibre dispersion and measurements manually was considered for this thesis because no suitable automated length measurement software was found to be applicable.

As seen commonly in literature, it was concluded that the injection moulded glass reinforced sample would be placed on an aluminium sheet where removal of the polymer matrix would be conducted in a furnace at high temperature for several hours.

A 20YM240 pellet (15 mm long glass fibre reinforced 20 wt. % polypropylene supplied by Sabic Stamax) sample was also analysed to see if a manual fibre dispersion method caused further attrition to fibre breakage. A fibre length distribution was created for the analysis of the pellet displayed below in Figure 2.14. The preparation and measurement procedure is described in more detail in Chapter 3.



**Figure 2.14. – Image J manual measurement: Pellet sample. (Material: 20YM240).**

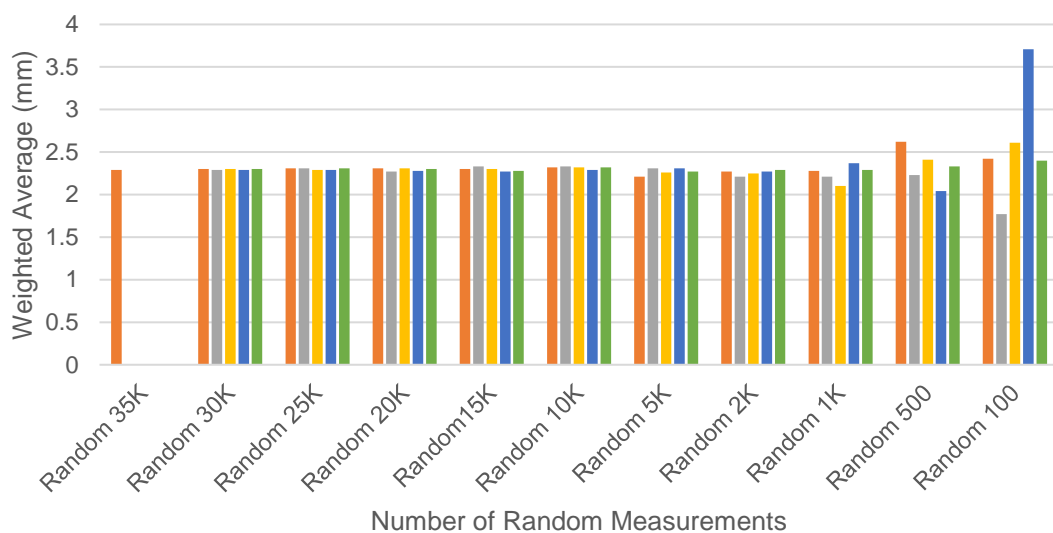
<b>20YM240 Pellet Sample 15 mm LGRPP (20 wt. %)</b>	<b>Image J manual preparation and measurement</b>
Number of Fibres Measured:	2019
Average Fibre Length	14.72
Weighted Average Length	14.87
Maximum Fibre Length Measured	16.91
Minimum Fibre Length Measured	2.02

**Table 2.1. - Summary of results for a 20YM240 pellet**

These results suggest minimal fibre degradation is achieved using the current method for fibre dispersion before manual fibre length measurements are made. From the summary of statistical results in Table 2.1, degradation of fibres during the manual dispersion process could be suggested due to the 2.02 mm minimum fibre length measured. Further to this, 75 fibres were counted to have a length less than 12.25 mm, however the presence of shorter fibres within the pellet could be due to the manufacturing of the pellet itself during the wire coating process and not the dispersion process or a combination. Nevertheless, the manual dispersion method was chosen as a valid option for future analyses.

Certain disadvantages with manual measurements need to be considered particularly the input of human error and interaction. A large variation in manual measurements of the same sample could be attained from researcher to researcher as seen in the literature review and this calls into question comparability, repeatability and accuracy of different long glass fibre measurement reports. There are also differences in fibre dispersion and fibre detection from study to study furthering a demand for an accurate and reliable standardized fibre length measurement technique.

Unlike short glass fibre reinforced materials there is no defined standard method for long glass fibre measurements (ISO: 22314). For an accurate representation of fibre length distribution a large number of fibres per sample must be measured. To assess the change in weighted average due to the number of fibre length measurements, an analysis of a random glass fibre sample was carried out with results showcased in Figure 2.15. A LabVIEW code with a random number generator function was created to select a specific amount of random fibre length measurements (100, 500, 1000, 2000 and so on) from the largest measured population data pool (35,000). These populations were evaluated for weighted average length and repeated to assess variance in sampling variation due to the number of fibres measured. The preparation and measurement procedure of the sample is described in Chapter 3.



**Figure 2.15. - Weighted average comparison of a different number of fibre length measurements**

It is also debatable whether a set of 1000 or fewer fibres can be statistically representative of the local fibre length distribution of the sample even though multiple cases in previous literature do so. From recent studies of long glass fibre length measurements and the results above which showcase minimal variance in the weighted average after 2000 random measurements, a decision was made to measure 2000 fibres manually for each glass fibre reinforced sample.

The breakage of fibres occurs predominantly in the feed and compression zones, such that the residual average fibre length of long-glass-fibres can reduce to 10% of its initial pellet length. Fibre attrition can thus be minimized by decreasing the residence time (shorter screw) and/or screw design, thereby decreasing fibre-fibre and fibre-wall interactions which were found to effect the level of fibre attrition. This will, however, be done at the expense of the quality of the melt to be injected (Patcharaphun and Opaskornkul 2008). Lafranche et al. (2005) suggested that fibre wall interactions due to the rotation of the screw are more significant than fibre melt interactions produced by back pressure.

As mentioned before, fibre attrition is a result of several fibre breakage mechanisms that the fibres are subjected to during processing. Although there is a considerable amount of research available concerning fibre attrition, there is further need for quantitative information on the fibre breakage mechanisms themselves and their impact throughout the injection moulding process. Following on from this, not very much has been done regarding modelling changes in fibre length during processing of glass fibre filled materials. None of the existing models were seen to benefit from the intended results so, in line with the project objectives, a novel phenomenological model is intended to be developed relating the results obtained to screw geometry, process control and fibre dispersion.



### **3. Experimental**

This chapters describes the experimental material, equipment, process conditions, geometries and procedures associated with this investigation. This includes the techniques used to evaluate fibre dispersion and fibre length of various injection mould geometries in order to study the effect of fibre dispersion and length degradation in the injection mould process. The method for the screw pull out test is also described in detail.

#### **3.1. Injection Moulding**

##### **3.1.1. Material**

Long glass fibre reinforced polypropylene was the material used to manufacture the components which are analysed in this study. Long glass fibre reinforced thermoplastics yield strong mechanical performance levels, heat resistance and formability. The selection of such a material would allow a better understanding of the effect of the screw and processing conditions on fibre breakage within the injection moulding process.

The material used in the evaluation of fibre length is a 15 mm long glass fibre reinforced grade homopolymer supplied by Sabic®. Three different grades of long glass fibre reinforced polypropylene were used in this study. The different grades consist of different levels of glass fibre content including 20 wt. % and 40 wt. %, and termed Sabic® Stamax 20YM240, and 40YM240/40YM243 respectively. 40YM243 is a ultra-violet (UV) stabilised grade of the 40YM240 material and bares the same mechanical properties. In this chapter and subsequent chapters, the material in question will be referred to as per their respective grade name (20YM240 or 40YM240/40YM243).

The virgin material is supplied in pellet form where 15 mm long glass fibre reinforced pellets are manufactured by means of a wire coating process. Glass fibres of uniform diameter are wired together to form a continuous multi-fibre glass strand. The glass strand initially passes through a 2% by mass chemical

coating before being passed through a wire coating die which coats the multi-fibre glass strand in molten polypropylene fed by an extruder. The glass fibre strands are coated along the longitudinal direction, and after the passing through a water bath, the strands are cut into the same desired length exposing the glass fibre core at either end. The glass fibres are chemically coupled to the polypropylene matrix via a silane coating, resulting in high stiffness and strength.

### **3.1.2. Injection Moulding Apparatus and Settings**

Samples evaluated in this study were manufactured using a Battenfeld BA750/315 CDK injection moulding machine (Figure 3.1) or an Arburg Allrounder 270C injection moulding Machine (Figure 3.2). Machine specifications for the Battenfeld injection moulding machine which consisted of a 40 mm screw within are found below in Table 3.1.



**Figure 3.1. - Battenfeld BA750/315 CDK injection moulding machine.**

<b>Details</b>	
Manufacturer:	Battenfeld
Type of machine:	BA750/315 CDK
Control Unit:	Unilog 2040
<b>Technical Details</b>	
Clamping Force:	750 kN
Screw Diameter:	40 mm
Length/Diameter Ratio:	20:1
Maximum Injection Speed:	106 mm/s
Maximum Screw Speed:	215 rpm
Back Pressure Range (hydraulic):	0 – 40 bar
Injection Pressure:	1575 bar
Holding Pressure (Specific) :	140 bar
Intensification Factor:	11.25
Mould Temperature Controller:	Regloplas 90S Temperature Control Unit – Maximum Temperature 90°C

**Table 3.1. - Battenfeld BA750/315 CDK machine specifications.**

Samples obtained using the Battenfeld BA750/315 CDK were evaluated using a 3 mm nozzle or 6 mm nozzle for which the process settings were kept constant and are shown below in Table 3.2. Each nozzle was processed using 20YM240 and 40YM240.

Battenfeld BA750/315 CDK machine settings	Sabic® Stamax 20YM240		Sabic® Stamax 40YM240	
	3 mm Nozzle	6 mm Nozzle	3 mm Nozzle	6mm Nozzle
Injection Time (secs)	0.74	0.75	0.74	0.76
Injection Speed (cm <sup>3</sup> /s)	40	40	40	40
Screw Speed (RPM)	49.5	49.5	49.5	49.5
Back Pressure (bar)	3	3	3	3
Packing Pressure (bar)	20	20	20	20
Packing Time (secs)	10	10	10	10
Melt Temperature (°C)	220	220	220	220
Mould Temperature (°C)	20	20	20	20
Cooling Time (secs)	30	30	30	30

**Table 3.2. - Battenfeld BA750/315 CDK injection moulding settings for all nozzle samples.**

The Arburg Allrounder (Figure 3.2) contained a 20 mm injection moulding screw and machine specifications are detailed below in Table 3.3.



**Figure 3.2. - Arburg Allrounder 270C injection moulding machine**

<b>Details</b>	
Manufacturer:	Arburg
Type of machine:	Allrounder 270C
Control Unit:	Selogica
<b>Technical Details</b>	
Clamping Force:	300 kN
Screw Diameter:	20 mm
Length/Diameter Ratio:	25:1
Maximum Injection Speed:	44.8 mm/s
Maximum Screw Speed:	445 rpm
Back Pressure Range:	0 – 18 bar
Injection Pressure:	2500 bar
Holding Pressure (specific):	2500 bar
Intensification Factor:	18.52
Mould Temperature Controller:	Regloplas 90S Temperature Control Unit – Maximum Temperature 90°C.

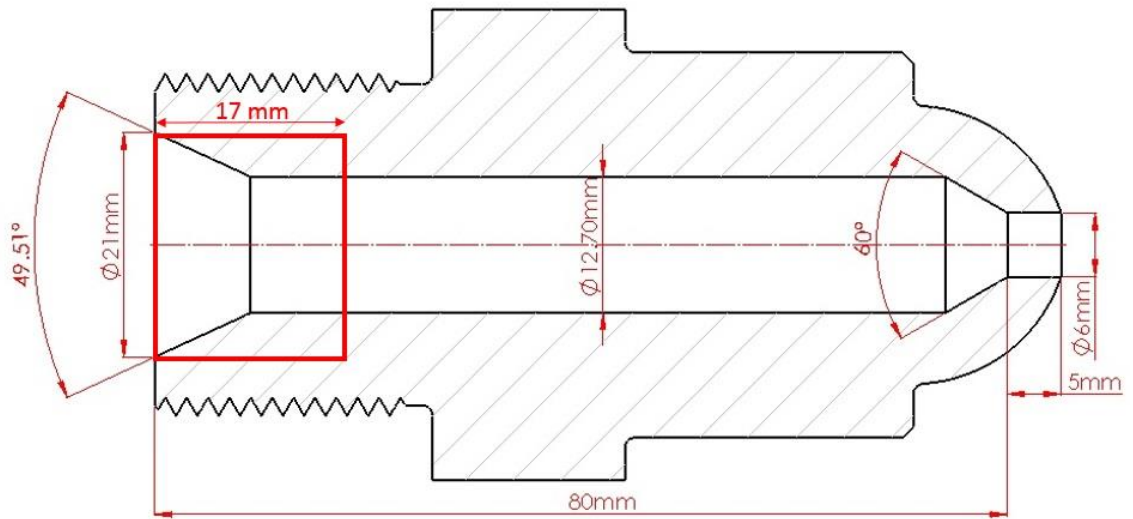
**Table 3.3. - Arburg Allrounder 270C machine specifications.**

Process settings for each screw test can be found below in Table 3.4. Back pressure and screw speed were the two process parameters evaluated. Screw tests 1 - 6 were processed using 20YM240 and screw tests 7 - 9 were processed using 40YM243. Nozzle and injection moulded part samples were taken from their corresponding screw test where possible. The combination of process parameters were determined mainly through literature and recommended settings given by the materials supplier. Being an industrially sponsored project some parameters had to be realistic and were kept in line with the industrial need for quick cycle times (such as the relatively high screw speed).

<b>Arburg Allrounder 270C Machine settings</b>	<b>Test 1</b>	<b>Test 2</b>	<b>Test 3</b>	<b>Test 4</b>	<b>Test 5</b>	<b>Test 6</b>	<b>Test 7</b>	<b>Test 8</b>	<b>Test 9</b>
<b>Injection Time (secs)</b>	0.84	0.72	0.84	1.07	1.07	0.84	0.86	0.71	0.84
<b>Injection Speed (cm<sup>3</sup>/s)</b>	20	20	20	20	20	20	20	20	20
<b>Screw Speed (RPM)</b>	150	150	150	300	300	300	150	150	150
<b>Back Pressure (bar)</b>	2.5	5	7.5	2.5	5	7.5	2.5	5	7.5
<b>Packing Pressure (bar)</b>	27	27	27	27	27	27	27	27	27
<b>Packing Time (secs)</b>	5	5	5	5	5	5	5	5	5
<b>Melt Temperature (°C)</b>	220	220	220	220	220	220	220	220	220
<b>Mould Temperature (°C)</b>	20	20	20	20	20	20	20	20	20
<b>Cooling Time (secs)</b>	30	30	30	30	30	30	30	30	30

**Table 3.4. - Arburg Allrounder 270C injection moulding settings for all screw pull out tests.**





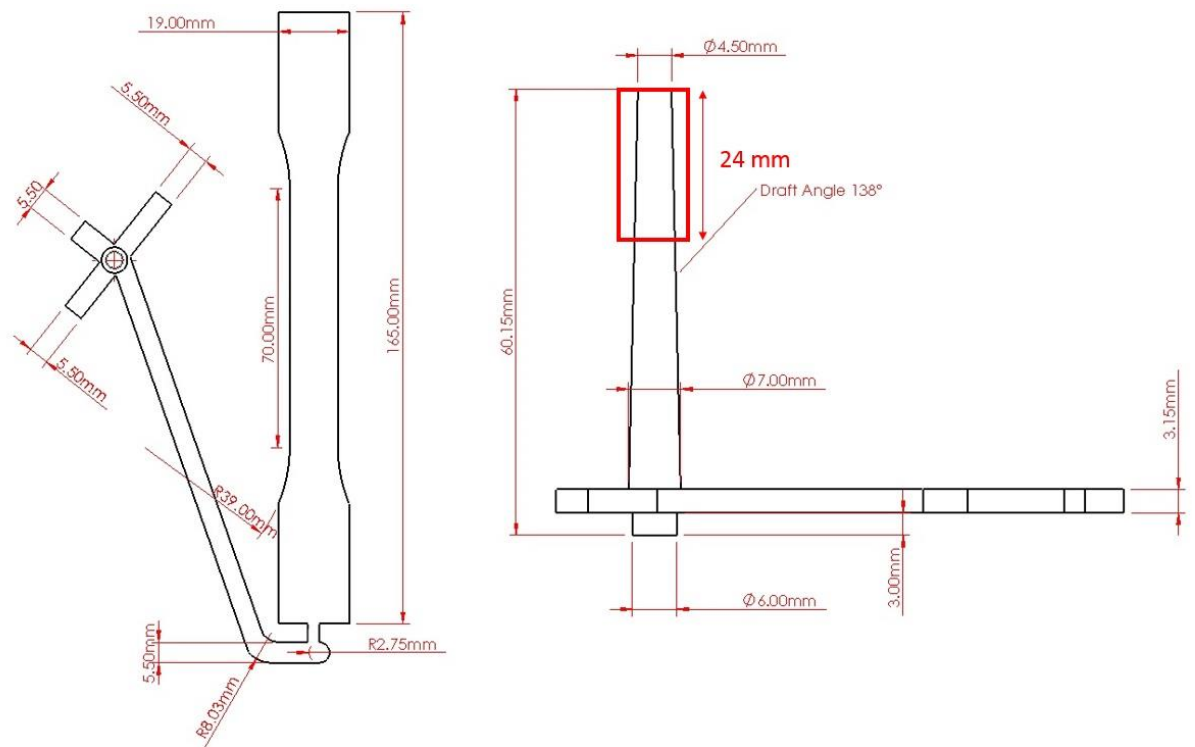
**Figure 3.4 - Technical drawing of 6 mm Battenfeld BA750/315 CDK injection moulding machine nozzle.**

The injection moulding conditions were kept constant for all nozzle samples and can be found in Table 3.2.

### **3.1.4. Injection Moulded Tensile Bar - Arburg Allrounder 270C**

As a result of the screw extraction tests performed on the Arburg Allrounder 270C, injection moulded components were manufactured. A detailed drawing of an injection moulded tensile test bar is shown below in Figure 3.5.





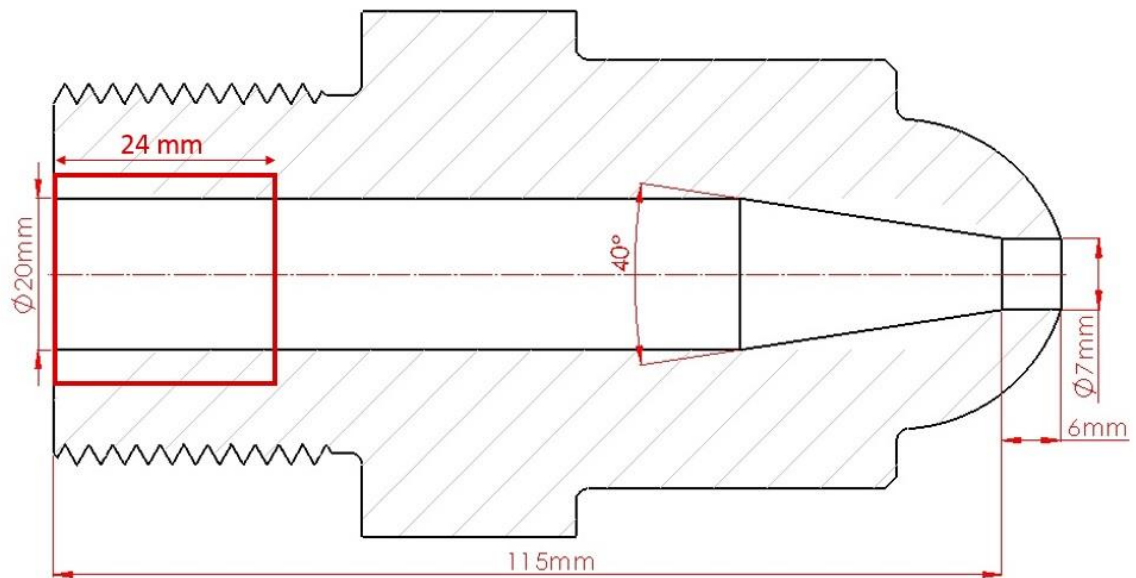
**Figure 3.5. – 2D drawing of injection moulded tensile bar**

The geometry was injection moulded using 20YM240 or 40YM243. For fibre length measurements, a 24 mm cut (highlighted in Figure 3.5) was taken from the top of the sprue (sprue entry) closest to the nozzle and used for further investigation.

### **3.1.5. Nozzle Geometry - Arburg Allrounder 270C**

Nozzle samples from an Arburg Allrounder 270C injection moulding machine were isolated concurrently with the screw extraction tests with various degrees of success for fibre length evaluation.

The geometry of the nozzle sample is shown below in Figure 3.6. For fibre dispersion and length measurements, a 24 mm cut (highlighted in red in Figure 3.6) was taken from the entry of each successfully acquired nozzle (nozzle entry) and used for further investigation.



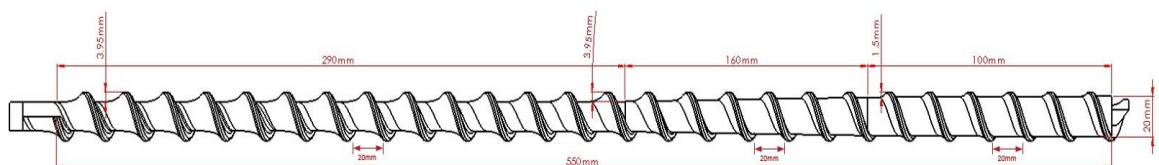
**Figure 3.6. Technical drawing of Arburg Allrounder 270C injection moulding machine nozzle.**

The injection moulding conditions for nozzle samples were the same as their corresponding screw test settings. Details of which can be found in Table 3.4.

### **3.1.6. Screw Geometry - Arburg Allrounder 270C**

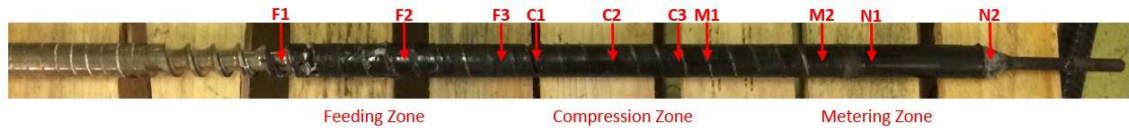
A 20 mm screw from an Arburg Allrounder 270C injection moulding machine was evaluated for fibre length dispersion and attrition along the injection moulding process using the same 20YM240 and 40YM243 grades as mentioned before.

The geometry of the screw is shown below in Figure 3.7. For fibre dispersion and length measurements, a 24 mm cut was taken from specified locations along the channels of the screw.



**Figure 3.7. - 2D Drawing of Arburg Allrounder 270C 20 mm injection moulding screw**

An example of specified sample locations mentioned above extracted for analysis are shown below in Figure 3.8. Process parameters for each screw test are detailed in Table 3.4.



**Figure 3.8. - Example of sample locations along Arburg Allrounder 270C injection moulding machine 20 mm screw**

## 3.2. Fibre Dispersion

### 3.2.1. $\mu$ -CT of Long Glass Fibre Filled Samples

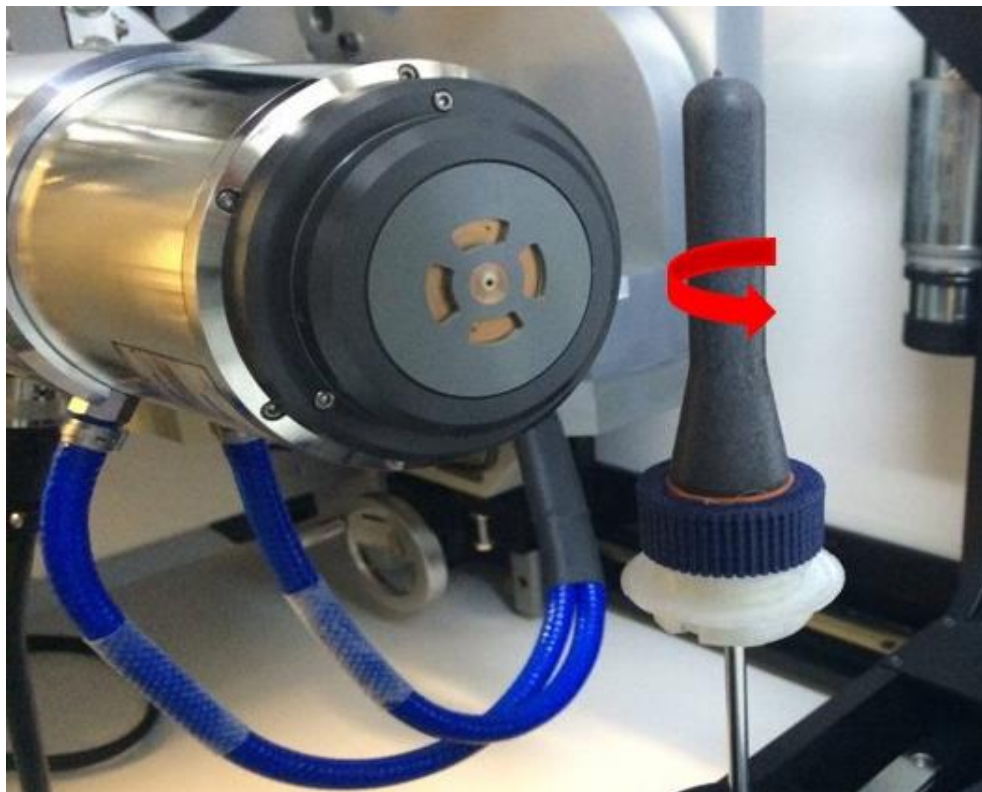
Fibre dispersion measurements can be obtained through the use of X-Ray imaging on a Micro-Computerised Tomography scanner. The scanner used to acquire such results in this study is a XT H 225 ST Industrial CT scanner manufactured by Nikon (Figure 3.9). This system enables high accuracy with a focal spot size of 3  $\mu\text{m}$  plus the ability to verify complex internal structures and detect and measure internal volumes simultaneously in a non-destructive way.



**Figure 3.9. - XT H 225 ST Industrial CT scanner.**

The system operates by emitting x-rays from a source, which travel through the sample and are recorded on a planar x-ray detector which collects the magnified projected images. The specimen is rotated in the X-ray beam capturing several thousands of projections for each sample enabling a 3D representation of the internal structure as presented in Figure 3.10. The resolution can be adjusted to attain more detailed images by increasing the number of projections and positioning the sample closer to the X-Ray source. However at very high magnifications, the resolution is limited by the focal spot size which is the size of the region of the target onto which the X-ray beam can be focused.

Fibre dispersion was measured within a 3 mm nozzle and 6 mm nozzle injection moulded sample taken from a Battenfeld BA750/315 CDK injection moulding machine. The details of which are described previously in Chapter 3.1.3. Fibre dispersion was also evaluated for successfully obtained nozzle and screw samples obtained from an Arburg Allrounder 270C injection moulding machine. Details of which can be found in Chapters 3.1.5 and 3.1.6.



**Figure 3.10. - Example of an injection moulded sample positioned in micro-CT scanner.**

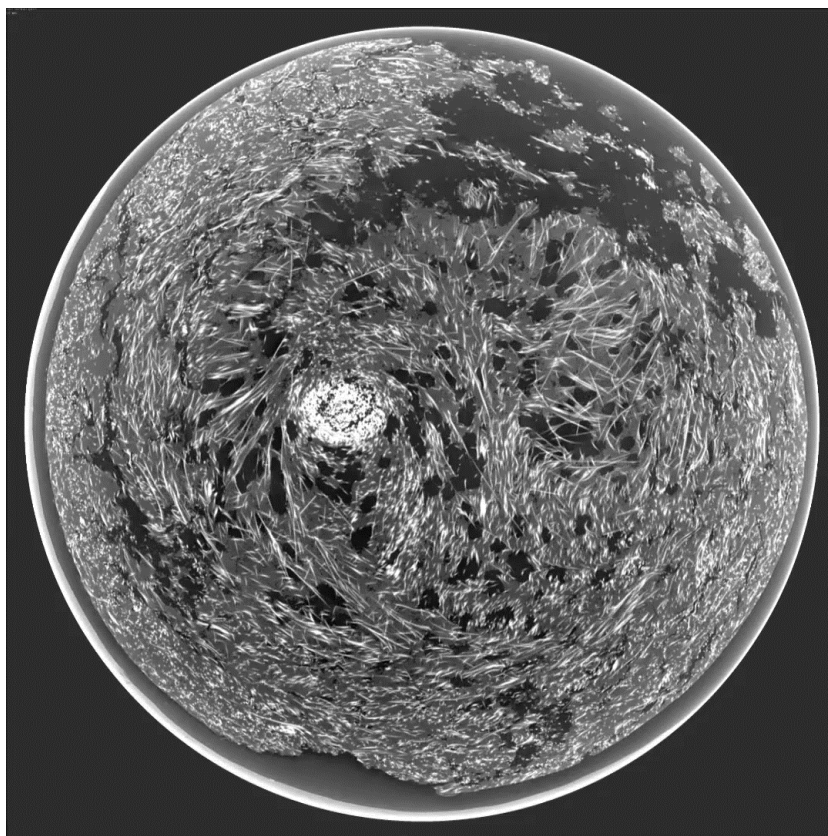
Each sample is positioned and secured on a rig which is locked firmly in place. To obtain a more detailed representation of the nozzles internal structure, the top (nozzle exit) and bottom (nozzle entry) sections of each nozzle are scanned. This applies for nozzles extracted from a Battenfeld BA750/315 CDK and Arburg Allrounder 270C injection moulding machine.

For nozzle samples, they are initially positioned in such a way that the nozzle exit is shown on an external monitor whilst keeping the sides of the sample within view. A shading correction is used to remove any artefacts caused by varying responses between pixels. The number of desired projections is entered, in this case 6000 projections are made within a 360° rotation and the scan is commenced. The same is done for the nozzle entry of each nozzle. For screw samples taken from an Arburg Allrounder 270C injection moulding machine, the specimen was positioned in such a way that it was wholly captured within the micro-CT's field of view before a shading correction is made and the number of projections entered.

Once each scan is completed, a reconstruction of all projected images is made to create a 3D representation in Volume Graphics software. Slices can be exported from the different screw and nozzle sections from the top, side, and bottom section views as shown below in Figure 3.11. The aim of this work is to relate fibre dispersion within the nozzle with fibre degradation. By examining the flow of the fibres we can eventually evaluate the effect of the screw and different nozzle geometries and see what characteristics can be most advantageous to retaining fibre length.

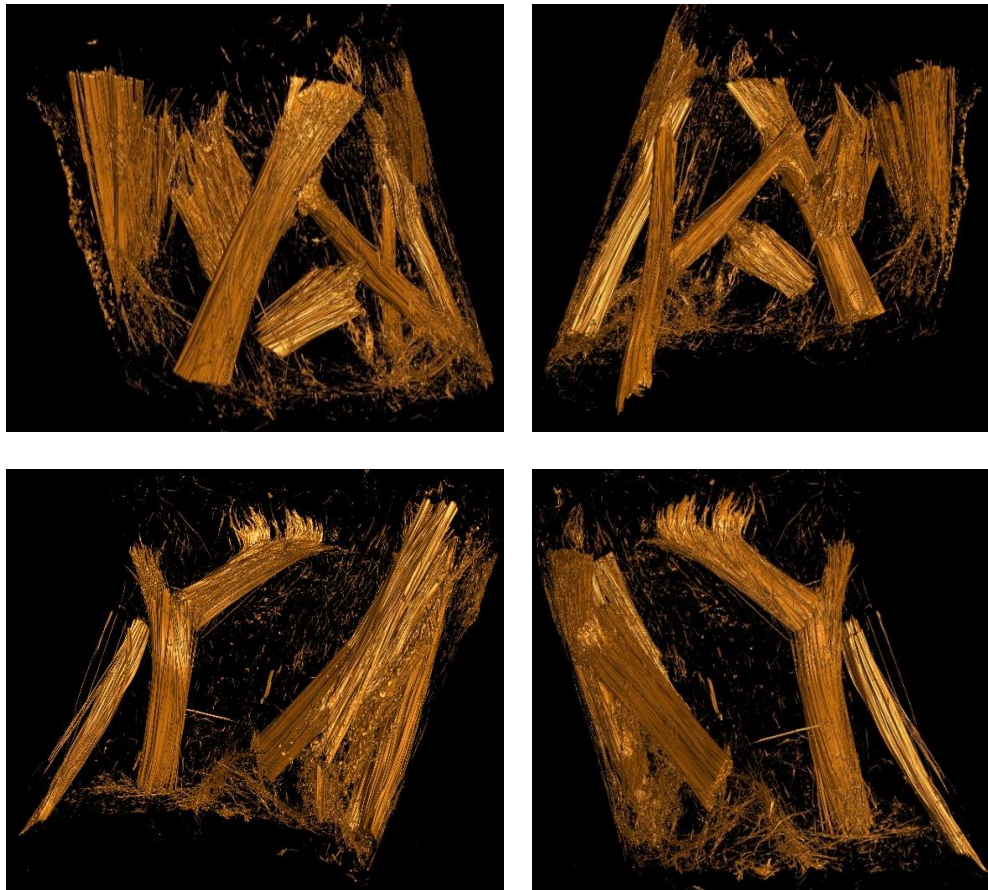
Nozzle sample scans generated in this study from  $\mu$ -CT had an isotropic voxel size of 10 microns, whilst all screw sample scans had a size of 11 microns.





**Figure 3.11. - Example of an image slice from the entry of a 3D reconstructed 3 mm nozzle manufactured using a Battenfeld BA750/315 CDK injection moulding machine.**

Ideally,  $\mu$ -CT would also be used to also analyse fibre length distributions within the sample of which Chapter 4.8 goes into more detail. An example of a screw sample which has been scanned using the XT H 225  $\mu$ -CT machine is shown below in Figure 3.12 with 4 different projected views of the sample. Clearly a complex glass fibre structure exists within the sample and  $\mu$ -CT would not only struggle in identifying and isolating individual long, short or curved fibres but also in recognising separate fibres in a cluster, of which there are many. No software to date has been found that can compute accurately and reliably fibre length distributions within a long glass fibre reinforced polymer sample.



**Figure 3.12. – Example of a long glass fibre reinforced screw sample scanned using the XT H 225  $\mu$ -CT machine.**

### **3.3. Fibre Length Measurement**

#### **3.3.1. Matrix Removal**

In order to obtain fibre length measurements, glass fibres have to be separated from the polymer matrix they were encased in. The section of interest from the manufactured component, specifically the nozzle or sprue, is removed with the use of a mini hack saw whilst the sample is secured in a vice.

The cut sample is then placed onto an aluminium sheet relative to the samples size which subsequently is positioned in a miniature ceramic bowl as shown below in Figure 3.13 similar to Rohde et al. (2011), Inceoglu et al. (2011) and Giusti et al. (2015), This allows for the expansion of glass fibres due to the stored elastic energy in bent fibres.



**Figure 3.13. - Example of isolated sample placed in ceramic dish (left) and furnace (right).**

The specimen is then left in a furnace (Figure 3.13) at 500°C for 4 hours enabling the complete removal of the polymer matrix, leaving behind an entangled mass of short and long fibres which are ready to be scanned.

### **3.3.2. Dispersion of Long Glass Fibres**

To obtain appropriate and quality fibre images for processing, the fibres must first be dispersed onto a number of thin transparent films. The transparent thin films measure 215 x 266 mm and have a thickness of 0.05 mm.

From the resultant burn off, great care needs to be taken whilst transferring the fibres onto the thin film, especially the long fibres which are susceptible to further breakage which may hamper the fibre length results. Ideally, physical interaction with the fibres needs to be avoided or at the very least kept to a minimum. Therefore, small portions or clumps of the glass fibres were gently transferred onto the film and dispersed using a miniature hand held suction pump which uses air to gradually scatter the fibres. However, long curved fibres which have become intertwined with one another and were usually found within the core of the burnt off sample can be very difficult to separate from each other. In this case, physical interaction must be applied and kept to a minimum to split up these curved fibres. Therefore, under a magnifying glass, a thin bristle from a brush is used to gently force separation between the fibres. Fibres should be spread out amply, preferably with minimal fibre cross overs across a number of thin



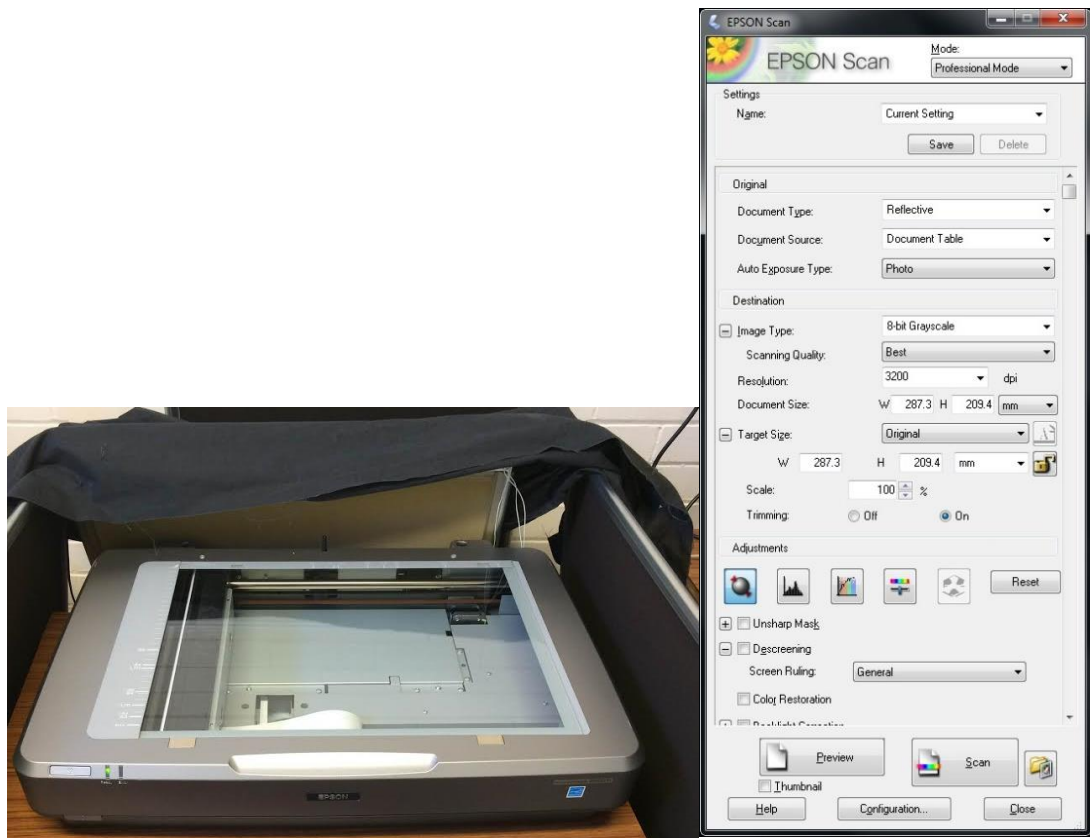
transparent films to ensure easier processing of fibre lengths later in the process. All fibres from the subsequent burn off were dispersed onto thin films for each sample in this investigation.

### **3.3.3. Capturing of Long Glass Fibres**

After correct dispersion of the long glass fibres, the fibres are scanned at a high resolution using an A3 Epson Expression 10000XL Pro scanner.

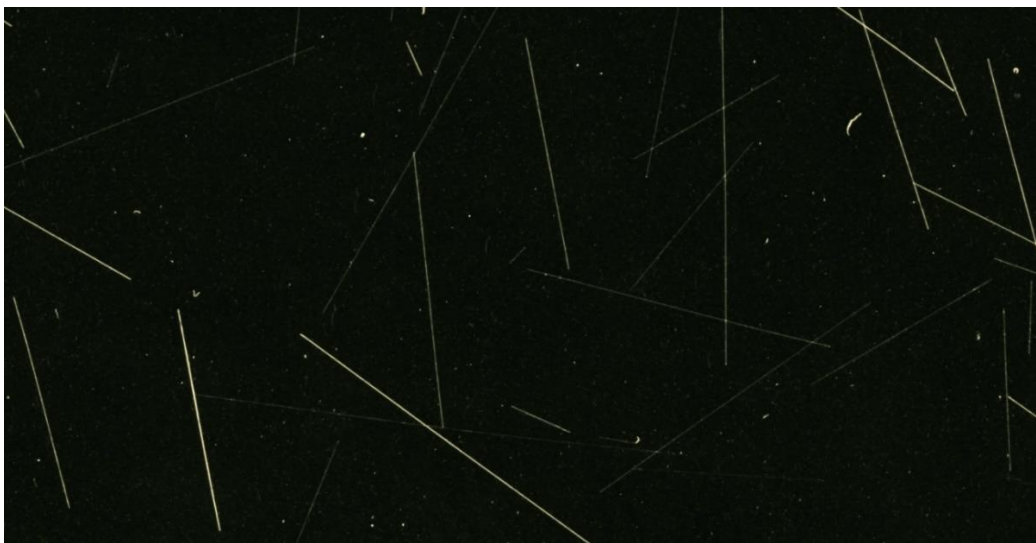
The glass surface of the scanner table must be made clean first (with the use of a screen cleaner) and free of any dust or marks to ensure no discrepancies are found in the scanned images and possibly be interpreted as glass fibres.

The scanner captures high resolution images of fibres with a maximum optical resolution of 9600 dpi. The scanner cover is removed and replaced with a 0.2 mm thick black fabric propped up with four make shift walls which encircle the scanner (Figure 3.14). This allows for a clear contrast between the glass fibres and the thin film due to the glass fibres being transparent and therefore difficult to capture with the original white cover on. Any external light source must be switched off and the room must be kept dark whilst the scan is in progress.



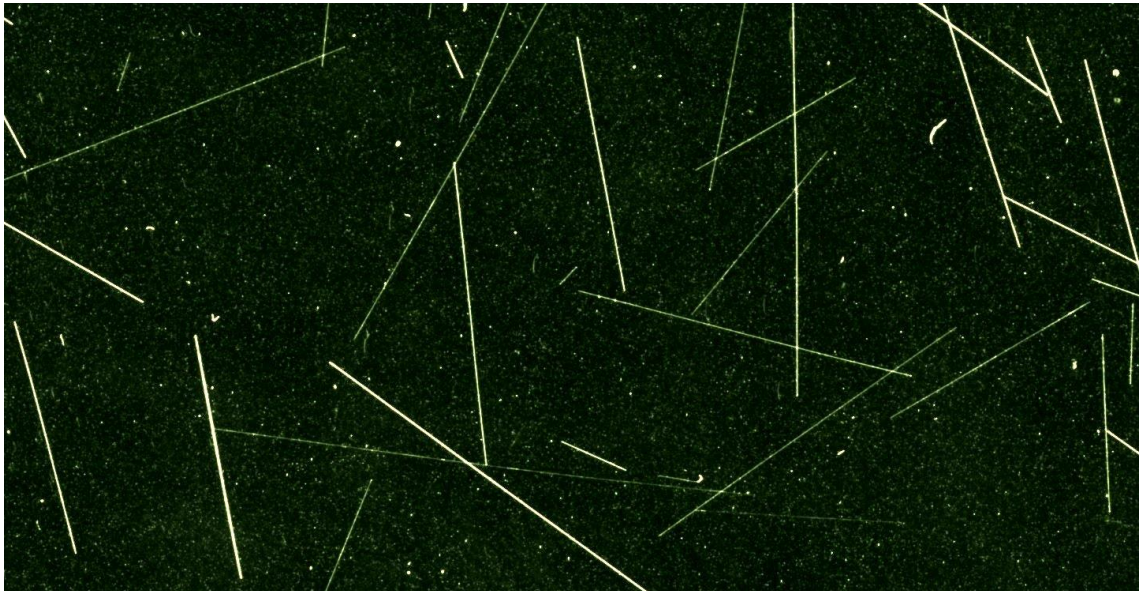
**Figure 3.14. - A3 Epson Expression 10000XL Pro Scanner (left), Settings used to scan glass fibres (right).**

The settings used to scan each thin film are shown above in Figure 3.14 resulting in an 8-bit grey-scale, 3200 dpi resolution image. An example of a scanned image is shown below in Figure 3.15.



**Figure 3.15. - Example of scanned fibre length image.**

The images can now be processed using the ImageJ software by means of manual measurement. Before this, the contrast of the image is enhanced on Image J as shown in Figure 3.16, increasing the brightness of the scanned glass fibres and revealing any fibres that might not have been identified in the original non-enhanced scanned image.



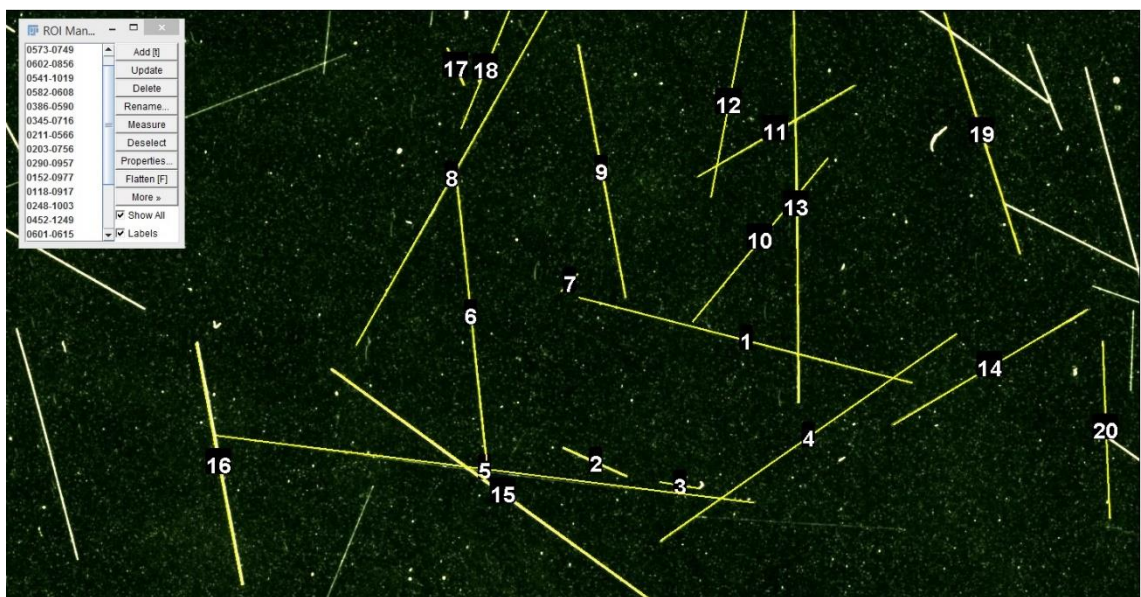
**Figure 3.16. - Example of improved scanned fibre length image.**

### **3.3.4. Measurement of Long Glass Fibres**

First, the scanned image file must be opened up onto ImageJ and a scale is set according to the resolution of the image. A calibration ruler was used to calculate the distance of 1 pixel in millimetres by overlaying the scanned length using a straight line selection tool and entering the known distance. This must be done otherwise the measured lengths of the fibres would be in pixels and not millimetres. In all cases, the scale used was 126.46 pixels/mm.

Typically, 10 films (+/- 1) are used to evenly disperse all fibres for each sample. 2000 is divided by the number of films used to scan each sample, and that amount of fibres is subsequently measured for each image; usually 200. Straight-Line and Segmented-Line tool features from ImageJ allow for manual measurement of short, long and curved fibres.

The 200 fibres are randomly measured from various selected areas. The areas chosen by the user are selected by zooming out completely from the image file and zooming into an area chosen by user. The area would be magnified to such a degree that a small dispersion of long glass fibres can be viewed. Around 20 fibres are then randomly measured. If a selected fibre lies outside the field of view, the image is simply moved using the hand tool, enabling complete measurement of the fibre before being returned to its original position. An example of a captured area of measured fibres using the Straight-Line tool is shown below in Figure 3.17.



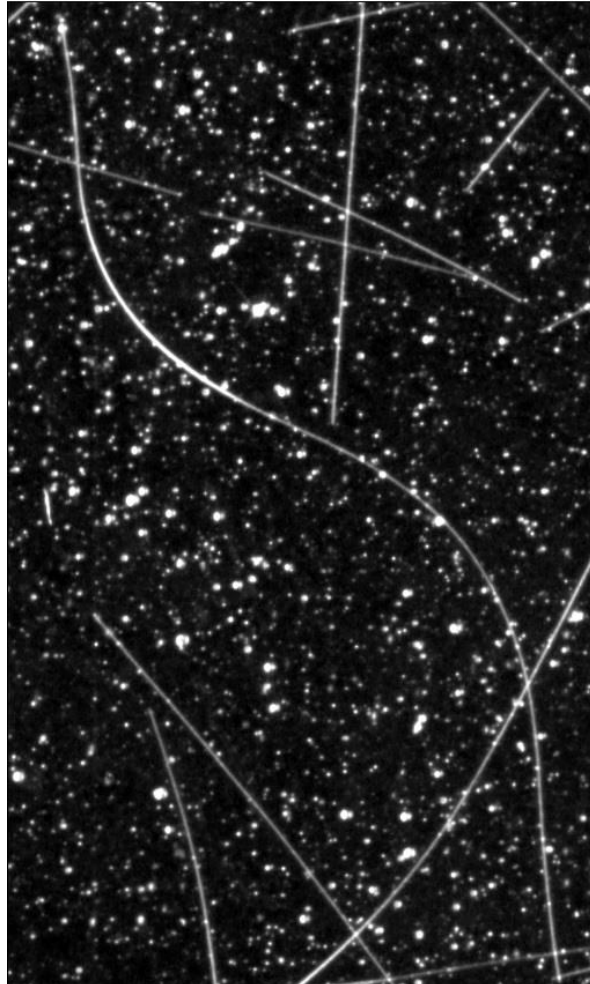
**Figure 3.17. - Example of a random area of measured fibres.**

The selected region of interests (measured fibres) are recorded in a ROI (region of interest) manager tool box displayed in the top left of Figure 3.17. “Show All” and “Label” boxes are ticked aiding the user in recording the correct number of fibres and ensuring no fibres are repeatedly measured.

This is repeated 10 times until 200 fibres are recorded. For samples with higher glass fibre content (40 wt. %), 15 films (+/- 1) were used in the dispersion of fibres and roughly 133 fibres were measured on each image with groups of approximately 13 fibres being measured for each zoomed in location.

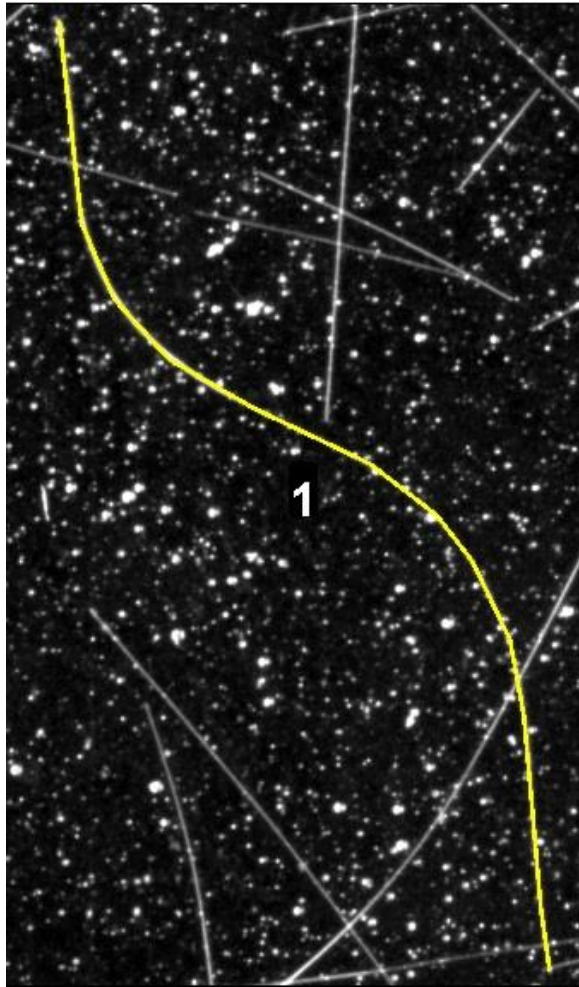


In the manual measurement of glass fibres, a curved fibre, such as the one shown in Figure 3.18 may be present which cannot be measured using the straight-line tool.



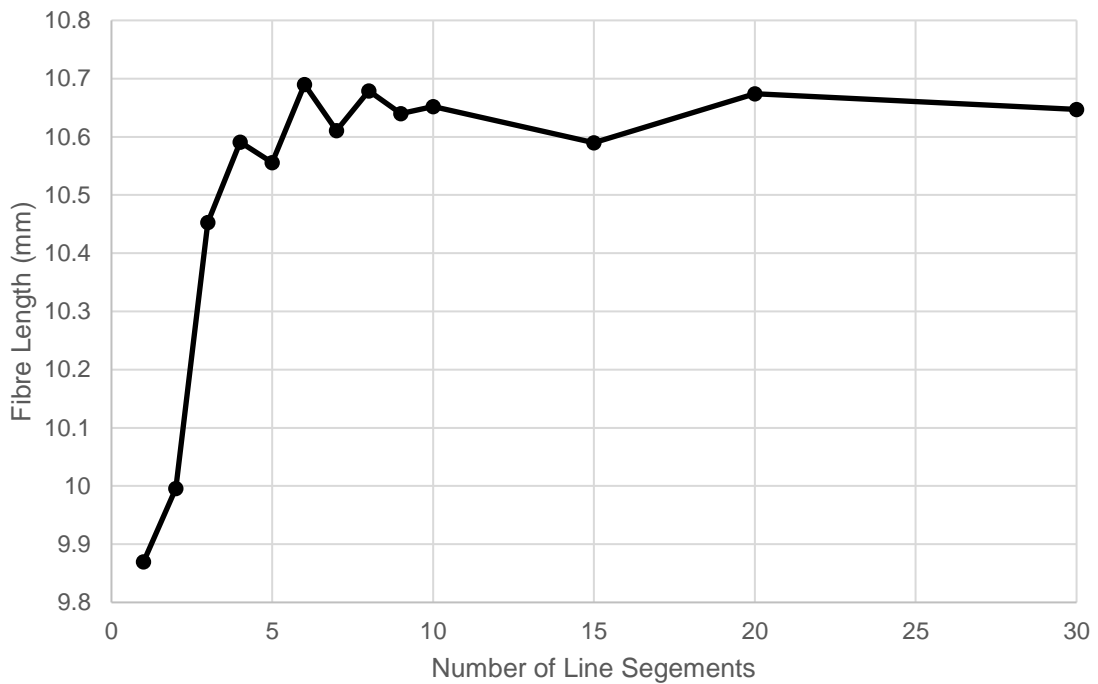
**Figure 3.18. – Example of a curved fibre.**

Instead the segmented-line tool is used which enables the user to overlay a curved fibre with multiple straight line segments leading to an accurate measurement of the fibre as seen in Figure 3.19.



**Figure 3.19. – Example of a measured curved fibre.**

Since the process of measuring a curved fibre involves superimposing a number of smaller straighter lines, a degree of error can arise from the number of straight line segments used, as showcased in Figure 3.20. Manually measuring the same glass fibre with 5 line segments as opposed to 30 can lead to a difference of 0.091 mm in the resulting computed length for that fibre.



**Figure 3.20. – Comparison of measurements using a different number of straight line segments.**

As expected, the results shown in Figure 3.20 indicate the greater number of straight line segments used in the measurement of a curved fibre, the greater the degree of accuracy in representing the true value of its length. Naturally, the number of segments applied to a curved fibre depend on the curvature and the fibre itself. To minimize the amount of error, a minimum of 6 line segments were utilized using the segmented-line tool feature in Image J to measure all curved fibres. More line segments were used if necessary.

### 3.3.5. Analysis of Data

From the obtained record of measurements, the data can be exported into Microsoft Excel and manipulated for statistical analysis which can be represented as a fibre length distributional plot. The output data is presented as minimum fibre length, maximum fibre length, number of recorded measurements, number average fibre length ( $L_n$ ) and weighted average fibre length ( $L_w$ ). The equations for ( $L_n$ ) and ( $L_w$ ) are shown below where  $L_i$  is the actual measured length of the fibre and  $n$  is the number of fibre length measurements.

$$L_n = \frac{\sum L_i}{n}$$

**Equation 3.1.**

$$L_w = \frac{\sum L_i^2}{L_i}$$

**Equation 3.2.**

The number average (Equation 3.1) is simply the sum of all the individually measured fibre lengths divided by the total number of measurements. However, this result can be interpreted as a poor statistical representation since longer fibres exhibit a disproportionately greater influence on mechanical properties. To attain a more real interpretation of results, as to give more emphasis on the longer fibres which carry a greater influence than shorter fibres, a weighting factor is established. It is statistically impossible to ascertain the weight of each individual fibre, so a mathematical derivation of the weighted average length is only based on fibre length, where fibres were assumed to have a constant diameter (Equation 3.2). The discrepancy in results between ( $L_n$ ) and ( $L_w$ ) is presented below in Table 3.5 and Equations 3.3 and 3.4. The results are a sample of the ones obtained from this study.

A full analysis for fibre length dispersion and distribution of one glass fibre filled sample following the methods described in this Chapter can be considered very time consuming. A full  $\mu$ -CT scan will take up to 6 hours with reconstruction of the projected images and post processing taking up the same amount of time. Following on, removal of the polymer matrix requires several hours in a muffle furnace with full dispersion of a glass fibre filled sample taking up to a day. Measurement of 2000 fibres is relatively laborious and subsequent processing of results also involves a number of hours to achieve accurate and coherent results.



Number	Length (mm)
1	1.128
2	0.77
3	1.395
4	2.582
5	1.234
6	2.218
7	2.674
8	1.461
9	0.155
10	0.775

**Table 3.5. - Example of a fibre length data sample.**

$$L_n = \frac{1.128 + 0.77 + 1.395 + 2.582 + 1.234 + 2.218 + 2.674 + 1.461 + 0.155 + 0.775}{10}$$

$$= 1.4392 \text{ mm}$$

**Equation 3.3.**

$$L_w = \frac{1.128^2 + 0.77^2 + 1.395^2 + 2.582^2 + 1.234^2 + 2.218^2 + 2.674^2 + 1.461^2 + 0.155^2 + 0.775^2}{1.128 + 0.77 + 1.395 + 2.582 + 1.234 + 2.218 + 2.674 + 1.461 + 0.155 + 0.775}$$

$$= 1.8642 \text{ mm}$$

**Equation 3.4.**

### **3.4. Sample Extraction**

#### **3.4.1. Nozzle – Battenfeld BA750/315 CDK**

Nozzle samples were obtained by halting the injection moulding process once 10 parts were manufactured. Once the screw had moved back to its original position, cooling of the mould had begun and with the injection unit left in its most forward position so as to prevent any leakage out the nozzle during cooling, the machine was turned off and left to cool overnight. Afterwards the injection moulding machine was heated up to 100°C apart from the nozzle heater band which was

switched off, too allow for successful extraction of the sample. The nozzle would then be gently unscrewed revealing a glass fibre reinforced polypropylene nozzle sample. If the nozzle was unscrewed with the nozzle sample still fixed inside, the nozzle would have to be left in a furnace at a high temperature for a number of hours to burn off the polymer matrix. Using a sand blaster, the nozzle would be cleaned and screwed back on and the test repeated. High temperature silicone lubricant was used beforehand and sprayed inside the nozzle to aid with removal and prevent the polymer from sticking inside. Multi-purpose copper grease was applied along the thread of the nozzle to help with the screwing and unscrewing of the nozzle.

### **3.4.2. Nozzle and Screw – Arburg Allrounder 270C**

Screw extraction tests took place at an external facility at KU Leuven Technology Campus in Ostend, Belgium. Due to the significance of the test regarding this investigation, the procedure is described in detail below.

- Screw samples were collected by stopping the injection moulding process on the Arburg Allrounder 270C injection moulding machine after 10 parts were produced and the process was stable. Once the screw had been pushed back, and cooling begun, the injection unit was left in its forward position before the machine was switched off and left to cool overnight.
- Once the injection moulding machine had cooled, the injection unit was moved to its most backward position. Zone 3 (screw heater band located closest to the screw) and the nozzle were heated to 70°C to allow for easier untightening of the nozzle. The nozzle heater band was then removed along with the bolts securing the injection moulding machine to the mould (Figure 3.21 (a) and (b)).
- The safety switch (Figure 3.21 (c)) was then disconnected from the nozzle safety guard and reconnected to override any errors that may arise later in the screw extraction process when the screw is pushed out.

- The whole injection unit was then carefully pulled back away from the mould (Figure 3.21 (d)). The corresponding heat sensor for the nozzle was then removed and the nozzle was gently unscrewed with a wrench (Figure 3.21 (e)). Ideally, a glass fibre polypropylene nozzle sample would be isolated which would then be detached. Again, silicon grease was sprayed inside a clean nozzle beforehand to help prevent the polymer from sticking inside and copper grease applied along the thread of the nozzle to facilitate screwing and unscrewing of the nozzle.
- Any excess virgin material was removed from the hopper so as not to interfere during the push out of the screw. The heating zones along the barrel are then set to 160°C. This was found to be the ideal temperature for the screw pull out test.
- Once the barrel has been reheated to the desired temperature level the safety guard on the back of the injection moulding machine is removed exposing the motor (Figure 3.21 (f)). The screw was then 'unclipped' from its electric motor drive (Figure 3.21 (g)) and was then pushed forward before the drive was brought back to its original position without pulling the screw back.
- This allows space for the placement of steel rods which can be positioned behind the screw (Figure 3.21 (h)) and pushed into the barrel one at a time carefully, leading to the slow push out of the screw.
- Once the screw has been pushed out sufficiently as pictured in Figure 3.21 (i), it can be simply removed from the barrel by hand.
- The screw was then placed in a large Venticell drying oven (Figure 3.21 (j)) at an optimum temperature of 170°C as shown in Figure 3.21 (k) for a short period of time to allow for successful sample removal.

- The screw was then positioned on a wooden palate with predetermined measurements marking out the different zones along the screw. Sample extraction was then carried out along the screw by first taking a 24 mm specimen, measured along the helical direction of the screw, from the first available section of material in the feeding zone. This sample was named F1. Subsequent 24 mm samples are then isolated, cut off and put into sample bags until the next selected sample location to be evaluated for fibre length analysis is reached (F2). Samples between each marked location are recorded and placed in sample bags too. F2 marks the mid-point of the screws feeding zone apart from one screw test which consisted of a shorter feeding zone where F2 was taken to be the location of the first available section of material to be removed. F3 indicates the end of the feeding zone and samples taken from C1 are the beginning of the screws compression zone. Sample C2 is the mid-point of the compression zone with C3 being the end of the compression zone. Samples M1 and M2 are each taken from the beginning and end of the screws metering zone, respectively. An example of sample locations is shown in Figure 3.8.
- Once all samples have been documented the screw was cleaned using a blow torch and a brass brush. The screw was then returned to the injection moulding machine which was set up as it was originally ready for the next screw pull out test.
- Due to the time consuming nature of the screw extraction and the fact this investigation is centred on the screw itself, if a nozzle sample was not successfully removed (shown in Figure 3.21 (I)) there was no opportunity to repeat the test.
- A range of temperatures were tested for optimum screw pull out before 160°C was found to be the most effective. Any less and the screw could not be pushed out, anymore and the polymer matrix would begin to melt exposing glass fibres on the outer surface of the polypropylene which would then be trapped back along the screw as it was pushed out, possibly

leading to further unnecessary fibre attrition as showcased in Figure 3.21 (m).

- Different temperatures were also examined when the screw was placed in the drying oven before sample removal. A temperature of 170°C was chosen because this allowed the material to be peeled off relatively easily off the screw without it being too hot for it to stick to the screws surface or too cold, consequently leading to difficult extraction of screw samples.
- As the screw cooled down, the samples would become increasingly difficult to isolate, thus the screw was returned to the drying oven for a minimal amount of time before being returned for the continuation of sample removal.
- Screw pull out tests were originally intended to be performed on an Arburg Allrounder 320S Injection moulding machine with a 25 mm screw. However, upon screw extraction, the glass fibre reinforced material appeared to not be feeding correctly as the screw was not filled along the compression and feed zones. However, the screw was filled with material in mixing zone. This is depicted in Figure 3.21 (n).
- Numerous tests were carried out to find a solution but action was taken due to the limited time available, to concentrate and complete as many screw tests on the 20 mm screw for the duration of the research placement.
- It was originally intended for more screw tests to be performed to evaluate the scatter of results for each test, however due to the availability of the machine being off-site (Belgium), time constraints at the location as well as the time required for each measurement analysis, repeat tests were not performed.

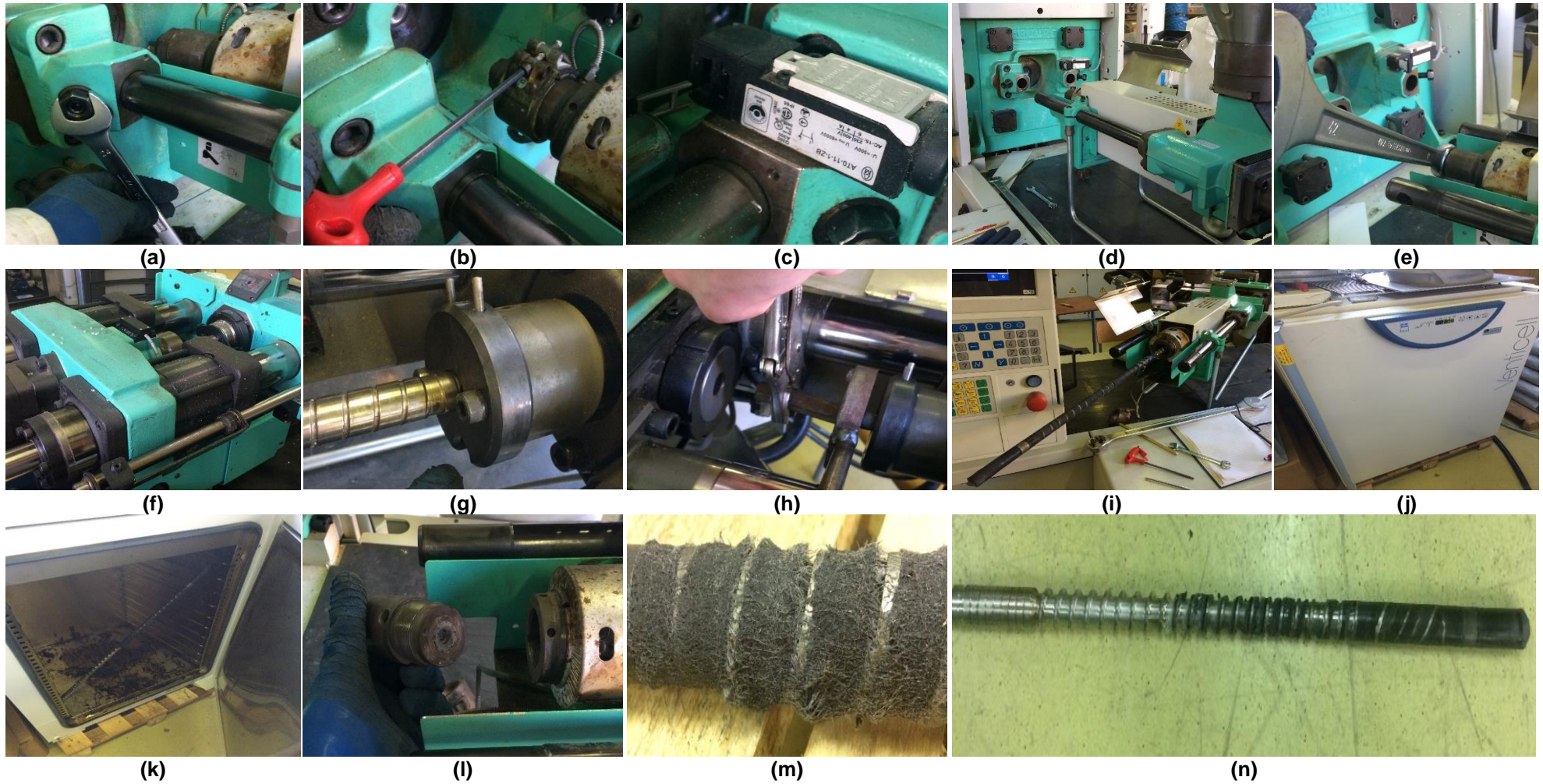


Figure 3.21. – Images showcasing various stages of the screw pull out method.

#### **4. Fibre Length Measurement – Evaluation of methods**

Due to the disadvantages of the current fibre dispersion, detection and measurement technique used in this thesis, a review of commercially available fibre length measurement systems was carried out and tested against the current system which is described in Chapter 3.3.

The main problem with automated fibre length measurement software is that it struggles in dealing with long, curved and intersecting fibres on a scanned image. The study utilised a manual fibre length measurement system via Image J. The process is not ideal, as pointed out in Chapter 2.7 with it being very time consuming, laborious and susceptible to human error and variation.

Thus, scanned image files taken using an A3 Epson Expression 10000XL Pro scanner of various samples were sent out to different companies and fibre length measurement results were compared. For each scanned image every single fibre was measured manually before being sent out. The data could then be directly compared to the automated system which would measure all the fibres automatically on the image.

Commercially available software's tested and utilised in various literature findings include: Image Pro Premier, Fibre Shape, FASEP, CT-FIRE and Clemex.

Chapters 4.2, 4.3, 4.4 and 4.6 evaluate the same scanned image of fibres which were isolated directly from an injection moulding screw sample before processing. This sample was taken from screw test 4 and identified as sample F3. The first scanned image (image 1001) obtained during the capture of glass fibres (as described in Chapter 3.3.3) for this particular sample was used for evaluation.

Chapter 4.1 assesses a different scanned image of fibres, taken from an injection moulded part which was acquired during the initial stages of this PhD in

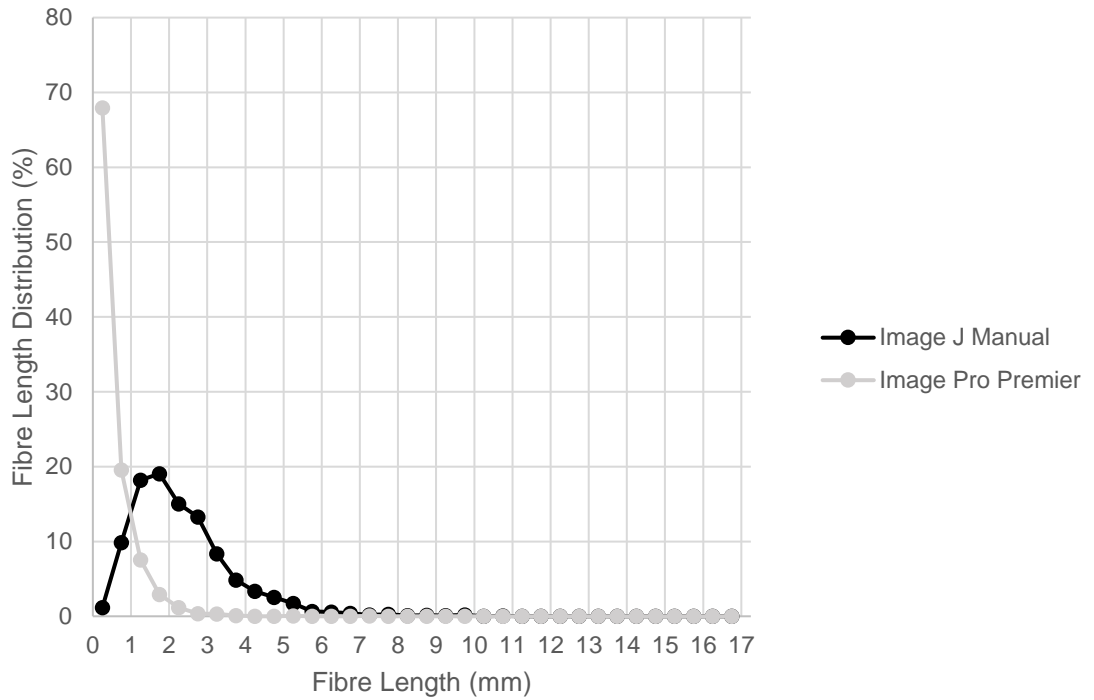
conjunction with Ticona as an industrial case study. An evaluation of Image Pro Premier software was carried out before any screw tests had been performed. The software was considered imprecise, as explained in further detail in Chapter 4.1, when measuring fibres taken from further along the injection moulding process. Samples taken from earlier stages in the injection moulding process have been subject to less fibre degradation and would exhibit longer and more curved fibres. Thus the decision was made to not repeat the evaluation of Image Pro Premier with the same scanned fibre image used in subsequent chapters as it had previously struggled measuring shorter glass fibres.

In Chapter 4.5, two consecutive 24 mm cuts were taken from the feeding zone section of a 20 mm injection moulding screw (screw test 6) and labelled as Samples F1 and F1b. Sample F1 was assessed using the manual fibre length measurement procedure as explained in Chapter 3.3, as well as one 20YM240 glass fibre reinforced polypropylene virgin pellet. Sample F1b, along with another 20YM240 reinforced polypropylene virgin pellet was sent to an external company so a direct comparison between the two fibre length measurement systems could be made.

#### **4.1. Image Pro Premier**

A 20 x 20 mm cut from the centre of the left plate of an injection moulded fan gated plate supplied by Ticona was burnt off in a furnace. The material used was a 15 mm long glass fibre filled (20 wt. %) polypropylene. Glass fibres were evenly dispersed across a number of films. The second scanned film image file was chosen for comparison between manual measurements as previously described in this study and sent to Image Pro Premier for automated measurements. A comparison of fibre length distribution results is shown below in Figure 4.1.





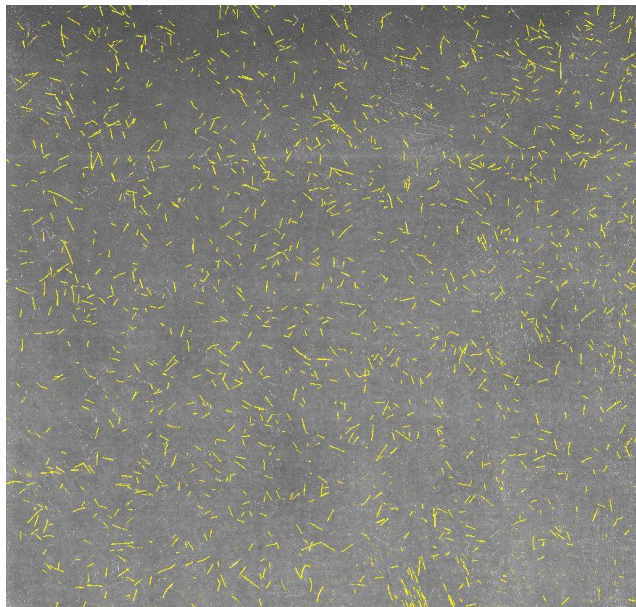
**Figure 4.1. - Image J manual measurement vs Image Pro Premier automated measurement - Ticona sample. Material: 20 wt. %. 15 mm LGFRPP (Scanned image 1002).**

<b>Ticona Sample. 15 mm LGFRPP (20 wt. %) Image 1002</b>	<b>Image J Manual Measurement</b>	<b>Image Pro Premier Automated Measurement</b>
Number of Fibres Measured:	2178	2497
Average Fibre Length	2.34	0.43
Weighted Average Length	3.11	1.12
Maximum Fibre Length Measured	10.58	7.27
Minimum Fibre Length Measured	0.13	0.004

**Table 4.1. – Summary of comparison results between Image J manual measurements against automated Image Pro Premier measurements.**

Above in Table 4.1 is a summary of numerical results from the two types of measurements.

Image Pro Premier is a 2D image analysis software developed by Media Cybernetics. Fibre length distribution results are obtained by the image first being opened in the software program itself. It is then segmented, identifying any fibres in the image. Object outlines are then created which are instantly counted and sized before the objects are separated into custom groups by specified interval parameters. Data is then analysed for making comparisons. The Image Pro Premier system only measures isolated fibres and ignores entangled fibres. The software struggled to handle a fully scanned image predominantly picking up short fibres as seen in Figure 4.2, an image supplied by Image Pro Premier after an analysis was completed. Version 9.1 of Image Pro Premier was evaluated.



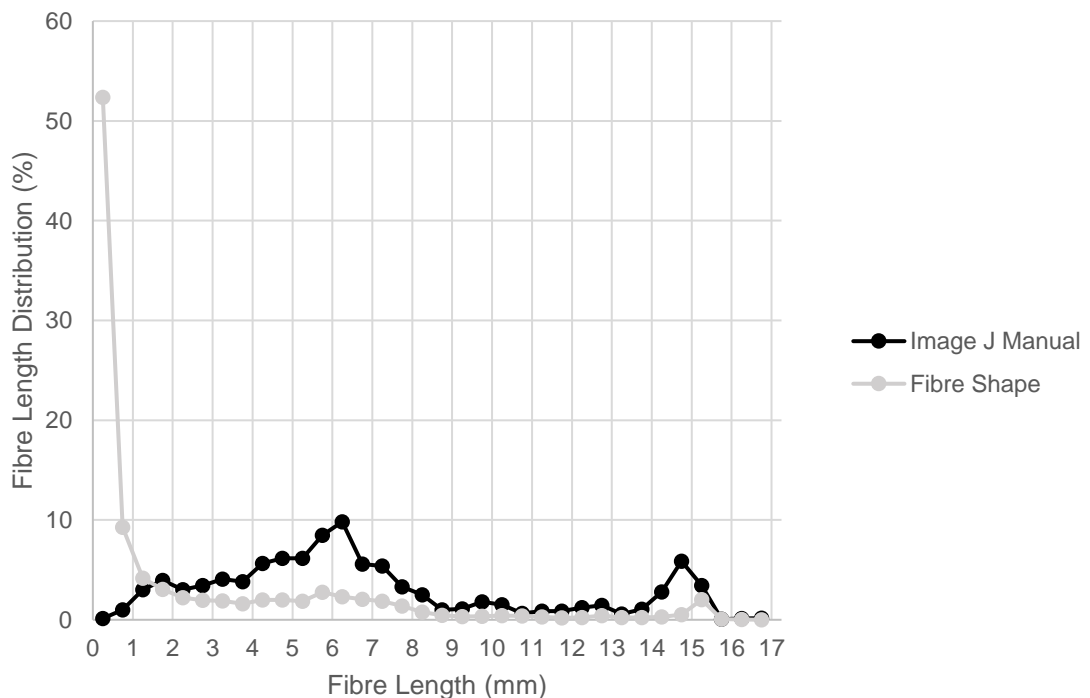
**Figure 4.2. - Image Pro Premier automated measurement - Ticona sample.  
Material: 20 wt. %. 15 mm LGFRPP (Scanned image 1002).**

The results seen above in Table 4.1 differ significantly, with a higher number and weighted average seen for the manual measurement technique. The automated measurement performed by Image Pro Premier can be considered relatively inaccurate. The software predominately measured short fibres, with only 2 fibres

being counted above 3.75 mm as opposed to 275 fibres for the manual measurement technique. Via the manual measurement technique, 100% of the fibres were counted, interestingly however Image Pro Premier totalled 319 more fibres. This is probably due to the software's inability to measure long, curved, and intersecting fibres, instead segmenting them into shorter fibre sections giving a bias towards the shorter fibre measurements.

#### 4.2. Fibre Shape

A 24 mm cut was taken from the feeding zone section of a 20 mm injection moulding screw and is labelled as F3. Sample was burnt off in a furnace and glass fibres were dispersed over a number of thin films as described in Chapter 3.3. The first scanned image file was chosen for comparison between manual measurements and automated measurements via Fibre Shape. The material used was 20YM240. A comparison of fibre length distribution results are shown below in Figure 4.3.



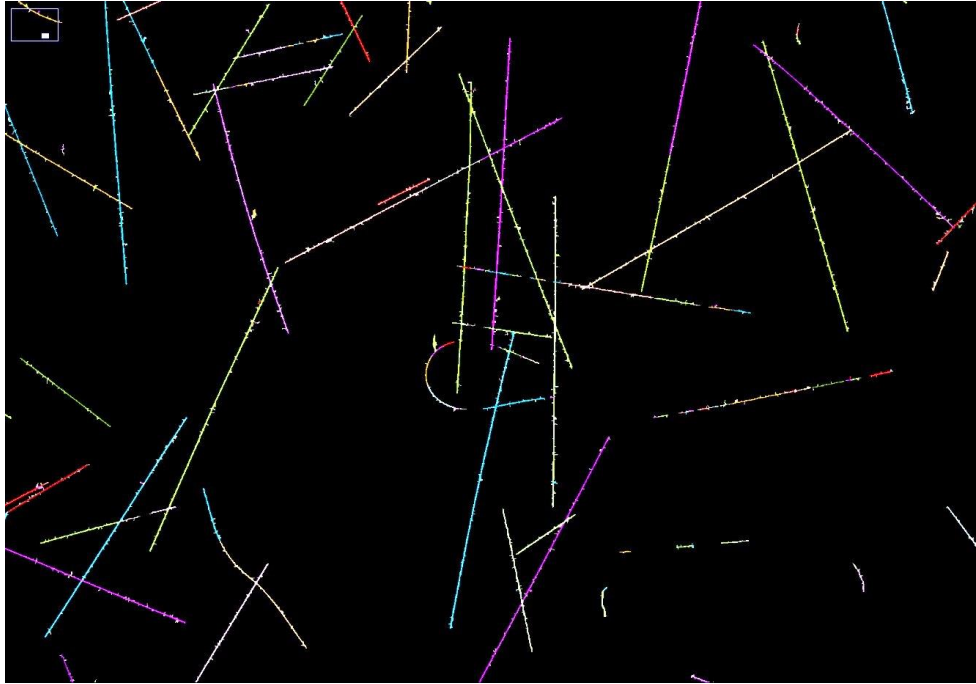
**Figure 4.3. - Image J manual measurement vs Fibre Shape automated measurement - Feeding zone sample. Material: 20YM240 (Scanned image 1001).**

<b>Sample F3 Screw Test 4 20YM240 Image 1001</b>	<b>Image J Manual Measurement</b>	<b>Fibre Shape Automated Measurement</b>
Number of Fibres Measured:	1670	4974
Average Fibre Length	7.02	2.36
Weighted Average Length	9.25	7.9
Maximum Fibre Length Measured	16.80	29.92
Minimum Fibre Length Measured	0.76	0.05

**Table 4.2. – Summary of comparison results between Image J manual measurements against automated Fibre Shape measurements.**

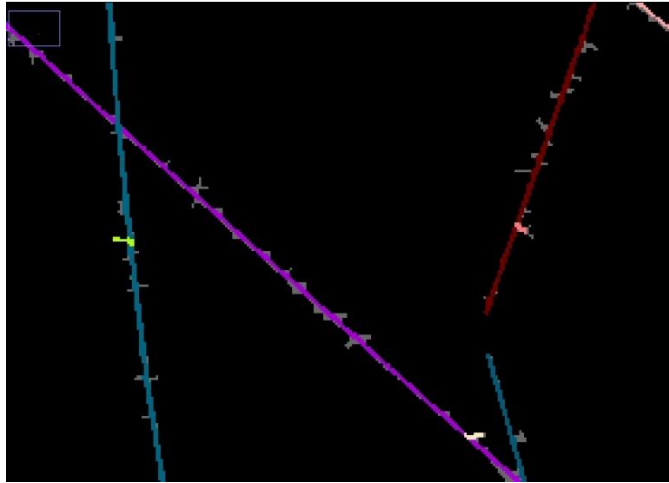
A summary of results obtained from the comparison of the two measurements is shown above in Table 4.2.

The Fibre Shape fibre length measurement software works similarly to Image Pro Premier and is developed by IST AG - Innovative Sintering Technologies, a company based in Switzerland. However, the image analysis software differs itself by reducing the data size of an image without losing resolution through the use of a fractal based algorithm. The maximum image file size the Fibre Shape software can handle is 150 mb. Resolution of the scanned image file used for manual measurements and sent to Fibre Shape was reduced to 950 dpi so a full image could be analysed by the software without splitting the image up. Fibre Shape suggested the scanner settings should be improved however did not go into any detail with further work/advice requiring an upfront payment. The version of Fibre Shape current at June 2017 was examined in this chapter.



**Figure 4.4. – Sample Fibre Shape automated measurement - Feeding zone sample. Material: 20YM240 (Scanned image 1001).**

The outcome of the comparison results are drastically different. Although the Fibre Shape software is similar to the Image Pro Premier system, it clearly has struggled in producing an accurate representation for the fibre length distribution of the supplied scanned image file. Although able to analyse a whole image file, the software has counted 3258 more fibres than were present on the original scan. Fibre Shape, like Image Pro Premier has again struggled dealing with long, curved and intersecting fibres as seen in Figure 4.4 which displays a sample area from an analysed image supplied by Fibre Shape. These long, curved fibres are ever present in a long glass fibre sample taken from the feeding section of the screw and the software instead segments the long fibres into smaller shorter fibres which accounts for the higher fibre count.



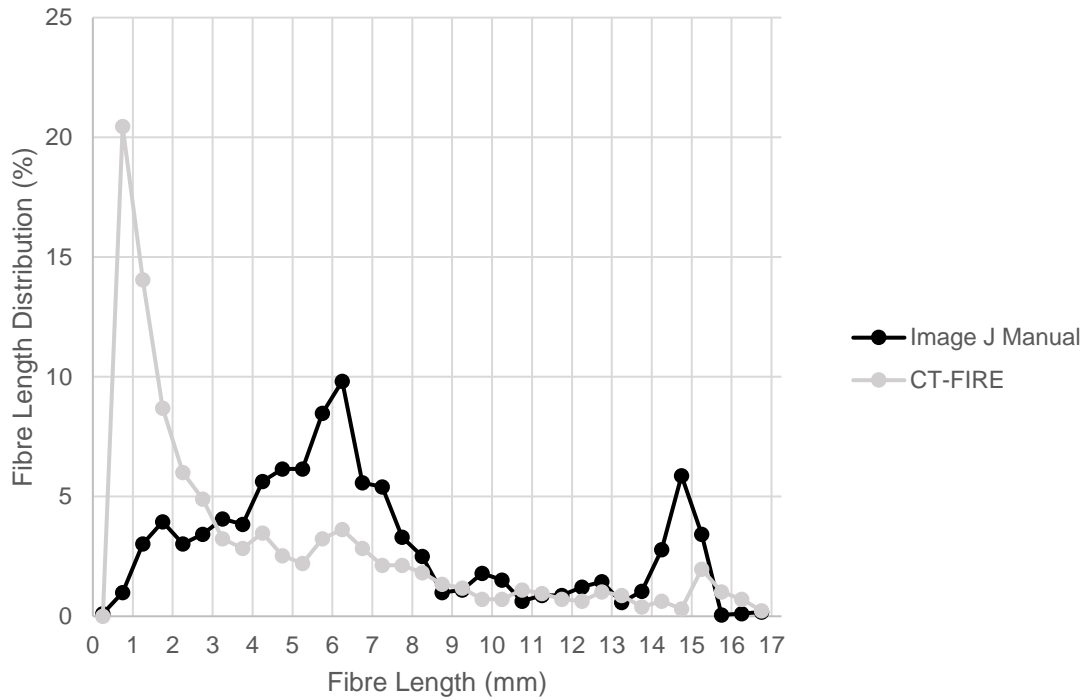
**Figure 4.5. – Sample Fibre Shape automated measurement – An example of fibre branches being computed.**

Another reason for the higher fibre count is possibly due to the low resolution of the image before analysis as the software appears to have computed minute fibre branches (which may have been a result from the skeletonization process) from a single fibre as a separate individual short fibre as shown in Figure 4.5.

The software also suggests to have stitched fibres together counting them as one which may explain the maximum fibre length measured on the Fibre Shape system was 29.92 mm.

### **4.3. CT-FIRE**

The same film as used in the previous comparison obtained from burning off and dispersing the glass fibres from a 24 mm sample cut taken along the feeding zone along a 20 mm injection moulding screw is evaluated in this particular assessment. The same scanned image file was again chosen for fibre length evaluation of the CT-FIRE automated system compared with the manual measurement technique. The sample is manufactured from the same material as mentioned before and a comparison of the results attained from the two different systems is shown below in Figure 4.6.



**Figure 4.6. - Image J manual measurement vs CT-FIRE automated measurement - Feeding zone sample. Material: 20YM240 (Scanned image 1001).**

<b>Sample F3 Screw Test 4 20YM240 Image 1001</b>	<b>Image J Manual Measurement</b>	<b>CT-FIRE Automated Measurement</b>
Number of Fibres Measured:	1670	1266
Average Fibre Length	7.02	4.51
Weighted Average Length	9.25	8.94
Maximum Fibre Length Measured	16.80	22.35
Minimum Fibre Length Measured	0.76	0.79

**Table 4.3. – Summary of comparison results between Image J manual measurements against automated CT-FIRE measurements.**

Table 4.3 displays a summary of results obtained from the comparison of the two different measurement techniques, manual measurement and CT-FIRE automated measurement.

CT-FIRE is an open source software developed by The Laboratory for Optical and Computational Instrumentation (LOCI) at the University of Wisconsin. It was originally developed for extracting collagen fibre data from an image file but was found to be applicable to this investigation. The software works via a curvelet transform 'CT' which denoises the image and enhances fibre edge features coupled with a fibre extraction 'FIRE' algorithm which extracts individual fibre data. Initial results seemed promising however an analysis of a fully scanned image is very time consuming (can take between 48-72 hours). The specifications of the computer used for the CT-FIRE analysis included a 2 x 12 core Xeon E5-2630 processor, 256 GB of RAM (Random-access memory), an Nvidia GTX 770 graphics card and a Windows 7 64-bit operating system. Version 2.0 Beta of CT-FIRE was used in this investigation.



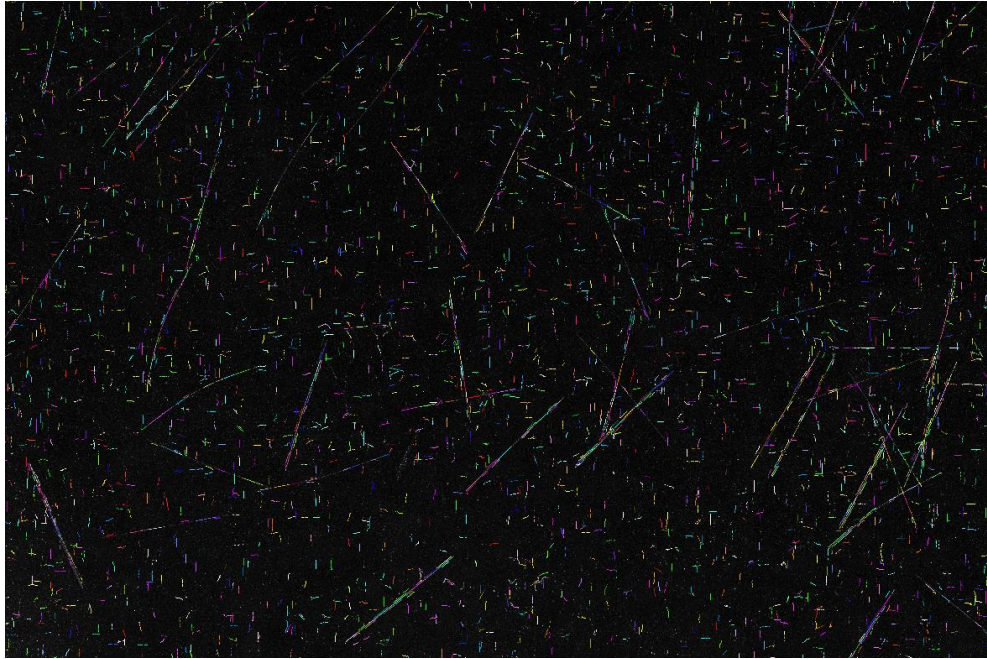
**Figure 4.7. – Sample CT-FIRE automated measurement: Parameters defined in-house.**



<b>Parameter</b>	<b>Value</b>
<i>thresh_im2</i>	30
<i>s_xlinkbox</i>	64
<i>thresh_ext</i>	40
<i>thresh_dang_L</i>	15
<i>thresh_short_L</i>	15
<i>s_fiberdir</i>	32
<i>thresh_linkd</i>	60
<i>thresh_linka</i>	-100
<i>thresh_flen</i>	15

**Table 4.4. – CT-FIRE automated measurement: Settings used in-house.**

Primarily, results displayed in Table 4.3 don't appear to be too dissimilar. This is supported in Figure 4.7, where a sample area has been selected from the overlaid image result from a CT-FIRE analysis with corresponding parameter values shown in Table 4.4. Figure 4.7 shows a large number of long and curved fibres being computed with relative success, compared to other automated fibre measurement systems that would segment them into smaller shorter fibres. Average and weighted average fibre length results measured from CT-FIRE from Table 4.3 only show a difference of 2.39 mm and 0.23 mm respectively when compared to the manual measurements taken from the same image. Notably, CT-FIRE is shown to count fewer fibres than were actually present, 450 to be precise on the scanned image file possibly due to the software not recognising a few fibres with a lower greyscale. However, similarly to previous comparison results, a significantly large number of shorter fibres were counted due to the software again struggling with long, curved and intersecting fibres as exhibited in Figures 4.6 and 4.7. Similarly to Fibre Shape, CT-FIRE appears to have linked two fibres together to produce a maximum fibre length of 22.35 mm.



**Figure 4.8. - Sample CT-FIRE automated measurement: Parameters defined by Giusti et al. (2015).**

<b>Parameter</b>	<b>Value</b>
<i>thresh_im2</i>	4.7
<i>s_xlinkbox</i>	1
<i>thresh_ext</i>	90
<i>thresh_dang_L</i>	15
<i>thresh_short_L</i>	15
<i>s_fiberdir</i>	10
<i>thresh_linkd</i>	10
<i>thresh_linka</i>	-150
<i>thresh_flen</i>	15

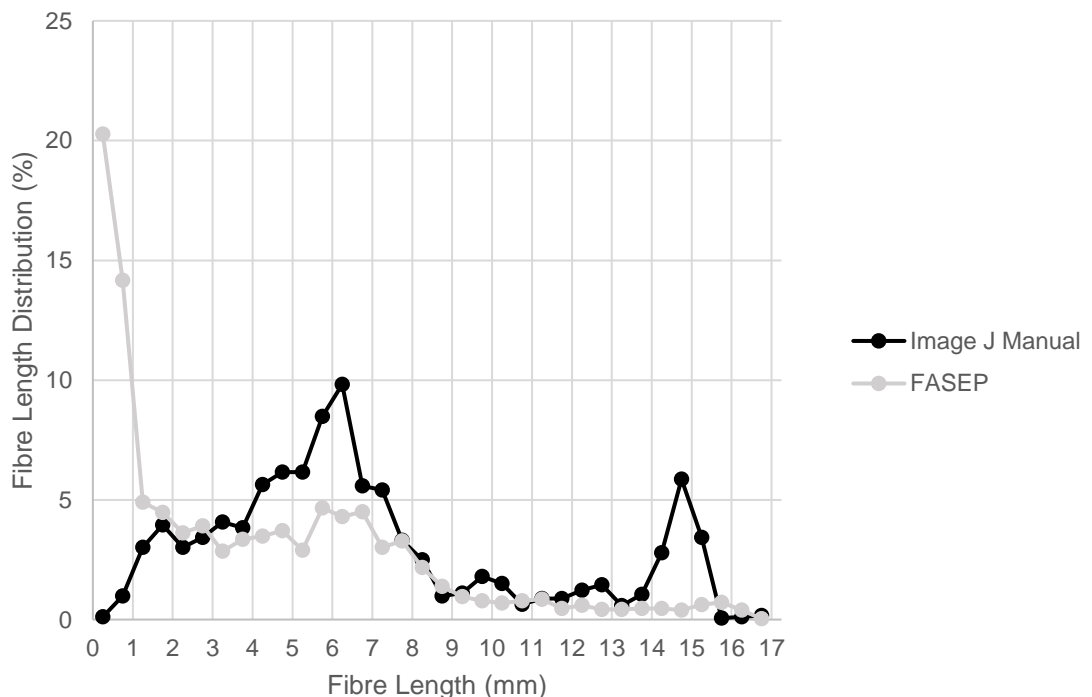
**Table 4.5. – CT-FIRE automated measurement: Settings used by Giusti et al. (2015).**

This investigation was not the only one to present CT-FIRE as a possible alternative for fibre length measurement of glass fibres. A study presented by Giusti et al. (2015) suggested CT-FIRE as a viable substitute to measure fibres automatically. However, applying the same CT-FIRE analysis parameters utilised in the research paper by Giusti et al. (2015), tabulated in Table 4.5,

revealed inaccurate results as shown in Figure 4.8. Not only are long individual fibres segmented into shorter fibres, the software settings appear to have computed multiple non-existent short fibres in the final output indicating fibre length results published by Giusti et al. (2015) are imprecise.

#### 4.4. FASEP

As with comparisons made with Fibre Shape and CT-FIRE, the same scanned image file described above was used in the assessment of the manual measurement technique against the automated measurements made by the FASEP fibre length measurement system. The sample is manufactured from the same material (as mentioned before) and fibre length distribution results are taken from the manual measurements of the scan and automated measurements by means of sending the scanned image file to the company that own the FASEP software and are compared in Figure 4.9.



**Figure 4.9. - Image J manual measurement vs FASEP automated measurement - Feeding zone sample. Material: 20YM240 (Scanned image 1001).**

<b>Sample F3 Screw Test 4 20YM240 Image 1001</b>	<b>Image J Manual Measurement</b>	<b>FASEP Automated Measurement</b>
Number of Fibres Measured:	1670	3044
Average Fibre Length	7.02	3.92
Weighted Average Length	9.25	7.50
Maximum Fibre Length Measured	16.80	16.59
Minimum Fibre Length Measured	0.76	0.16

**Table 4.6. – Summary of comparison results between Image J manual measurements against automated FASEP measurements.**

Table 4.6 shows a summary of numerical results calculated from the manual measurements of the image file along with the automated measurements from the FASEP fibre length measurement system of the scanned image file.

FASEP, a company based in Germany have created their own fibre length measurement system which can supposedly measure glass fibre lengths in a polymer sample accurately and reliably. The FASEP measurement software works by first analysing the image with a customized module of the image analysing software mentioned previously, Image-Pro. The software can detect most fibres semi-automatically. Thus completely isolated long and curved fibres can be detected automatically, on the other hand, intersecting fibres or clusters require manual input. The version of FASEP current at October 2017 was evaluated in this study.

Fibre length distribution results are of a similar nature to all previous comparisons made against other fibre length measurement systems. An inaccurate greater

distribution of shorter fibres, which are in fact segmented longer fibres which the FASEP software cannot compute, are seen in Figure 4.9. Summarised numerical results support this with almost double the amount of fibres being counted by the automated system than are actually present on the scanned image file.

An overlaid image of the captured fibres from the analysis was not supplied by FASEP in either case.

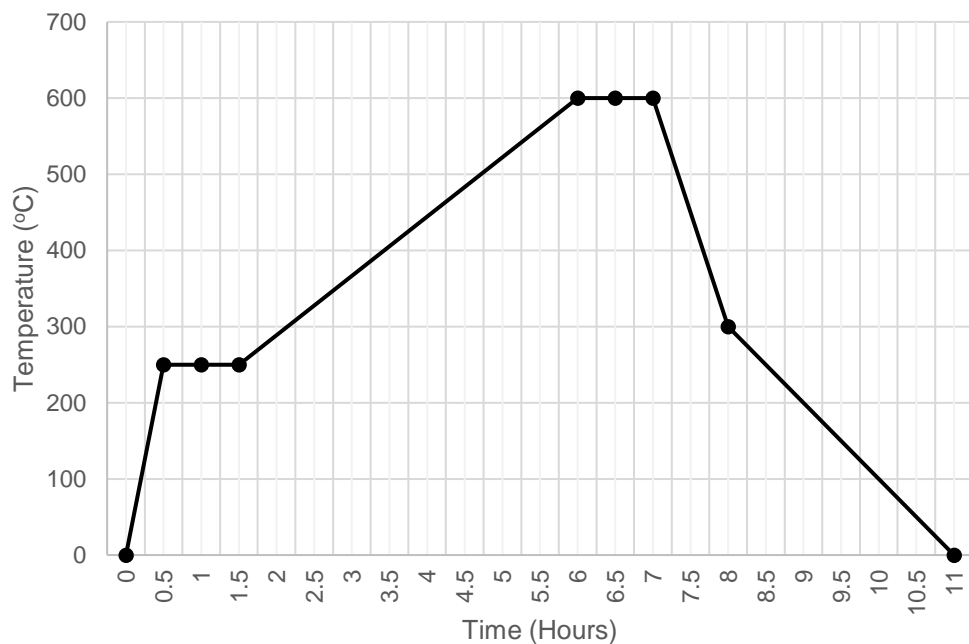
#### **4.5. FASEP (ii)**

The FASEP system was further tested by sending out two glass fibre reinforced polymer samples to the company so sample preparation of the long glass fibre sample would be done on-site using their own sample preparation system. The sample preparation and measurement system could then be directly compared with the fibre length measurement protocol described in Chapter 3.3 where glass fibres are dispersed manually onto thin films and around 2000 fibres are then randomly measured.

Two 24 mm cuts were taken from the feeding zone section of a 20 mm injection moulding screw, Sample F1 and Sample F1b. These samples are different to the ones used for the comparisons previously in this chapter as they are taken from a different screw test entirely. Sample F1 is the first 24 mm sample obtainable after the material has entered the screw and Sample F1b being the second, taken directly after along the screw channel. This is because no repeat screw pull out test was conducted thus the same sample location could not be evaluated, It was assumed the fibre distribution would not be too dissimilar between sample F1, which would be evaluated by manual fibre dispersion and measurement (Chapter 3.3) and sample F1b, which was sent to FASEP. This was supported by micro-CT results which showed no large visual differences and similar levels of fibre clustering in both samples.

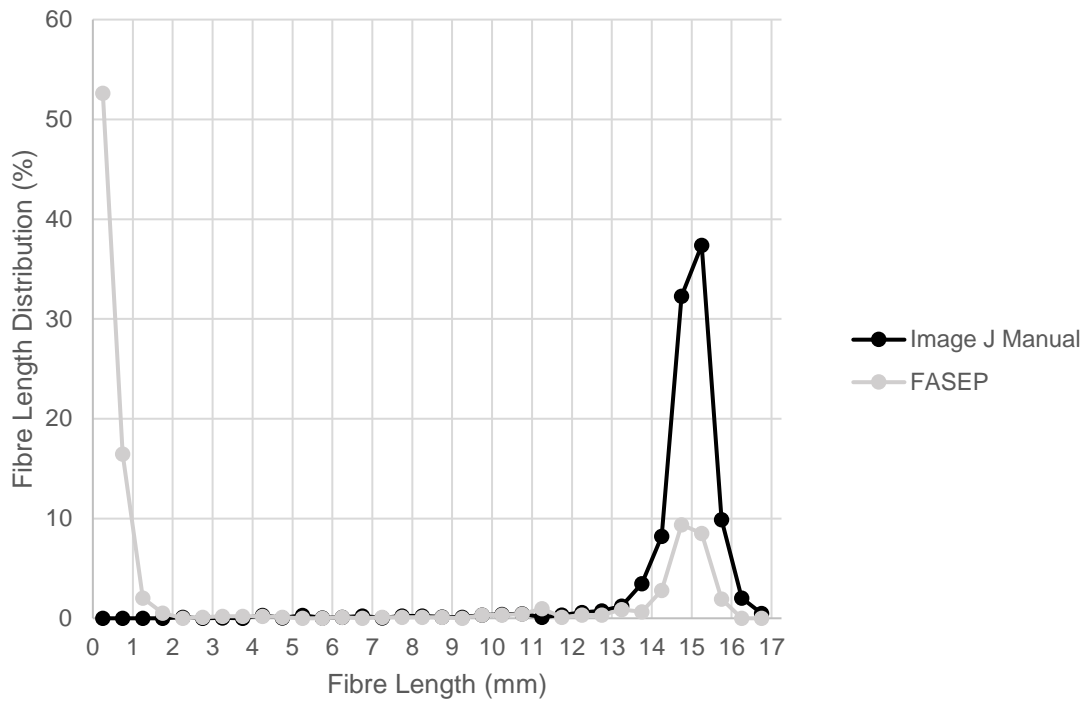
Also, one 20YM240 reinforced polypropylene virgin pellet was sent along with the screw sample to FASEP. The FASEP preparation protocol for long glass fibres

states that the higher the content of glass fibres in the polymer sample, the less sample mass you need for the analysis. For a 20 wt. % sample, FASEP use a granulate mass of 1.88g for fibre length analysis. First, the glass fibres are ashed applying the suggested temperature profile exposing the long glass fibres which is displayed below in Figure 4.10.



**Figure 4.10. – Temperature profile for fibre ashing suggested by FASEP.**

After the polymer matrix has been separated from the glass fibres, the glass fibres are mixed in a solution of water and glycerine. The solution is manually stirred so fibres are uniformly dispersed in the mixture. If clusters are visible, the solution is placed in an ultrasonic bath to disentangle and disperse the fibres. Subsequently, a set of diluting steps is performed by adding more water and glycerine. 500ml of the original solution is poured into an empty 1l beaker. The second beaker is filled up to 1l with distilled water. This process is repeated 7 times whilst continuously manually stirring the mixture. Finally, after the last dilution step, small portions of the liquid are extracted randomly with a pipette into a Petri dish, ready to be scanned, creating a digital image of the sample. The sample is ready for fibre length analysis. Two images were analysed for the pellet and 5 images for the injection moulded feeding zone sample.



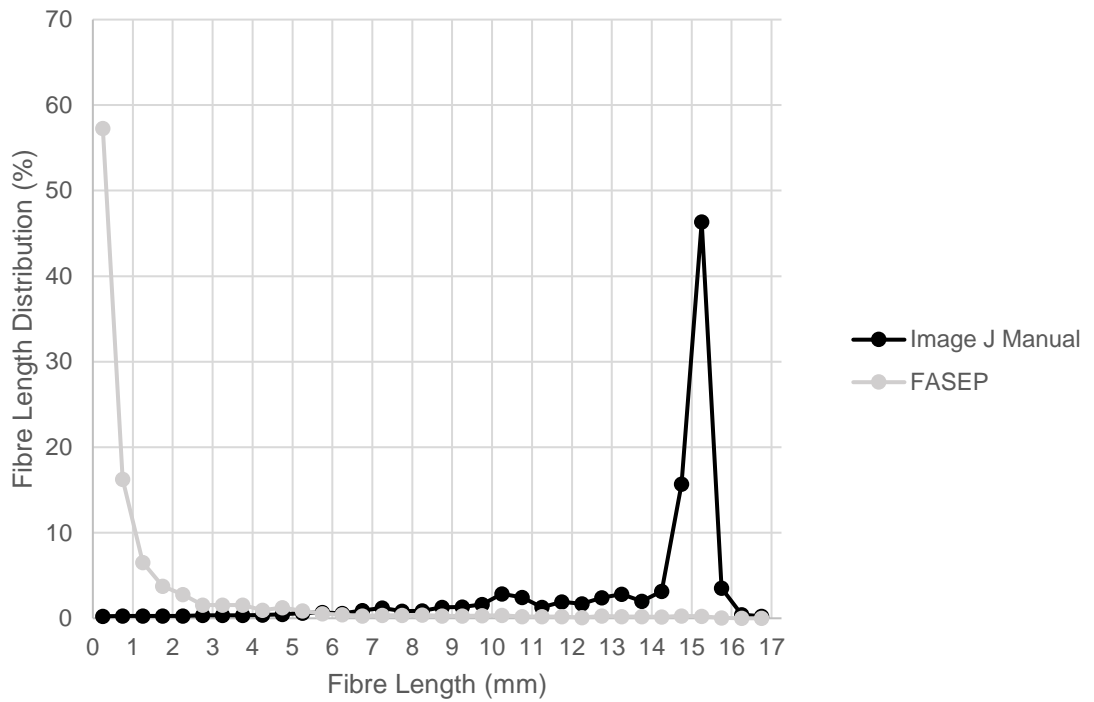
**Figure 4.11. - Fibre length manual measurement protocol vs FASEP automated measurement protocol - Pellet Sample. Material: 20YM240.**

<b>Pellet Sample 20YM240</b>	<b>Image J manual preparation and measurement</b>	<b>FASEP preparation and automated measurement</b>
Number of Fibres Measured:	2019	929
Average Fibre Length	14.72	4.27
Weighted Average Length	14.87	13.5
Maximum Fibre Length Measured	16.91	15.9
Minimum Fibre Length Measured	2.02	0.11

**Table 4.7. – Summary of comparison results of a 20YM240 pellet between Image J manual preparation and measurements against automated FASEP preparation and automated measurements.**

Figure 4.11 showcases the fibre length distribution results using the dispersion and measurement protocol employed in this study against the one developed by FASEP of a glass fibre reinforced pellet. The results are accompanied with a summary of results shown in Table 4.7. There is a clear contrast of results between the two methods. The manual technique could be viewed as more accurately representative of a fibre length distribution in a pellet as a much larger expected distribution of long fibres is present in the manual technique whereas the results presented by FASEP suggest there is a greater distribution by almost 4 times of shorter fibres than longer fibres in a raw virgin pellet sample. Only 929 fibres were measured by FASEP but this was deemed to be a sufficient enough to produce a precise fibre length distribution of the pellet. These results indicate the dilution process for the FASEP system does not allow for a reasonable representation of glass fibre distribution in a fibre filled sample, coupled with the fact that the measurement software segments long, curved and intersecting fibres into smaller shorter sections, leading to this erroneous display of results. This is supported by the fact that the FASEP software measured 663 fibres with a length less than 1.75 mm as opposed to 0 fibres in the manual measurement procedure.





**Figure 4.12. - Fibre length manual measurement protocol vs FASEP automated measurement protocol - Sample F1 vs Sample F1b. Material: 20YM240.**

<b>Feeding Zone Sample Screw Test 6 20YM240</b>	<b>Image J Manual Preparation and Measurement. Sample F1</b>	<b>FASEP preparation and automated measurement. Sample F1b</b>
Number of Fibres Measured:	2017	2484
Average Fibre Length	8.86	1.33
Weighted Average Length	11.38	5.74
Maximum Fibre Length Measured	16.81	15.85
Minimum Fibre Length Measured	0.08	0.1

**Table 4.8. – Summary of comparison results between Image J manual preparation and measurements against automated FASEP preparation and automated measurements of an injection moulded screw sample.**

A fibre length distribution plot of two samples measured using two different fibre length measurement systems is shown in Figure 4.12 with corresponding numerical results shown in Table 4.8 detailing notable statistics pulled from the fibre length measurements of each sample.

Even though two different samples are being compared, the micro-CT data suggests fibre clusters are still present in Sample F1b although they are slightly more predominant in sample F1. Results suggest that 918 measured fibres with a length greater than 9.75 mm have degraded to such a degree that only 66 fibres were found to have a length greater than 9.75 mm in sample F1b. The software is again indicated to have struggled in dealing with long, curved and intersecting fibres, ever present in screw samples, as the largest distribution of fibres is seen to be in the range of 0 – 1.25 mm, with 1927 fibres being counted. It is however unclear as to how many of those fibres are actually short fibres or segmented long fibres.

An overlaid image of the captured fibres from the analysis was not provided by FASEP in Chapters 4.4 or 4.5.

#### **4.6. Others**

Other fibre length measurement systems evaluated included Clemex Vision PE, image analysis software developed by Clemex. However the software was originally created for measuring short glass fibres only and thus proved impractical in relation to this study.

A fibre length measurement system was present at the KU Leuven Technology Campus in Ostend, Belgium where the screw pull out tests were performed. A custom MATLAB module was developed for previous glass fibre length measurement studies conducted at the Technology Campus. The software was unsuccessful in creating an accurate fibre length distribution for long glass fibres as it segmented all long and curved fibre into smaller shorter segments computing

them as short fibres. The software was primarily developed for automatically measuring short glass fibres.

#### **4.7. Conclusion of Trialled Fibre Length Measurement Methods.**

From the comparison results it is clear that current commercially available software for fibre length measurement analysis is still struggling to deal with long, curved and intersecting fibres instead segmenting them into shorter fibres giving an inaccurate data set. Whilst the manual dispersion and measurement of fibres is time consuming and perceived as inaccurate in some literature, it was chosen to be applied to this investigation due no viable or reasonable priced alternative. It is judged that the fibre length dispersion and measurement protocol used for this study is accurate enough to represent a reasonable and reliable fibre length distribution as supported from the literature review conclusions in Chapter 2.7.

This investigation is centred on long glass fibres, specifically along the screw, where such fibres are predominant. The majority of literature is centred on fibre length distributions of injection mouldings where short fibres are considered to be prevalent. Automated dispersion and measurement systems may achieve reasonable success in such studies, as long, curved or intersecting fibres found earlier in the injection moulding process have largely broken down into smaller fragments. Such systems were probably originally designed for these particular studies and consequently struggle to compute fibre length distributions earlier on in the injection moulding process.

#### **4.8. Fibre Length Measurement through the use of Micro-CT**

The fibre length measurement technique used in this thesis involving pyrolysis and image analysis can be considered inaccurate due to its susceptibility to human error. Thus there is a need for it to become more standardized, especially when it comes to the measurement of long fibres which can heavily influence the outcome of results. Results can vary if repeated and from person to person which is not ideal. A more standardized process needs to be introduced to allow for accurate and repetitive measurements of fibres with minimal error. If the same

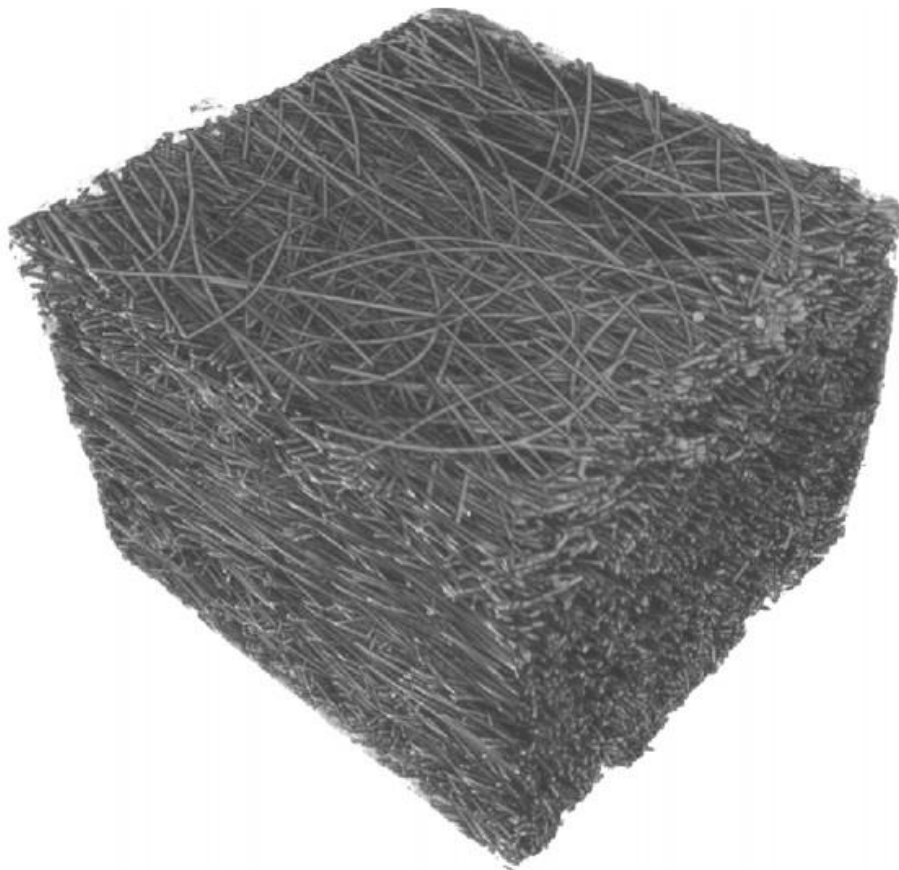
test was repeated, one researcher may measure less long fibres compared to another researcher by simply selecting a different area of interest, presenting a discrepancy in results. A large enough dataset was collected for each experiment (compared to previous literature) to allow for such an error, but this 'correction method' is not perfect as it is very time consuming and not very standardized.

Conventional methods as used in this study measure approximate fibre length distribution in such a way that requires destruction of the sample component. One mechanical process, not used in this investigation is to sieve the fibres with different sieve sizes. However, this method does not work successfully with long fibres that are intertwined with one another. Another is the usage of scanners but the fibres have to be singularized in order to reduce any errors in measurements due to entanglement or overlapping which can require mechanical action. The fibres are then segmented using a digital analysis system which is very time consuming and inefficient as long fibres have to be generally measured manually.

However, one of the main problems which arise from all conventional fibre length measurement procedures is the destruction of the component in order to determine fibre lengths. It would be advantageous to have a means of evaluating in-use products or parts thereof for quality assessment without the need to destroy the sample. Nevertheless, this area of research is relatively new and is ongoing, thus there are only a limited number of non-destructive fibre evaluation technologies.

New methods have been introduced recently into the polymer engineering world which involves a computerised tomography system used for scientific and industrial applications. High resolution computed tomography can be and is used as an imaging method, together with subsequent image analysis for evaluation of fibre length distributions. This allows for an automatic and non-destructive analysis of materials, specifically the determination of fibre length distribution in long glass fibre reinforced samples (Zauner et al. 2015).

The use of Micro-CT allows for 3D imaging of structures with a very high spatial resolution, up to 70 nanometres. With the diameter of glass fibres well below 0.1 mm, this system enables the user to acquire high-quality images of the inside of a fibre reinforced polymer sample. The system works by rotating the specimen in an X-ray beam as described in Chapter 3.2.1. The subsequent projection of the specimen is captured by a digital detector. More than a thousand projections can be produced from different angles. These projections can then be computed and reconstructed in a 3D data set consisting of volumetric pixels, known as voxels with varying grey values. A complete 3D image of the specimen is produced once it has been rotated a full 360°. An example of a scanned sample is shown in Figure 4.13.



**Figure 4.13. - CT scan of a long glass reinforced polymer sample  
(Teßmann et al. 2010)**

Due to the high resolution scanning technology resulting in high image quality, the development of non-destructive evaluation algorithms has become more and more practical. Resolution of the image depends on the CT equipment used but also the size of the sample. To enable accurate results of fibre length distribution and orientation, a compromise has to be found between sample size and representative volume. The CT scan above has an isotropic voxel size of 4.36  $\mu\text{m}$ .

An original, model-based algorithm proposed by Teßmann et al. (2010) allowed for the automatic detection, segmentation, and calculation of length distributions of fibres in CT data for fibre reinforced polymers by a hessian based procedure. The algorithm was shown to handle curved fibres and image noise successfully, as well as tightly packed and crossing fibres, though the accuracy suffers in these cases, as not all fibres may be detected fully or gaps may occur within single fibres. To obtain such a high resolution image of 4.36  $\mu\text{m}$  for the algorithm to work successfully a small sample size must be scanned. This means fibres were being cut off affecting their true value and giving a bias towards short fibres. This unfortunately limits the practical applicability of the method proposed by Teßmann et al. (2010).

Limitations that have to be overcome with X-Ray computed tomography analysis arise from the dependency of resolution on sample size and limited data quality. Constraints also arise with the complexity of fibre tracking in 3D which can lose connected fibre paths resulting in a bias in the fibre length distribution results, especially in large scans (Salaberger et al. 2010).

As well as Teßmann et al. (2010), Kastner et al. (2008) and Shen et al. (2004) all reported 3D image processing algorithms for obtaining quantitative information about fibre orientation and length distribution in fibre reinforced material components. Salaberger et al. (2011) presented a study through the use of synchrotron CT, a sub- $\mu\text{m}$ -CT scanner which is able to operate at higher resolutions compared to conventional  $\mu\text{-CT}$  scanners such as the one present at

this University, enabling data quality good enough to separate single fibres, which is possible with a  $\mu$ -CT system but at half the size of measurement volume.

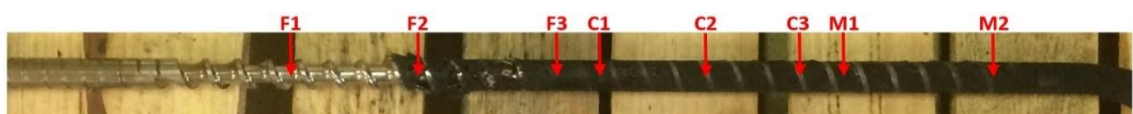
The accuracy of the approach shown suffered from the ability to segment fibres at high fibre content, dropping considerably with samples containing 20 wt. % glass or more. This is because there is a more complex fibre network with an increasing fibre content thus a higher fibre-fibre interaction and cluster regions. Zauner et al. (2015) attempts to overcome the detected problems in CT data analysis in higher fibre content samples, specifically 30 wt. %, by using a template matching approach. Using a spherical template was shown to improve the accuracy in detecting the centrelines of individual fibres without increasing processing time severely. Another researcher (Pinter et al. (2016)) was able to integrate local orientation data to their 3D fibre tracking algorithm to improve separation of individual fibres and apply tensor-voting methods to differentiate any noise or erroneous particles from glass fibres. Results were relatively successful of long glass fibre reinforced samples (20 wt. %) with a thickness of 5 mm and potentially could lead to improved characterization of larger long glass fibre reinforced samples in the future.

However, research in this field has mainly focused on relatively small sample sizes, no more than a few hundred fibres. Samples obtained in this study have a significantly larger sample size and can contain hundreds of thousands of fibres. To date, no fibre length measurement system which used micro-CT was found to be applicable to this study and thus further work in terms of comparisons with the current manual measurement systems was not made.

## 5. Long Glass Fibre Distribution Results.

Fibre length measurements were initially taken from samples extracted at the nozzle entry of a 3 and 6 mm nozzle utilised in a Battenfeld BA750/315 CDK injection moulding machine. A 17mm cut was taken from the nozzle entry, the side closest to the screw. Process parameters were kept constant and the nozzles were evaluated with 20YM240 and 40YM240 material. Details of the nozzle and sample extraction can be found in Chapter 3.1. Roughly 2000 fibres were measured for each sample. A sampling bias correction has not been applied for fibre length measurement data presented in Chapter 5 or Appendix 1 but discussed in detail in Chapter 6.

Fibre length distribution measurements were subsequently taken from a maximum of 10 different sample locations along an injection moulding machine. In all cases, a 20 mm screw was extracted from an Arburg Allrounder 270C. Samples F1, F2 and F3 are taken from the beginning, middle and end of the feeding zone. Due to a shorter feeding zone the screw test that will be evaluated in Chapter 5.1, only samples F2 and F3 were removed. Samples C1, C2 and C3 are also taken from the beginning, middle and end but of the compression zone. Finally sample M1 is obtained from the start of the metering zone and M2 is taken from the end of the metering zone. Nozzle samples N1 and N2 were also obtained but only from screw tests 1 and 5. N1 being nozzle entry and N2 being the nozzle exit. The sprue sample is taken from the top region of the sprue closest to the screw from the resultant injection moulded component. Nozzle and sprue samples are taken from the same extracted screw test. Finally, a single pellet sample from the processing material is also analysed. Various process parameters are evaluated with 20YM240 and 40YM243 material and further details of sample and screw extraction can be found in Chapter 3.1. Roughly 2000 fibres were measured for each sample. Injection moulding settings can be found in Appendix 1.



**Figure 5.1. – Example of extracted sample locations from a 20 mm Arburg Allrounder 270C injection moulding screw.**



## 5.1. Nozzle Extraction Tests Numerical Results - Battenfeld BA750/315 CDK

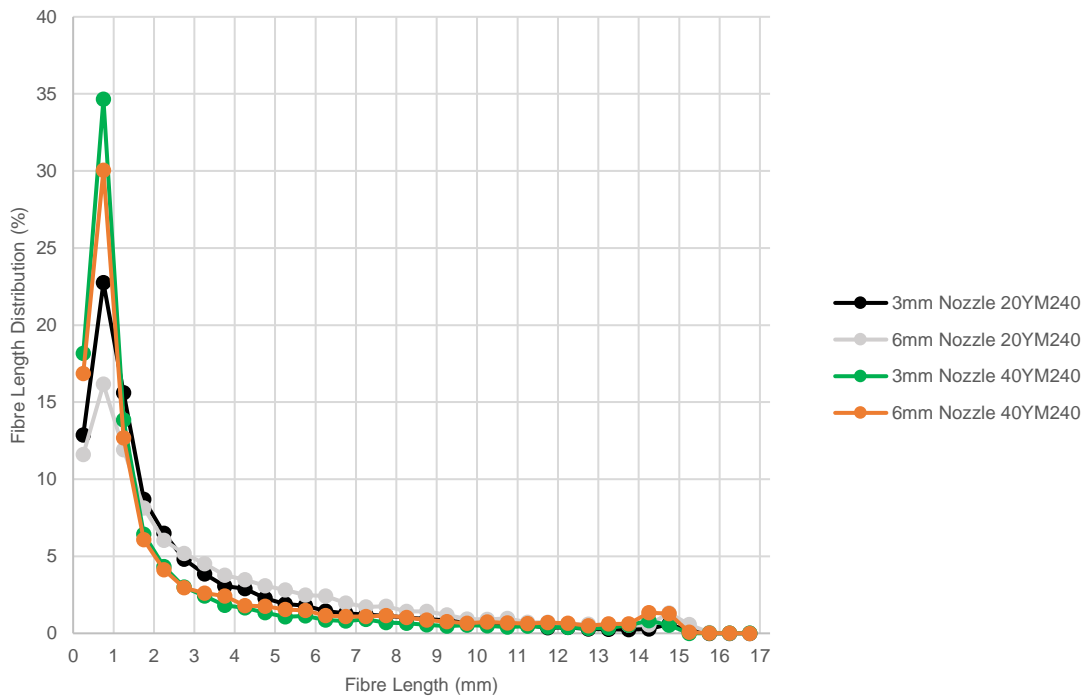
Below in Table 5.1 is a summary of numerical results taken from 4 injection moulding nozzle extraction tests.

Samples were processed using 20YM240 and 40YM240 with the process parameters being kept constant throughout all nozzle extraction tests, details of which can be found in Chapter 3.1. The 3 mm nozzle geometry included a long tapered entry and the 6 mm nozzle contained a short tapered entry. 17 mm cuts at the nozzle entry were evaluated for fibre length distribution. This would allow for any longer fibres to be measured in the subsequent fibre length measurement analysis.

<b>Sample</b>	<b>Average Fibre Length (mm)</b>	<b>Weighted Average Length (mm)</b>	<b>Maximum Fibre Length Measured (mm)</b>	<b>Minimum Fibre Length Measured (mm)</b>
3 mm Nozzle 20YM240	2.70	6.04	15.49	0.08
6 mm Nozzle 20YM240	3.60	7.25	16.61	0.08
3 mm Nozzle 40YM240	2.20	6.31	16.94	0.03
6 mm Nozzle 40YM240	2.83	7.49	16.36	0.08

**Table 5.1. - Summary of results (Battenfeld BA750/315 CDK)**

### 5.1.1. Fibre Length Distribution Results - Battenfeld BA750/315 CDK



**Figure 5.2. - Fibre length distribution results from nozzle extraction tests.**

Figure 5.2 shows the fibre length distribution plot for each nozzle entry processed with 20YM240 and 40YM240 material. It is initially clear from the results in Figure 5.2 that a greater concentration of shorter fibres was found in the 40YM240 material when compared against the lower glass fibre content 20YM240 material. However, weighted average results are higher for the 40 wt. % set of data. This could suggest that at increased fibre content, there is an increase of fibre-fibre interactions leading to clusters of fibres being forced which are able to protect each other from the high shear forces present in the nozzle, preserving their length. This clustering on the other hand is not desirable in the final part as it leads to poor homogeneity resulting in decreased mechanical properties and a poor surface finish. Both 6 mm nozzles with a short tapered entrance appear to minimise fibre attrition with higher weighted averages when processing both materials of 7.25 mm for 20YM240 and 7.49 mm for 40YM240. Compared to their 3 mm nozzle long tapered end equivalent, the weighted average is smaller for both materials, evaluated to be 6.04 mm and 6.31 mm respectively.

## 5.2. Screw Pull Out Test Numerical Results - Arburg Allrounder 270C

Below in Table 5.2 is a summary of numerical results taken from a screw pull out test.

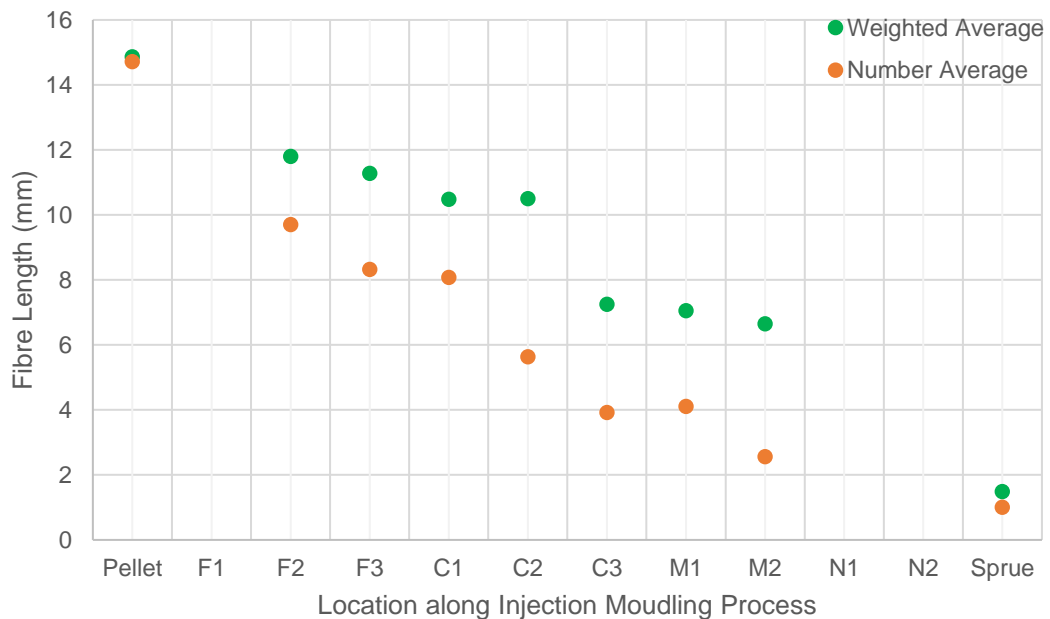
Samples were processed using 20YM240 at a low back pressure (2.5 bar) and high RPM (300 RPM) and identified as screw test 4. 24 mm cuts along the thread of the screw were taken from each of the specified locations shown in Figure 5.1 from F2 through to M2. 24 mm cuts were also made at the sprue entry but no nozzle samples were successfully obtained for this particular screw test. This would allow for any longer fibres to be measured in the subsequent fibre length measurement analysis.

<b>Sample</b>	<b>Average Fibre Length (mm)</b>	<b>Weighted Average Length (mm)</b>	<b>Maximum Fibre Length Measured (mm)</b>	<b>Minimum Fibre Length Measured (mm)</b>
Pellet	14.72	14.87	16.91	2.021
F1	<i>n/a</i>	<i>n/a</i>	<i>n/a</i>	<i>n/a</i>
F2	9.71	11.80	15.70	0.08
F3	8.33	11.28	15.77	0.07
C1	8.08	10.48	15.54	0.05
C2	5.64	10.50	16.01	0.05
C3	3.92	7.25	15.05	0.09
M1	4.11	7.06	14.99	0.11
M2	2.75	6.65	15.08	0.03
N1	<i>n/a</i>	<i>n/a</i>	<i>n/a</i>	<i>n/a</i>
N2	<i>n/a</i>	<i>n/a</i>	<i>n/a</i>	<i>n/a</i>
Sprue	1.01	1.49	7.74	0.05

**Table 5.2. – Summary of results (Arburg Allrounder 270C)**

### 5.3. Summary of Screw Pull Out Test Results – 20YM240. 20 mm Screw Test (Low Back Pressure / High RPM) - Arburg Allrounder 270C

Figure 5.3 shows a comparison of number and weighted average along the injection moulding process from the initial stage of the material being in pellet form through to the sprue entry at location S1.



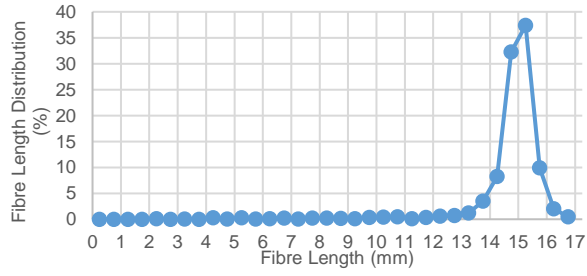
**Figure 5.3. – Number and weighted average distribution of each 24 mm cut taken from various locations along the injection moulding process**

Overall, it can be suggested that there is a decreasing linear trend present in terms of fibre breakage for both number and weighted average along the injection moulding process, from a raw pellet sample through to the sprue of an injection moulded component. From the initial stages of the injection moulding process, it can be seen there is a gradual decline of overall fibre length through the feeding zone to the beginning of the compression zone. However, at the beginning of the compression zone a drastic step change is displayed until the end of the compression zone highlighting significant fibre breakage has occurred. The weighted average however, does not initially follow the decreasing trend of the number average between samples C1 and C2, indicating although an increase in fibre breakage and thus short fibres is evident, a fibre bundle of long fibre lengths, not present in C1 but C2 may have been preserved along the injection moulding

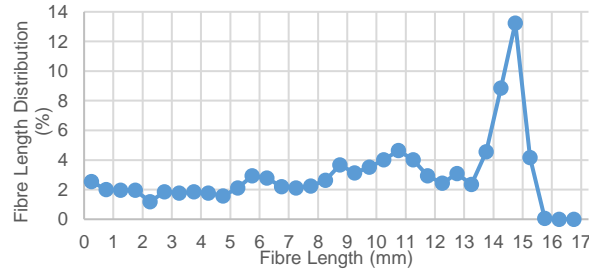
process. Thereafter, the number and weighted average results follow the earlier trend of gradually decreasing along the metering zone through to the sprue.

A summary of all fibre length distribution results is shown below in Figure 5.4 taken from screw test 4. the first data point is plotted at 0.25 mm. The

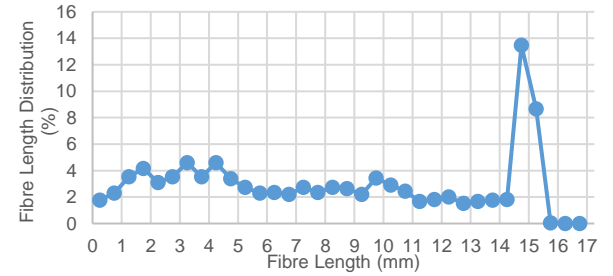
In all fibre length distribution graphs, the population of fibres is categorised into various bins for easy graphical display. The bin labels range from 0.25 mm, 0.75 mm, 1.25 mm, etc., up to 16.75 mm but the nominal length of each bin is the mid-point of the band of lengths it represents, i.e., the count of fibres in each bin is those of fibres which have lengths within a  $\pm 0.25$ mm band of the nominal length. That is, the bin labelled 14.75 mm would count the fibres which have lengths between 14.5 mm and 15.0mm.



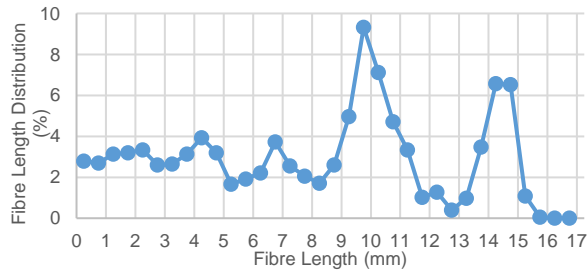
**Sample Location – Pellet**



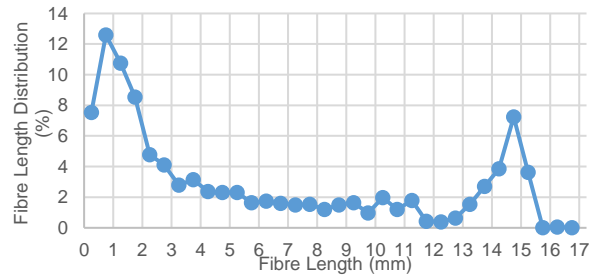
**Sample Location – F2**



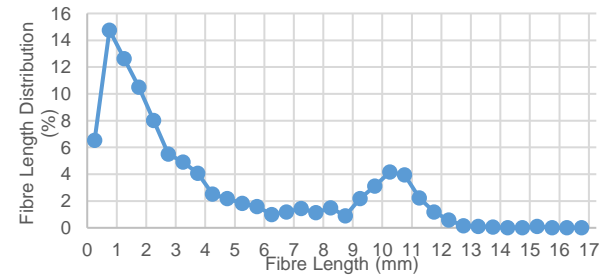
**Sample Location – F3**



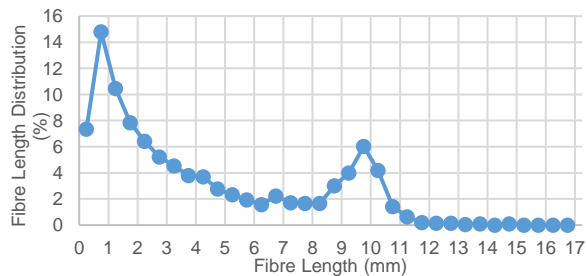
**Sample Location – C1**



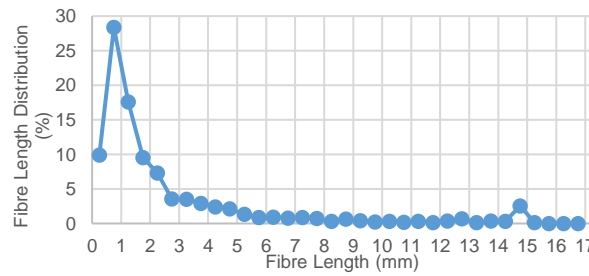
**Sample Location – C2**



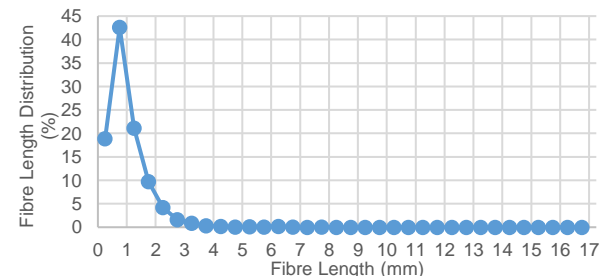
**Sample Location – C3**



**Sample Location – M1**



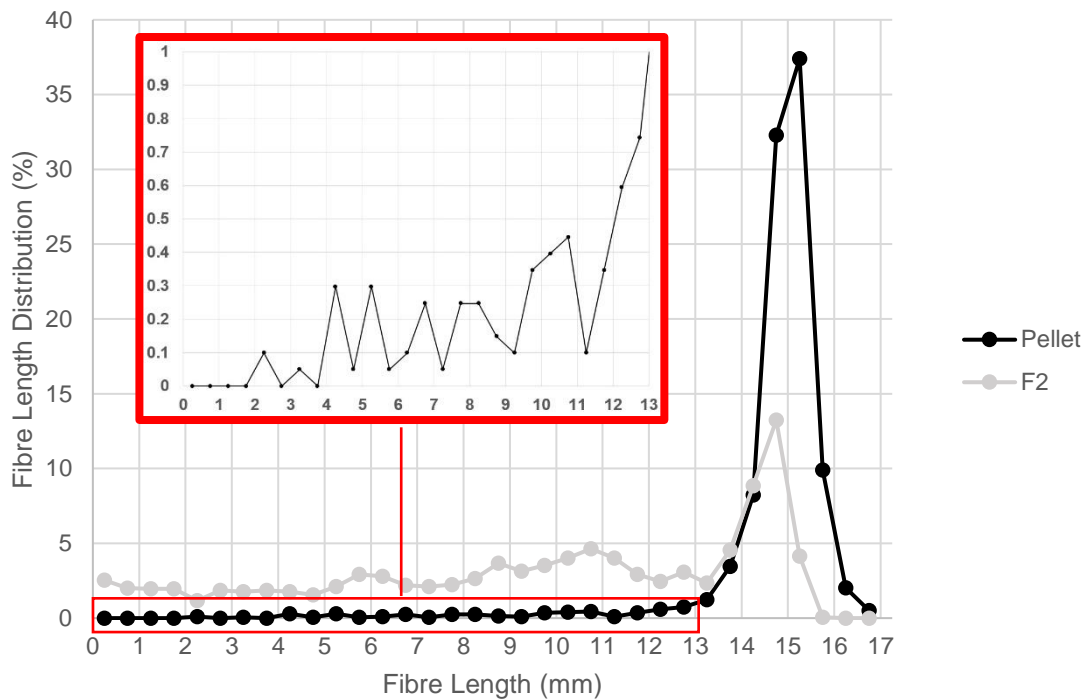
**Sample Location – M2**



**Sample Location – Sprue**

**Figure 5.4. - Summary of fibre length distribution results**

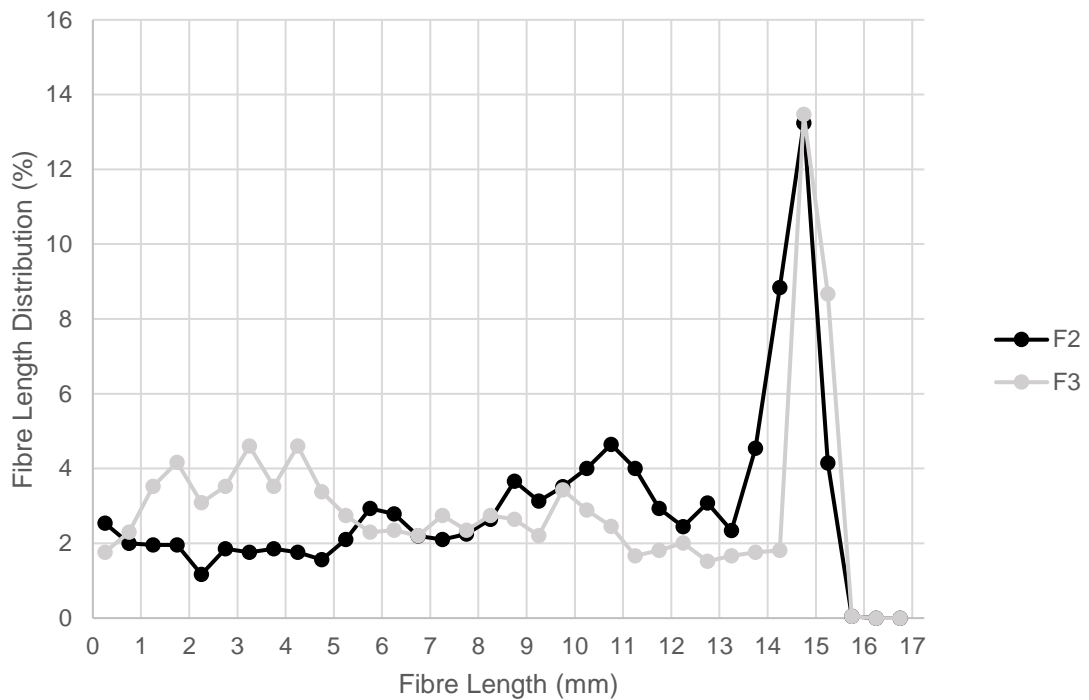
### 5.3.1. Fibre Length Distribution Results: Pellet – F2



**Figure 5.5. - Pellet and F2 fibre length distribution results from screw pull out test.**

Figure 5.5 shows the fibre length distribution plot for the pellet and F2 sample location. The graph results for the pellet sample between 0 – 13 mm is highlighted to show that there is a distribution present albeit very minute. This distribution of shorter glass fibre lengths within the long glass reinforced pellet is surprising and could be attributed to the manual measurement preparation method or the manufacturing process of the pellet itself not being perfect and leading to minor fibre attrition. Nevertheless, there is a higher distribution of longer fibres in the pellet sample when compared to sample F2 as expected with a number and weighted average of 14.72 mm and 14.87 mm respectively. Both averages drop drastically at the beginning of the feeding zone to 9.71 mm and 11.80 mm. The higher distribution of shorter fibre lengths within sample F2 can be attributed to the long fibres between lengths of 14 mm and 17 mm within the pellet sample being expectedly broken in the injection moulding process as they enter the feeding zone.

### 5.3.2. Fibre Length Distribution Results: F2 – F3



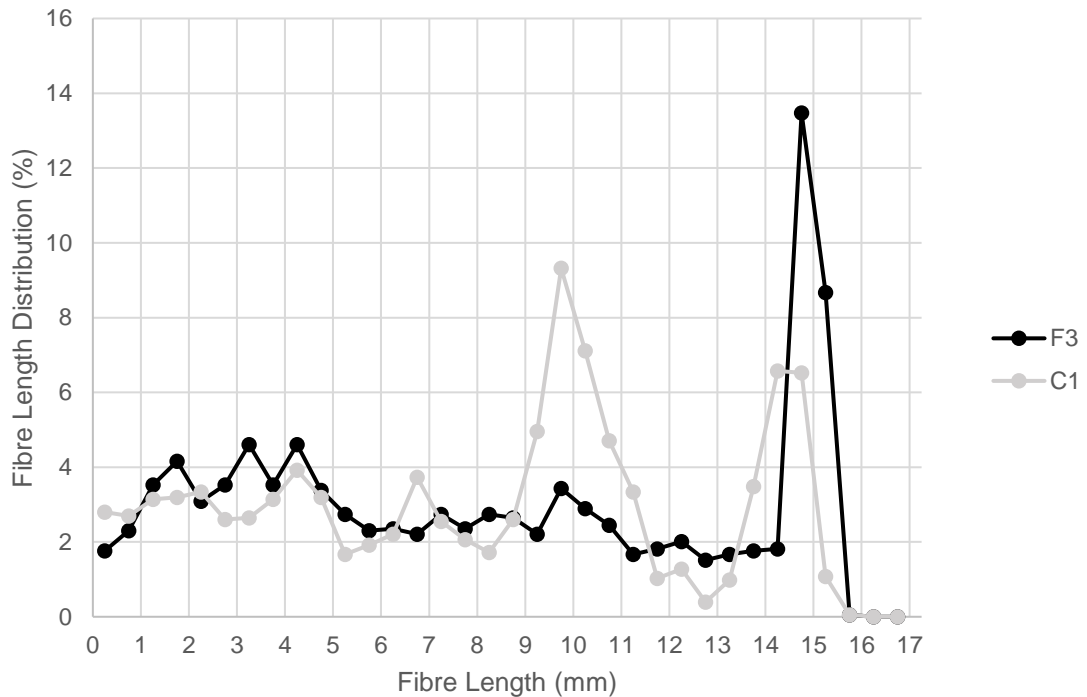
**Figure 5.6. – F2 and F3 fibre length distribution results from screw pull out test.**

Figure 5.6 shows the fibre length distribution plot for sample locations F2 and F3. Although there is larger distribution of glass fibres of 4.75% measured between lengths of 14.5 mm – 16 mm for Sample F3 compared to F2, the weighted and number average are marginally larger for Sample F2 at 11.80 mm and 9.71 mm respectively compared to 11.28 mm and 8.33 mm for F3. This is predominantly due to Sample F2 having a larger measured distribution at 40.35% (compared to 21.02% for F3) of longer fibres found within the length interval of 9.5 mm – 14.5 mm, which are seemingly subsequently broken along the injection moulding process as they reach sample location F3 giving a rise to a higher distribution of shorter fibres between 0.5 mm – 5.5 mm. However, if fibres of length 9.5 - 14.5 mm have broken, then the total number of fibres per unit volume at F3 should be higher than F2, since each long fibre is broken down to create two or more shorter fibres. Therefore, the fibre population between 14.5 - 16 mm even if it had all remained unbroken, would now be a smaller percentage of the total population at F3. Therefore the results suggest that there is some natural variation in the



results due to the randomness of the measurement method and the randomness of fibre bundles which are not yet dispersed along the screw.

### 5.3.3. Fibre Length Distribution Results: F3 – C1

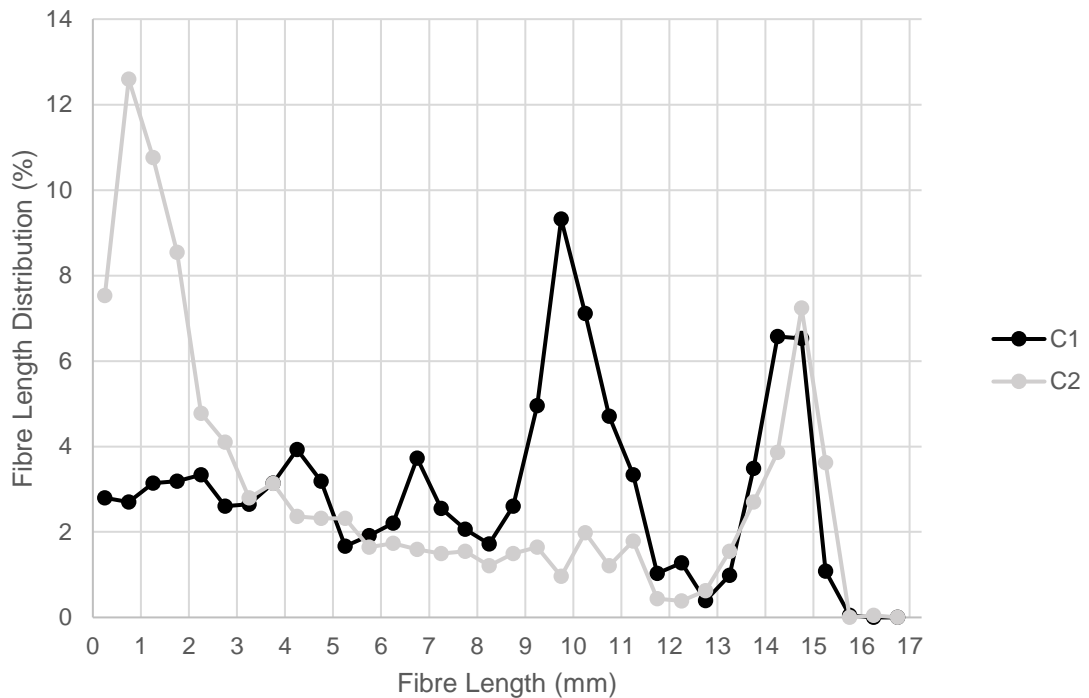


**Figure 5.7. – F3 and C1 fibre length distribution results from screw pull out test.**

Figure 5.7 shows fibre length distribution results for sample locations F3 and C1. On first observation, both Samples F3 and C1 have surprisingly similar fibre length distributions for fibres measured between 0 mm and 9 mm as they leave the feeding zone and flow into the compression zone of the screw (+/- 1.96%). However, fibre attrition for longer fibres found in both samples with lengths measured greater than 9 mm is more evident as seen in the Figure 5.7. The highest fibre length distribution found in Sample F3 was for fibres found to have lengths between 14.5 mm and 15 mm, this is no longer the case for sample C1. As these longer fibres flow into the compression zone they are significantly degraded which would suggest the reason for drop in overall fibre length distribution from 28.96% to 19.09% for length intervals 12.5 mm – 16 mm. This could account for the higher overall fibre length distribution found in sample C1

for lengths between 8.5 mm – 12 mm, an increase of 17.10 % in F3 to 33.07% in C1. However, if the breakage of long fibres accounts for the shift in peaks from the two results there would expectedly be a higher distribution of shorter fibres found in sample C1, however this is not the case and fibre dispersion data would need to be evaluated.

#### 5.3.4. Fibre Length Distribution Results: C1 – C2

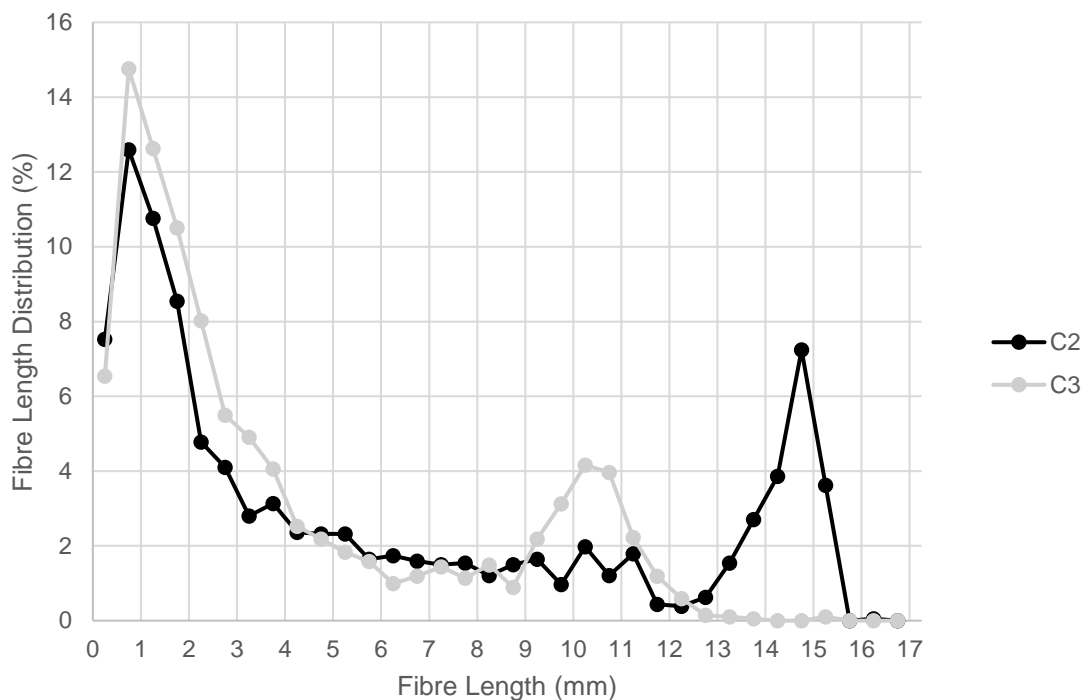


**Figure 5.8. – C1 and C2 fibre length distribution results from screw pull out test.**

Figure 5.8 shows the fibre length distribution plot for sample locations C1 and C2. Firstly, it is interesting to note that both samples C1 and C2 have relatively similar fibre length distributions for measured length intervals between 12.5 mm – 16 mm at 19.08% and 19.59% respectively. However, as anticipated, significant fibre attrition of fibres measured between 5.5 mm - 12 mm has occurred along the compression zone which accounts for the sharp decrease in number average from 8.08 mm in C1 to 5.64 mm in C2. This also accounts for the larger distribution of shorter fibre lengths which the longer fibres have broken down into found between 0 mm and 3.5 mm at 51.11%, an increase of 30.70% for the same

length interval. Conversely, the weighted average for both samples remains relatively the same at 10.48 mm for sample C1 and an increase to 10.50 mm for sample C2. From first inspection it could be suggested sample C1 would have a higher weighted average, however a slight increased difference for C2 of longer fibre lengths specifically between 14.5 mm – 16.5 mm (increase of 3.25%) can impact weighted average results.

### 5.3.5. Fibre Length Distribution Results: C2 – C3

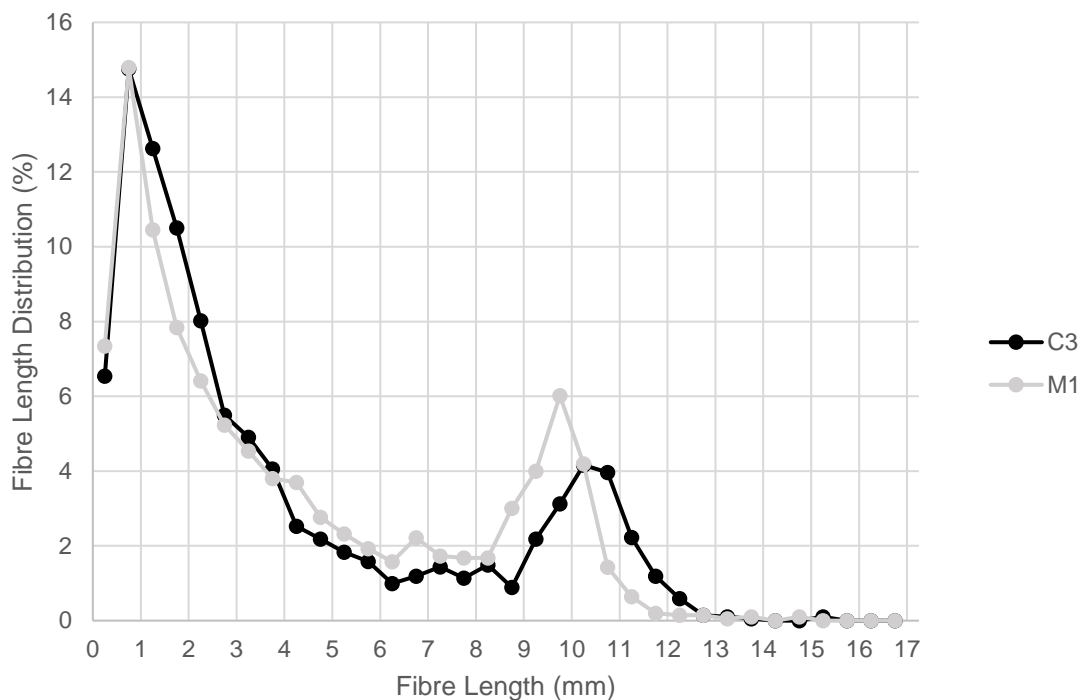


**Figure 5.9. – C2 and C3 fibre length distribution results from screw pull out test.**

The fibre length distribution plot for samples C2 and C3 from screw pull out test 4 is displayed above in Figure 5.9. The majority of the longer fibres found in C2 with lengths between 12.5 mm – 16.5 mm have virtually all broken down into smaller fibre lengths with only 3 fibres being measured to have lengths between 12.5 mm – 13 mm, 2 fibres between 13 mm – 13.5 mm, 1 fibre between 13.5 mm – 14 mm and a final 2 fibres between 15 mm – 15.5 mm. This has led to a significant decrease in both number and weighted average lengths, falling from 5.64 mm and 10.5 mm respectively in C2 to 3.92 mm and 7.25 mm in C3. Upon

further examination of the fibre length distribution plot, the results suggest fibres with lengths of 12.5 mm – 16.5 mm presented in Figure 5.9 for sample C2 have suffered significant attrition and increased the distribution of measured fibre lengths in the ranges of 0 – 4.5 mm and 9 mm - 12.5 mm for sample C3. This suggests that fibre ends are being chipped off as they travel down the flight of the screw towards the end of the compression zone.

### 5.3.6. Fibre Length Distribution Results: C3 – M1

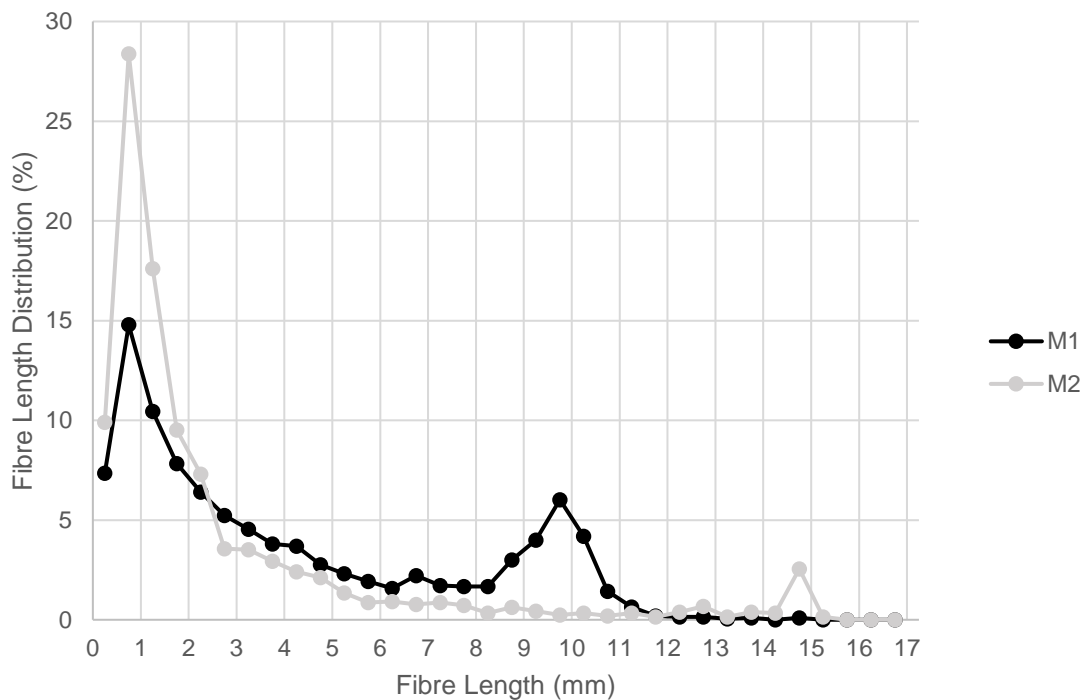


**Figure 5.10. – C3 and M1 fibre length distribution results from screw pull out test.**

The fibre length distribution plot for samples C3 and M1 are shown above in Figure 5.10 taken from a screw pull out test. It appears that both fibre length distribution plots for samples C3 and M1 are relatively similar. This is supported by the alike results for number and weighted averages, 3.92 mm and 7.25 mm correspondingly for C3 and 4.11 mm and 7.06 mm for M1. The results display a shift in fibre length distributions occurred from 9 mm – 11.5 mm in C3 to 8.5 mm – 11 mm in sample M1, again possibly due to the ends of the fibres continuously being degraded. The measured short fibre populations within a length interval

range of 0 mm – 1.5 mm however remain relatively similar evaluated at 33.93% for C3 and 32.59 % for M1.

### 5.3.7. Fibre Length Distribution Results: M1 – M2

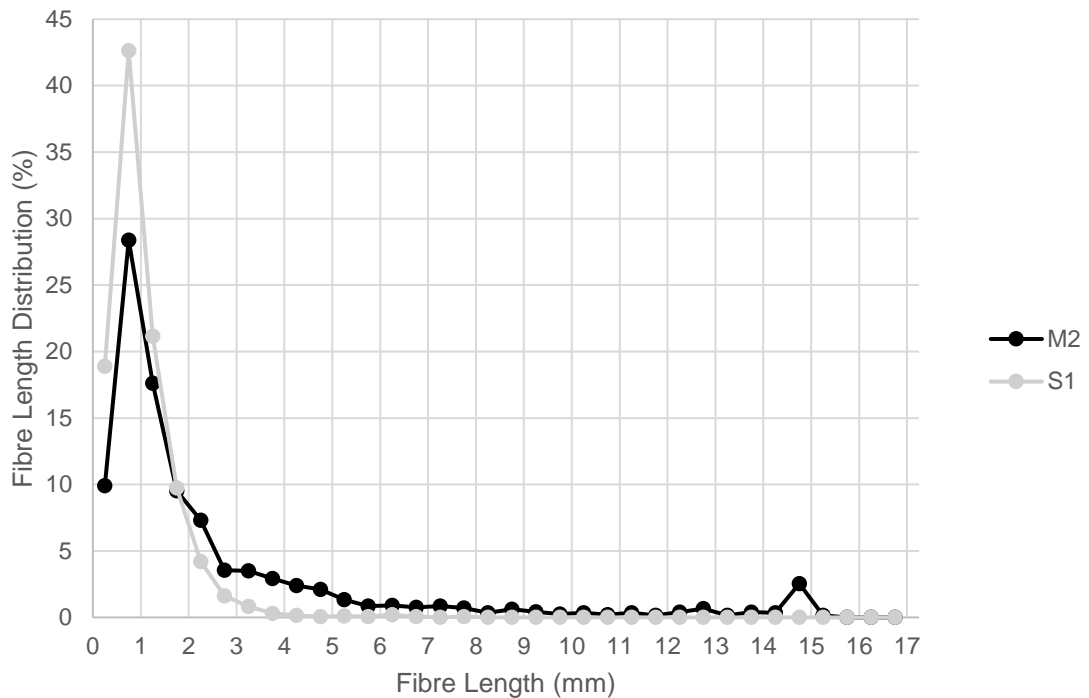


**Figure 5.11. – M1 and M2 fibre length distribution results from screw pull out test.**

The fibre length distribution plots for samples M1 and M2 are displayed above in Figure 5.11. The graph above indicates that the remaining longer fibres (8 mm – 11.5 mm) found at the beginning of the metering zone have virtually all succumbed to fibre attrition with a subsequent increase of overall shorter fibre distributions (0 mm – 3 mm) found at the end of the metering zone. Fibres computed with lengths greater than 3 mm accounted for 47.93% of overall measured fibre length distribution and 52.07% for fibres measured below lengths of 3 mm for M1. However this changes for sample M2, as fibre length distributions for fibre lengths greater than 3 mm is shown to be at 23.71% and 76.29% for fibres less than 3 mm. Although the number average falls by 1.54 mm to 2.57 mm in sample M2, the weighted average decreases only fractionally from 7.06 mm in M1 to 6.65 mm in M2. A small distribution of 2.55% of longer fibre lengths (14.5

mm – 15 mm) are present in sample M2 which accounts for this. This highlights that even as the fibres continuously break along injection moulding process, increasing the amount of short fibres, some fibre bundles are still preserved which can still hold relative significance in terms of final mechanical properties in the injection moulded component.

### 5.3.8. Fibre Length Distribution Results: M2 – Sprue



**Figure 5.12. – M2 and Sprue fibre length distribution results from screw pull out test**

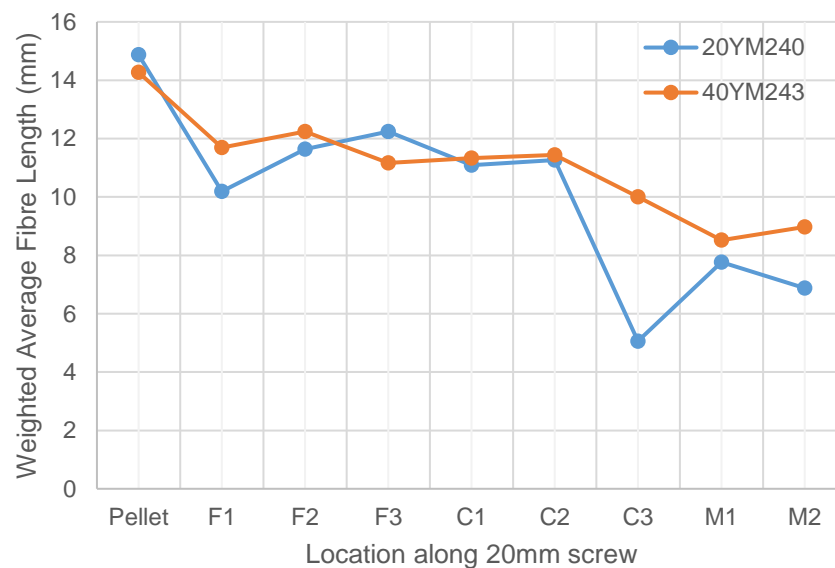
Figure 5.12 displays a fibre distribution plot against fibre length for sample M2 and the nozzle entry sample, where the sample area is located at the closest end to the injection moulding screw. It should be noted that a nozzle sample was not obtained for this particular screw test thus fibre length distribution is evaluated straight from the end of the metering zone to the sprue. As the fibres flow through the constricting geometry of the nozzle, they are subjected to greater shear forces increasing fibre breakage. They are then forced through the very narrow and crowded area of the sprue furthermore intensifying fibre breakage through shear and increased fibre-fibre interaction. This is evident in the 2 plots shown in the

figure above. Any remaining longer fibres with lengths greater than 8 mm found in sample M2 have all been seemingly broken down to shorter fibre lengths as no fibres were measured to have lengths greater than 8 mm in the sprue. From the graph, the nozzle and sprue have evidently had a big effect on fibre breakage along the injection moulding process, increasing the overall fibre length distribution of fibres found between 0 mm – 2 mm from 65.42% in sample M2 to 92.41% in the sprue.

#### 5.4. Summary of All Screw Pull Out Test Results - Arburg Allrounder 270C

##### 5.4.1. Effect of Fibre Content

Screw pull out tests were conducted to evaluate the effect of fibre content at different back pressure levels (2.5, 5 and 7.5 bar) whilst maintaining a constant screw speed of 150 RPM.

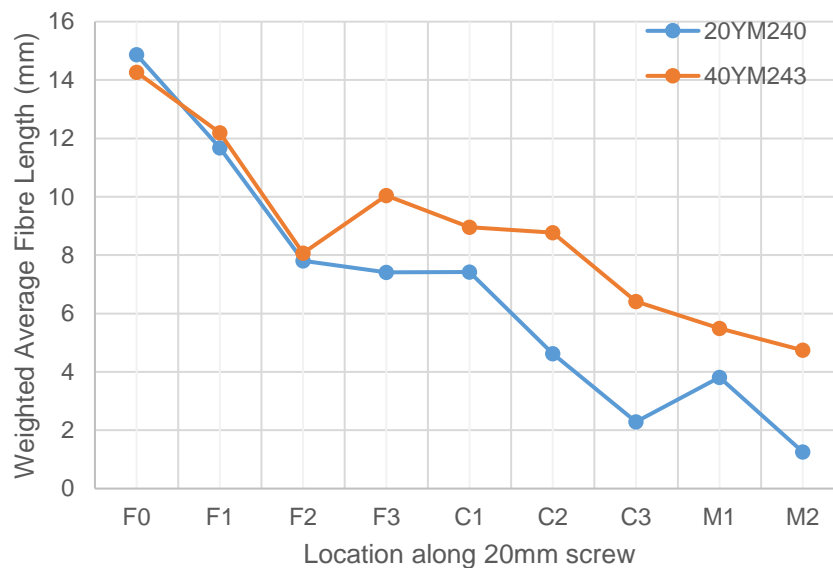


**Figure 5.13. – Effect of fibre content at low RPM (150 RPM) and low back pressure (2.5 bar)**

Figure 5.13 shows a comparison of the weighted average for two different materials with differing fibre contents processed along the injection moulding

process from the initial stage of the material being in pellet form through to the end of the metering zone at M2.

Overall, it can be suggested that for the 40YM243 material there is a gradual attrition process along the injection moulding screw. Compared with the lower weight % glass filled material, 20YM240, there is sharp decrease of weighted average fibre length at F1 and C3 to 10.19 mm and 5.06 mm respectively. However, at both instances the weighted average is seen to increase at the subsequent sample location at F2 to 11.64 mm and M1 to 7.77 mm, indicating that fibre bundles are still intact but were simply not captured during the sample extraction process at F1 and C3. And since the 40YM243 material contains more glass fibres, the likelihood of clusters being captured at each sample location is higher than the 20YM240 material.

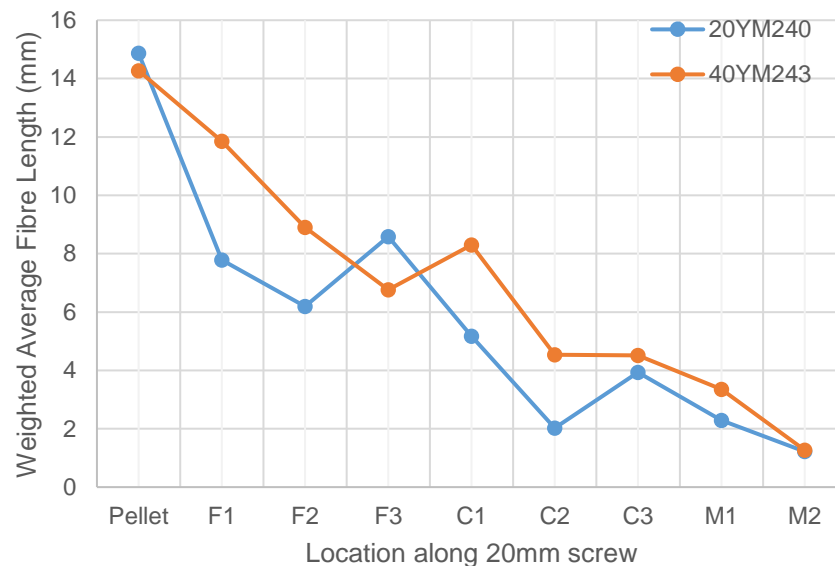


**Figure 5.14. – Effect of fibre content at low RPM (150 RPM) and medium back pressure (5 bar)**

Figure 5.14 displays a similar comparison but each differently weighted material is processed at a higher back pressure of 5 bar whilst the screw speed remains the same at 150 RPM.



Both materials exhibit similarly high levels of fibre breakage along the feeding zone with weighted average values within +/- 0.6 mm of each other. The weighted average drops by 47% and 43% for 20YM240 and 40YM243 respectively from the initial pellet average. As both polymers flow into the compression and metering zones, fibre attrition is clearly more apparent for the 20YM240 material in contrast to the 40YM243 material. Whereas in the higher glass filled material, the rate of fibre breakage appears to decrease from the initial feeding zone region with a final weighted average value of 4.74 mm at sample location M2, a decrease of 41% from F2. The lower glass filled material on the other hand appears to suffer significant fibre breakage with a final weighted average of 1.26 mm, a decrease of 84% from the measured weighted average at sample location F2.



**Figure 5.15. – Effect of fibre content at low RPM (150 RPM) and high back pressure (7.5 bar)**

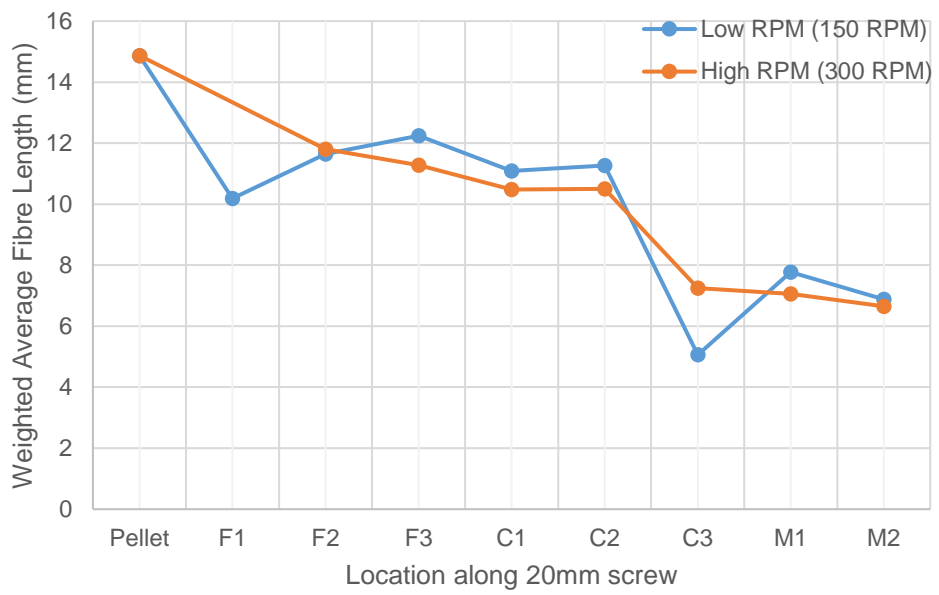
Figure 5.15 shows an assessment of the effect of fibre content on fibre length along the injection moulding process at a back pressure of 7.5 bar and a screw speed of 150 RPM.

Both plots exhibit similar trends of fibre breakage, with both materials weighted average fibre length decreasing significantly to 6.19 mm for 20YM240 and 6.76

mm for 40YM243 along the feeding zone. This drop is achieved at a quicker rate in the lower glass filled material as 6.19 mm is measured at sample location F2 compared to sample location F3 for the corresponding 6.76 mm value for the 40YM243 material before both materials see an increase in weighted average. Again, the weighted average fibre length falls as the fibres travel further along the screw before another increase is observed for both materials, albeit more apparent in the 20YM240 material. Both sets of results appear to have developed similar levels of overall fibre degradation along the injection moulding process at a higher back pressure value as the weighted average is nearly identical for both materials at sample location M2 and are within 0.5 mm of each other.

#### 5.4.2. Effect of Screw Speed

Screw pull out tests were conducted to evaluate the effect of screw speed at different back pressure levels (2.5, 5 and 7.5 bar) processing the same grade material, 20YM240 for all tests.

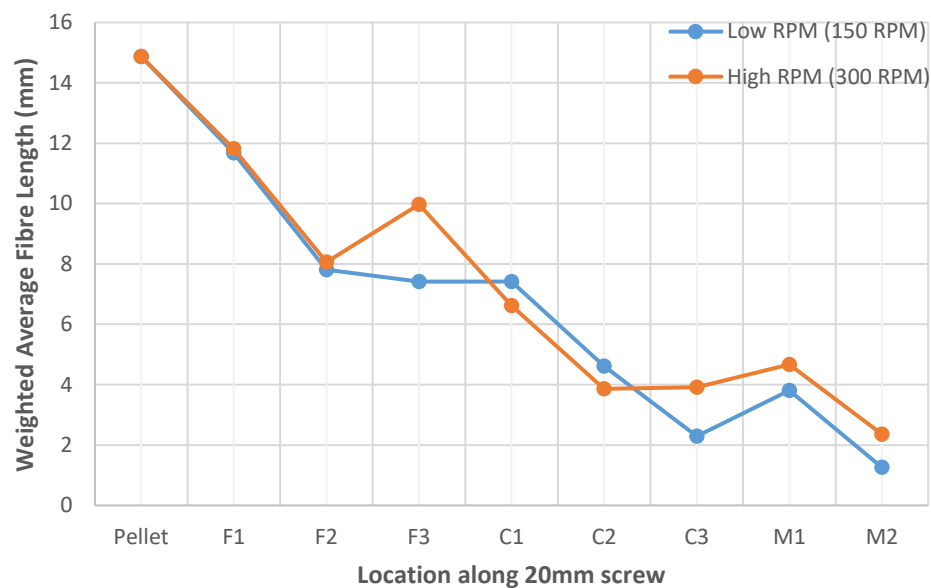


**Figure 5.16. – Effect of screw speed at low back pressure (2.5 bar):  
20YM240**

Figure 5.16 shows a comparison of the weighted average fibre length along an injection moulding screw from the initial glass fibre reinforced pellet through to

the end of the metering zone at sample location M2 whilst evaluating a low and high screw speed at a constant back pressure of 2.5 bar.

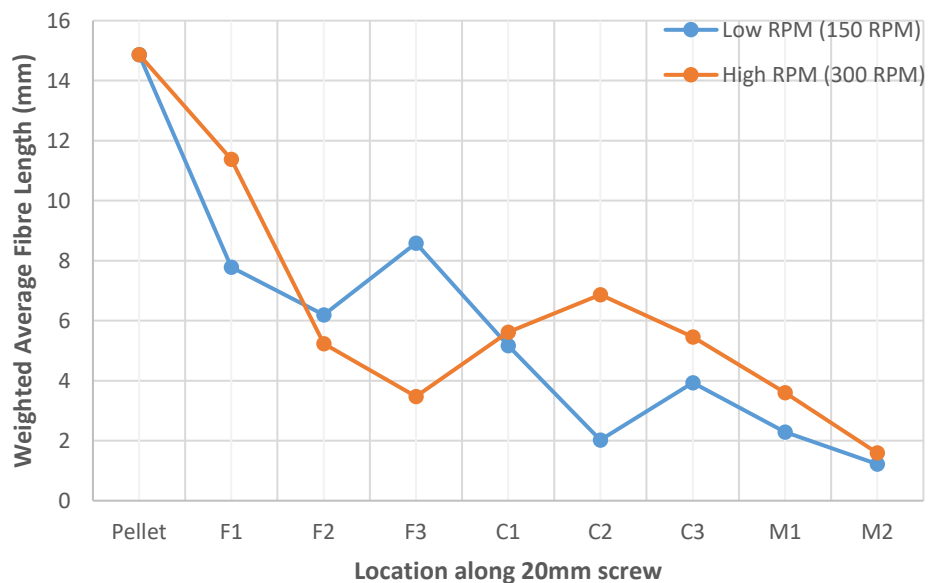
Both plots appear to show comparable weighted average results along the screw evident with a final value of 6.88 mm for results processed at a low RPM and 6.65 mm for results processed at a higher screw speed at sample location M2. This suggests that fibres will suffer considerable breakage irrespective of a higher or lower screw speed. However, two sudden transitions to a lower weighted average fibre length is seen at samples location F1 and C3 for the screw test conducted at a lower screw speed. This could be simply due to clusters of fibres not being captured within the sampling region at that moment in time as their distribution along the screw appears random.



**Figure 5.17. – Effect of screw speed at medium back pressure (5 bar):  
20YM240**

Figure 5.17 displays results from screw pull out tests evaluating high and low screw speeds whilst maintaining a constant back pressure of 5 bar and processing the same material grade, 20YM240.

Much like in the previous evaluation of screw speed at a lower back pressure, both sets of weighted average fibre length are in line with each other. Weighted average results decrease from an initial 14.87 mm to 7.81 mm at sample location F2 before steadying out until C1 where another drop is seen along the compression zone of the screw. The weighted average increases a small amount thereafter at location M1 but again decreases to a value of 1.26 mm at the end of the screw for the screw test performed at a lower screw speed. A similar trend is observed for the screw test completed at a higher screw speed of 300 RPM. However, an increase in weighted average fibre length is observed between sample locations F2 and F3 before decreasing severely from 9.97 mm at F3 to 3.86 mm at C2. Fibre breakage is then seen to stabilise somewhat between sample locations C2 and M1 before reaching a final weighted average length akin to the screw test performed at 150 RPM of 2.36 mm at M2.



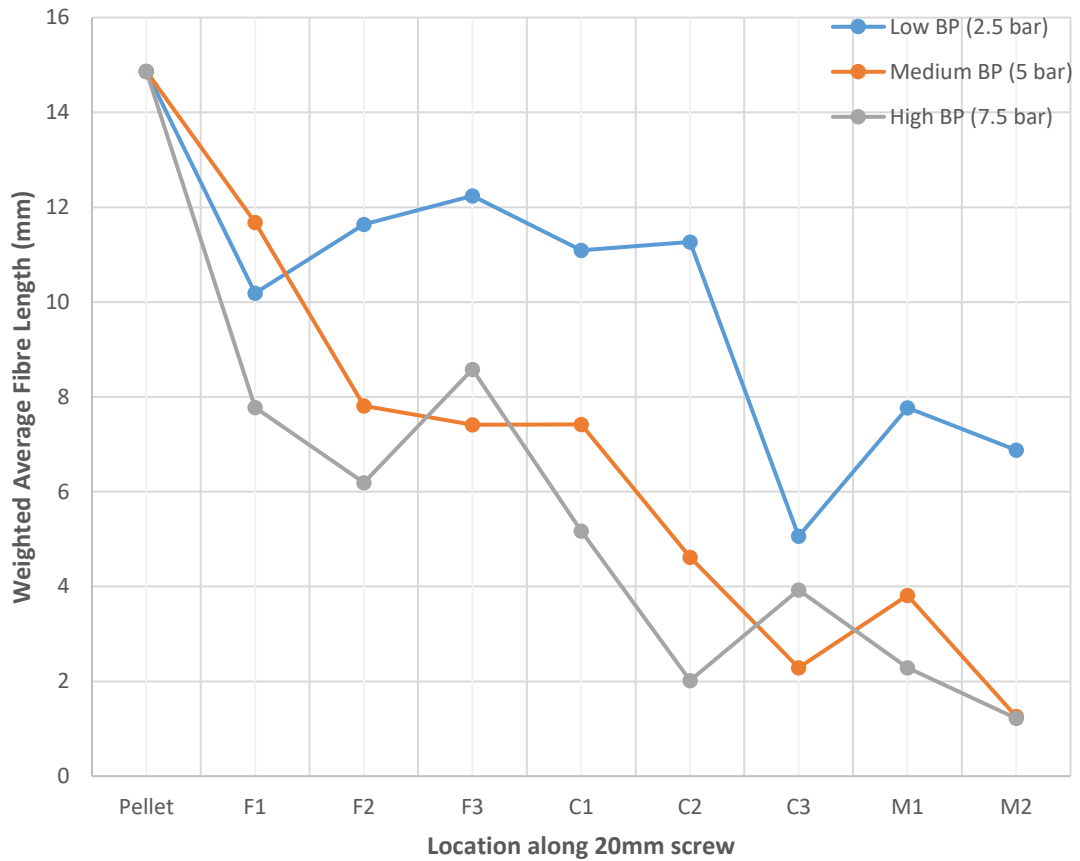
**Figure 5.18. – Effect of screw speed at high back pressure (7.5 bar):  
20YM240**

Figure 5.18 exhibits the final evaluation of the effect of screw speed on fibre length distribution along an injection moulding screw. Results were obtained after two screw tests were performed, one at a high screw speed of 300 RPM and the other at a lower speed of 150 RPM. Both tests processed the same grade of material as before, 20YM240.

As in other studies assessing screw speed, weighted average results suggest altering the speed of the screw does not improve or aggravate overall fibre length along the injection moulding process. Both sets of data begin at weighted average fibre length values of 14.87 mm, and as the glass fibre reinforced polymer is processed along the screw at either screw speed, fibres undergo similar levels of attrition as the weighted average fibre length at the end of the screw is 1.22 mm for the 150 RPM test and 1.59 mm for the 300 RPM test. On the other hand, weighted average fibre length appears to fluctuate quite noticeably in between the start and end of the screw with increases and decreases seen for both the higher screw speed and the lower. This is probably due to the dispersion of clusters along the screw being considerably uneven leading to multiple clusters being unexpectedly present in sample locations where less clusters were present in the preceding sample location.

#### **5.4.3. Effect of Back Pressure**

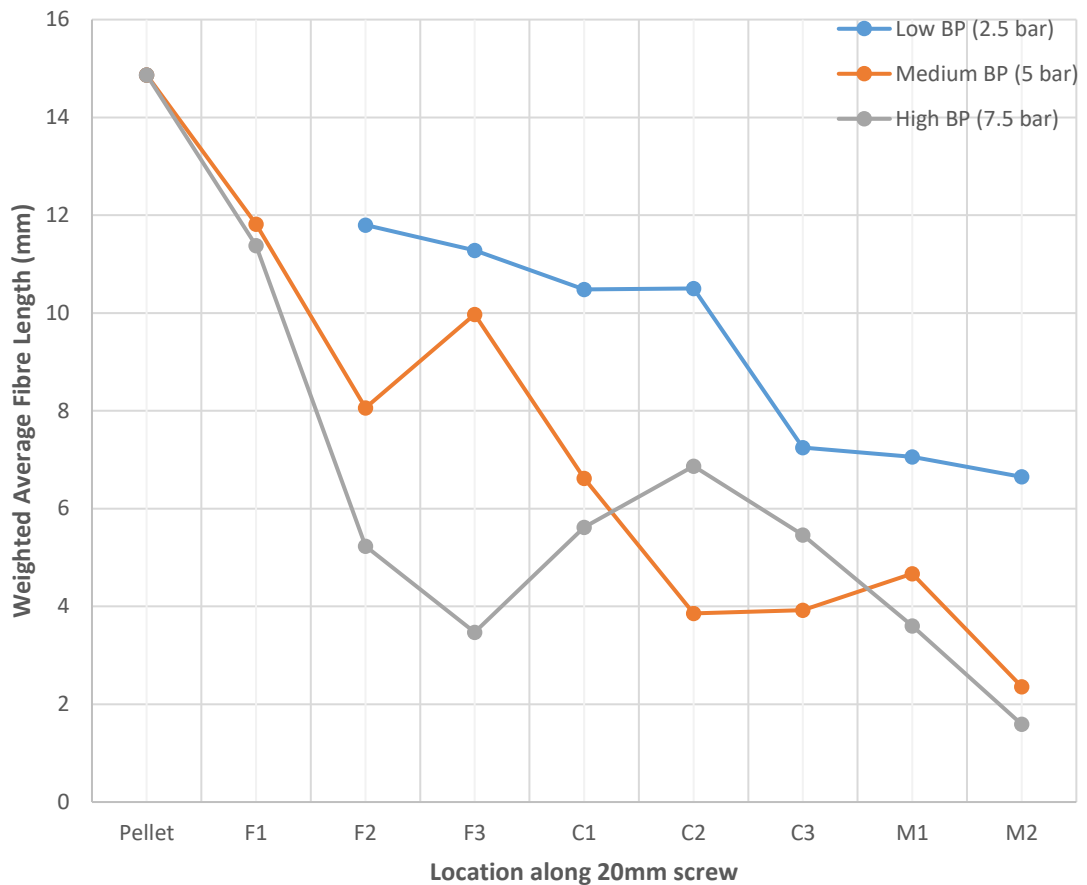
Screw pull out tests were performed to examine the effect of low (2.5 bar), medium (5 bar) and high (7.5 bar) back pressures at varying screw speeds (150 RPM and 300 RPM). The same grade of material, 20YM240, was processed for these investigations.



**Figure 5.19. – Effect of back pressure at low RPM (150 RPM): 20YM240**

Figure 5.19 presents a comparison of different back pressures at a low screw speed of 150 RPM and their effect on overall fibre length along the injection moulding process.

Results clearly indicate that back pressure does indeed affect the weighted average fibre length as fibre lengths are suggested to be much more preserved at a lower back pressure of 2.5 bar (6.88 mm) by the time they reach the end of the metering zone compared to a higher back pressure of 5 bar (1.26 mm) or 7.5 bar (1.22 mm). Fibre length degradation is shown to be of a similar level for the higher back pressures of 5 bar and 7.5 bar as the plots are very much in line with each other and both equate to a final weighted average fibre length within 0.4 mm of each other.



**Figure 5.20. – Effect of back pressure at high RPM (300 RPM): 20YM240**

Figure 5.20 presents a final evaluation of back pressure on weighted average fibre length but at a higher screw speed of 300 RPM for the same glass fibre reinforced material used previously.

Once more, back pressure comparison results at a low screw speed seem to match those seen at a higher injection moulding screw speed. Glass fibres appear again to break significantly when exposed to higher back pressures of 5 bar and 7.5 bar. This is evidenced by the numerical results computed at the end of the screw at sample location M2 with weighted average fibre length values of 2.36 mm and 1.59 mm respectively. Whereas for glass fibres processed at a lower back pressure of 2.5 bar, fibre breakage is less evident as the weighted average fibre length at location M2 is 6.65 mm, considerably higher than the tests performed at higher back pressures.

## **6. Discussion**

### **6.1. Experimental Technique**

The variance shown in fibre length measurement methods in Chapter 2 highlight the significance of a standardised measurement technique for fibre length investigations as it creates a certain amount of uncertainty with regards to comparability, repeatability, and precision of the various fibre length evaluations.

A manual fibre length measurement system was evaluated and developed for this study based on past and present methods to measure the fibre length distributions within long glass fibre reinforced injection mouldings. The method is able to produce statistically representative data which is used to create comparative datasets of samples along the injection moulding process.

The method was assessed and showed fibre length results can be precisely generated following a manual sample preparation and measurement method. This manual measurement system was also benchmarked against other automated systems found on the market as of 2018 and shown to provide much more accurate and reliable representations of fibre length distributions within long glass fibre reinforced samples.

However, the manual technique utilised in this study is relatively laborious and requires manual input to handle, prepare and measure a glass fibre sample. Also, the sample extraction method utilised in this study will lead to additional cutting of fibres as samples are cut from their location given specified dimensions. This could unavoidably lead to a bias in shorter fibres and a misrepresentation of the measured fibre length distribution within the sample. This should be accounted for and the data accordingly corrected if a more accurate estimate of fibre length distribution within an injection moulded samples is to be attained.



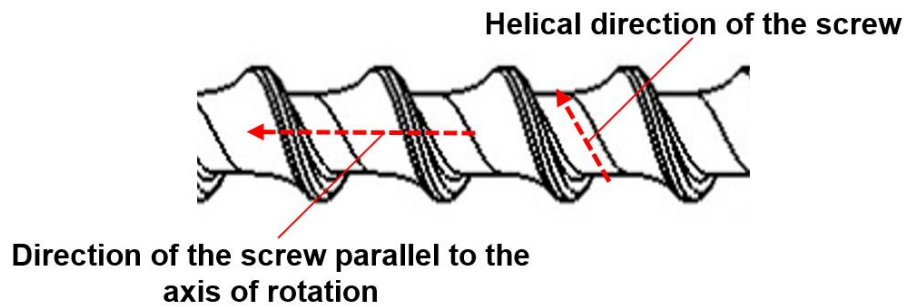
### **6.1.1. Compensation for Cut Sample Size**

For fibre length distributions, 24 mm samples in length were extracted from various locations along the injection moulding process, all taken from either the sprue, nozzle or screw of an injection moulding machine. The correction methods proposed in Chapters 6.1.2 – 6.1.4 are very specific to the technique the data was collected in this investigation.

Other studies of fibre length distributions of samples along the screw which also extract their samples in a similar fashion would have also suffered from cut fibres and required a correction, but no correction was proposed to overcome the cutting of fibres at the sample edge. However, the need for a correction method is governed by the sample preparation method which may have been tailored to avoid this breakage. For example, Kunc et al. (2007) developed a method of using an epoxy plug to collect all the fibres from a small sample region of the fibre matrix which remained after pyrolysis of which the sampling method required its own correction method. However, as the fibres get shorter or as the sample gets larger, the need for correction decreases.

The original fibre lengths are quite long when in pellet form (15 mm) in comparison to the sample size (24 mm) and since the extraction process involves the cutting of polymer material from the screw channels, nozzle or sprue to achieve this sample size, it will inevitably lead to cutting of fibres at the sample edges. This additional breakage should be accounted for and the data accordingly corrected if an accurate estimate of fibre length distributions within the screw, nozzle or sprue is to be achieved.

The helical direction and direction of the screw parallel to the axis of rotation are defined and highlighted below in Figure 6.1.

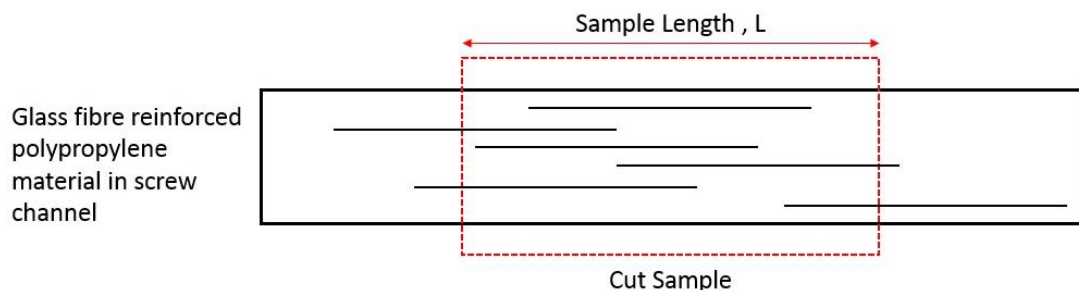


**Figure 6.1. – Helical direction and direction of the screw parallel to the axis of rotation**

### 6.1.2. 1D Correction for Cut Sample Size

In collaboration with Autodesk Moldflow, a linear 1D theory of fibre breakage probability was developed with the intention of correcting resultant length distributions obtained from the sprue, nozzle and screw of an injection moulding machine.

Considering the population of fibres of length 16.75 mm +/- 0.25 mm existing in the screw channels before extraction. (These were the longest fibres observed in the F2 measured sample of the 20YM240 material processed in screw test 4). Of these long fibres in the screw channel, some will fall entirely within the cut 24 mm sample, while others will lie across the sample cut boundary and will be cut during the sample extraction process and therefore will appear in the measurement data as shorter fibres as depicted in Figure 6.2.



**Figure 6.2. – Example of glass fibres falling within and across the sample cut boundary.**

Given that the sample length extracted from the screw channel is denoted by  $L$ , and that this sample length is greater than the length of the longest fibre found in the sample, then the probability ( $P_l$ ) of a fibre of length  $l_l$  (where the centroid of the fibre is located within the sample region) being sliced during sample extraction and having only some fragment of the fibre present in the removed sample is shown in Equation 6.1. This probability is derived by assuming that all fibres are aligned along the screw channel path in the helical direction of the screw

$$P_l = \frac{l_l}{L}$$

**Equation 6.1.**

The probability of a fibre of length  $l_l$  surviving the sample extraction process and being fully present within the sample is defined in Equation 6.2.

$$1 - P_l$$

**Equation 6.2.**

Therefore, the population of measured fibres will contain a combination of whole fibres of length  $l_l$  in addition to fragments of such fibres which spanned the sample cut boundary (plus fibres and fragments originating from fibres of other lengths). Some of the fibre fragments measured will also be from fibres which had their centroid outside the cut sample region.

Taking into account the fibres of the longest length bin (16.75 mm +/- 0.25 mm), if the number of fibres which were measured to have a length  $l_l$  is denoted by  $M_l$ , then the true number of fibres of length  $l_l$  which had their centroids within the cut sample region before sample cutting is governed by Equation 6.3.

$$N_l = \frac{M_l}{1 - P_l}$$

**Equation 6.3.**

Substituting  $P_I$  in Equation 6.3 leads to Equation 6.4.

$$N_I = \frac{M_I}{1 - \frac{l_I}{L}}$$

**Equation 6.4.**

However, the correction defined in Equation 6.4 only accounts for the number of fibres in the longest length bin but for all smaller length bins, the measured population of fibres at any given length includes fibres fragments of fibres which had longer lengths before sample extraction.

Inevitably, the measured population of glass fibres will contain fibres that have been cut during the sample extraction process. Before cutting the sample, some fibres would have had their centroids within the sample length area whilst others would have had their centroids outside the sample area whilst having some fragment of the fibre within the sampling region.

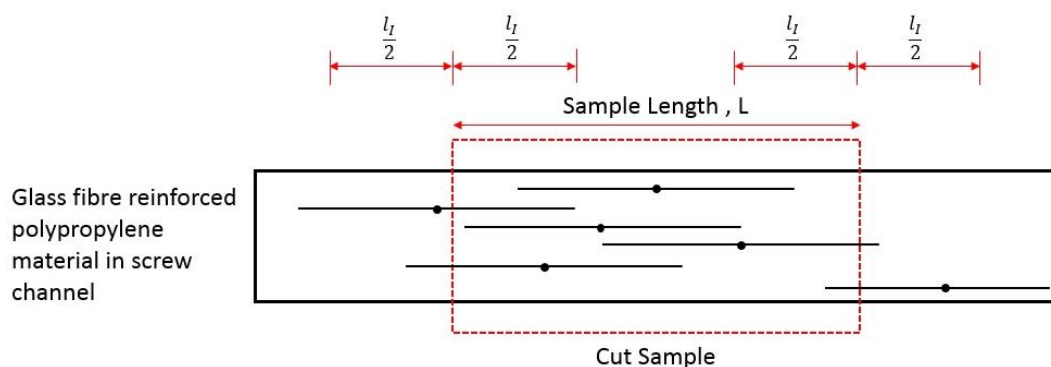
Ideally, one could assume that the fibre fragments created from the cutting of fibres of length  $l_I$  will create a uniform distribution of lengths spanning from zero to  $l_I$ . But this assumption relies on a random, well dispersed population of fibres in the screw channel. This is certainly not the case as evidenced by fibre dispersion results through  $\mu$ -CT, which show fibres are still in ordered bundles which originated from individual pellets along the screw, even more so in the early stages of the injection moulding process (feeding zone). For that reason, an alternative assumption may be made that the length distribution of the fibre fragments created is in proportion to the distribution of shorter fibres that were measured.

Additionally, the number of fibre fragments which are created from the fibres of length  $l_l$  is governed by Equation 6.5.

$$2N_l P_l$$

**Equation 6.5.**

Where  $P_l$  is the probability of a fibre of length  $l_l$  (where the centroid of the fibre is located within the sample region) being cut during the sample extraction process. This is multiplied by a factor of 2 since each cut fibre will yield two fragments, generally consisting of one which is greater than  $\frac{l_l}{2}$  in length and another which is less than  $\frac{l_l}{2}$ , depicted in Figure 6.3.



**Figure 6.3. – Example of glass fibres falling within and across the sample cut boundary creating two fragments.**

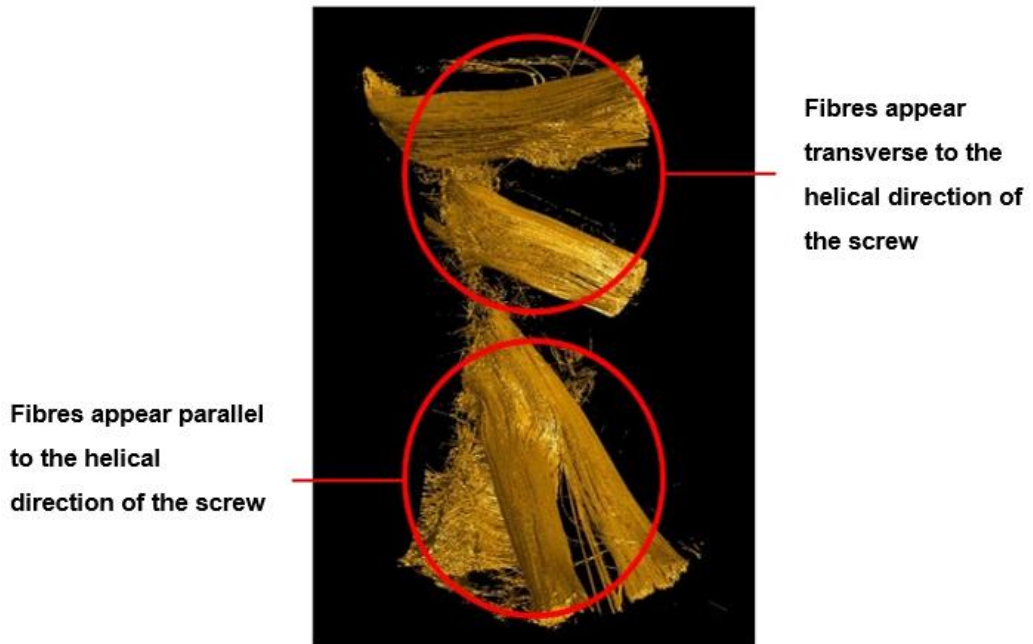
In view of the fact that only glass fibres which have had their centroids within the sampling region have been considered, the shorter fibre fragments from the fibres will be outside the sampling region (and so not collected for measurement). Nevertheless, there will be an equivalent number of short fibre fragments in the sampling region of length  $l_l$  where their centroid is located outside the cut sample area. Therefore, the number of fibre fragments in the measured sample will be as though both fragments from each fibre of length  $l_l$  with its centroid inside the sample region have been included in the cut sample. It is assumed that these

fibres will be distributed amongst the bins of shorter fibre lengths in the same proportions as their measured population distribution.

The creation of these fibre fragments means that the total number of fibres measured at any length  $l_i$  will include fibre fragments from fibres of greater length. These additional contributions need to be removed if a true representation of fibre length distribution which existed prior to the sample extraction process is to be established. Fibres measured within the longest length bin (16.75 mm +/- 0.25 mm) do not necessitate a correction for fibre fragments created from longer fibre lengths as their lengths have not been reduced from the sample extraction process. And so, a sequential process is employed beginning from the length bin containing the longest fibres and applying a correction to the number of measured fibres of all length bins of shorter fibres. This correction is then applied progressively to each length bin in descending length order.

### **6.1.3. 2D Correction for Cut Sample Size**

The previous 1D correction (Chapter 6.1.2) assumed that fibres are fully aligned in the helical direction of the screw. However, due to the relatively large screw channel width (approximately 20 mm) some fibres were found to be somewhat inclined away from the helical direction as evidenced by  $\mu$ -CT in Figure 6.4.

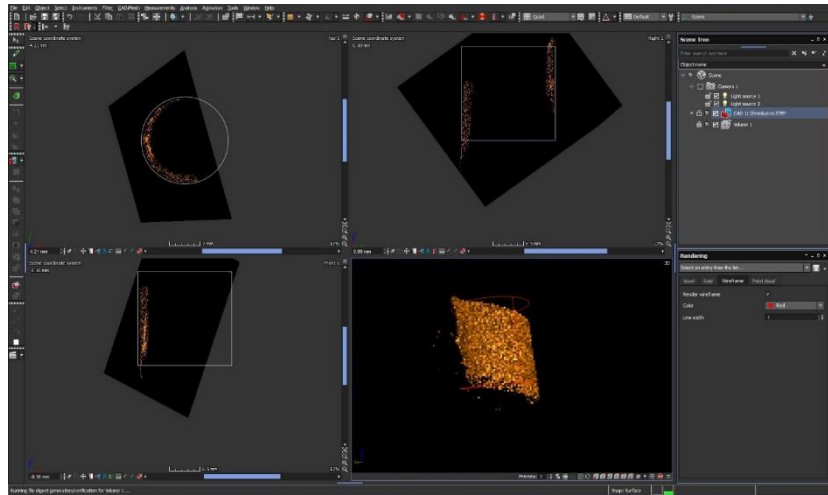


**Figure 6.4. – Example  $\mu$ -CT of fibres appearing parallel and transverse to the helical direction of the screw.**

This can be accounted for by considering the projection of the fibre length in the helical direction rather than the full fibre length and is done according to the cosine of the average inclination angle measured for each sample location.

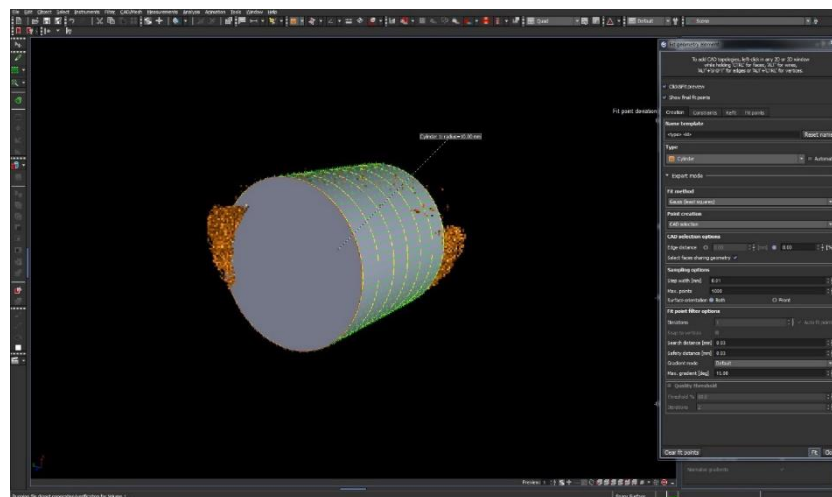
This can be achieved via the analysis of slice data from the glass fibre sample which is obtained after a sample is scanned and reconstructed via  $\mu$ -CT. To obtain slice data the sample must be ‘unrolled’ using Volume Graphics software due to the inability of being able to create a plane that follows the helical screw channel path and the curved nature of the sample.

A CAD cylinder reference geometry is first imported in VG Studio Max 3.2.0. The geometry is based on the original injection moulding machine barrel geometry (20 mm in diameter). The cylinder is locked into position and rendered as a wireframe for clearer visualization of the differences between the sample and the reference geometry as shown in Figure 6.5.



**Figure 6.5. – CAD cylinder wire positioned around glass fibre reinforced screw sample.**

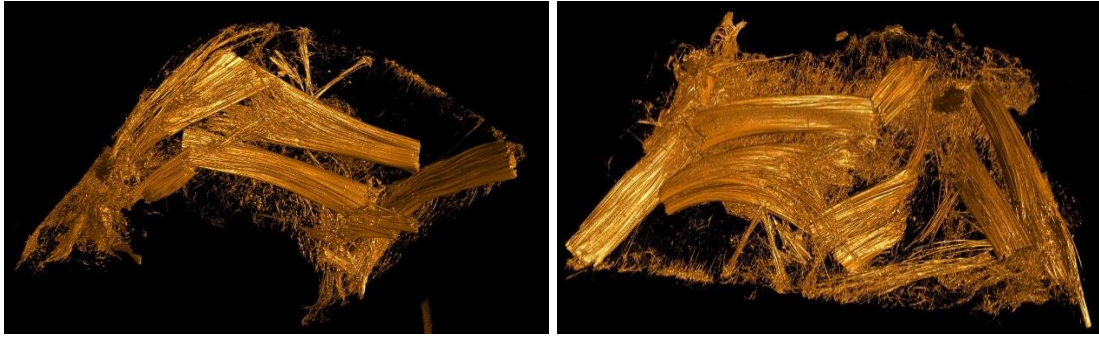
The CT dataset is rotated and translated, via numerical input, so that it locates within the cylindrical reference geometry. Using a measurement tool, a reference cylinder is created based on the original CAD geometry as displayed below in Figure 6.6.



**Figure 6.6. – Example of a CAD cylinder fitted to a glass fibre reinforced screw sample.**

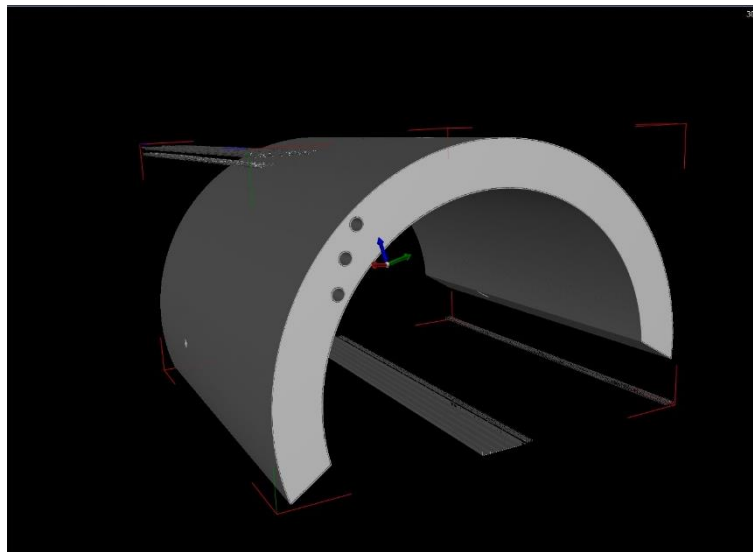
The sample is then unrolled and the unrolled data can then be resampled to create a stand-alone dataset with a comparison between the two shown below in Figure 6.7.





**Figure 6.7. – Example of a CAD cylinder fitted to a glass fibre reinforced screw sample before unrolling (left) and after unrolling (right)**

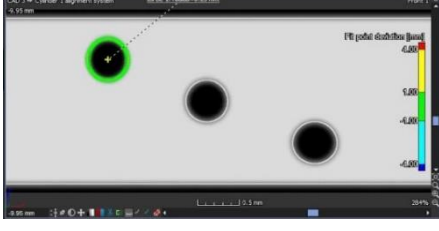
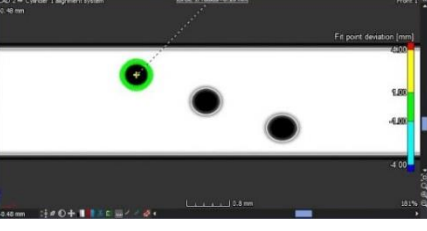
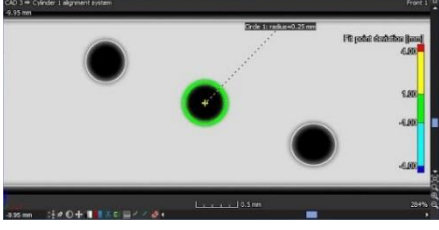
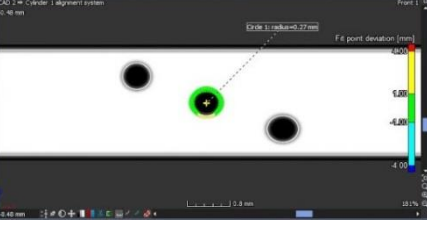

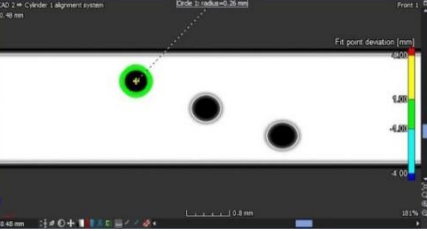
An idealised computer aided design (CAD) model, pictured in Figure 6.8, was imported into VG Studio Max to assess the effects of unrolling on the glass fibres themselves as there may be a concern the software stretches or compresses the glass fibres during the unrolling process.



**Figure 6.8. – Idealised CAD model imported into VG Studio Max**

The CAD model was based upon a feeding zone screw sample and defined with a 20 mm diameter and 4 mm wall thickness consisting of holes (0.25 mm in diameter) punched along the screw and also transverse to the screw in 2 axes.

Because the channel height (4 mm) is relatively small compared to the cylinder (screw) diameter, the amount of stretch introduced by the unrolling is minimized. However, stretching in one direction will alter the angles measured. A comparison was made between unrolling with a 20 mm CAD cylinder that would fall on the top surface of the screw channel height closest to the barrel and a 16 mm CAD cylinder diameter that would fall half-way between the top and bottom surfaces of the screw channel height, so that some fibres are slightly stretched and some are slightly compressed by the unrolling.

16 mm CAD unroll (middle of screw channel height)	20 mm CAD unroll (top of screw channel height)	Fit circle dimensions (Original hole = 0.25 mm)	
		Top (closest to the barrel surface)	
		16 mm	20 mm
		0.25 mm	0.26 mm
		Middle	
		16 mm	20 mm
		0.25 mm	0.27 mm
		Bottom (closest to the screw surface)	
		16 mm	20 mm
		0.26 mm	0.29 mm

**Table 6.1. – Results comparing diameter of imported CAD cylindrical geometry during unrolling**

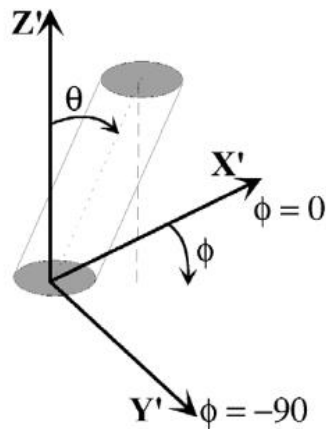
The results of the comparison (presented above in Table 6.1) show there is slight ovality present in the unrolling of the idealised CAD geometry using a 20 mm fitted cylinder, but even less so when unrolling at the middle of the sample between the top and bottom surfaces using a 16 mm fitted cylinder. This suggests the software maintains the geometry of the fibres with a high degree of reliability

enabling an accurate measurement of the inclination of fibres along the screw channels helical path. The distortion of the fibres when unrolling in the compression and metering zones (smaller screw channel depths) is even less apparent due to the presence of shorter fibres and the fibre bundles being predominantly dispersed.

Depending on the location of the screw sample, a corresponding CAD geometry is imported into Volume Graphics for the unrolling process. For feeding zone samples located within a screw channel depth of approximately 4 mm, a 16 mm CAD cylinder is selected. A 17.5 mm CAD cylinder is chosen for compression samples where the channel depth ranges from approximately 4 mm to 1.5 mm. For metering zone samples an 18.5 mm CAD cylinder is imported for the unrolling where channel depth is roughly 1.5 mm.

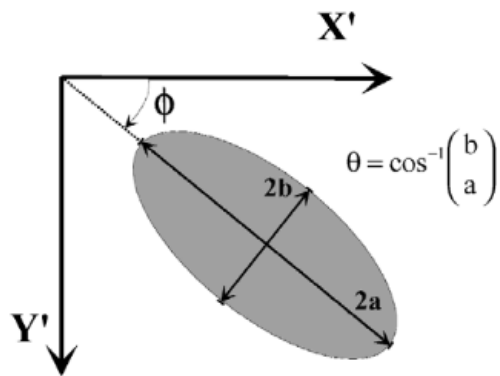
An image stack of the unrolled sample is generated taking slices of the sample (0.082 mm apart) along the length of the sample. Three images are selected from the image stack for further analysis. Depending on the amount of images produced from the image stack, one image is taken from the middle of the sample and two from either end close to the location from where the sample was cut (specifically one-tenth of the way in from either side). The three images are then imported into LabVIEW Vision Assistant (VA) to be processed where the inclination angle can be calculated from the elliptical footprint of the fibres, and also the clusters. (Clusters are defined as having a width greater than 20 microns).

The orientation of a single fibre can be defined by the angles  $\varphi$  and  $\theta$  (Advani and Tucker III 1987). The angle phi ( $\varphi$ ) is defined as the angle the projection of the fibre in the XY plane makes with the  $x$  – axis and theta ( $\theta$ ) is the angle which the fibre makes with the  $z$  –axis perpendicular to the sectioned surface as visualised in Figure 6.9.



**Figure 6.9. – Definition of the orientation angles from the fibres elliptical footprint (Hine and Duckett 2004)**

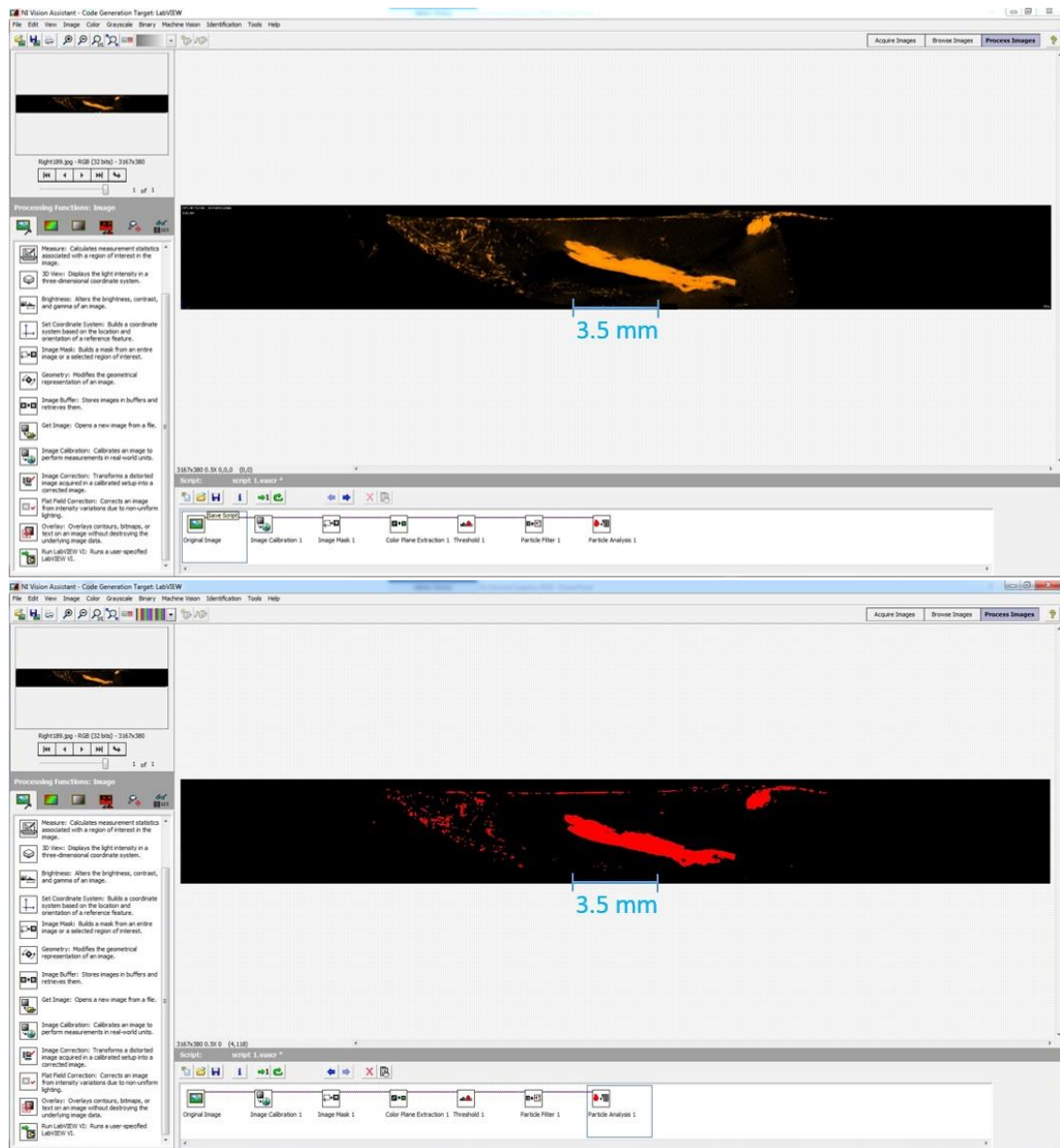
The inclination angle theta ( $\theta$ ) can be calculated by Equation 6.6 which is derived from the elliptical footprint of the fibre as presented in Figure 6.10. The measurements signify the major axis length  $2a$ , and the minor axis length  $2b$  of the fibre ellipse (Hine and Duckett 2004).



**Figure 6.10. - Determination of the orientation angles from the fibres elliptical footprint (Hine and Duckett 2004)**

$$\theta = \cos^{-1} \frac{b}{a}$$

**Equation 6.6.**



**Figure 6.10. – Image slice imported into LabVIEW VA pre particle analysis (top). Image slice post particle analysis (bottom).**

A labview script was created to analyse the inclination of fibres for all samples extracted along the injection moulding screw, presented in Figure 6.10. The sliced image is imported into Volume Graphics before a number of processing functions are performed, including calibrating the image, thresholding, and an image mask to remove any unwanted data that was imported along with the image such as the scale bar, image file name etc. Next a particle filter function is applied to separate and define individual fibres and clusters before a particle analysis is executed which outputs the calibrated cross sectional area and minor/major elliptical axis for each identified fibre. From this information the

inclination angle can be calculated for each individual fibre/cluster. The cosine of each inclination angle is computed for each fibre across all 3 image slices leading to an average cosine theta value

A weighting factor according to the cross sectional area of each fibre is also applied to the cosine theta value for each fibre as a larger cluster will have more significance on length distribution data with regards to the probability of it being cut during sample extraction compared to an individual fibre. The cross sectional area for each fibre is divided by the sum of cross sectional areas for that particular sample. This value is multiplied by the fibres cos theta value and the sum of all these values in the sample generates a final average cos theta value which can be used to modify the length in the probability calculation.

The probability of a fibre of length  $l_i$  (which had its centroid within the sample region) being cut during the sample extraction and having only some fragment of the fibre present in the cut sample was originally defined in Equation 6.1. However, this probability needs to be modified according to the length which is projected into the helical direction, described in Equation 6.7 below.

$$P_i = \frac{l_i \times \cos(\theta)}{L}$$

**Equation 6.7.**

Consequently, the probability of a fibre of length  $l_i$  (which had its centroid within the sample area) being cut during sample extraction is now reduced for the reason that the projected length in the helical direction is reduced.

#### **6.1.4. Proposed Correction Method for Cut Sample Size**

The total proposed correction sequence for the analysis of fibre length distribution in injection moulded screw, nozzle and sprue samples is described as follows:

For each fibre length bin ( $l$ ), in descending order starting from the longest length bin:

1. Estimate the number of fibres of that length which existed in the screw channels prior to sample cutting (Equation 6.8):

$$N_l = \frac{M_l}{1 - \frac{l \times \cos(\theta)}{L}}$$

**Equation 6.8.**

2. Estimate the total number of fibre fragments created by sample cutting from fibres of that length (Equation 6.9):

$$2N_l \frac{l \times \cos(\theta)}{L}$$

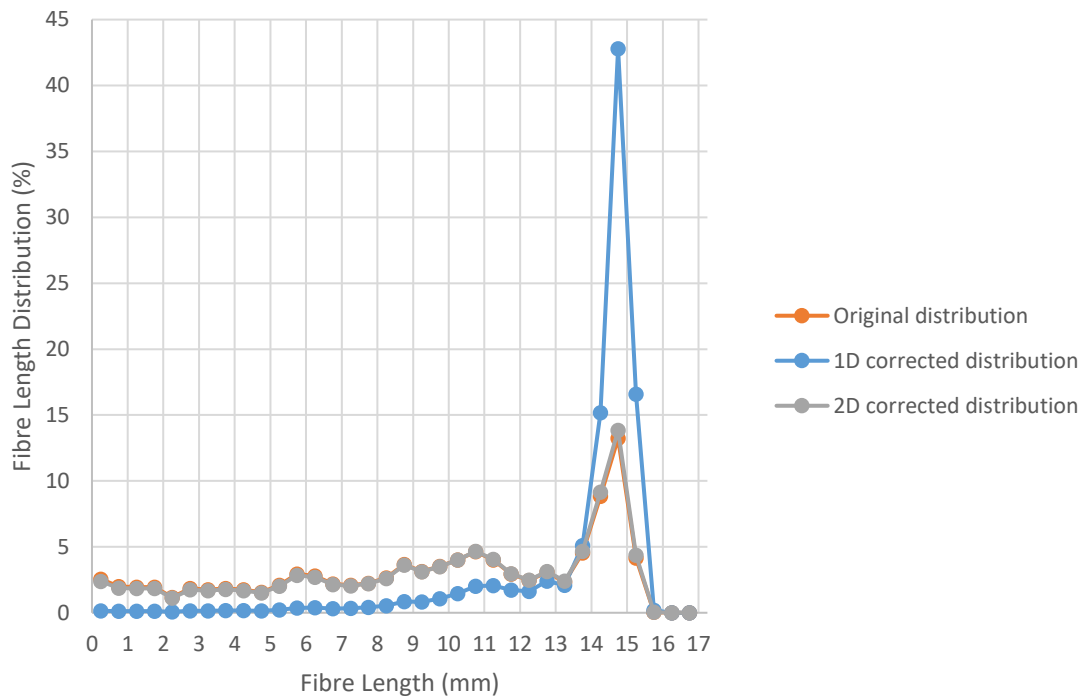
**Equation 6.9.**

3. Subtract these fibre fragments from the bins of all shorter length in proportion to the current number of fibres in those bins.

This method could be extended into 3D but due to the constricting nature of the screw channel height on fibre alignment, which becomes more prevalent further along the screw, assumed inclination in the third direction is negligible.

### **6.1.5. Review of Correction Methods for Cut Sample Size**

The fibre length distribution of screw sample F2 (taken from the feeding zone of screw test 4) obtained after a 1D and 2D correction procedure is applied and compared against the raw (uncorrected) distribution result in Figure 6.10 below.



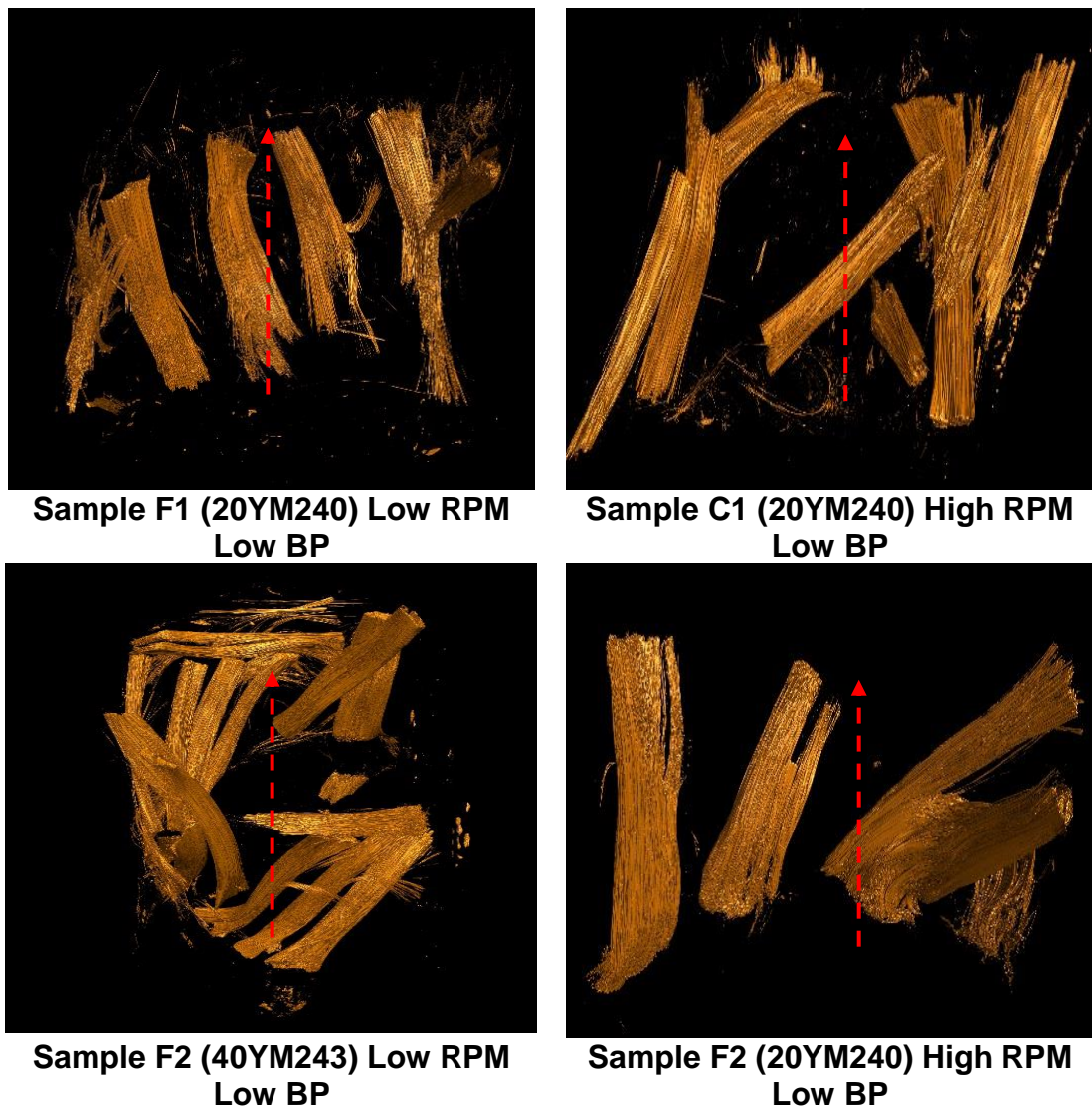
**Figure 6.11. – Comparison of Original, 1D and 2D corrected fibre length distribution results (F2 Screw Test 4).**

As can be seen from this comparison, the difference in outcome due to the 1D correction for sample cutting is significant. Whereas in the raw fibre length distribution data, the length average was 9.72 mm and the weighted average length was 11.81 mm, in the 1D corrected data the length average is 13.80 mm and the weighted average is 14.16 mm. However, minimal variance in fibre length distribution data is seen between the 2D correction and the original distribution data set. This suggests either all fibres are perfectly perpendicular to the helical direction or there is an error in the orientation data obtained and applied to the 2D correction. These results are similar across all sample locations for screw test 4 as shown in Appendix 2.2 where a further comparison of original, 1D and 2D corrected fibre length distribution results are made for samples F3, C1, C2, C3, M1, M2 and S1.

The original 1D correction assumes all fibres are aligned parallel to the helical direction. However, a great deal of pellets/clusters are shown to be inclined more in the direction of the screw (perpendicular to the helical direction) in the feeding and initial compression stages from  $\mu$ -CT results shown in Figure 6.12. The screw



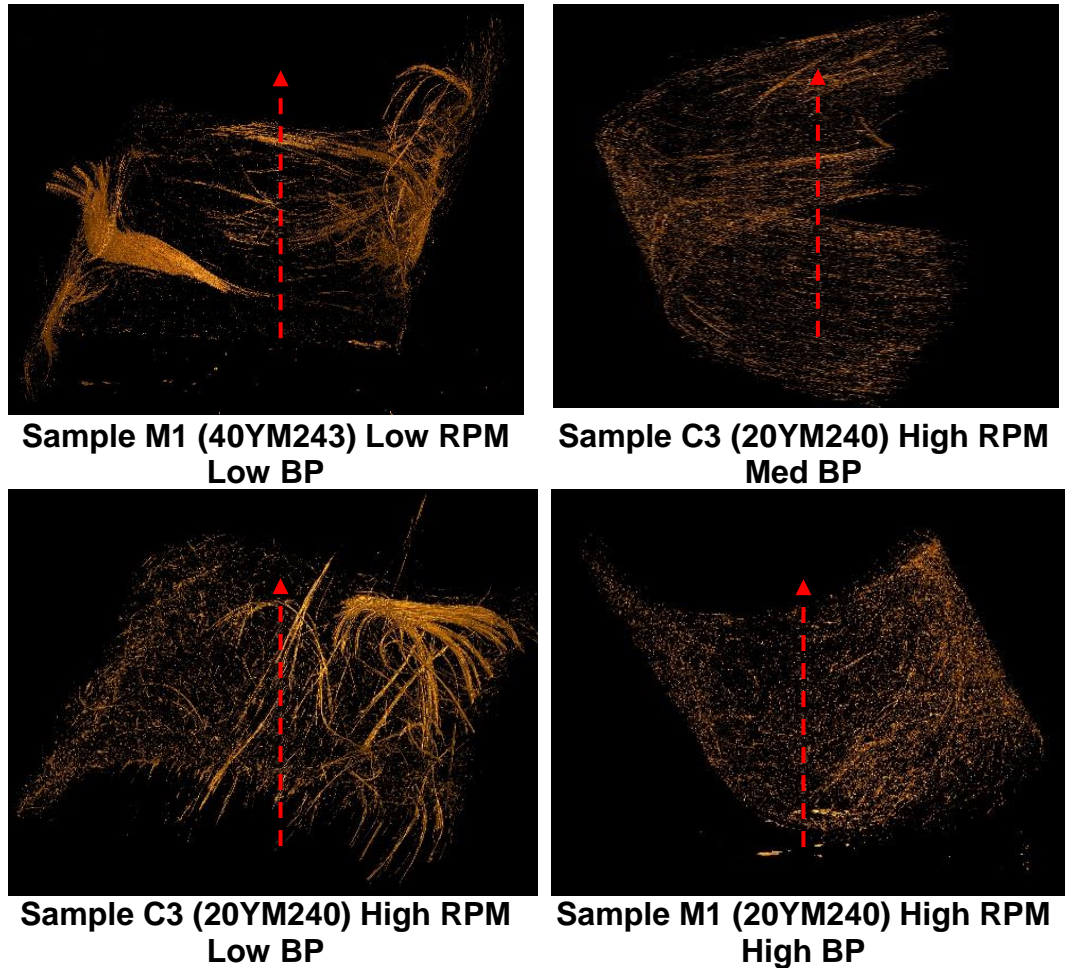
direction parallel to the axis of rotation for each sample is indicated with a red arrow.



**Figure 6.12. – Example of clusters found in various samples aligned perpendicular to the helical direction**

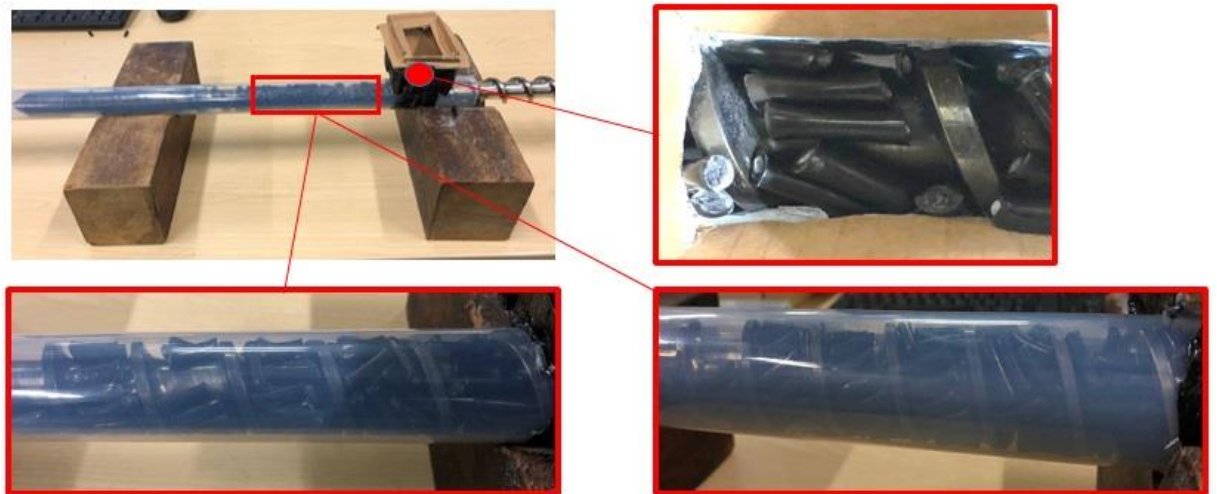
This suggests fibres are more naturally inclined to follow the direction of the screw as the pellets are fed into the screw. It is easier for them to fill and be packed into the screw channel if filled along the screw direction. Further down the screw, in the latter stages of compression and metering, the clusters are subject to more shearing and begin to align in the helical direction. As the polymer matrix melts, the drag flow created forces the fibres in the helical direction. But in these zones the fibres have predominantly dispersed and broken down significantly as shown in Figure 6.13 below and the need for a correction decreases (since they are

shorter relative to the 24 mm sample size, the proportion of fibres cut during sample extraction is decreased). Again, the direction of the screw parallel to the axis of rotation is indicated by the red arrows in Figure 6.13.



**Figure 6.13. – Example of dispersed clusters in the latter stages of the injection moulding process.**

A very basic model of a screw in a polypropylene tube was constructed to see the natural inclination of a pellet as it is fed from the hopper into the screw. Naturally they would fit in a cylindrical tube given a large enough screw channel width along the screw direction due to their long length (15 mm). However, some pellets were seen to align in the helical direction as well as being caught between the lip of the feeder and mouth of the screw, forcing them into the screw channel and significantly breaking them as evidenced in Figure 6.14.



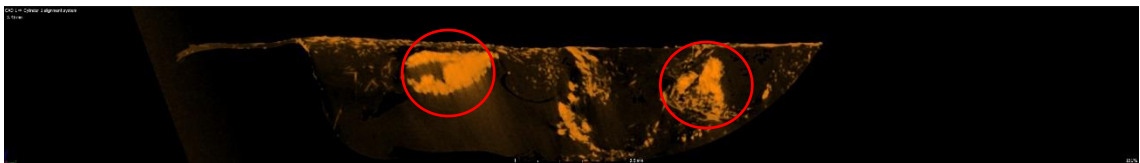
**Figure 6.14. – Basic model of natural inclination of pellets along an injection moulding screw**

Pellets were also seen to not align exactly in the screws direction as expected but at a slight angle in line with the screw flights, highlighted in Figure 6.15. This indicated that since the sample extraction involved cutting the samples off the screw at an angle in line with the screw flight, the need for a correction is minimised as the 1D correction assumes fibres align parallel to the helical direction and calculates the probability of them being cut during sample extraction. If a large quantity of fibres are shown to be perpendicular to the helical direction then it could be proposed that sample extraction at the same angle of the screw flight does not need a correction.



**Figure 6.15. – Overlaid lines showcasing example of pellets inclination along an injection moulding screw**

The proposed method via Volume Graphics to obtain orientation data for the 2D correction (described in Chapter 6.1.3) is considered to be inaccurate. The particle analysis function on LabVIEW assumes fibres are circular and straight and it is hard to obtain accurate orientation data if not. The larger fibres clusters (circled in red in Figure 6.16 below) are irregular in shape and not straight (as well as smaller fibre clusters) and to derive an ellipse major and minor axis is quite difficult if the clusters are not circular.



**Figure 6.16. – Example of clusters from slice data**

These average  $\cos(\theta)$  values applied to the 2D correction probability model and charted in Figure 6.11 are detailed in Table 6.2. A weighted average according to cluster cross-section is also applied to the average  $\cos(\theta)$  for each sample. This explains why the 2D corrected results are similar with the original raw data set seen in Figure 6.11 as the average  $\cos(\theta)$  values are surprisingly low, suggesting the majority of fibres are inclined perpendicular to the helical direction and not being cut during sample extraction. The average  $\cos(\theta)$  was calculated without a weighting factor and the results differ significantly to the ones with. However, a weighting factor is important as the inclination of a larger cluster compared with a single isolated fibre will have more of an impact on measured fibre length distribution data. Therefore, a rough manual measurement of the inclination angle of fibres in the helical direction was performed from a reconstructed unrolled screw sample data set, examples of which are shown in Appendix 2.1. Clear clusters of fibres were identified and using the angle measurement tool in Volume Graphics an inclination angle of the cluster was calculated. These average  $\cos(\theta)$  results are also tabulated in Table 6.2.

Screw Test 4 (20YM240)			
Sample	Average cos ( $\theta$ )		
	2D Correction with weighting factor	2D Correction without weighting factor	Manual 2D correction
F2	0.05	0.49	0.53
F3	0.1	0.57	0.49
C1	0.13	0.56	0.44
C2	0.17	0.63	0.87
C3	0.28	0.62	0.99
M1	0.32	0.57	n/a
M2	0.23	0.55	n/a
Sprue	0.5	0.67	n/a
Average cos ( $\theta$ ) = 1: Inclined parallel to helical direction of the screw			
Average cos ( $\theta$ ) = 0: Inclined perpendicular to helical direction of the screw			

**Table 6.2. – Comparison of orientation data**

Results for M1, M2 and the sprue were not computed as no clear individual clusters were seen but rather a matte of entangled fibres inclined in various directions was presented by the fibre dispersion analysis.

Both sets of 2D correction orientation data with and without a weighting factor differ to the manual 2D correction orientation data, signifying orientation data obtained from Vision Assistant is indeed imprecise and would lead to an erroneous fibre length distribution data set. But since it can also be assumed that fibres are not inclined along the helical direction but in the screw direction, a 1D correction would also lead to a misinterpretation of results. Details of how the 2D correction can be expanded to 3D to accurately account for the bias introduced into the fibre length distribution results from sample extraction are described in Chapter 8.



## 6.2. Experimental Results

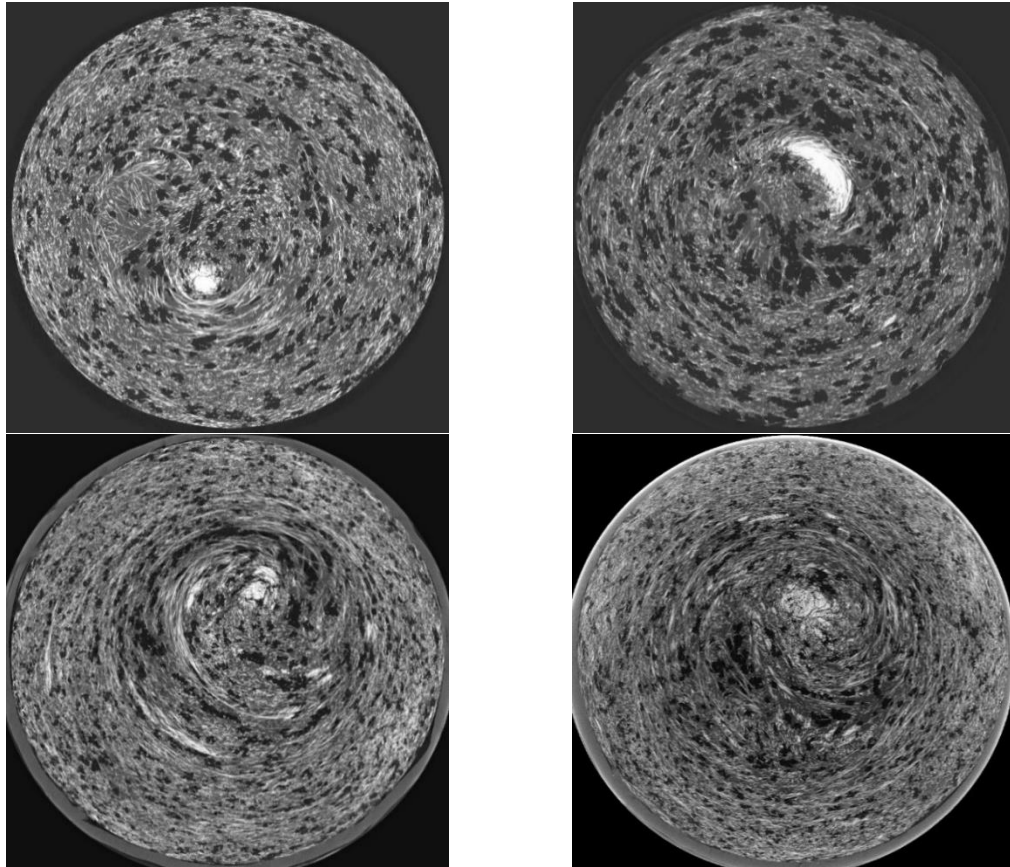
It is accepted and observed in this investigation that within the injection moulding process, long glass fibres are drastically shorter within the manufactured injection moulded part compared to their initial length in pellet form before processing. Fibre breakage inside the injection moulding process is inevitable and is a consequence of multiple fibre damage mechanisms that are present during the materials flow through the process.

It is particularly challenging to isolate each fibre breakage mechanism and understand its influence on fibre length. These mechanisms within the process are relatively understudied and research in this field is still ongoing as it is necessary to understand their importance within the injection moulding process, thus measurable information of fibre length distributions along the process can be collected. These damage mechanisms within the injection moulding process would ideally be studied through the use of computer simulations similarly to the way fibre breakage is assessed in the manufactured LGFRP part. Therefore, complete and accurate injection moulding simulations could be performed with such mechanisms implemented which could then be optimized to decrease fibre breakage and thus improve mechanical properties in the final part.

Initial investigations showed a large amount of fibre degradation had already occurred by the time fibres had reached the end of the screw and entered the nozzle. It is clear that fibre attrition is mostly attributed during the polymers flow through the screw during the injection moulding process with over 74% of 15 mm long fibres having reduced in length to between 0 mm – 5 mm by the time they enter the nozzle for both 20YM240 and 40YM240.

Lower weight percentage composites (20YM240) showed an agglomeration of glass fibres close to the screw at the nozzle entry as evidenced in Figure 6.17 which would dissipate by the time the fibres reached the nozzle exit. This indicated that fibres were not evenly dispersing along the injection moulding screw as previously thought and exhibited a cluster 'memory' from the screws rotation into the nozzle. These bundles of fibres were not so prevalent in the

higher weight percentage polymer (40YM240), suggesting when processing with a higher weight percent, fibres were more evenly dispersed along the injection moulding screw.



**Figure 6.17. -  $\mu$ -CT top cross section from the entry a 3mm nozzle (top left) & 6mm nozzle (top right) (20YM240) and  $\mu$ - CT top cross section from the entry of a 3 mm nozzle (bottom left) & 6 mm nozzle (bottom right) (40YM240)**

It was suggested in the results from the nozzle extraction tests that the higher weighted average fibre length in the 40YM240 material was due to the greater fibre-fibre interaction within the sample. This in turn might lead to clusters being formed from which glass fibres can protect themselves within from the shear forces present during the moulding process. However, larger central clusters are seen to be more apparent in the 20YM240 nozzle samples compared to the higher weighted glass nozzle samples. It could be deduced that there are a larger quantity of smaller clusters in the 3 and 6 mm nozzles processed using 40YM240 as opposed to one large well defined cluster in the nozzles processed with

20YM240. This suggests processing with higher glass fibre content material yields more advantageous results in preserving glass fibre length in the final injection moulded part.

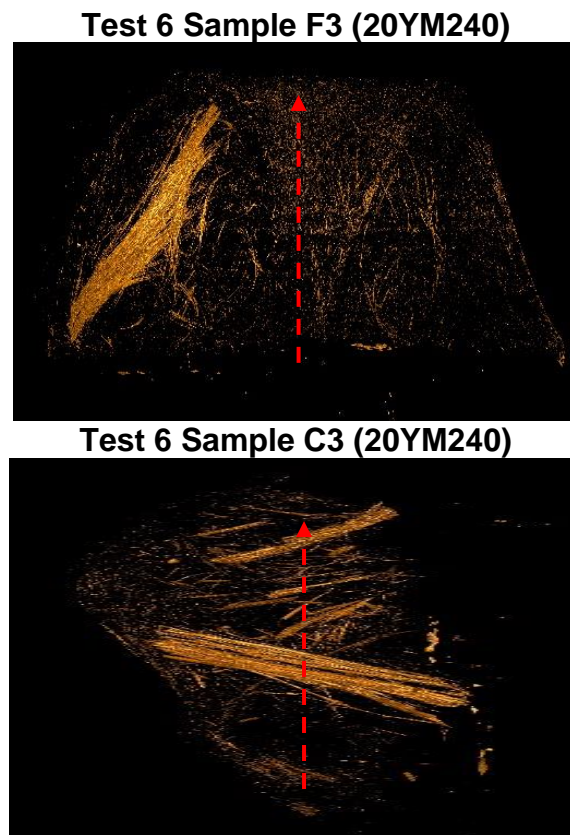
From this, the investigation was centred on evaluating fibre length and dispersion along an injection moulding screw. In general, results presented did not indicate a gradual attrition of average and weighted average fibre length along the injection moulding process but a localised sudden transition to the loss of overall fibre length. This is evidenced particularly at the beginning of the feeding zone where the pellets are fed from the hopper into the screw and along the compression zone where the glass fibre pellets break up and disperse within a complete pool of molten polymer.

A drastic decrease of glass fibre length from initial pellet form to sample location F1 is seen across all tests. This suggests how the reinforced polypropylene pellets are fed into the screw is a significant factor. A pellet is more naturally inclined to follow the screw direction and if the screw channel width is large enough for a pellet to lie across it, they will suffer minimal degradation. Pellet-pellet interactions and the random nature of the feeding of pellets lead to them being filled and packed in various directions as they enter the screw. Since their length is relatively large compared to the screw channel width, they will consequently experience significant breakage due to being forced into a constricting geometry.

Further along the injection moulding process another severe level of fibre breakage occurs along the compression zone. The average and weighted average fibre length drop considerably from the end of the feeding zone, F3 to the end of the compression zone, C3 for all screw tests bar one (screw test 6). At the compression stage, not only are clusters packed into a narrowing screw channel depth, the clusters are also subject to more shearing forces created from the increasing melt pool size. For screw test 6, this increase in average fibre length can be largely attributed to the fact there simply being more clusters present in the C3 sampling region compared to the F3 sampling region at that

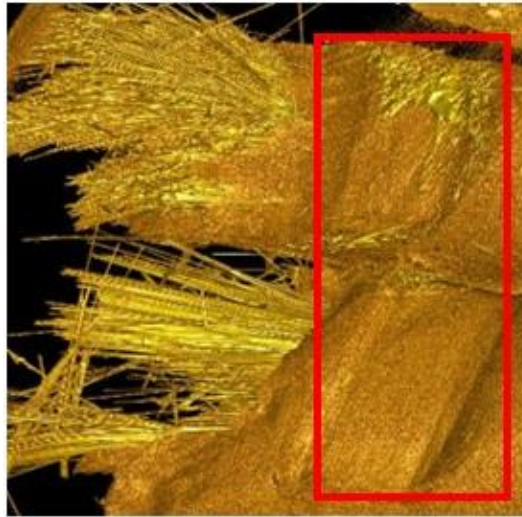


moment in time as evidence by Figure 6.18. The screw direction, parallel to the axis of rotation is denoted by a red arrow.



**Figure 6.18. –  $\mu$ -CT results showing the random nature of the dispersion of clusters along the injection moulding process**

Evidence of certain fibre breakage mechanisms were revealed in the fibre dispersion analysis of glass fibre reinforced samples extracted from the screw. Figure 6.19 below supports the theory that as the raw virgin material flows through the hopper exit and the pellets are compacted into the screw channels, a small percentage of pellets are compressed between the edge of the hopper exit and screw flights.



**Figure 6.19 -  $\mu$ -CT evidence of pellet and screw flight interaction at hopper exit**

Additionally,  $\mu$ -CT supported the suggestion that due to a clearance gap between the top of the screw flight and the inside diameter of the barrel there is a certain degree of fibre attrition since fibres touching or passing through will be damaged due to shear and frictional forces subjected on the fibres shown in Figure 6.20 below.



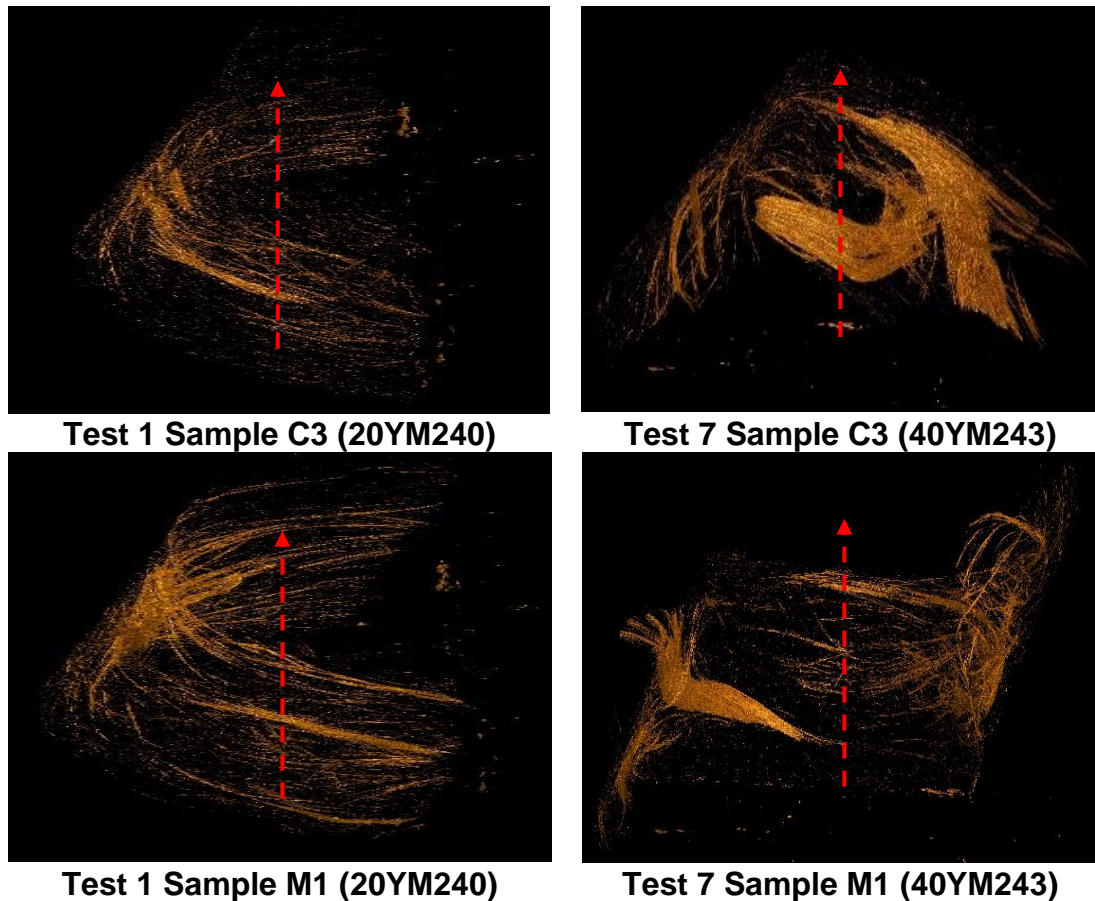
**Figure 6.20 -  $\mu$ -CT evidence of pellet and screw flight interaction along injection moulding screw**

### 6.3. Fibre Length Distribution & Dispersion

The investigation also focused on analysing the effect of glass fibre content, back pressure and screw speed on fibre dispersion and fibre length distribution of long glass fibre reinforced polypropylene along the injection moulding process. The direction of the screw, parallel to the axis of rotation is denoted by a red arrow in the following  $\mu$ -CT images highlighting fibre dispersion within an extracted sample.

Results evaluated the effect of fibre content with two different grades of material. One was reinforced with 20 wt. % 15 mm long glass fibres (20YM240) and the other with 40 wt. % 15 mm long glass fibres (40YM243). Different back pressures were assessed (2.5, 5 and 7.5 bar) whilst maintaining a constant screw speed of 150 RPM.

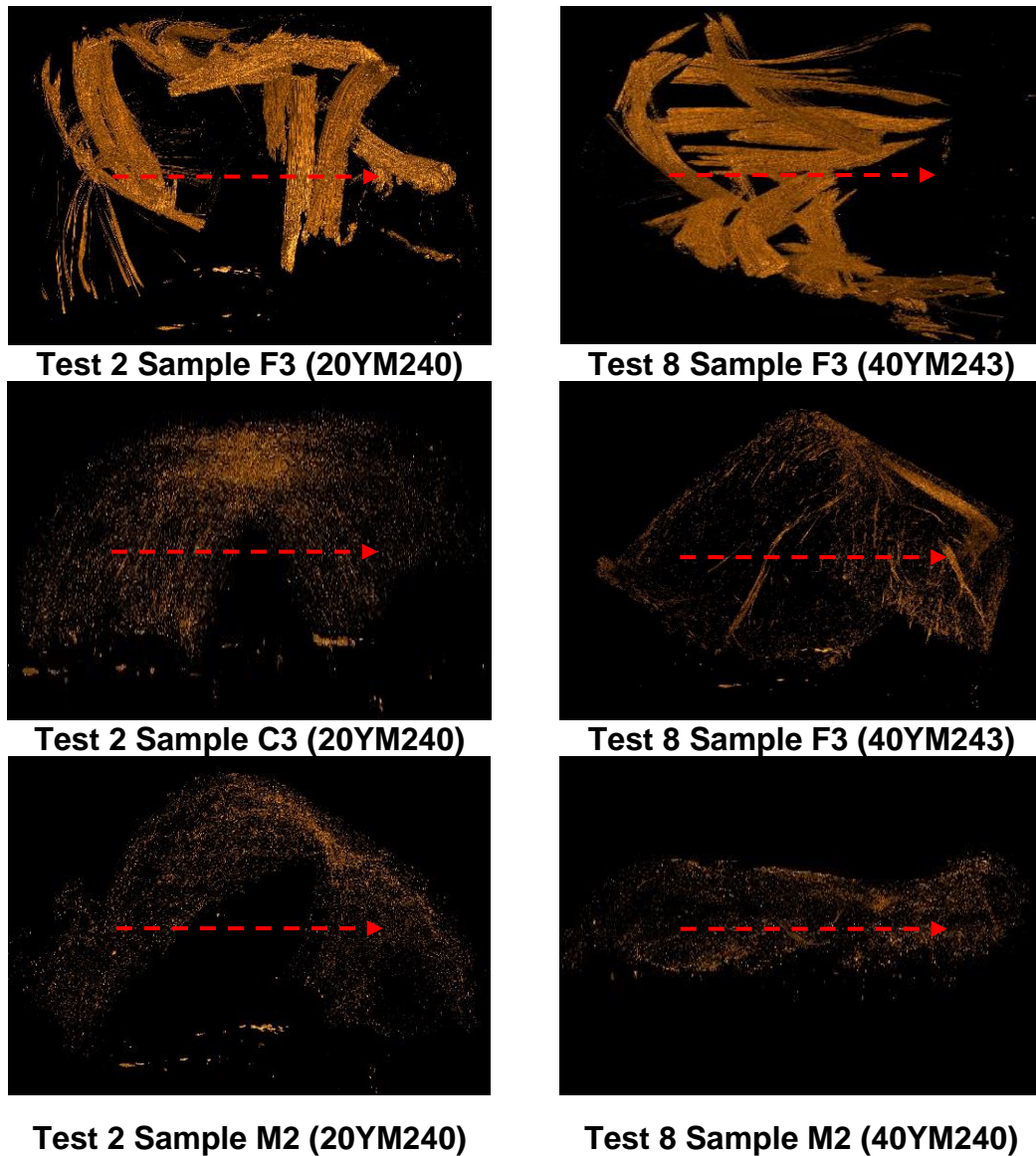
For screw tests processed at a lower back pressure, fibre length degradation appeared to be a gradual process along the screw for the 40YM243 material. But for the 20YM240 material, fibre length degradation showed localised sudden transitions of decreasing fibre length at F1 and specifically C3 sample locations. However, at subsequent sample locations, F2 and M1 for the 20 wt. % filled material, the weighted average fibre length increases to a similar value to its 40 wt. % filled counterpart result suggesting overall fibre degradation is not dissimilar. This increase can be attributed to fewer clusters of longer fibre lengths being present in the preceding sample at that moment in time as evidenced by  $\mu$ -CT results displayed in Figure 6.21. Comparing samples C3 and M1 for the 20YM240 material it is clear clusters of fibres are more prominent in the latter sample akin to the similar level of fibre dispersion seen in sample M1 for the 40YM243 which is why weighted average fibre length results are much closer at M1 and shows the random nature of the clustering of fibres along the screw. Clusters may not be present in one sampling region but may be present in the subsequent sampling area and since more fibre-fibre interactions would naturally occur within a higher glass filled polymer, more clusters will be present along the screw, increasing the likelihood of them being captured for analysis which is why no sudden transitions of decreasing fibre length were seen in the 40YM243 tests.



**Figure 6.21 –  $\mu$ -CT results showing the effect of fibre content on the dispersion of fibres in the compression and metering zones at low back pressures**

Analysing the effect of fibre content at a medium back pressure yields contrasting results however. Fibre attrition appears to be similar for both glass filled materials at first along the feeding zone, but as the glass fibres flow from the end of feeding zone into the latter zones of the screw, fibre length degradation is much more apparent in the lower wt. % glass filled material. This suggests that processing with higher wt. % glass filled materials will yield higher levels of clustering (as evidenced in Figure 6.22 below of samples at the end of each zone) which although is undesirable in terms of homogeneity in the final part leads to the preservation of fibre length as fibres are able to protect each other within these structures from the shear forces present during the moulding process.





**Figure 6.22. –  $\mu$ -CT results showing the effect of fibre content on the dispersion of fibres at end of each zone at medium back pressures**

The effect of fibre content at a higher back pressure of 7.5 bar was also evaluated. The findings showed similarities between tests ran at a back pressure of 2.5 bar as fibre content again did not appear to have an overall effect on fibre degradation along the screw. This suggests fibres processed at higher pressures will suffer severe attrition regardless of fibre content and the level of clustering along the screw as both weighted average values are near identical at the end of the screw for both sets of glass filled material at 1.22 mm (20YM240) and 1.27 mm (40YM243). It is noted that 40YM243 material suffers less degradation in the initial feeding zone of the screw as the material reaches a weighted average fibre length value of 6.76 mm at sample location F3, similar to the average value of

6.19 mm for the 20YM240 but earlier on in the process at location F2 suggesting the increased fibre content does yield some protection of fibre length but is inevitably meaningless by the time the polymer reaches the compression and metering zones.

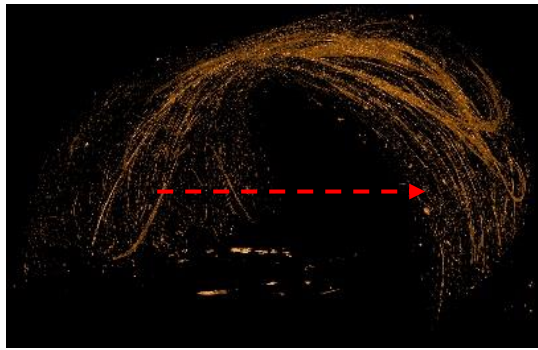
The effect screw speed has on fibre length degradation during the injection moulding process was also evaluated, specifically at 150 RPM and 300 RPM using a 20 mm screw. The two different screw speeds were evaluated at 3 different back pressures (2.5, 5 and 7.5 bar) whilst processing the same grade of polymer material, 20YM240.

Across all three back pressures, the effect the screw speed has on fibre length degradation is minimal. Both the low (150 RPM) and high (300 RPM) screw speed show minimal differences with regards to preserving fibre length or increasing fibre degradation along the screw as the level of fibre degradation is parallel for both sets of screw speeds. For the low back pressure screw test, both screw speeds yield similar final weighted average fibre length results of 6.65 mm for the lower screw speed and 6.88 mm for the higher screw speed, a difference of 0.23 mm. Similar negligible differences in the results for the low and high screw speeds evaluated at different back pressures are seen with final weighted average fibre lengths within 1.14 mm and 0.37 mm of each other for the medium (5 bar) and high back pressure (7.5 bar) tests respectively. This could be partly due to the relatively high screw speeds evaluated in this investigation particularly the 'low' screw speed of 150 RPM. However, such screw speeds need to be evaluated due to the fact that this investigation is an industrial collaboration, and high screw speeds are a necessity in industry due to the need for fast cycle times.

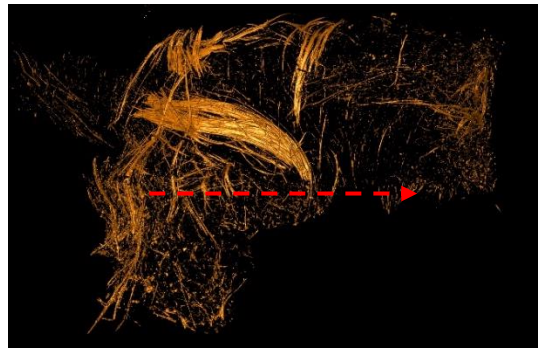
Finally, an analysis was carried out on back pressure and its influence on weighted average fibre length along the injection moulding process. Three different back pressures were assessed from low (2.5 bar), medium (5 bar) and high (7.5 bar) back pressure whilst processing the same 20YM240 grade of material for all screw tests. The different back pressures were evaluated at a low screw speed of 150 RPM and a high screw speed of 300 RPM.

It is evident from both sets of back pressure results evaluated at a low and high screw speed that a low back pressure of 2.5 bar yields the most advantageous result with regards to preserving fibre length along the injection moulding process for the 20YM240 material. Processing at a lower back pressure of 2.5 bar produced measured final weighted average fibre length results of 6.88 mm and 6.65 mm for the low and high screw speed tests respectively. This in clear contrast to the measured final weighted average fibre length results for the higher back pressure screw tests conducted at 5 and 7.5 bar. Processing at a medium back pressure yielded weighted average length results of 1.26 mm (150 RPM) and 2.36 mm (300 RPM) and a high back pressure gave results of 1.22 mm (150 RPM) and 1.59 mm (300 RPM). This clearly indicated that attrition of fibre length in a glass fibre reinforced polymer sample is intensified at higher back pressures. This is in support of previous literature findings that argued back pressure has a significant effect on fibre degradation as opposed to injection moulding screw speed.

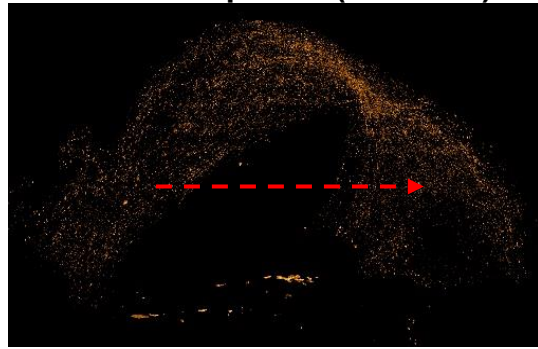
As seen in Figure 6.23 fibre clusters are much more preserved in Tests 1 and 4 by the time they reach the end of the screw as they are processed with a back pressure of 2.5 bar. Little or no clustering is seen for screw tests 2, 5, 6 and 9 which processed the polymer material at higher back pressures. As mentioned before these clusters of long fibres are suggested to protect themselves from the higher pressures and shear forces exerted on them and since the forces acting on them are lowered by processing with a lower back pressure, naturally less fibres will be broken along the injection moulding process as supported by the higher weighted average values seen at M2. This will in turn lead to more favourable mechanical properties in the manufactured part as long as the clusters are able to disperse homogeneously but more importantly able to preserve the fibres original length as much or as close to it as possible.



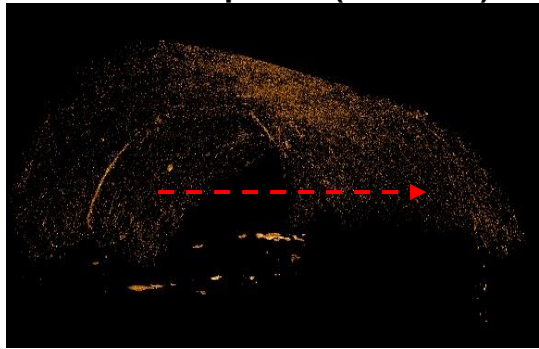
**Test 1 Sample M2 (20YM240)**



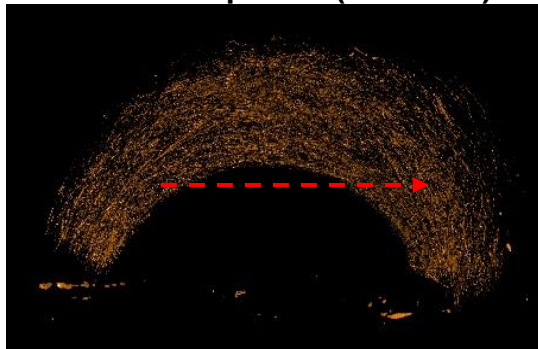
**Test 4 Sample M2 (20YM240)**



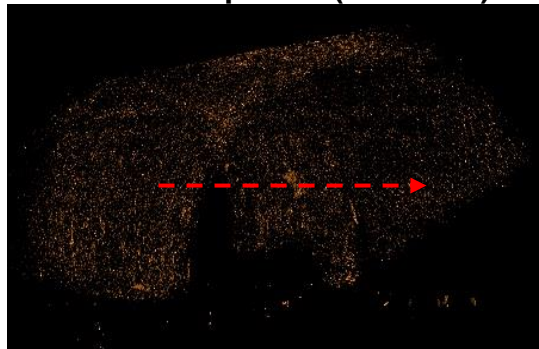
**Test 2 Sample M2 (20YM240)**



**Test 6 Sample M2 (40YM243)**



**Test 5 Sample M2 (20YM240)**



**Test 9 Sample M2 (20YM240)**

**Figure 6.23. -  $\mu$ -CT results showing the effect of back pressure on the dispersion of fibres at end of the screw at sample location M2**



## 7. Conclusions

The conclusions derived from this thesis are listed below; these conclusions relate to the objectives to evaluate fibre length breakage and dispersion along an injection moulding screw. Fibre length dispersion and distribution measurements were taken from long glass fibre reinforced injection mouldings.

In terms of fibre length measurement techniques, the following conclusions have been made:

- The fibre length measurement method described in this thesis can be used to generate more accurate results for the evaluation of fibre length distributions in glass fibre reinforced injection mouldings compared to other commercially available systems currently on the market as of 2018 as evidenced in Chapter 4.
  - Image Pro Premier produced results which had shorter fibres than those found by the manual method as the software appeared to segment long and curved fibres into shorter fragments.
    - Specifically, Image Pro Premier showed an average fibre length of 0.43 mm compared to the manual method value of 2.34 mm, weighted average length of 1.12 mm compared to 3.11 mm and maximum fibre length of 7.27 mm compared to 10.58 mm.
  - Fibre Shape not only produced results which had shorter fibres present than those found by the manual method, but also longer fibres as well due to the software stitching separate shorter fibres together.

- Fibre Shape showed an average fibre length of 2.36 mm compared to the manual method value of 7.02 mm, weighted average length of 7.9 mm compared to 9.25 mm and maximum fibre length of 29.92 mm compared to 16.80 mm.
- CT-FIRE also produced results which had shorter and longer fibres than those found by the manual method by both segmenting and stitching scanned glass fibres.
  - CT-FIRE showed an average fibre length of 4.51 mm compared to the manual method value of 7.02 mm, weighted average length of 8.94 mm compared to 9.25 mm and maximum fibre length of 22.35 mm compared to 16.80 mm.
- FASEP produced results which had a significant amount of shorter fibres present than those found by the manual method in the evaluation of a raw virgin glass fibre reinforced pellet and screw sample. The software struggled to compute multiple long glass fibres, overlaying them with smaller shorter fibre segments.
  - For the pellet sample, FASEP showed an average fibre length of 4.27 mm compared to the manual method value of 14.72 mm, weighted average length of 13.5 mm compared to 14.87 mm and maximum fibre length of 15.9 mm compared to 16.91 mm.
  - For the screw sample, FASEP showed an average fibre length of 1.33 mm compared to the manual method value of 8.86 mm, weighted average length of 5.74 mm compared to 11.38 mm and maximum fibre length of 15.85 mm compared to 16.81 mm.

- It is debated in literature whether a set of 1000 or fewer fibres can be statistically representative of the local fibre length distribution within a sample. Therefore, from the results shown in Chapter 2.7 it is vital for a suitably large number of fibres to be measured of at least 2,000 to acquire an accurate, reliable and representative fibre length distribution within a sample.
- A minute amount of short fibres (0 – 7.5 mm) were measured within a long glass fibre reinforced pellet before processing for both 20YM240 (25 fibres) and 40YM243 (10 fibres) which suggests that fibres suffer additional fibre breakage either due to the manufacturing of the pellet itself during the wire coating process or the dispersion process of the fibre length measurement method utilised in this study, or a combination.
  - If the manufacturing of the raw virgin pellet does not supposedly lead to fibre attrition then it is proposed that fibres suffer minimal inadvertent attrition during the developed manual method for fibre dispersion before manual fibre length measurements are made.
- Depending on the method used for extraction of long glass fibre reinforced samples a valid and accurate correction needs to be developed and applied to account for the cutting of fibres at the cut sample boundary which can lead to a bias in shorter fibres as discussed in this thesis.
  - The proposed 1D correction assumes all fibres are aligned parallel to the helical direction of the screw, perpendicular to the axis of rotation. However  $\mu$ -CT contradicts this which could lead to an inaccurate fibre length distribution data set.
  - The 2D correction which accounts for the inclination of fibres in the helical direction of the screw, relies on orientation data obtained from Vision Assistant. Applying the correction leads to similar fibre

length distribution results to distributions obtained without a correction.

- Further work in the acquisition of the angle of inclination from clustered fibres is required to improve the accuracy of this method, see future work chapter 8.
- There is a need for the development of a universally accepted ISO standard for the measurement of long glass fibres as per short glass fibres. A regulated measurement system would allow for an unbiased and accurate comparison between various fibre length investigational reports.

In terms of fibre length dispersion, the following conclusions have been made:

- For a 20 mm screw with a screw channel depth ranging from 3.95 mm to 1.5 mm and a width of 20 mm, glass fibre reinforced pellets are initially more naturally inclined to align in the direction of the screw, parallel to the axis of rotation during feeding. This can lead to the preservation of fibre length as pellets are not forced into the constricting nature of the screw channel, perpendicular to the axis of rotation.
  - Some pellets were shown via  $\mu$ -CT to deform by interacting with the screw flights during initial feeding of the glass fibre reinforced pellet from the hopper into the screw as described in Chapter 6.2.
- The preservation of glass fibre clusters from their original pellet form along the screw appears to be random in nature. Larger clusters of fibres can be found in one sample location further along the screw than the preceding one. Increased fibre content appears to aid in the conservation of fibre clusters which are beneficial in protecting residual fibre length.

- Glass fibres are clearly not as well dispersed along the screw as previously thought from their initial pellet bundle form with clusters found all along the screw but more predominantly in the feeding and compression zones of the screw. However, bundles are still present in the metering zone and nozzle.
- This uneven dispersion can lead to a central clusters of fibres as the reinforced polymer flows into the nozzle, exhibiting a cluster 'memory' from the screws rotation.

In terms of fibre length distribution, the following conclusions have been made:

- Initial measurements taken from the nozzle of a Battenfeld BA750/315 CDK injection moulding machine showed that fibres break significantly during the melting process in the machine barrell, thus highlighting the need for fibre length distribution tests along the screw.
  - Weighted average fibre length reduced by 92% from 14.87 mm in original pellet form to 1.22 mm at the end of the metering zone for a 20 wt. % glass fibre filled material.
- Results showed that changes in fibre content had an effect on the overall fibre length distribution at all stages of processing
  - In the Battenfeld BA750/315 CDK nozzle studies, the effect of fibre content on fibre length distribution showed no clear trends apart from the effect of nozzle geometry.
    - For the 3 mm nozzle the 20% LGF material had average fibre length of 2.70 mm, weighted average of 6.04 mm and

maximum fibre length of 15.49 mm compared to 2.20 mm, 6.31 mm and 16.94 mm for the 40% LGF material.

- For the 6 mm nozzle the 20% LGF material had average fibre length of 3.6 mm, weighted average of 7.25 mm and maximum fibre length of 16.61 mm compared to 2.83 mm, 7.49 mm and 16.36 mm for the 40% LGF material
- Results taken from the screw pull tests performed on an Arburg Allrounder 270C injection moulding machine showed that a higher fibre content in the reinforced polymer reduced fibre length attrition along the injection moulding screw.
  - For a fixed low back pressure of 2.5 bar, and fixed screw speed of 150 RPM, the weighted average fibre length reduced by 53.74 % for a 20% LGF material and 35.64 % for the 40% material.
  - For a fixed medium back pressure of 5 bar, and fixed screw speed of 150 RPM, the weighted average fibre length reduced by 91.53 % for a 20% LGF material and 64.09 % for the 40% material.
  - For a fixed high back pressure of 7.5 bar, and fixed screw speed of 150 RPM, the weighted average fibre length reduced by 91.80 % for a 20% LGF material and 87.42 % for the 40% material.
- $\mu$ -CT showed that increasing fibre content leads to an increased number of ordered bundles along the screw which in turn leads to the preservation of fibre length as fibres are able to protect each other from the forces exerted on them.

- Screw speed is of little influence with regards to minimising fibre length degradation along the screw which concurs with published work (Rohde et al. 2011) and contradicts others (Lafranche et al. 2005; Kumar et al. 2009).
  - For a fixed back pressure of 2.5 bar, the weighted average fibre length reduced from 14.87 mm in initial raw virgin pellet form, to 6.88 mm at the end of the metering zone at 150 RPM and 14.87 mm to 6.65 mm at 300 RPM.
  - For a fixed back pressure of 5 bar, the weighted average fibre length reduced from 14.87 mm in initial raw virgin pellet form, to 1.26 mm at the end of the metering zone at 150 RPM and 14.87 mm to 2.36 mm at 300 RPM.
  - For a fixed back pressure of 7.55 bar, the weighted average fibre length reduced from 14.87 mm in initial raw virgin pellet form, to 1.22 mm at the end of the metering zone at 150 RPM and 14.87 mm to 1.59 mm at 300 RPM.
- Back pressure is a controlling factor for process optimization to reduce fibre length degradation without impacting cycle time.
  - Processing at a low back pressure of 2.5 bar has the most positive influence on maintaining weighted average fibre length along the injection moulding screw compared to higher back pressures of 5 bar and 7.5 bar.
    - For a fixed screw speed of 150 RPM, the weighted average fibre length reduced from initial raw virgin pellet form to the end of the metering zone by 53.73 % for a processing back

pressure of 2.5 bar, 91.53 % for 5 bar and 91.80 % for 7.5 bar.

- For a fixed screw speed of 300 RPM, the weighted average fibre length reduced from initial raw virgin pellet form to the end of the metering zone by 55.28 % for a processing back pressure of 2.5 bar, 84.13 % for 5 bar and 89.31 % for 7.5 bar.



## 8. Further Work

Based on the outcomes of this research, further studies would be recommended in the following areas:

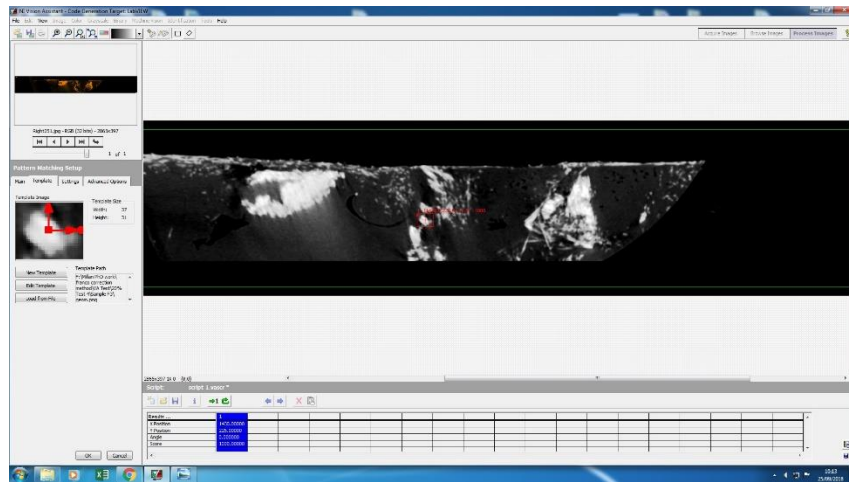
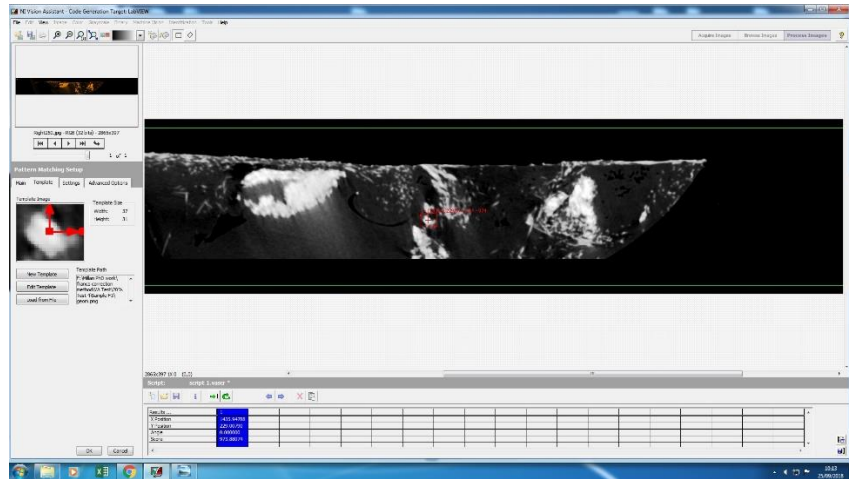
- In order to optimise a long glass fibre length distribution model, reliable test data for the fibre length distribution is required. Instead of destroying a sample to measure the fibre length distribution it would be useful to measure fibre length distribution through the use of  $\mu$ -CT. Fibre orientation modules for the measurement of fibre orientation from a scanned and 3D reconstructed sample are already available thus expanding this technique with the development of complex algorithms that would be able to track each individual fibre and its length would prove invaluable within this area of research.
- A separate study to investigate further the effect that varying injection moulding parameters has on fibre length and mechanical properties. The injection speed and melt temperature along the screw are parameters which should also be investigated similarly to contrasting investigations conducted by Hafellner et al. (2000) who suggested elevated injection speeds increased fibre length degradation and Rohde et al. (2011) who observed injection speed had a minimal effect on fibre length.
- Improving the screw geometry to reduce shear stresses exerted on the glass fibres which would subsequently lead to less fibre degradation whilst maintaining homogeneity of the composite could also be investigated. This could be done by increasing the depth of the screw flights, maintaining constant flight depth in all zones but varying the flight pitch, incorporating a mixing zone into the screw, or a combination as investigated by Inoue et al. (2015).
- Future work should also attempt to compare experimental results along a screw to simulate fibre breakage. This knowledge will be important in

understanding complex fibre flow fields and how these parameters ultimately affect final mechanical properties in the moulded part. Moldex3D, a direct competitor to Autodesk Moldflow have attempted to do this but with data at the point of injection not along screw (Huang and Tseng 2018).

- Not enough data was acquired for the refinement and optimisation of a fibre length distribution prediction model along the screw which was aimed to be incorporated into Autodesk Moldflow. The Phelps-Tucker model is based upon the initial long glass fibre length material and seen to under predict measured findings inside the mould as the default fibre length at the sprue of an injection moulded component is the fibres original length .
- The fibre breakage prediction substantially improves if measured fibre length distributions at the end of plasticisation is entered. Instead of evaluating various sample locations along a screw it could be more efficient to evaluate screw data for each screw test from the extrudate or nozzle instead.
  - Instead of measuring 8 samples for one screw test, one sample could be measured for each screw test increasing the number of variables and repeatability. Different academic or industrial institutions could be contacted to perform a screw test on their injection moulding machinery with the desired material to be evaluated sent beforehand. Injection moulding apparatus and settings would be recorded and the extrudate or nozzle sample (if obtainable) can be sent back for further analysis of fibre length distribution.
  - Also, different screw geometries would process the glass fibre reinforced material at external facilities thus evaluating another variable and one which would be able to correlate shear data along

the screw with fibre breakage. This in turn would increase the data pool for the development of a more accurate fibre length distribution model to be incorporated into Autodesk Moldflow.

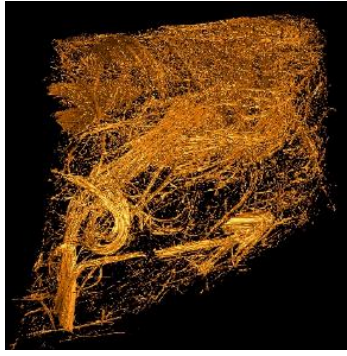
- The correction proposed for fibres cut at the sample boundary in this investigation would need to be improved significantly before being considered to be applicable to such methods of sample extraction.
  - One possible method is to pattern match fibre clusters by identifying a cluster on an unrolled slice and tracking its movement with a subsequent slice along the sample. The x, y and known z shift are evaluated to create a vector in 3D space. This assumes fibres are straight. A straight 17mm long fibre would have a high probability of being cut during sample extraction but if it is curved the probability decreases.
  - Fibres are indeed shown to curve a great deal so an iterative pattern match (Figure 8.1) could be conducted of all slices along sample. This would track all the fibres along the sample to correct for any curvature. On the other hand clusters are shown to fray at the ends (Figure 8.2), are not circular and irregular in shape and curve back on themselves (Figure 8.3), thus pattern matching could prove challenging. A higher resolution scan would be ideal (current method comparatively low resolution) to track each individual fibres start and end point so an effective length and orientation could be achieved.



**Figure 8.1. - Example of iterative pattern matching of fibre clusters taken from a slice view.**



**Figure 8.2. - Example of a frayed fibre clusters along the injection moulding process**



**Figure 8.3. - Example of curved fibres within an injection moulded screw sample**

- Would be interesting to conduct a fibre length degradation study of glass fibre reinforced pellets fed directly onto the screw channels so that they lie in the screw direction, perpendicular to the helical direction, minimising pellet-pellet interaction and compare it to the conventional method of feeding.
- Since it is suggested from the results that an increased fibre content material of 40 wt. % reduces fibre attrition along an injection moulding screw compared to a 20 wt. % glass filled material. A study examining higher glass filled materials such as 50 wt. % and 60 wt. % could also be performed to evaluate the effects of increased fibre content on fibre length degradation along the screw.

## References

- Advani, S. G. and Tucker III, C. L. (1987) The use of tensors to describe and predict fiber orientation in short fiber composites. *Journal of rheology* 31 (8), 751-784.
- Ahmad, F., Mujah, D., Hazarika, H. and Safari, A. (2012) Assessing the potential reuse of recycled glass fibre in problematic soil applications. *Journal of Cleaner Production* 35, 102-107.
- Akay, M. and Barkley, D. (1992) Jetting and fibre degradation in injection moulding of glass-fibre reinforced polyamides. *Journal of materials science* 27 (21), 5831-5836.
- Arroyo, M. and Avalos, F. (1989) Polypropylene/low density polyethylene blend matrices and short glass fibers based composites. I. mechanical degradation of fibers as a function of processing method. *Polymer composites* 10 (2), 117-121.
- Bailey, R. and Kraft, H. (1987) A study of fibre attrition in the processing of long fibre reinforced thermoplastics. *International Polymer Processing* 2 (2), 94-101.
- Bajracharya, R. M., Manalo, A. C., Karunasena, W. and Lau, K.-t. (2016) Experimental and theoretical studies on the properties of injection moulded glass fibre reinforced mixed plastics composites. *Composites Part A: Applied Science and Manufacturing* 84, 393-405.
- Bereaux, Y., Charmeau, J. Y. and Mogueudet, M. (2008) Modelling of fibre damage in single screw processing. *International Journal of Material Forming* 1 (SUPPL. 1), 827-830.
- Bernasconi, A., Davoli, P., Basile, A. and Filippi, A. (2007) Effect of fibre orientation on the fatigue behaviour of a short glass fibre reinforced polyamide-6. *International Journal of Fatigue* 29 (2), 199-208.
- Berton, M., Cellere, A. and Lucchetta, G. (2010) Influence of reinforcement volume fraction on fibers length reduction in injection molding of LGFRT. In *PPS-26*. Banff, Canada.
- Bijsterbosch, H. and Gaymans, R. J. (1995) Polyamide 6—long glass fiber injection moldings. *Polymer Composites* 16 (5), 363-369.
- Brydson, J. A. (1990) *Handbook for plastics processors*. Butterworth-Heinemann.
- Bumm, S. H., White, J. L. and Isayev, A. I. (2012) Glass fiber breakup in corotating twin screw extruder: Simulation and experiment. *Polymer Composites* 33 (12), 2147-2158.
- Bürkle, E., Sieverding, M. and Mitzler, J. (2003) Process Comparison: Injection Moulding of Long Glass Fibre reinforced PP. *Kunststoffe* 93 (3), 47-50.
- Bush, S. F., Torres, F. G. and Methven, J. M. (2000) Rheological characterisation of discrete long glass fibre (LGF) reinforced thermoplastics. *Composites Part A* 31 (12), 1421-1431.
- Callister Jr, W. D. and Rethwisch, D. G. (2008) *Fundamentals of materials science and engineering: an integrated approach*. 3rd edition. John Wiley & Sons.

- Carneiro, O. S., Covas, J. A., Bernardo, C. A., Caldeira, G., Van Hattum, F. W. J., Ting, J. M., Alig, R. L. and Lake, M. L. (1998) Production and assessment of polycarbonate composites reinforced with vapour-grown carbon fibres. *Composites Science and Technology* 58 (3), 401-407.
- Caton-Rose, P., Gilson, M.-J. and Hine, P. (2017) Orientation, Dispersion and Length Reduction of Fibres in Long Glass Fibre Reinforced Injection Moulding. In *21st International Conference on Composite Materials*. Xi'an, China.
- Cattanach, J. B., Guff, G. and Cogswell, F. N. (1986) *The Processing of Thermoplastics Containing High Loadings of Long and Continuous Reinforcing Fibers*.
- Chen, H., Cieslinski, M. and Baird, D. G. (2015) Progress in modeling long glass and carbon fiber breakage during injection molding. *AIP Conference Proceedings*. Vol. 1664. AIP Publishing.
- Correia, J. R., Almeida, N. M. and Figueira, J. R. (2011) Recycling of FRP composites: reusing fine GFRP waste in concrete mixtures. *Journal of Cleaner Production* 19 (15), 1745-1753.
- Creasy, T., Advani, S. and Okine, R. (1996) Transient rheological behavior of a long discontinuous fiber-melt system. *Journal of Rheology* 40 (4), 497-519.
- Cunliffe, A. M. and Williams, P. T. (2003) Characterisation of products from the recycling of glass fibre reinforced polyester waste by pyrolysis☆. *Fuel* 82 (18), 2223-2230.
- Çuvalcı, H., Erbay, K. and İpek, H. (2014) Investigation of the Effect of Glass Fiber Content on the Mechanical Properties of Cast Polyamide. *Arabian Journal for Science and Engineering* 39 (12), 9049-9056.
- Denault, J., Vu-Khanh, T. and Foster, B. (1989) Tensile properties of injection molded long fiber thermoplastic composites. *Polymer composites* 10 (5), 313-321.
- Desplentere, F., Soete, K., Vandenweghe, L., Bonte, H. and Debrabandere, E. (2012) Fiber length along injection molding screw. 69-75.
- Durin, A., De Micheli, P., Ville, J., Inceoglu, F., Valette, R. and Vergnes, B. (2013) A matricial approach of fibre breakage in twin-screw extrusion of glass fibres reinforced thermoplastics. *Composites Part A: Applied Science and Manufacturing* 48, 47-56.
- El Haggag, S. and El Hatow, L. (2009) Reinforcement of thermoplastic rejects in the production of manhole covers. *Journal of Cleaner Production* 17 (4), 440-446.
- Folgar, F. and Tucker III, C. L. (1984) Orientation behavior of fibers in concentrated suspensions. *Journal of reinforced plastics and composites* 3 (2), 98-119.
- Forgacs, O. L. and Mason, S. G. (1959) Particle motions in sheared suspensions: IX. Spin and deformation of threadlike particles. *Journal of Colloid Science* 14 (5), 457-472.
- Fu, S. Y., Lauke, B., Mäder, E., Yue, C. Y. and Hu, X. (2000) Tensile properties of short-glass-fiber- and short-carbon-fiber-reinforced polypropylene

- composites. *Composites Part A: Applied Science and Manufacturing* 31 (10), 1117-1125.
- Gérard, P. (1998) *Control and optimisation of anisotropy and heterogeneity of injection-moulded short glass fibre reinforced thermoplastic composites*. University of Lille I – Ecole des Mines de Douai.
- Giusti, R., Dubrovich, I. and Lucchetta, G. (2015) Rapid and accurate image analysis procedure for fiber length measurements. *SPE Annual Technical Conference*. Florida, USA.
- Gleissle, W. and Curry, J. (2003) Characterisation of Finite Length Composites: Rheological Studies of Processed PP-Glass Composites. *International Polymer Processing* 18 (1), 20-32.
- Goodship, V. (2004) *Practical guide to injection moulding*. iSmithers Rapra Publishing.
- Goris, S., Back, T., Yanev, A., Brands, D., Drummer, D. and Osswald, T. A. (2017) A novel fiber length measurement technique for discontinuous fiber-reinforced composites: A comparative study with existing methods. *Polymer Composites*.
- Gupta, V., Mittal, R., Sharma, P., Mennig, G. and Wolters, J. (1989a) Some studies on glass fiber-reinforced polypropylene. Part I: Reduction in fiber length during processing. *Polymer composites* 10 (1), 8-15.
- Gupta, V. B., Mittal, R. K., Sharma, P. K., Mennig, G. and Wolters, J. (1989b) Some studies on glass fiber-reinforced polypropylene. Part II: Mechanical properties and their dependence on fiber length, interfacial adhesion, and fiber dispersion. *Polymer Composites* 10 (1), 16-27.
- Hafellner, R., Picher, M. and Worndle, R. (2000) Injection moulding of long fibres. *Kunststoffe* 90 (1), 44-48.
- Hartwich, M. R., Höhn, N., Mayr, H., Sandau, K. and Stengler, R. (2009) FASEP ultra-automated analysis of fibre length distribution in glass-fibre-reinforced products. *Optical Measurement Systems for Industrial Inspection VI*. Vol. 7389. International Society for Optics and Photonics.
- Hernandez, J. P., Raush, T., Rios, A., Strauss, S. and Osswald, T. A. (2002) Analysis of fiber damage mechanisms during processing of reinforced polymer melts. *Engineering Analysis with Boundary Elements* 26 (7), 621-628.
- Hine, P. J. and Duckett, R. A. (2004) Fiber orientation structures and mechanical properties of injection molded short glass fiber reinforced ribbed plates. *Polymer Composites* 25 (3), 237-254.
- Ho, M. H., Wang, P. N. and Fung, C. P. (2011) The Effect of Injection Molding Process Parameters on the Buckling Properties of PBT/Short Glass Fiber Composites. *Advanced Materials Research*. Vol. 284. Trans Tech Publ.
- Holbery, J. and Houston, D. (2006) Natural-fiber-reinforced polymer composites in automotive applications. *JOM* 58 (11), 80-86.
- Huang, C. T. and Tseng, H. C. (2018) Simulation prediction of the fiber breakage history in regular and barrier structure screws in injection molding. *Polymer Engineering & Science*.



- Huilier, D. and Patterson, W. I. (1991) Simulation of the packing and cooling phases of thermoplastic injection moulding. In Isayev, A. I. (editor) *Modeling of polymer processing: recent developments*. Oxford: Oxford University Press.
- Huq, A. and Azaiez, J. (2005) Effects of length distribution on the steady shear viscosity of semiconcentrated polymer-fiber suspensions. *Polymer Engineering & Science* 45 (10), 1357-1368.
- Inceoglu, F., Ville, J., Ghamri, N., Durin, A., Valette, R. and Vergnes, B. (2010) A Study of Fiber Breakage During Compounding of Glass Fiber Reinforced Composites. *Proceedings 27th Congr Polym Proc Soc Banff (Canada)*.
- Inceoglu, F., Ville, J., Ghamri, N., Pradel, J. L., Durin, A., Valette, R. and Vergnes, B. (2011) Correlation between processing conditions and fiber breakage during compounding of glass fiber-reinforced polyamide. *Polymer Composites* 32 (11), 1842-1850.
- Inoue, A., Morita, K., Tanaka, T., Arai, Y. and Sawada, Y. (2015) Effect of screw design on fiber breakage and dispersion in injection-molded long glass-fiber-reinforced polypropylene. *Journal of Composite Materials* 49 (1), 75-84.
- International Organization for Standardization: ISO 22314: Plastics - Glass-fibre-reinforced products - Determination of fibre length, Switzerland* (2006)
- Jeffery, G. B. (1922) The motion of ellipsoidal particles immersed in a viscous fluid. *Proc. R. Soc. Lond. A* 102 (715), 161-179.
- Jin, G., Lin, X., Tian, G., Zhang, S., Wang, M. and Wang, X. (2016) Entrance flow of long glass fiber reinforced polypropylene through contraction die. *Journal of Reinforced Plastics and Composites* 35 (2), 111-123.
- Job, S. (2013) Recycling glass fibre reinforced composites – history and progress. *Reinforced Plastics* 57 (5), 19-23.
- Kastner, J., Salaberger, D., Zitzenbacher, G., Stadlbauer, W. and Freytag, R. (2008) Determination of diameter, length and three-dimensional distribution of fibres in short glass-fibre reinforced injection moulded parts by  $\mu$ -computed tomography. *Proceedings 24th annual meeting polymer processing society, Salerno, Italy*. Vol. 15.
- Kelleher, P. G. (1993) *Reinforced Thermoplastics: Composition, Processing and Applications*. Vol. 66. iSmithers Rapra Publishing.
- Kelly, A. and Tyson, a. W. (1965) Tensile properties of fibre-reinforced metals: copper/tungsten and copper/molybdenum. *Journal of the Mechanics and Physics of Solids* 13 (6), 329-350.
- Kim, S.-W. and Turng, L.-S. (2004) Developments of three-dimensional computer-aided engineering simulation for injection moulding. *Modelling and Simulation in Materials Science and Engineering* 12 (3), S151.
- Krasteva, D. L. (2009) *Integrated prediction of processing and thermomechanical behavior of long fiber thermoplastic composites*. PhD. Portugal: University of Minho.

- Kraus, T., Kühnel, M. and Witten, E. (2014) Composites market report 2014; Market developments, trends, challenges and opportunities. *The Global CRP Market*.
- Ku, H., Wang, H., Pattarachaiyakoop, N. and Trada, M. (2011) A review on the tensile properties of natural fiber reinforced polymer composites. *Composites Part B: Engineering* 42 (4), 856-873.
- Kumar, K. S., Bhatnagar, N. and Ghosh, A. K. (2007a) Development of long glass fiber reinforced polypropylene composites: mechanical and morphological characteristics. *Journal of reinforced plastics and composites* 26 (3), 239-249.
- Kumar, K. S., Ghosh, A. K. and Bhatnagar, N. (2007b) Mechanical properties of injection molded long fiber polypropylene composites, part 1: tensile and flexural properties. *Polymer Composites* 28 (2), 259-266.
- Kumar, K. S., Patel, V., Tyagi, A., Bhatnagar, N. and Ghosh, A. (2009) Injection Molding of Long Fiber Reinforced Thermoplastic Composites. *International Polymer Processing* 24 (1), 17-22.
- Kunc, V., Frame, B. J., Nguyen, B. N., Tucker III, C. L. and Velez-Garcia, G. (2007) Fiber length distribution measurement for long glass and carbon fiber reinforced injection molded thermoplastics. *7th Annual Automotive Composites Conference and Exhibition*. Michigan, USA.
- Lafranche, E., Krawczak, P., Ciolczyk, J.-P. and Maugey, J. (2005) Injection moulding of long glass fiber reinforced polyamide 66: Processing conditions/microstructure/flexural properties relationship. *Advances in Polymer Technology* 24 (2), 114-131.
- Lafranche, E., Krawczak, P., Ciolczyk, J. and Maugey, J. (2007) Injection moulding of long glass fibre reinforced polyamide 6-6: guidelines to improve flexural properties. *Express Polym Lett* 1 (7), 456-466.
- Lee, S. M. (1992) *Handbook of composite reinforcements*. John Wiley & Sons.
- Lohr, C., Menrath, A., Elsner, P. and Weidenmann, K. A. (2017) Influence of the Manufacturing Process (Comparison MuCell and Direct-LFT) of Foamed and Fiber Reinforced Polymer Sandwich Structures on the Fiber Length. *Key Engineering Materials*. Vol. 742. Trans Tech Publ.
- Lunt, J. and Shortall, J. (1979) The effect of extrusion compounding on fibre degradation and strength properties in short glass-fibre-reinforced nylon 6.6. *Plastics Rubber Process* 4 (3), 108-111.
- Marsh, G. (2014) Composites flying high. *Reinforced Plastics* 58 (3), 14-18.
- Martin, G. A. (2005) Direct Compounding: New Directions in Plastics Processing. *Kunststoffe* (8), 26-33.
- Matsuoka, T. (1995) Fiber orientation prediction in injection molding. *Polypropylene Structure, blends and Composites*. Springer. 113-141.
- McCrum, N. G., Buckley, C. and Bucknall, C. B. (1997) *Principles of polymer engineering*. Oxford University Press, USA.
- Metten, M. and Cremer, M. (2000) Injection Moulding of long-fibre-reinforced thermoplastics. *Kunststoffe* 75 (1), 80-83.

- Mittal, R. K., Gupta, V. B. and Sharma, P. K. (1988) Theoretical and experimental study of fibre attrition during extrusion of glass-fibre-reinforced polypropylene. *Composites Science and Technology* 31 (4), 295-313.
- Nguyen, B. N., Bapanapalli, S. K., Holbery, J. D., Smith, M. T., Kunc, V., Frame, B. J., Phelps, J. H. and Tucker III, C. L. (2008) Fiber length and orientation in long-fiber injection-molded thermoplastics—Part I: Modeling of microstructure and elastic properties. *Journal of composite materials* 42 (10), 1003-1029.
- Ning, F., Cong, W., Qiu, J., Wei, J. and Wang, S. (2015) Additive manufacturing of carbon fiber reinforced thermoplastic composites using fused deposition modeling. *Composites Part B: Engineering* 80, 369-378.
- O'Regan, D. and Akay, M. (1996) The distribution of fibre lengths in injection moulded polyamide composite components. *Journal of materials processing technology* 56 (1-4), 282-291.
- Ogawa, T., Mima, T. and Taya, N. (1995) Change of Fiber Length in Injection Molding of Carbon Fiber Reinforced Nylon 66. *Japanese Society Polymer Processing* 7 (5), 315-320.
- Palmer, J., Ghita, O. R., Savage, L. and Evans, K. E. (2009) Successful closed-loop recycling of thermoset composites. *Composites Part A: Applied Science and Manufacturing* 40 (4), 490-498.
- Parveen, B. (2014) *Fibre Orientation and Breakage in Glass Fibre Reinforced Polymer Composite Systems: Experimental Validation of Models for Injection Mouldings. Validation of Short and Long Fibre Prediction Models within Autodesk Simulation Moldflow Insight 2014*. PhD. University of Bradford.
- Patcharaphun, S. and Opaskornkul, G. (2008) Characterization of Fiber Length Distribution in Short and Long-Glass-Fiber Reinforced Polypropylene during Injection Molding Process. *Kasetsart J.(Nat. Sci.)* 42, 392-397.
- Pechulis, M. and Vautour, D. (1998) The effect of thickness on the tensile and impact properties of reinforced thermoplastics. *Journal of reinforced plastics and composites* 17 (17), 1580-1586.
- Phelps, J. H. (2009) *Processing-microstructure models for short-and long-fiber thermoplastic composites*. PhD. University of Illinois.
- Phelps, J. H., Abd El-Rahman, A. I., Kunc, V. and Tucker, C. L. (2013) A model for fiber length attrition in injection-molded long-fiber composites. *Composites Part A: Applied Science and Manufacturing* 51, 11-21.
- Pickering, S. J. (2006) Recycling technologies for thermoset composite materials—current status. *Composites Part A: applied science and manufacturing* 37 (8), 1206-1215.
- Pinter, P., Bertram, B. and Weidenmann, K. A. (2016) A Novel Method for the Determination of Fibre Length Distributions from  $\mu$ CT-data. *6th Conference on Industrial Computed Tomography, Wels, Austria (iCT 2016)*.

- Priebe, M. and Schledjewski, R. (2011) Processing and properties of glass/polypropylene in long fibre compounding extrusion. *Plastics, Rubber and Composites* 40 (6-7), 374-379.
- Ramani, K., Bank, D. and Kraemer, N. (1995) Effect of screw design on fiber damage in extrusion compounding and composite properties. *Polymer composites* 16 (3), 258-266.
- Ren, P. and Dai, G. (2014) Fiber dispersion and breakage in deep screw channel during processing of long fiber-reinforced polypropylene. *Fibers and Polymers* 15 (7), 1507-1516.
- Rohde-Tibitz, M. (2015) *Direct Processing of Long Fiber Reinforced Thermoplastic Composites and their Mechanical Behavior under Static and Dynamic Load*. Carl Hanser Verlag GmbH Co KG.
- Rohde, M., Ebel, A., Wolff-Fabris, F. and Altstädt, V. (2011) Influence of processing parameters on the fiber length and impact properties of injection molded long glass fiber reinforced polypropylene. *International Polymer Processing* 26 (3), 292-303.
- Rubin, I. (1974) *Injection Molding: Theory and Practice*. John Wiley & Sons.
- Salaberger, D., Gleiß, S. and Kastner, J. (2013) Comparison of Methods to Determine Fibre Length Distribution: X-Ray CT Versus Standard Method. In *International Conference Structural Analysis of Advanced Materials*. Kos, Greece. University of Applied Sciences Upper Austria.
- Salaberger, D., Kannappan, K., Kastner, J., Reussner, J. and Auinger, T. (2010) CT Data Evaluation of Fibre Reinforced Polymers to Determine Fibre Length Distribution. In *PPS-26*. Banff, Canada.
- Salaberger, D., Kannappan, K., Kastner, J., Reussner, J. and Auinger, T. (2011) Evaluation of Computed Tomography Data from Fibre Reinforced Polymers to Determine Fibre Length Distribution. *International Polymer Processing* 26 (3), 283-291.
- Salinas, A. and Pittman, J. (1981) Bending and breaking fibers in sheared suspensions. *Polymer Engineering & Science* 21 (1), 23-31.
- Sawyer, L. C. (1979) Determination of fiberglass lengths: Sample preparation and automatic image analysis. *Polymer Engineering & Science* 19 (5), 377-382.
- Schemme, M. (2003) Long fibre reinforced thermoplastics. *Kunststoffe, Plast Europe* 93 (8).
- Schemme, M. (2008) LFT – development status and perspectives. *Reinforced Plastics* 52 (1), 32-39.
- Schijve, W. (2000) High performance at medium fibre length in long glass fibre polypropylene. *Plastics, Additives and Compounding* 12 (2), 14-21.
- Schmid, B. (1989) Spritzgießen von langfaserverstärkten Thermoplasten. *Kunststoffe* 79 (7), 624-630.
- Selzer, R. and Friedrich, K. (1997) Mechanical properties and failure behaviour of carbon fibre-reinforced polymer composites under the influence of moisture. *Composites Part A: Applied Science and Manufacturing* 28 (6), 595-604.

- Servais, C., Luciani, A. and Månson, J.-A. E. (1999) Fiber–fiber interaction in concentrated suspensions: dispersed fiber bundles. *Journal of rheology* 43 (4), 1005-1018.
- Shen, H., Nutt, S. and Hull, D. (2004) Direct observation and measurement of fiber architecture in short fiber-polymer composite foam through micro-CT imaging. *Composites science and technology* 64 (13-14), 2113-2120.
- Shon, K., Liu, D. and White, J. (2005) Experimental studies and modeling of development of dispersion and fiber damage in continuous compounding. *International Polymer Processing* 20 (3), 322-331.
- Shon, K. and White, J. L. (1999) A comparative study of fiber breakage in compounding glass fiber-reinforced thermoplastics in a buss kneader, modular Co-rotating and counter-rotating twin screw extruders. *Polymer Engineering & Science* 39 (9), 1757-1768.
- Shuaib, N. A. and Mativenga, P. T. (2016) Energy demand in mechanical recycling of glass fibre reinforced thermoset plastic composites. *Journal of Cleaner Production* 120, 198-206.
- Singh, R., Chen, F. and Jones, F. (1998) Injection molding of glass fiber reinforced phenolic composites. 2: Study of the injection molding process. *Polymer composites* 19 (1), 37-47.
- Skourlis, T., Pochiraju, K., Chassapis, C. and Manoochchri, S. (1998) Structure-modulus relationships for injection-molded long fiber-reinforced polyphthalamides. *Composites Part B: Engineering* 29 (3), 309-319.
- Stokes, V., Inzinna, L., Liang, E., Trantina, G. and Woods, J. (2000) A phenomenological study of the mechanical properties of long-fiber filled injection-molded thermoplastic composites. *Polymer composites* 21 (5), 696-710.
- Teixeira, D., Giovanela, M., Gonella, L. and Crespo, J. (2015) Influence of injection molding on the flexural strength and surface quality of long glass fiber-reinforced polyamide 6.6 composites. *Materials & Design* 85, 695-706.
- Teßmann, M., Mohr, S., Gayetskyy, S., HaSZler, U., Hanke, R. and Greiner, G. (2010) Automatic Determination of Fiber-Length Distribution in Composite Material Using 3D CT Data. *EURASIP Journal on Advances in Signal Processing* 2010 (1), 545030.
- Thomason, J. and Vlug, M. (1996) Influence of fibre length and concentration on the properties of glass fibre-reinforced polypropylene: 1. Tensile and flexural modulus. *Composites Part A: Applied science and manufacturing* 27 (6), 477-484.
- Thomason, J. and Vlug, M. (1997) Influence of fibre length and concentration on the properties of glass fibre-reinforced polypropylene: 4. Impact properties. *Composites Part A: Applied Science and Manufacturing* 28 (3), 277-288.
- Thomason, J., Vlug, M., Schipper, G. and Krikor, H. (1996) Influence of fibre length and concentration on the properties of glass fibre-reinforced polypropylene: Part 3. Strength and strain at failure. *Composites Part A: Applied Science and Manufacturing* 27 (11), 1075-1084.

- Thomason, J. L. (2002) The influence of fibre length and concentration on the properties of glass fibre reinforced polypropylene: 5. Injection moulded long and short fibre PP. *Composites Part A: Applied Science and Manufacturing* 33 (12), 1641-1652.
- Thomason, J. L. (2005) The influence of fibre length and concentration on the properties of glass fibre reinforced polypropylene. 6. The properties of injection moulded long fibre PP at high fibre content. *Composites Part A: Applied Science and Manufacturing* 36 (7), 995-1003.
- Thomason, J. L. (2007) The influence of fibre length and concentration on the properties of glass fibre reinforced polypropylene: 7. Interface strength and fibre strain in injection moulded long fibre PP at high fibre content. *Composites Part A: Applied Science and Manufacturing* 38 (1), 210-216.
- Thomason, J. L. (2009) The influence of fibre length, diameter and concentration on the impact performance of long glass-fibre reinforced polyamide 6,6. *Composites Part A: Applied Science and Manufacturing* 40 (2), 114-124.
- Timmis, A. J., Hodzic, A., Koh, L., Bonner, M., Soutis, C., Schäfer, A. W. and Dray, L. (2015) Environmental impact assessment of aviation emission reduction through the implementation of composite materials. *The International Journal of Life Cycle Assessment* 20 (2), 233-243.
- Truckenmüller, F. and Fritz, H. G. (1991) Injection molding of long fiber-reinforced thermoplastics: A comparison of extruded and pultruded materials with direct addition of roving strands. *Polymer Engineering & Science* 31 (18), 1316-1329.
- Tucker CL, P. J., Abd El-Rahman, AI, Kunc V, Frame BJ (2010) Modeling fiber length attrition in molded long-fiber composites. *PPS-26*. Banff, Canada.
- Von Bradsky, G., Bailey, R., Cervenka, A., Zachmann, H. and Allan, P. (1997) Characterization of finite length composites: Part IV-Structural studies on injection moulded composites (Technical Report). *Pure and Applied Chemistry* 69 (12), 2523-2540.
- Von Turkovich, R. and Erwin, L. (1983) Fiber fracture in reinforced thermoplastic processing. *Polymer Engineering & Science* 23 (13), 743-749.
- Wambua, P., Ivens, J. and Verpoest, I. (2003) Natural fibres: can they replace glass in fibre reinforced plastics? *Composites Science and Technology* 63 (9), 1259-1264.
- Wang, H. (2007) *Fiber property characterization by image processing*.
- Wang, J., Geng, C., Luo, F., Liu, Y., Wang, K., Fu, Q. and He, B. (2011) Shear induced fiber orientation, fiber breakage and matrix molecular orientation in long glass fiber reinforced polypropylene composites. *Materials Science and Engineering: A* 528 (7-8), 3169-3176.
- Wolf, H. (1994) Screw plasticating of discontinuous fiber filled thermoplastic: Mechanisms and prevention of fiber attrition. *Polymer composites* 15 (5), 375-383.

- Wollan, E. (2017) Glass & carbon fiber reinforcement combine in hybrid long fiber thermoplastic composites to bridge price & performance gap. *Reinforced Plastics* 61 (1), 55-57.
- Yamamoto, S. and Matsuoka, T. (1995) Dynamic simulation of flow-induced fiber fracture. *Polymer Engineering & Science* 35 (12), 1022-1030.
- Yilmazer, U. and Cansever, M. (2002) Effects of processing conditions on the fiber length distribution and mechanical properties of glass fiber reinforced nylon-6. *Polymer Composites* 23 (1), 61-71.
- Young, E. (2010) UK Composites Supply Chain Scoping Study.
- Zauner, H., Salaberger, D., Heinzl, C. and Kastner, J. (2015) 3D image processing for single fibre characterization by means of XCT. *Acta Stereologica*.
- Zhang, G. and Thompson, M. R. (2005) Reduced fibre breakage in a glass-fibre reinforced thermoplastic through foaming. *Composites Science and Technology* 65 (14), 2240-2249.
- Zhuang, H., Ren, P., Zong, Y. and Dai, G. (2008) Relationship between fiber degradation and residence time distribution in the processing of long fiber reinforced thermoplastics. *Exp Polym Lett* 2, 560-568.

**Appendix 1: Injection Moulding Settings and Fibre Length Distribution Results for Screw Pull Out Tests Performed on an Arburg Allrounder 270C**

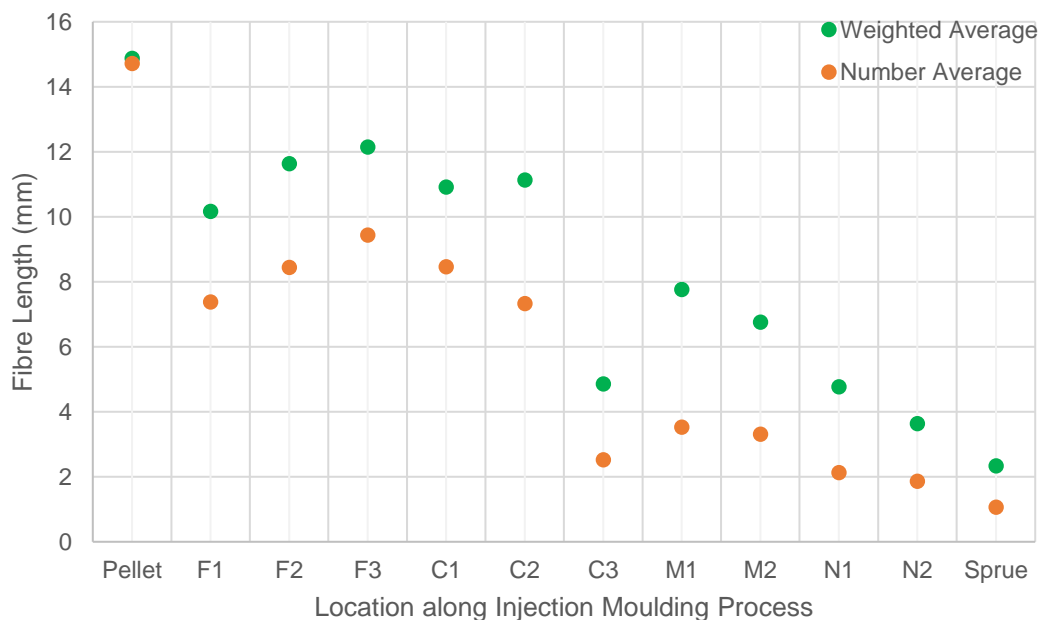
<b>Machine Settings</b>	<b>Arburg Allrounder 270C</b>
<b>Injection Time (secs)</b>	0.84
<b>Injection Speed (cm<sup>3</sup>/s)</b>	20
<b>Screw Speed (RPM)</b>	150
<b>Back Pressure (bar)</b>	2.5
<b>Packing Pressure (bar)</b>	27
<b>Packing Time (secs)</b>	5
<b>Melt Temperature (°C)</b>	220
<b>Mould Temperature (°C)</b>	20
<b>Cooling Time (secs)</b>	30

**Table A1.1. - Injection moulding settings for 20 mm screw pull out test – Low BP / Low RPM. Material: 20YM240.**

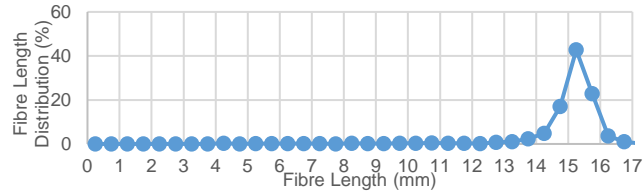


Sample	Average Fibre Length (mm)	Weighted Average Length (mm)	Maximum Fibre Length Measured (mm)	Minimum Fibre Length Measured (mm)
Pellet	14.72	14.87	16.91	2.02
F1	7.38	10.17	15.69	0.14
F2	8.44	11.63	16.24	0.12
F3	9.44	12.15	16.57	0.13
C1	8.46	10.91	16.82	0.11
C2	7.33	11.13	16.40	0.09
C3	2.52	4.86	14.71	0.04
M1	3.53	7.76	15.62	0.12
M2	3.31	6.76	16.41	0.08
N1	2.13	4.77	16.00	0.03
N2	1.86	3.64	13.55	0.05
Sprue	1.06	2.34	14.06	0.03

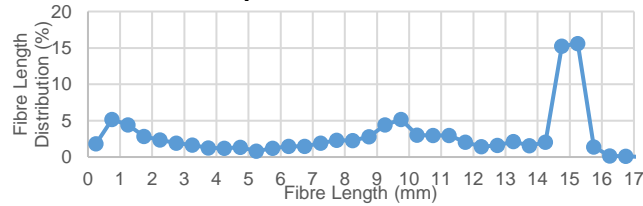
**Table A1.2. – 20 mm screw pull out test - Low BP (2.5 bar) / Low RPM (150 RPM). Material: 20YM240.**



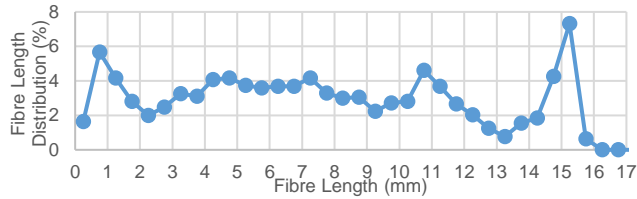
**Figure A1.1. - Number and weighted average distribution of each 24 mm cut taken from various locations along the injection moulding process**



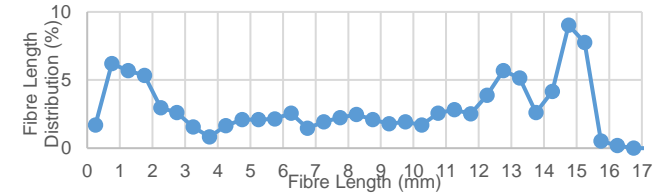
**Sample Location – Pellet**



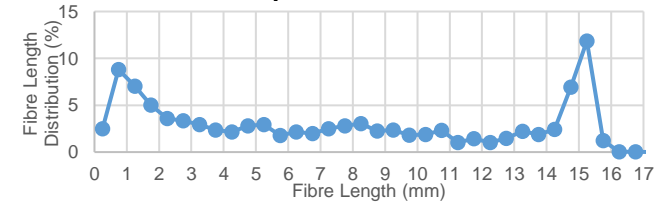
**Sample Location – F1**



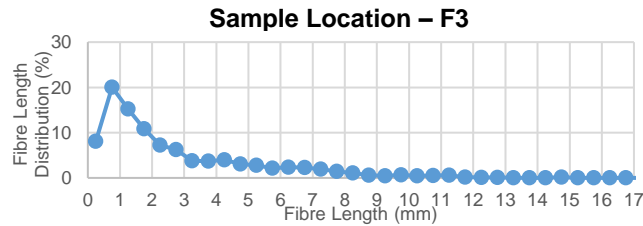
**Sample Location – F2**



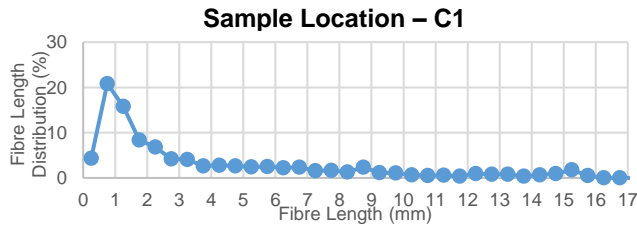
**Sample Location – C2**



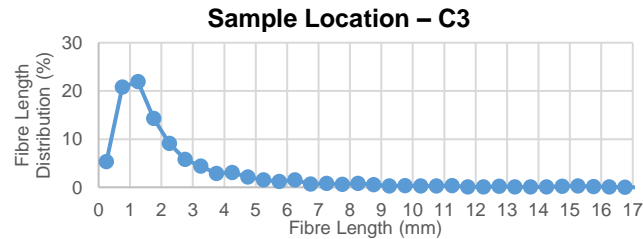
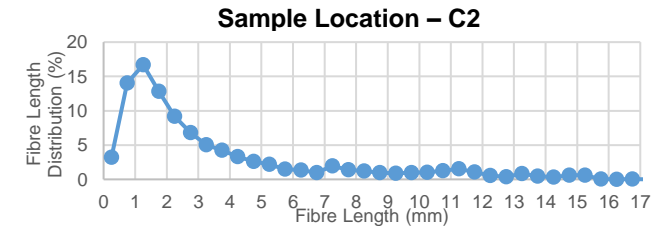
**Sample Location – C3**



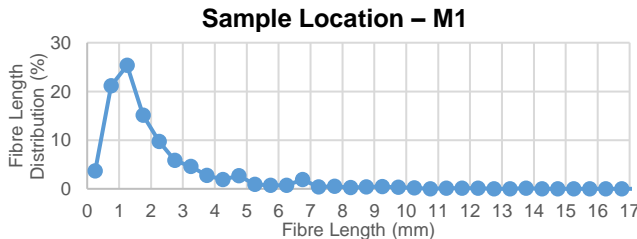
**Sample Location – M2**



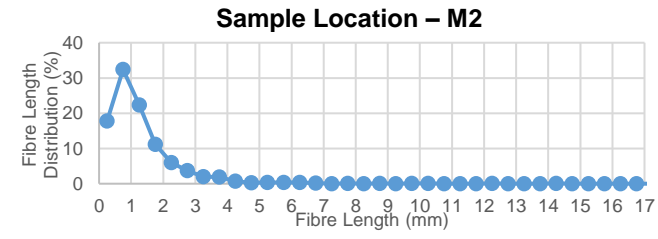
**Sample Location – M2**



**Sample Location – N1**

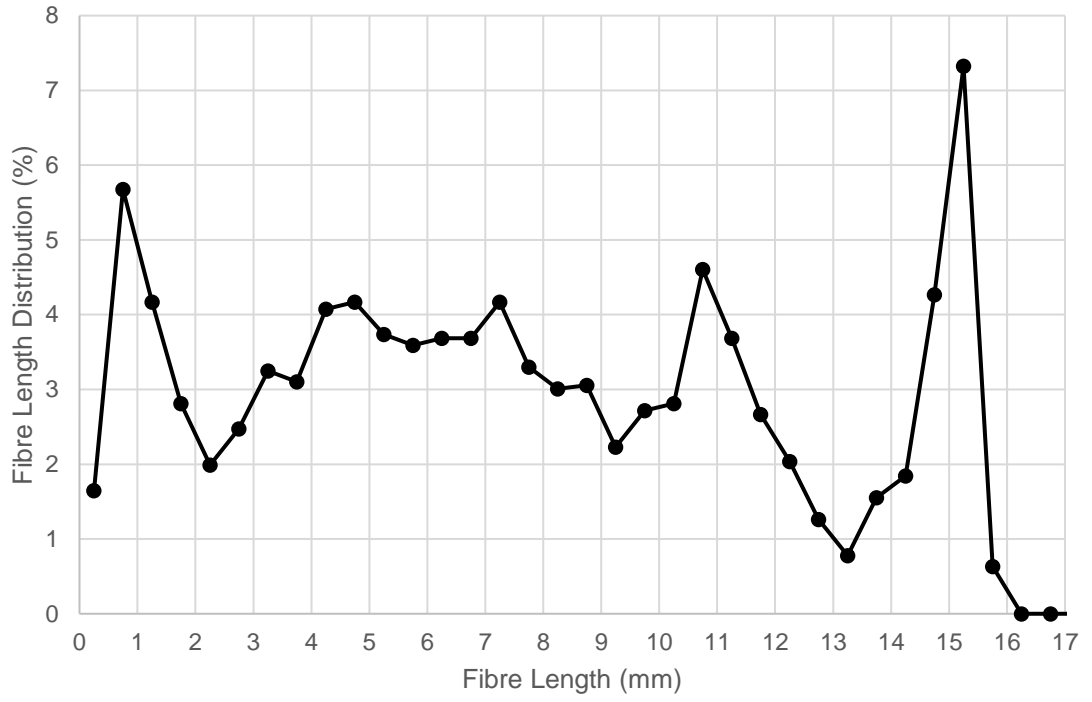


**Sample Location – N2**

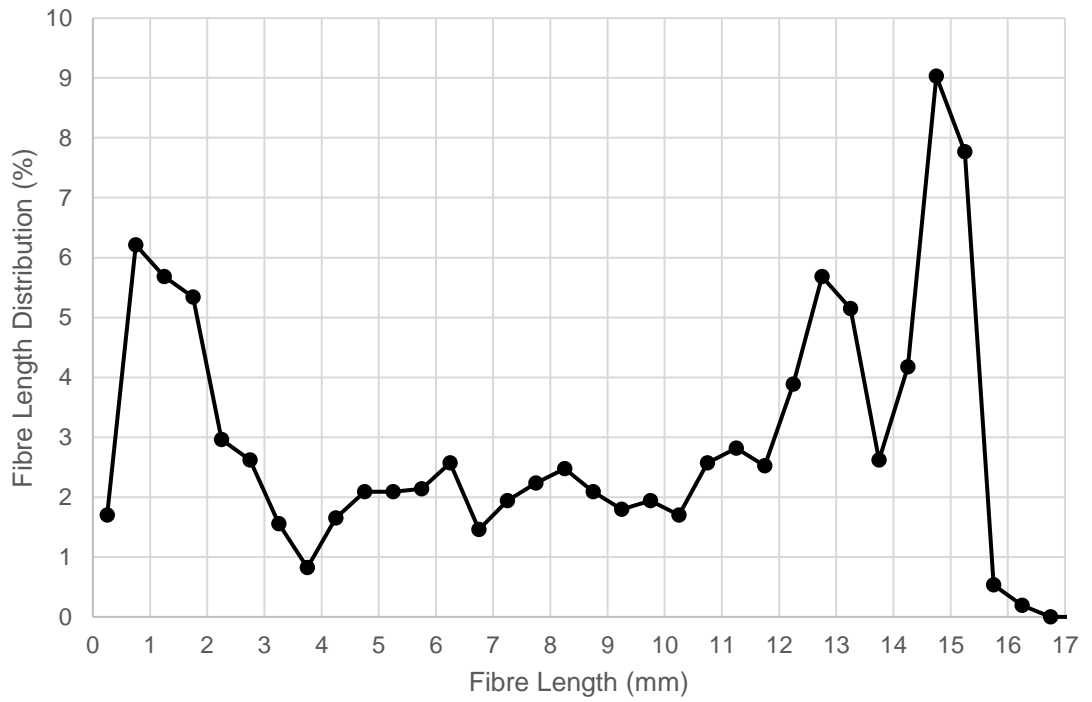


**Sample Location – Sprue**

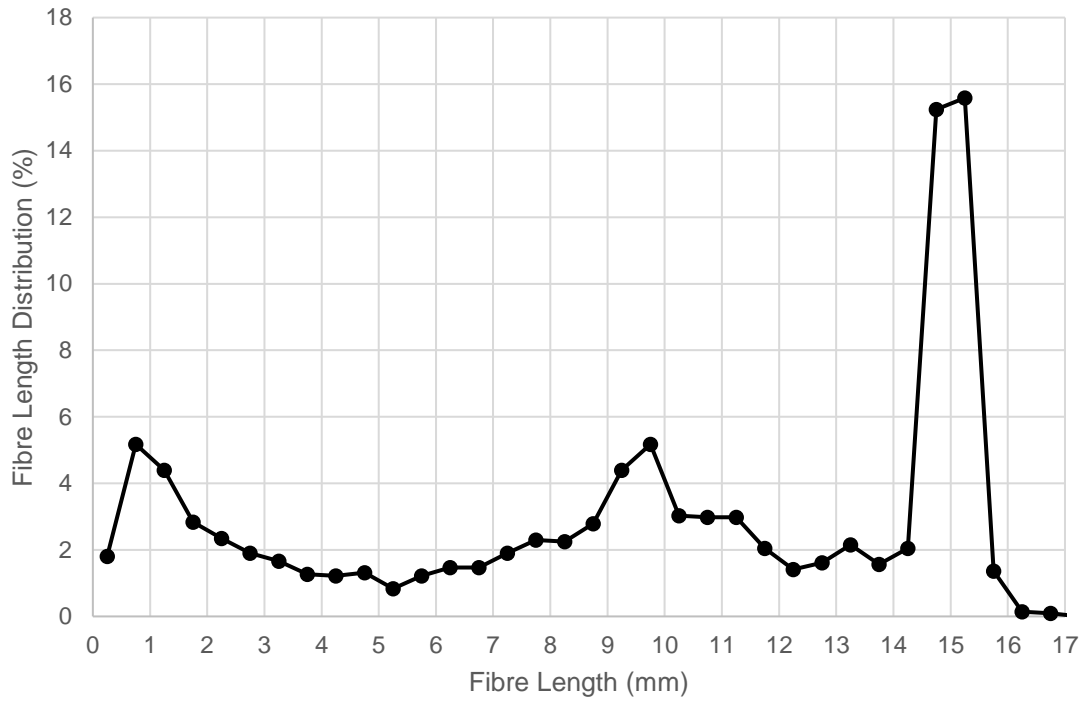
**Figure A1.2. - Summary of fibre length distribution results**



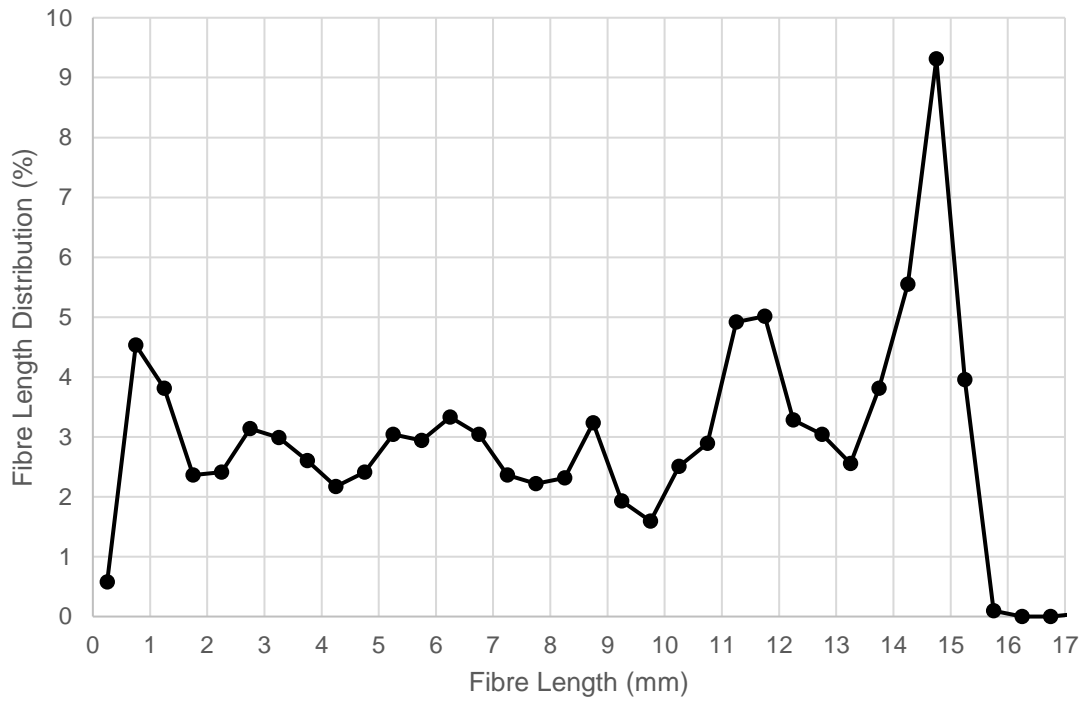
**Figure A1.3. - Sample: F1**



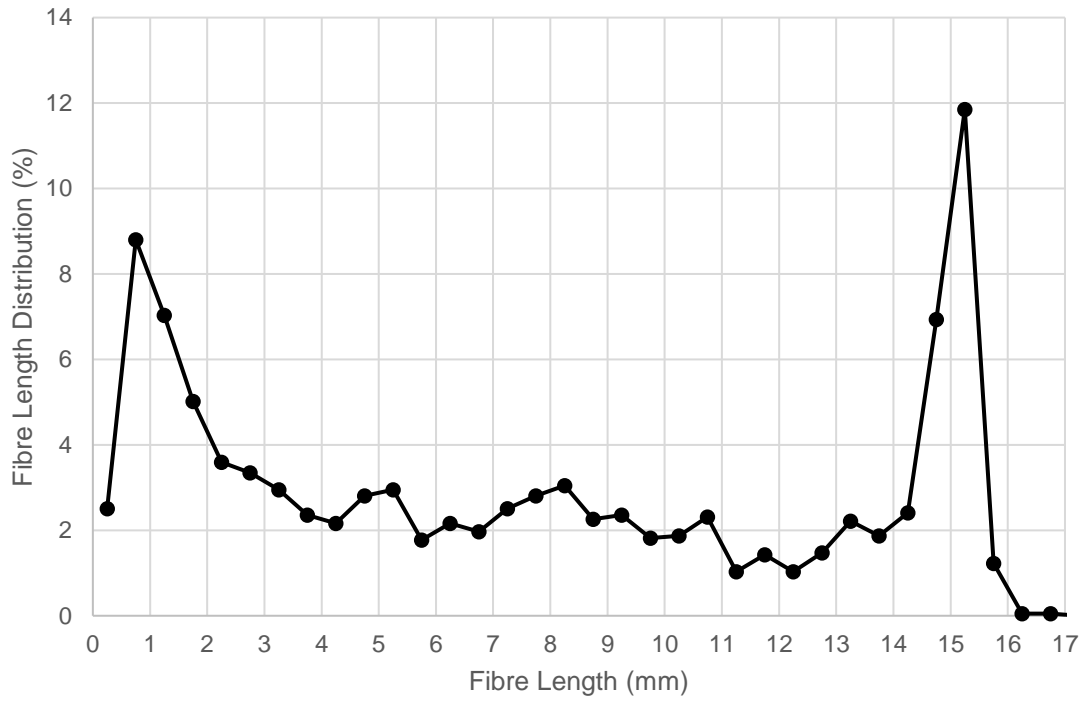
**Figure A1.4. - Sample: F2**



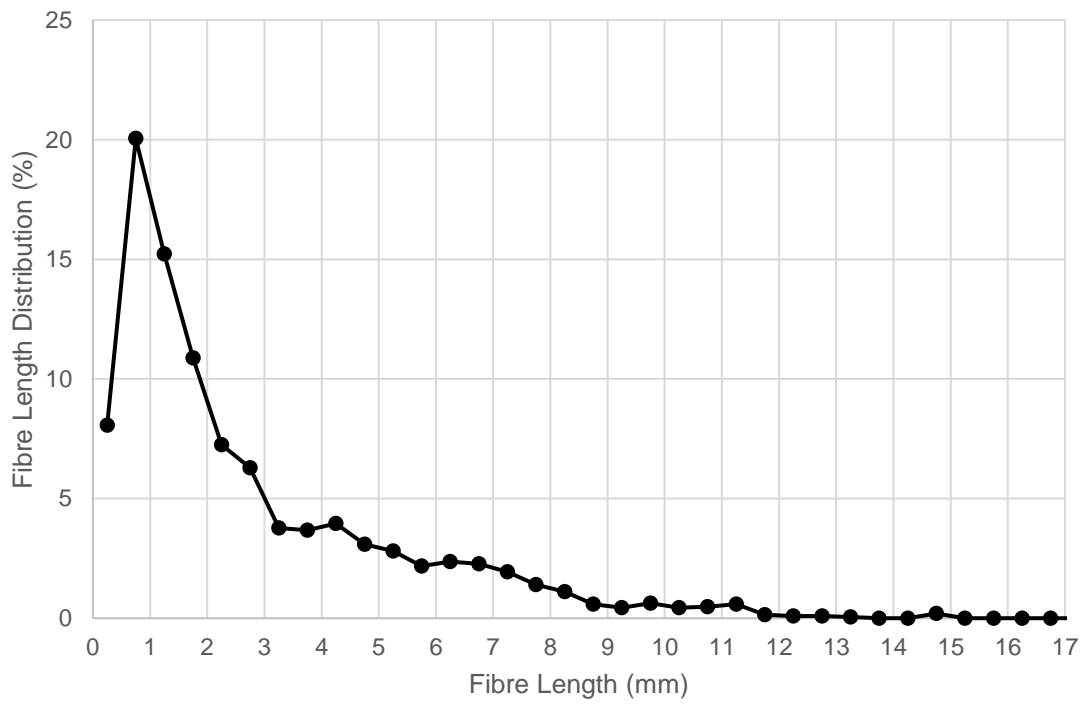
**Figure A1.5. - Sample: F3**



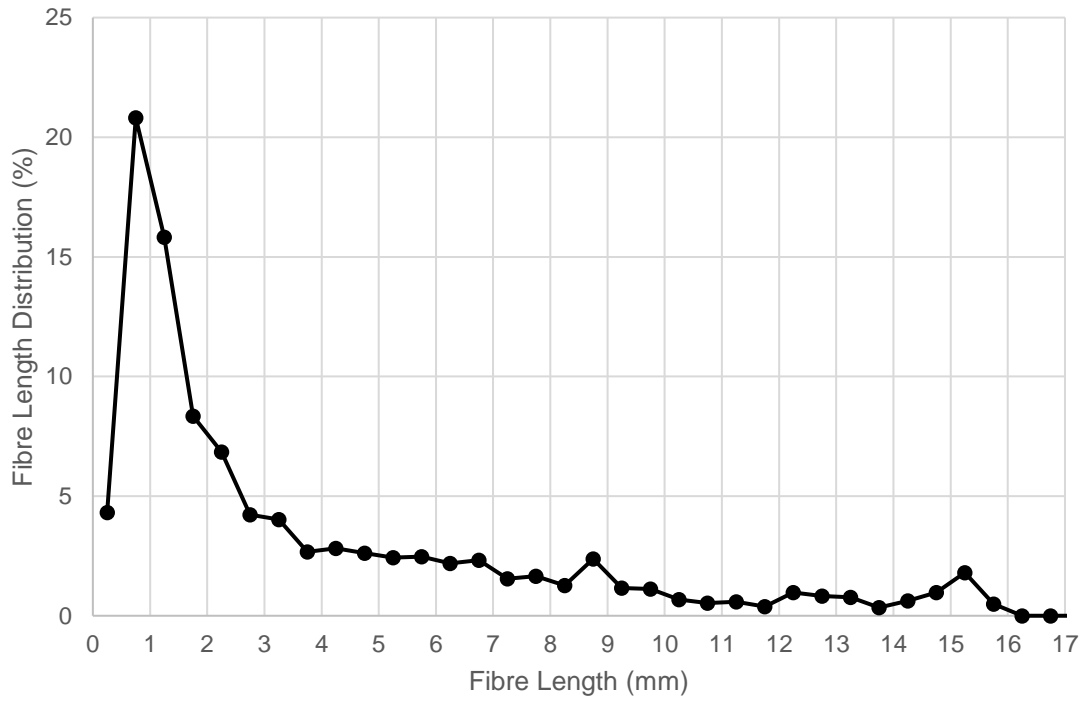
**Figure A1.6. - Sample: C1**



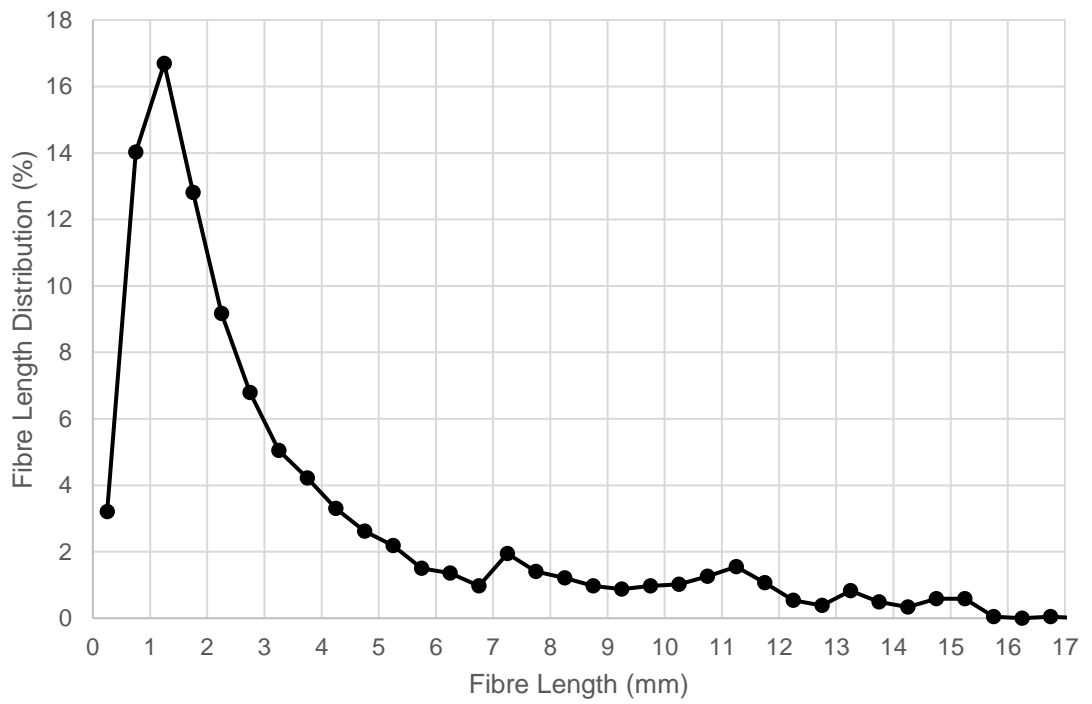
**Figure A1.7. - Sample: C1**



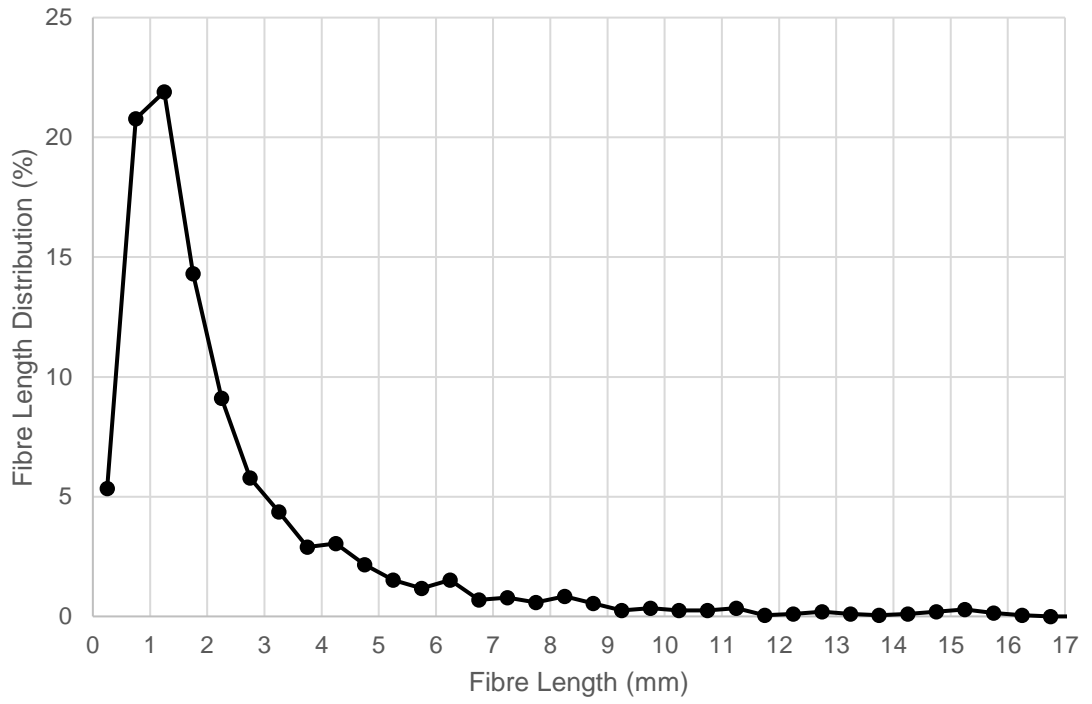
**Figure A1.8. - Sample: C3**



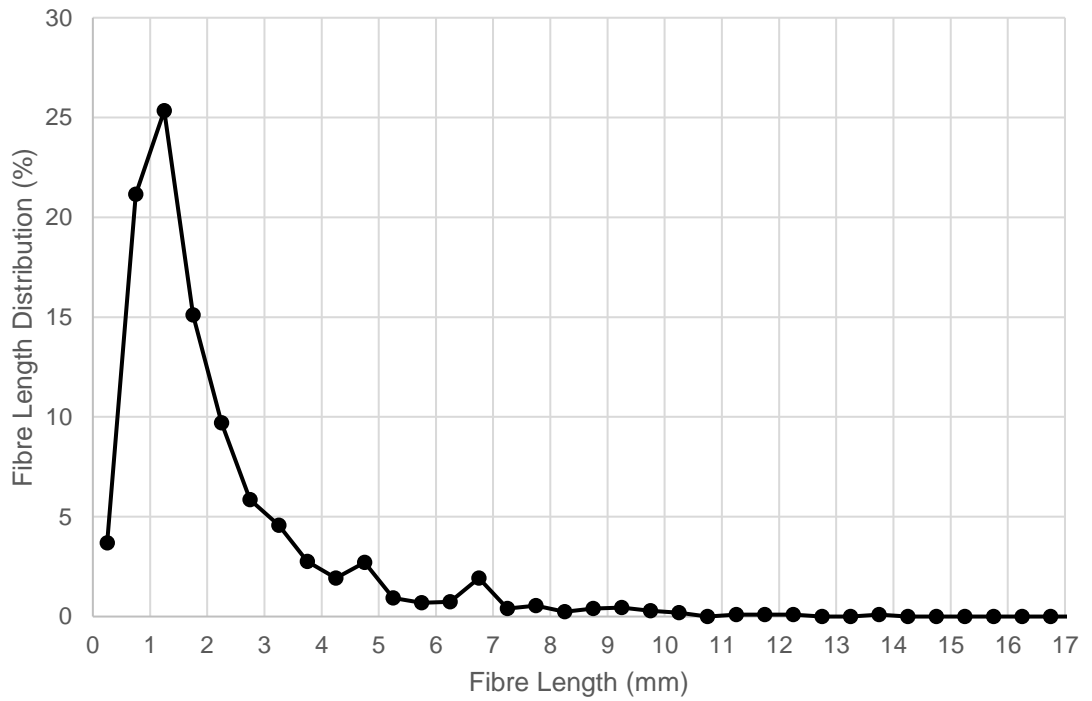
**Figure A1.9. - Sample: M1**



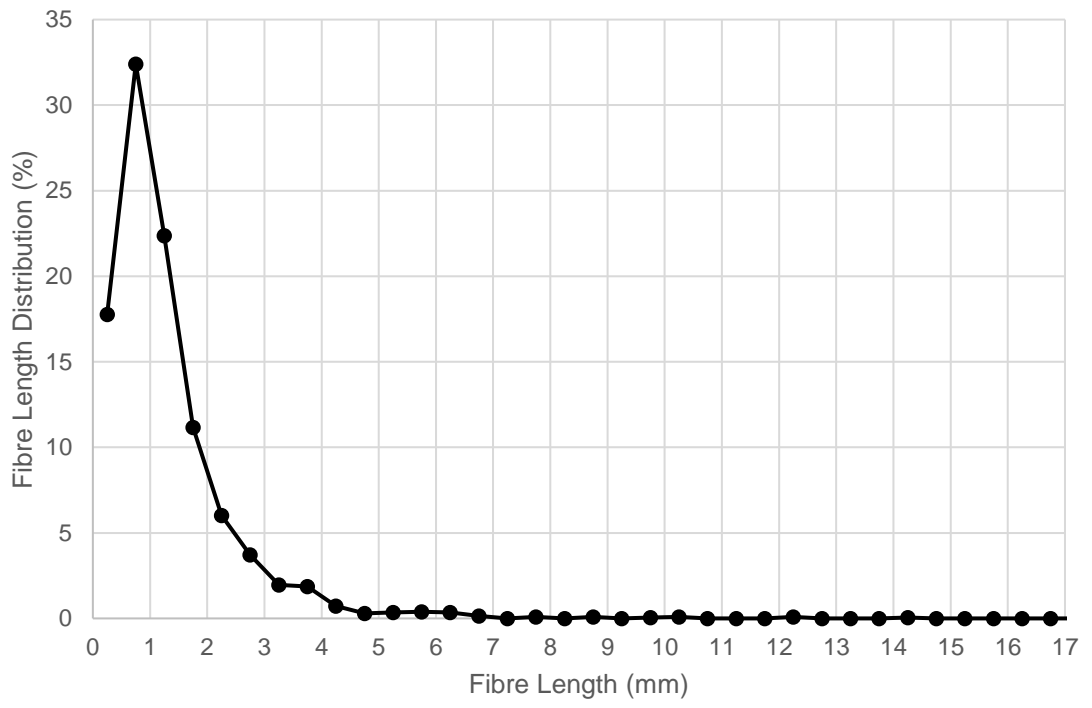
**Figure A1.10. - Sample: M2**



**Figure A1.11. - Sample: N1**



**Figure A1.12. - Sample: N2**



**Figure A1.13. - Sample: Sprue**

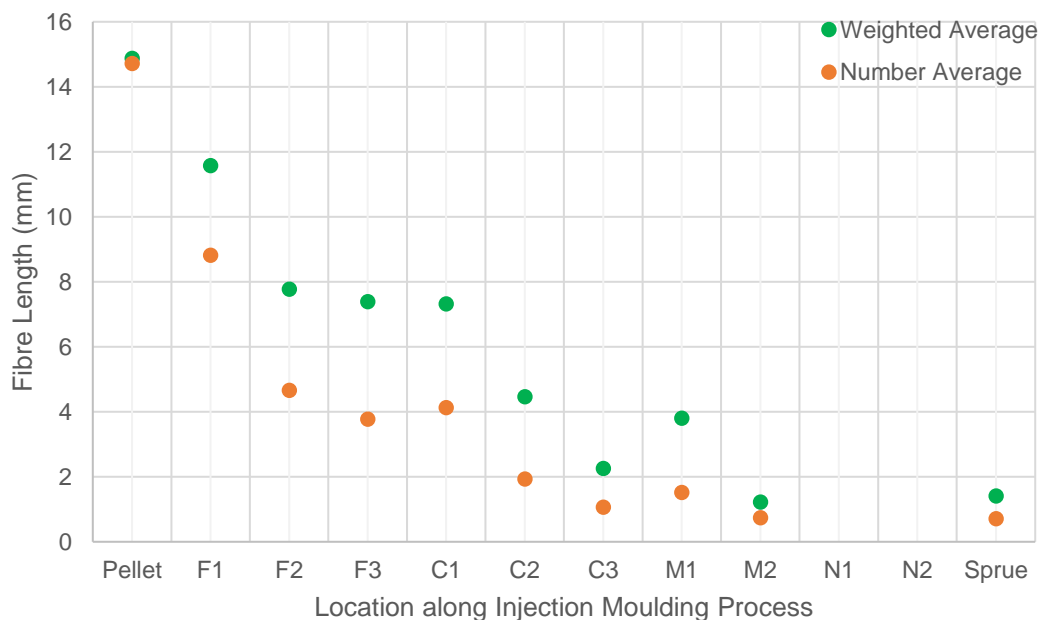


<b>Machine Settings</b>	<b>Arburg Allrounder 270C</b>
<b>Injection Time (secs)</b>	0.72
<b>Injection Speed (cm<sup>3</sup>/s)</b>	20
<b>Screw Speed (RPM)</b>	150
<b>Back Pressure (bar)</b>	5
<b>Packing Pressure (bar)</b>	27
<b>Packing Time (secs)</b>	5
<b>Melt Temperature (°C)</b>	220
<b>Mould Temperature (°C)</b>	20
<b>Cooling Time (secs)</b>	30

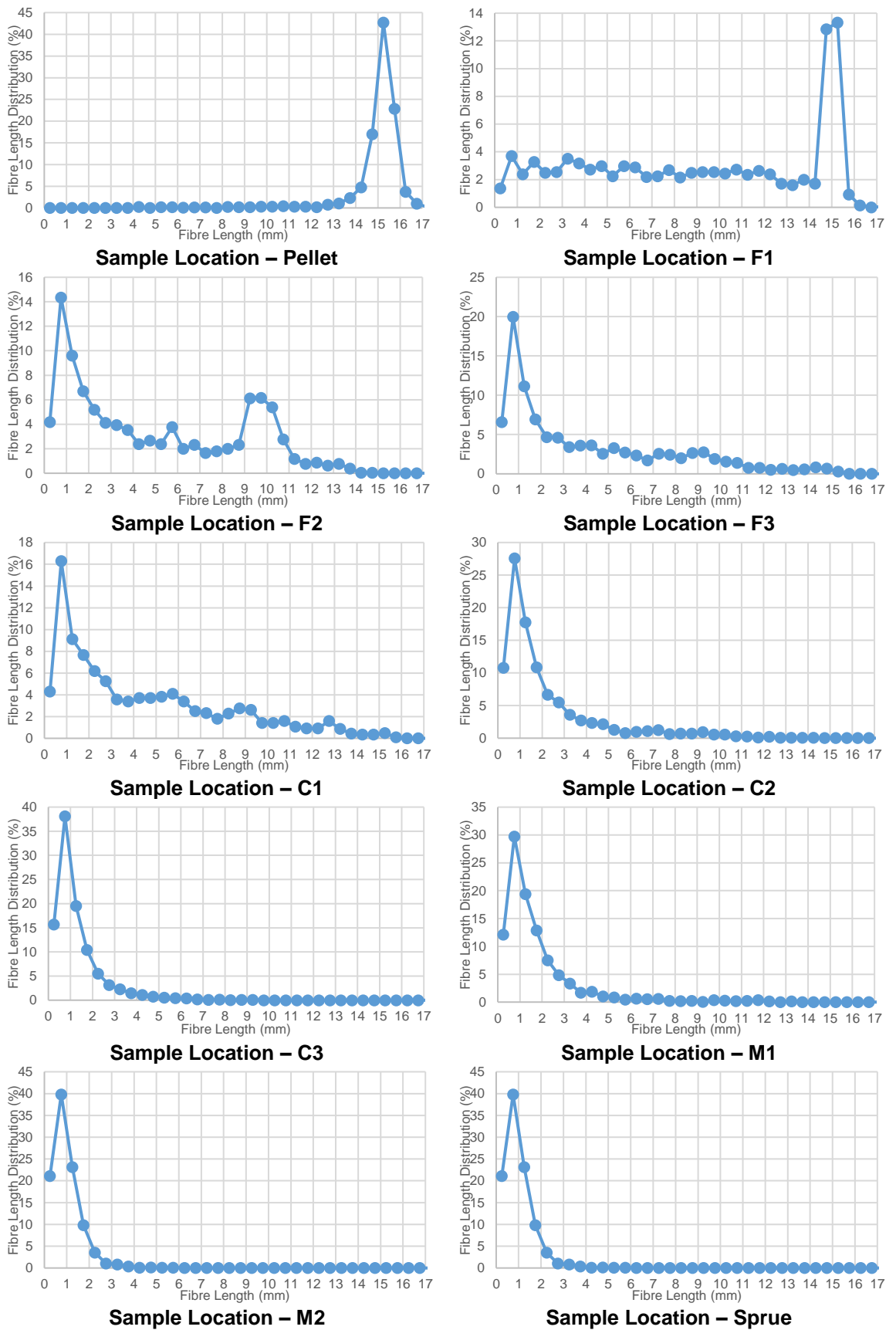
**Table A1.3. - Injection moulding settings for 20 mm screw pull out test -  
Medium BP / Low RPM. Material: 20YM240.**

Sample	Average Fibre Length (mm)	Weighted Average Length (mm)	Maximum Fibre Length Measured (mm)	Minimum Fibre Length Measured (mm)
Pellet	14.72	14.87	16.91	2.02
F1	8.82	11.57	16.93	0.09
F2	4.66	7.77	14.57	0.05
F3	3.77	7.39	15.01	0.07
C1	4.13	7.32	15.47	0.09
C2	1.93	4.46	14.25	0.07
C3	1.06	2.26	9.12	0.06
M1	1.52	3.8	13.20	0.06
M2	0.74	1.22	5.55	0.05
N1	<i>n/a</i>	<i>n/a</i>	<i>n/a</i>	<i>n/a</i>
N2	<i>n/a</i>	<i>n/a</i>	<i>n/a</i>	<i>n/a</i>
Sprue	0.71	1.41	5.82	0.03

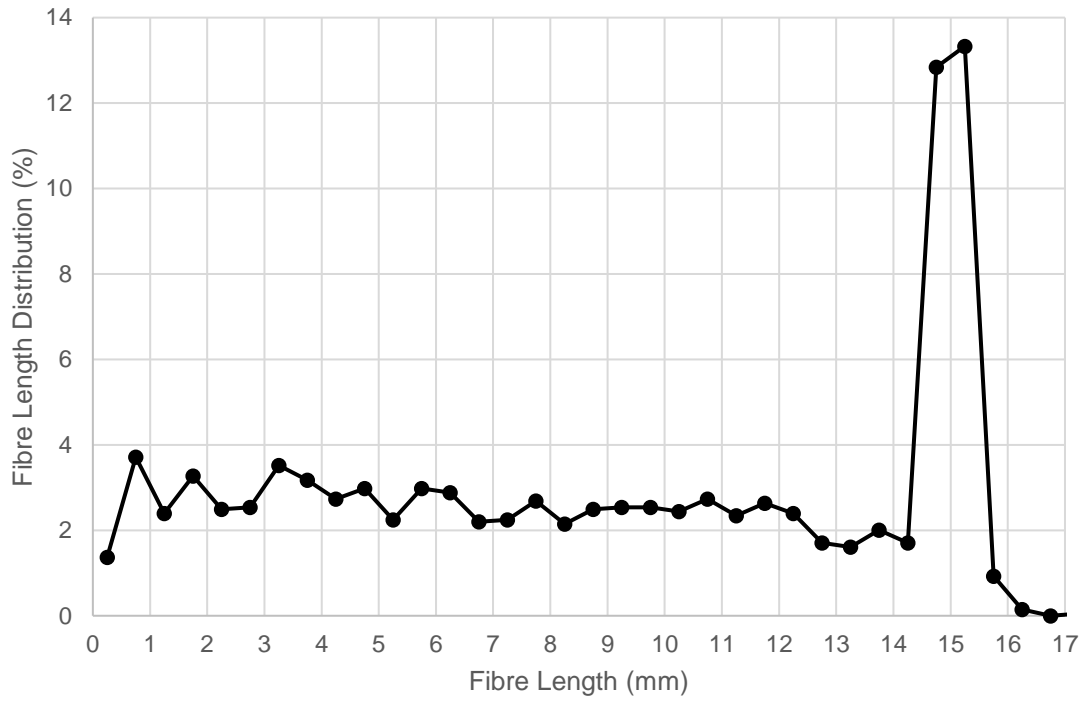
**Table A1.4. - 20 mm screw pull out test - Medium BP (5 bar) / Low RPM (150 RPM). Material: 20YM240.**



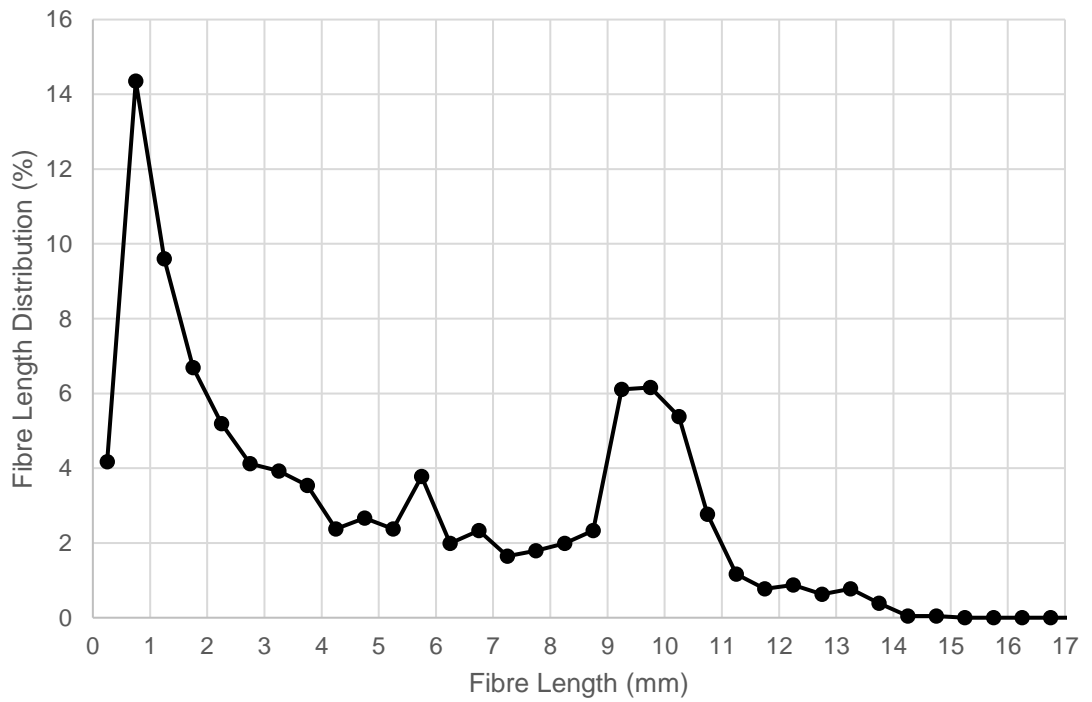
**Figure A1.14. - Number and weighted average distribution of each 24 mm cut taken from various locations along the injection moulding process**



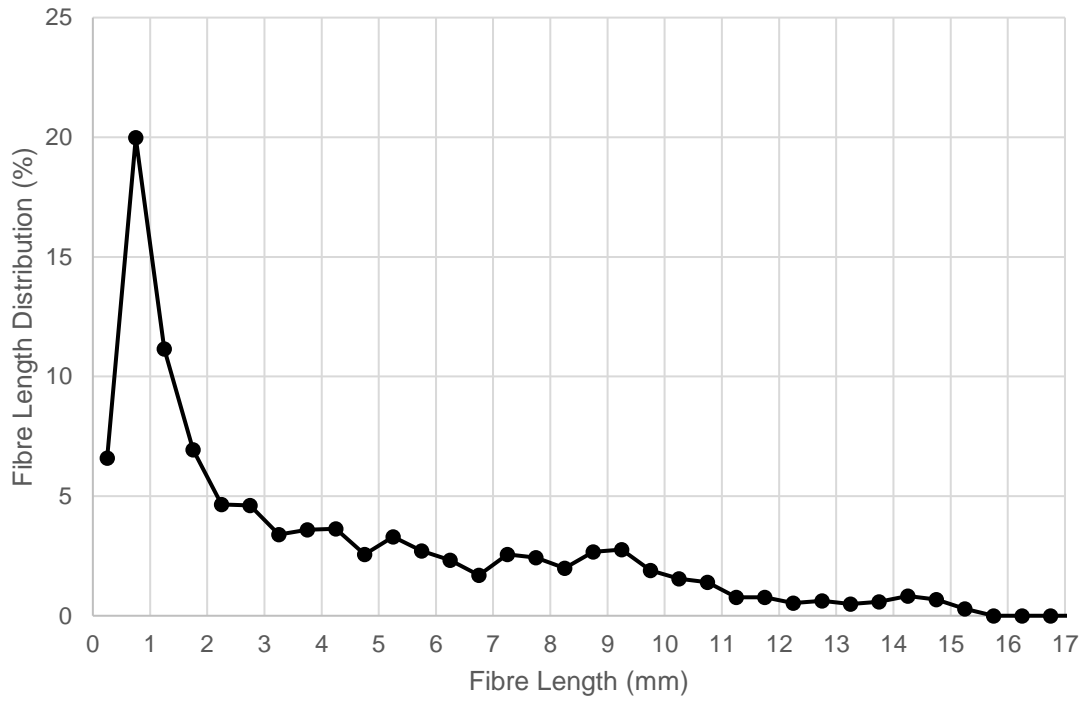
**Figure A1.15. - Summary of fibre length distribution results**



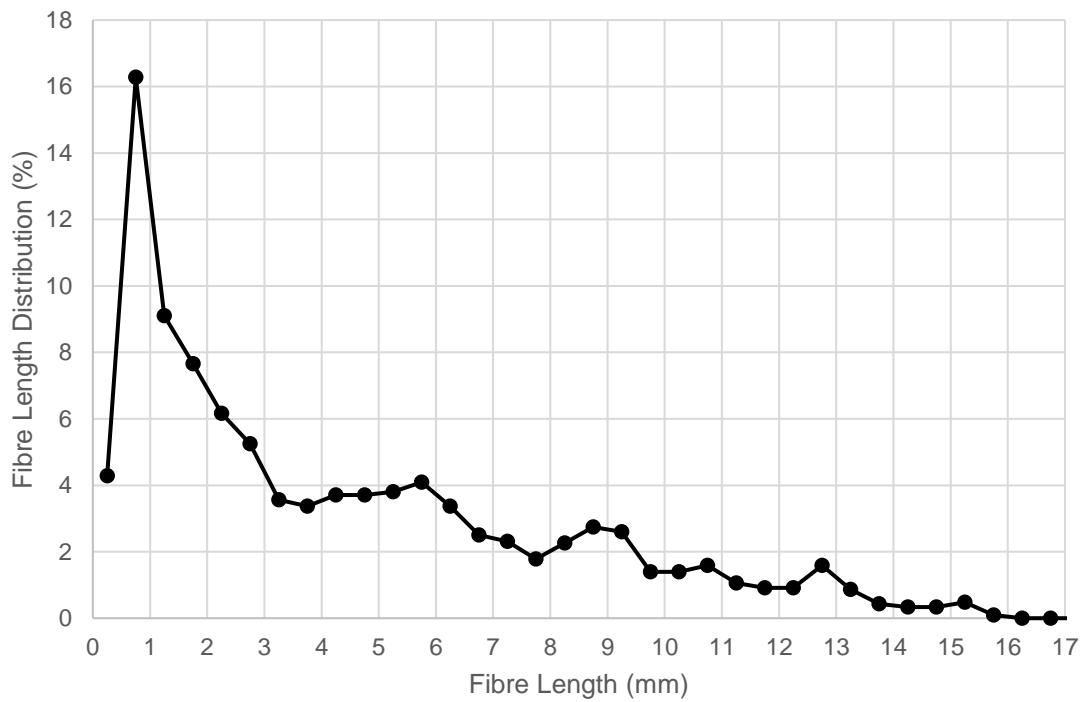
**Figure A1.16. - Sample: F1**



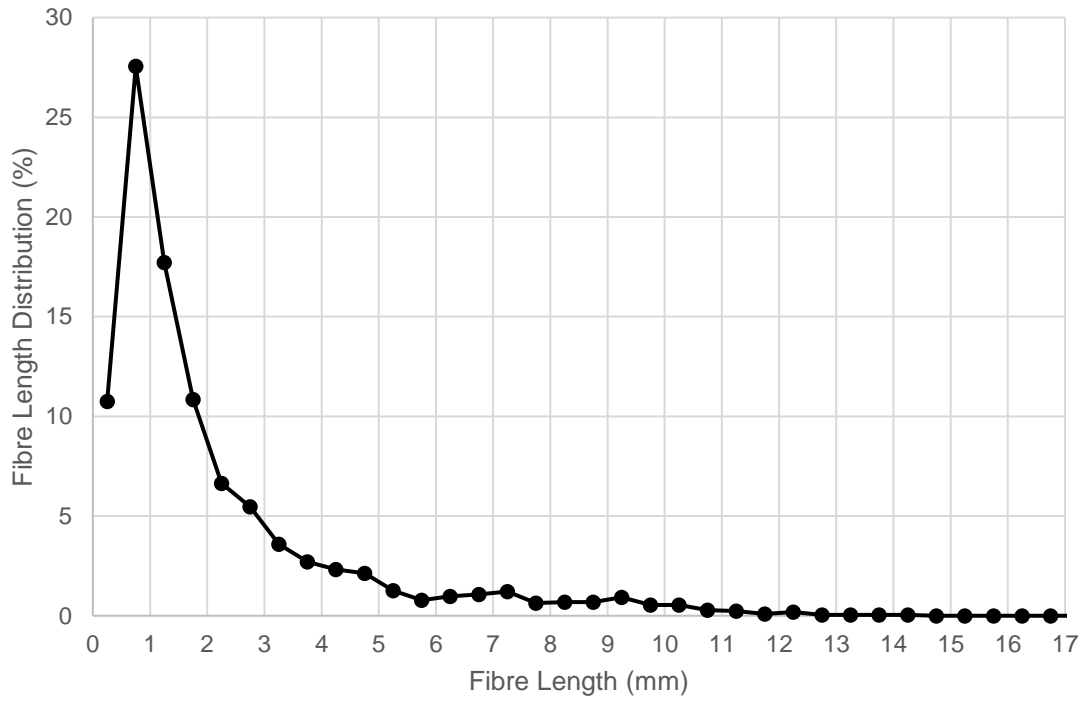
**Figure A1.17. - Sample: F2**



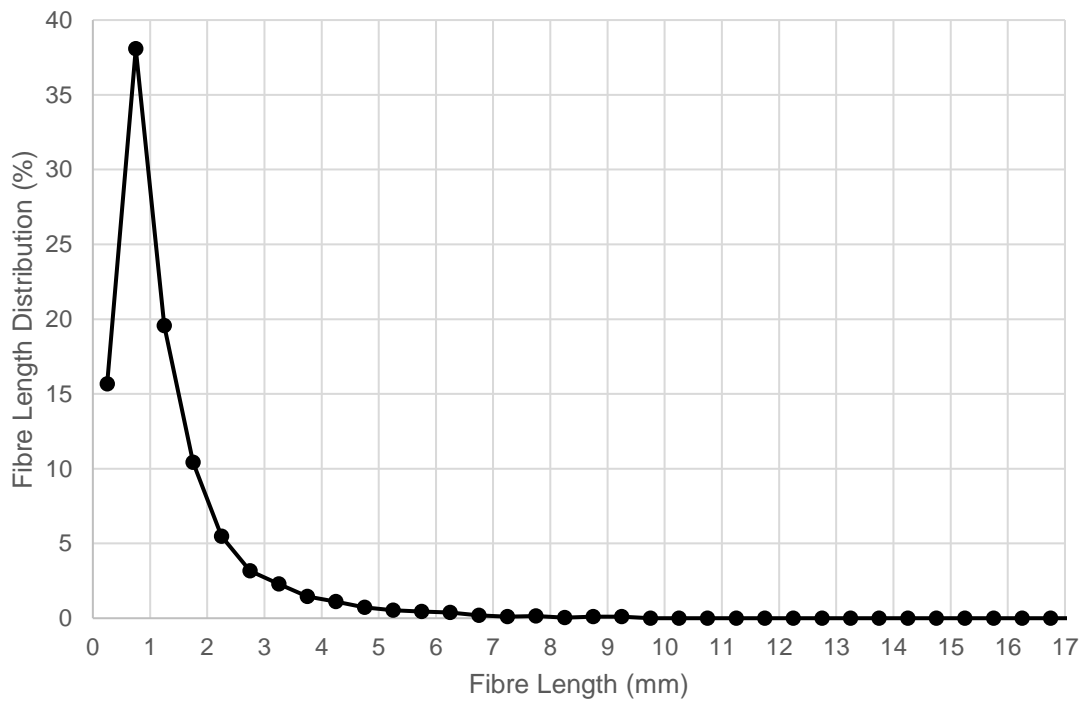
**Figure A1.18. - Sample: F3**



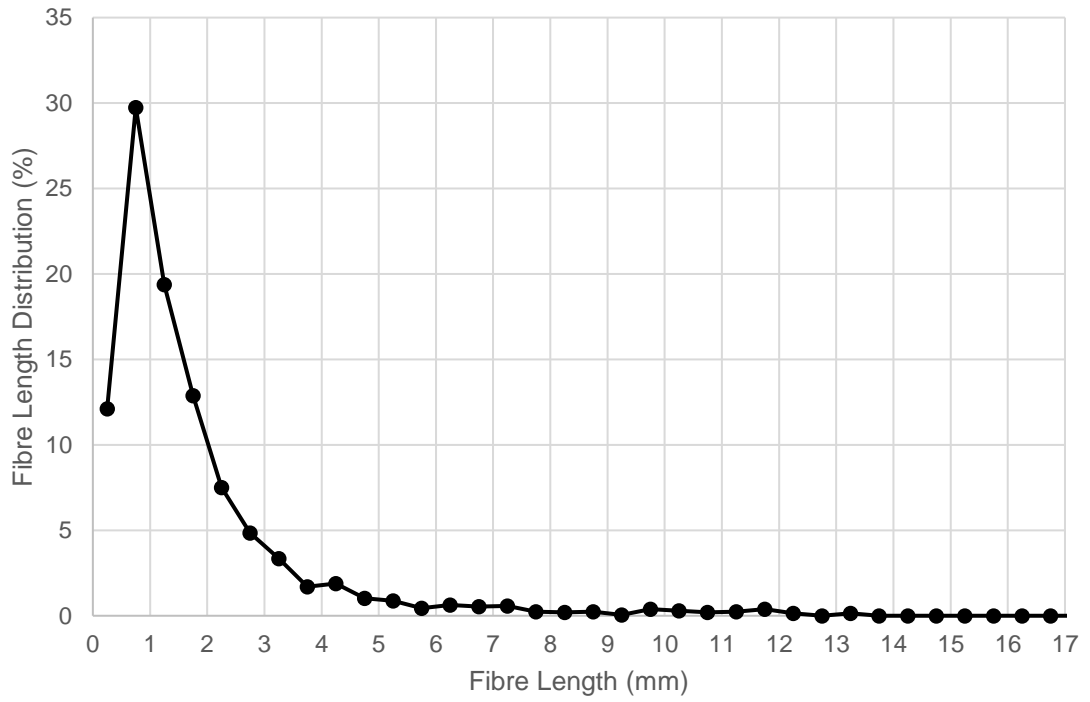
**Figure A1.19. - Sample: C1**



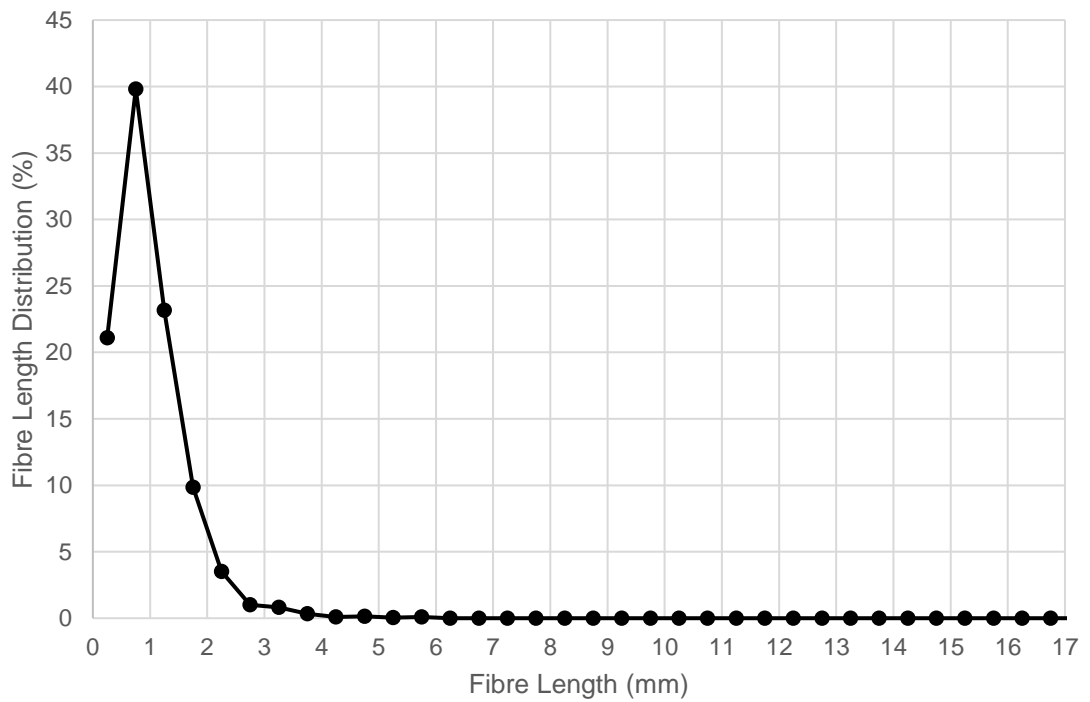
**Figure A1.20. - Sample: C2**



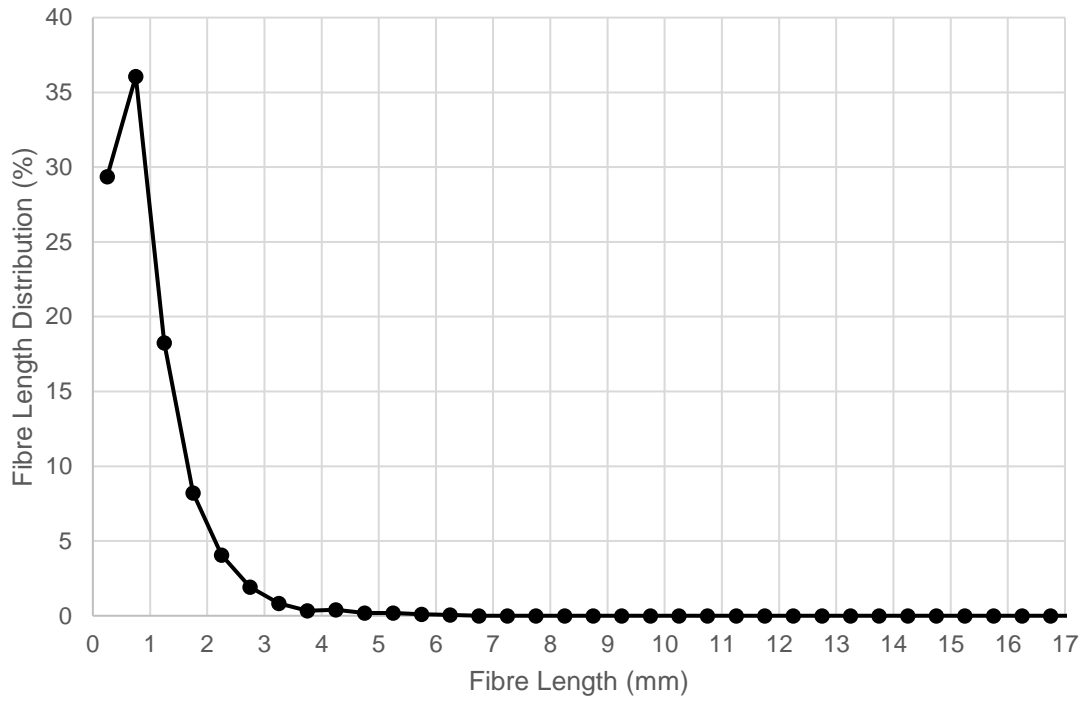
**Figure A1.21. - Sample: C3**



**Figure A1.22. - Sample: M1**



**Figure A1.23. - Sample: M2**



**Figure A1.24. - Sample: Sprue**

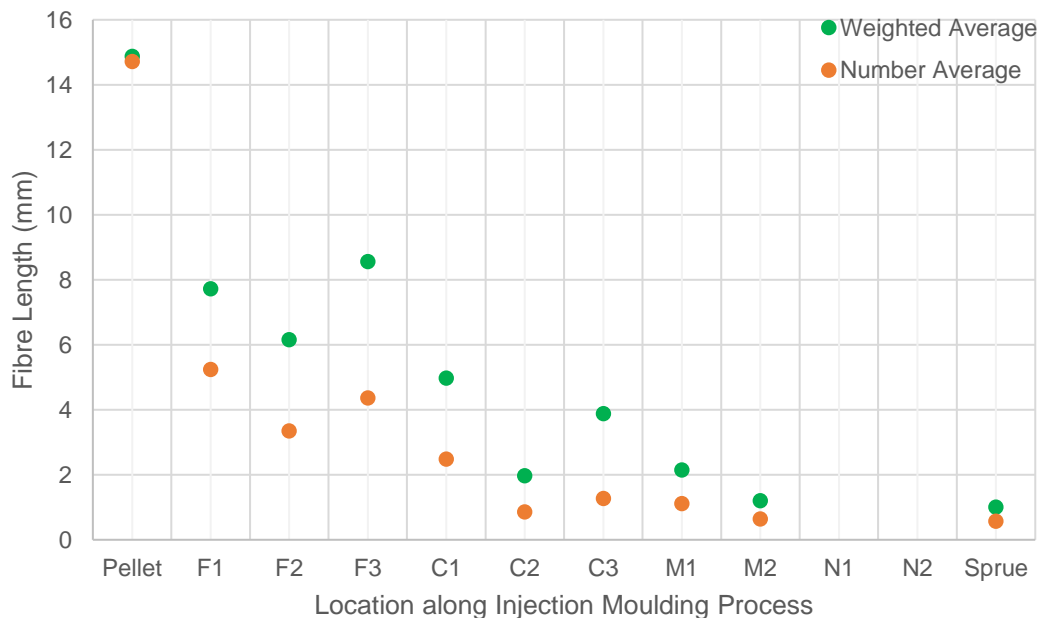


<b>Machine Settings</b>	<b>Arburg Allrounder 270C</b>
<b>Injection Time (secs)</b>	0.84
<b>Injection Speed (cm<sup>3</sup>/s)</b>	20
<b>Screw Speed (RPM)</b>	150
<b>Back Pressure (bar)</b>	7.5
<b>Packing Pressure (bar)</b>	27
<b>Packing Time (secs)</b>	5
<b>Melt Temperature (°C)</b>	220
<b>Mould Temperature (°C)</b>	20
<b>Cooling Time (secs)</b>	30

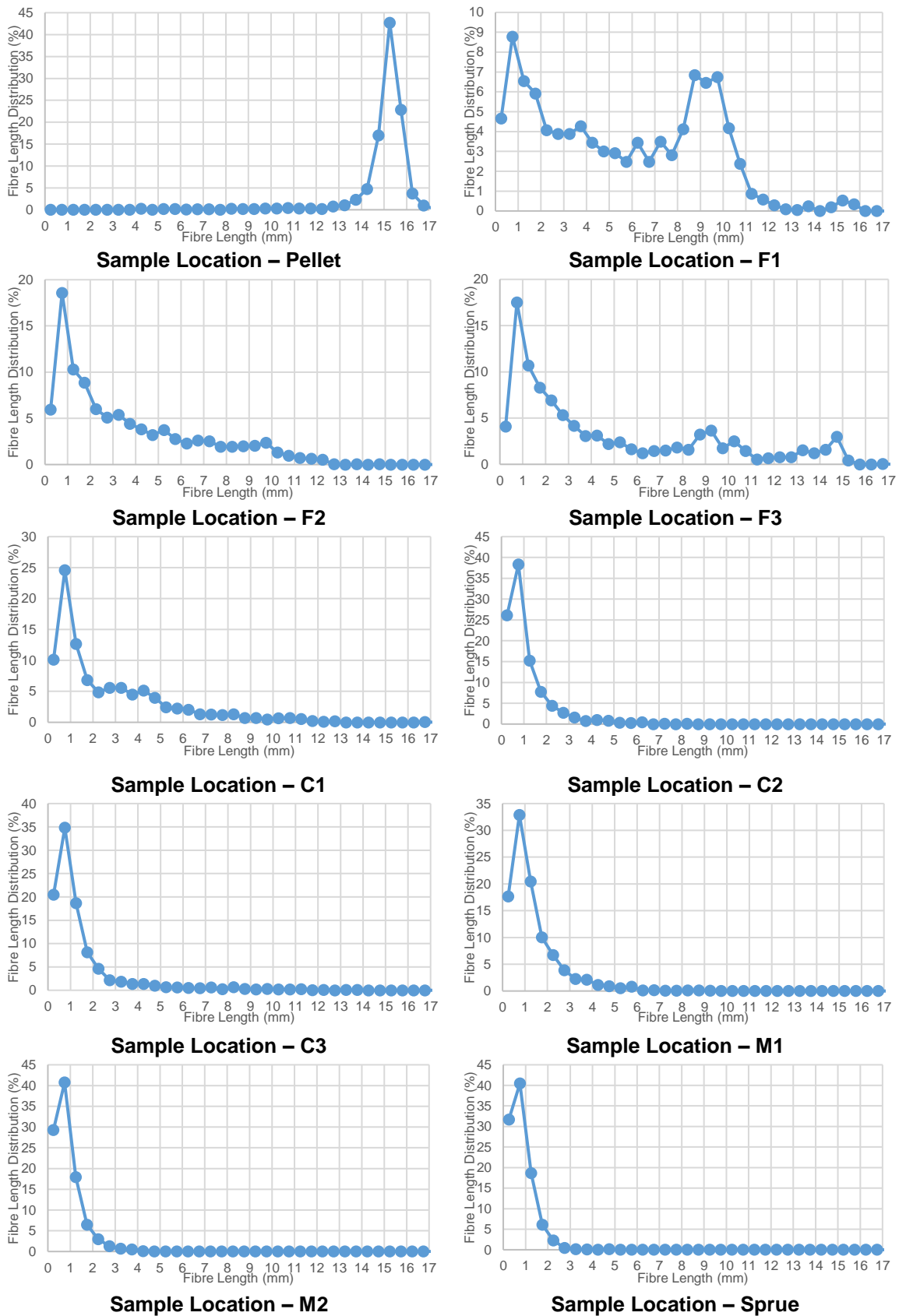
**Table A1.5. - Injection moulding settings for 20mm screw pull out test - High BP / Low RPM. Material: 20YM240.**

Sample	Average Fibre Length (mm)	Weighted Average Length (mm)	Maximum Fibre Length Measured (mm)	Minimum Fibre Length Measured (mm)
<b>Pellet</b>	14.72	14.87	16.91	2.02
<b>F1</b>	5.24	7.72	15.50	0.05
<b>F2</b>	3.35	6.16	14.56	0.05
<b>F3</b>	4.36	8.56	16.30	0.07
<b>C1</b>	2.48	4.98	16.58	0.06
<b>C2</b>	0.86	1.97	8.19	0.06
<b>C3</b>	1.27	3.88	13.57	0.06
<b>M1</b>	1.11	2.15	8.83	0.05
<b>M2</b>	0.64	1.20	6.42	0.05
<b>N1</b>	<i>n/a</i>	<i>n/a</i>	<i>n/a</i>	<i>n/a</i>
<b>N2</b>	<i>n/a</i>	<i>n/a</i>	<i>n/a</i>	<i>n/a</i>
<b>Sprue</b>	0.57	1.01	4.62	0.04

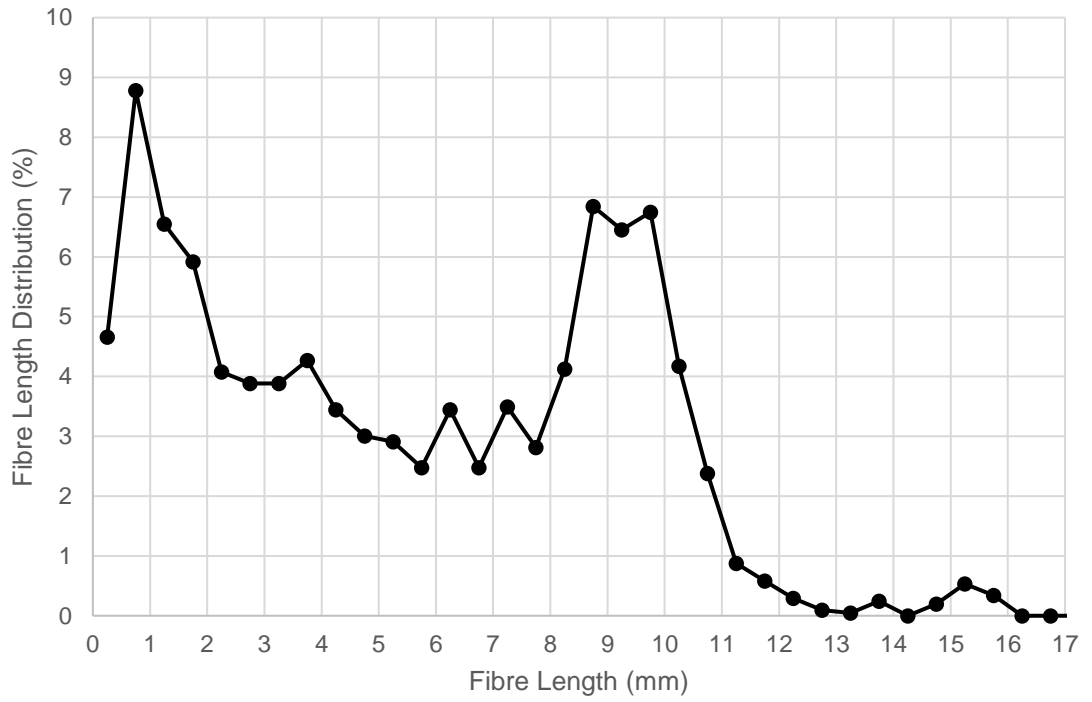
**Table A1.6. - 20mm screw pull out test - High BP (7.5 bar) / Low RPM (150 RPM). Material: 20YM240.**



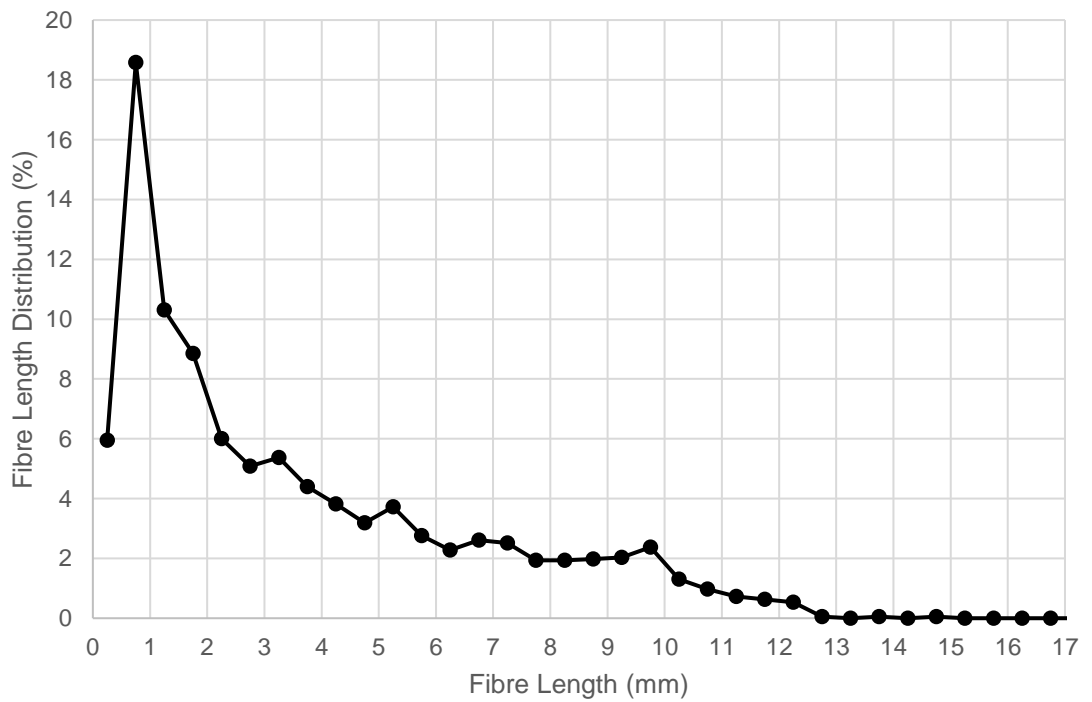
**Figure A1.25. - Number and weighted average distribution of each 24 mm cut taken from various locations along the injection moulding process**



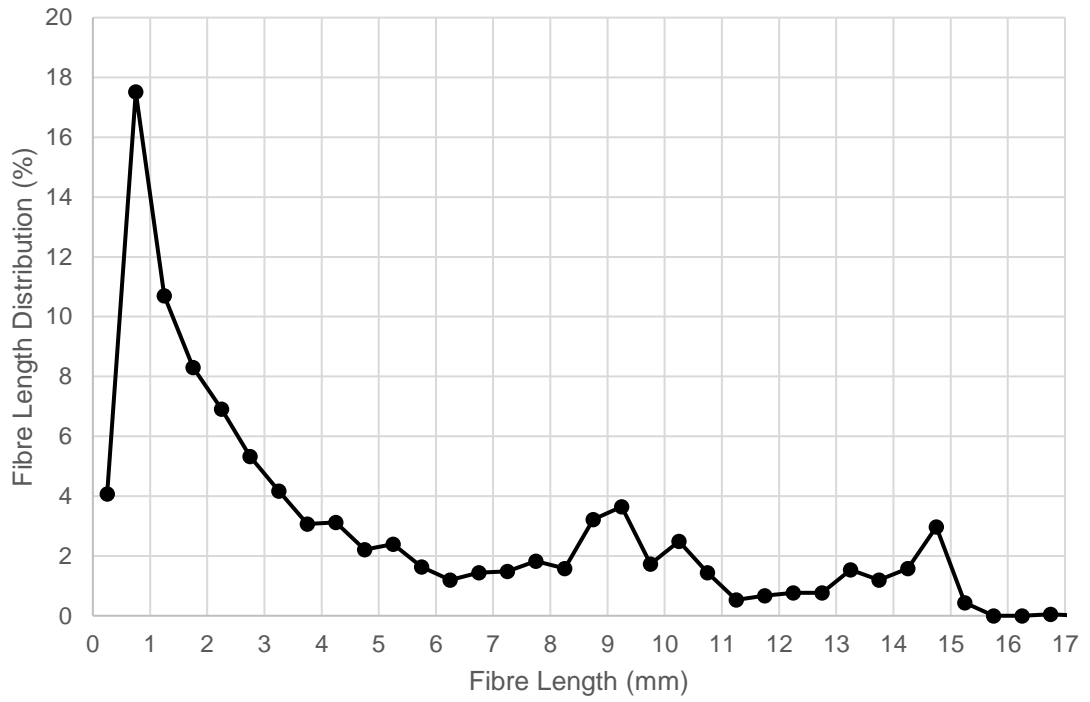
**Figure A1.26. - Summary of fibre length distribution results**



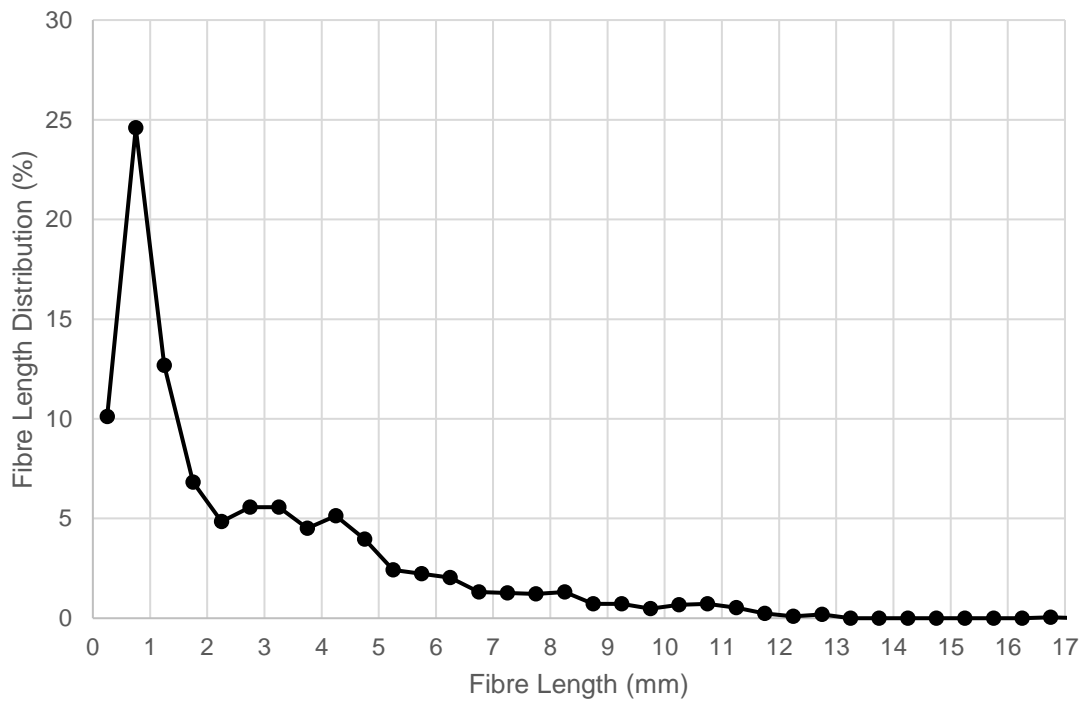
**Figure A1.27. - Sample: F1**



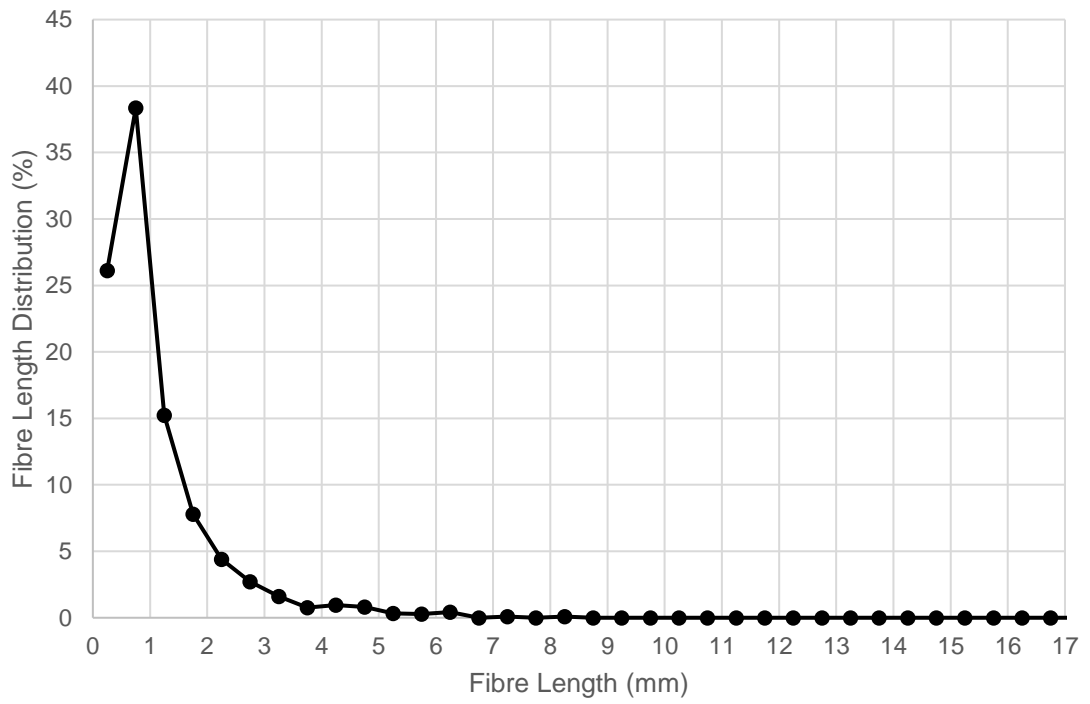
**Figure A1.28. - Sample: F2**



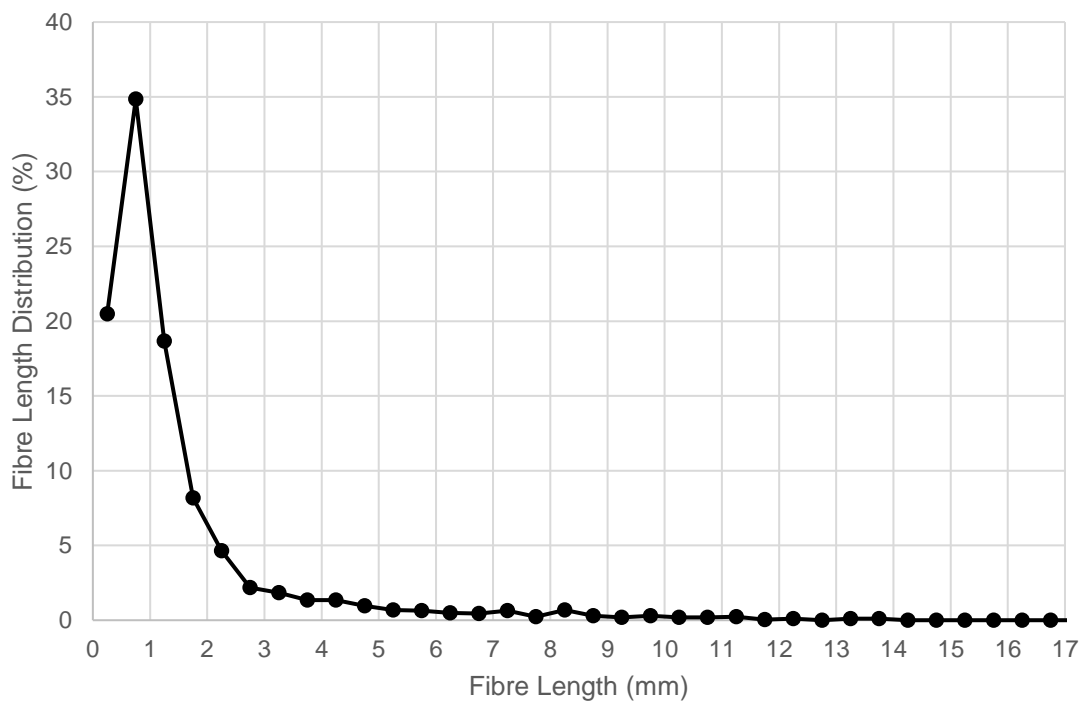
**Figure A1.29. - Sample: F3**



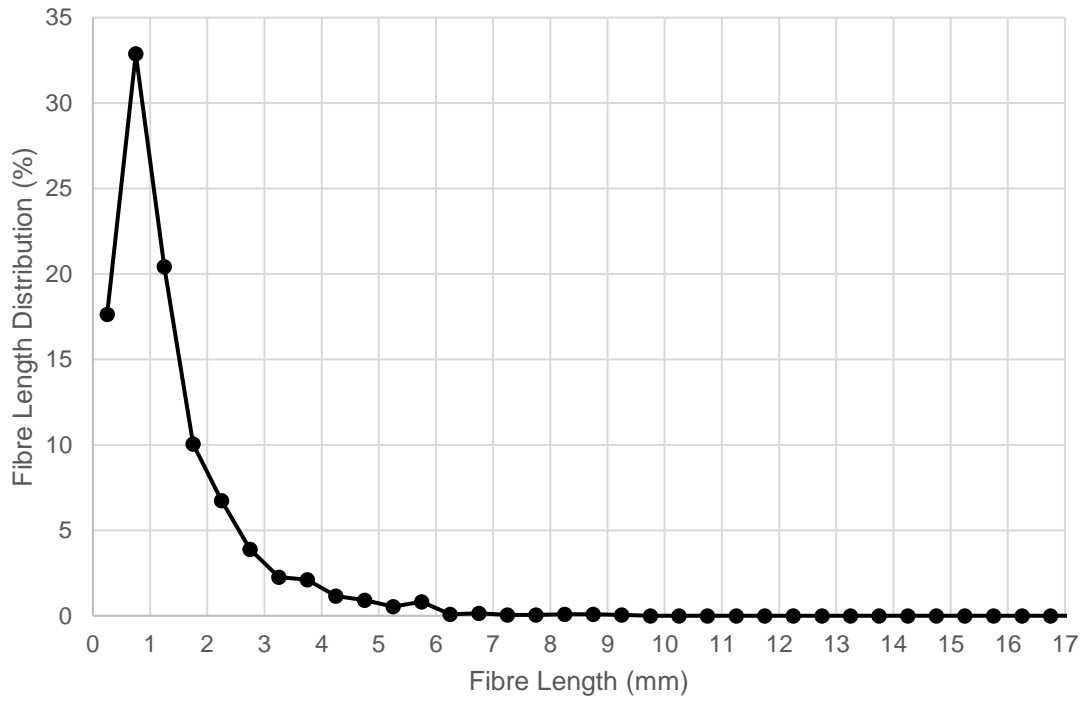
**Figure A1.30. - Sample: C1**



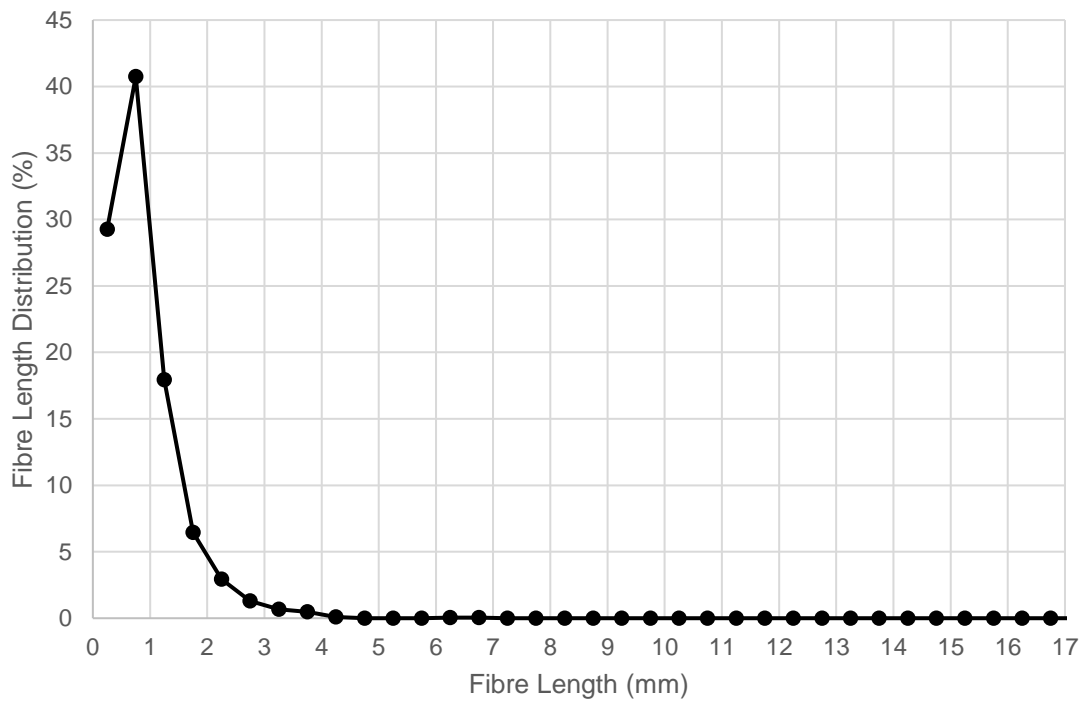
**Figure A1.31. - Sample: C2**



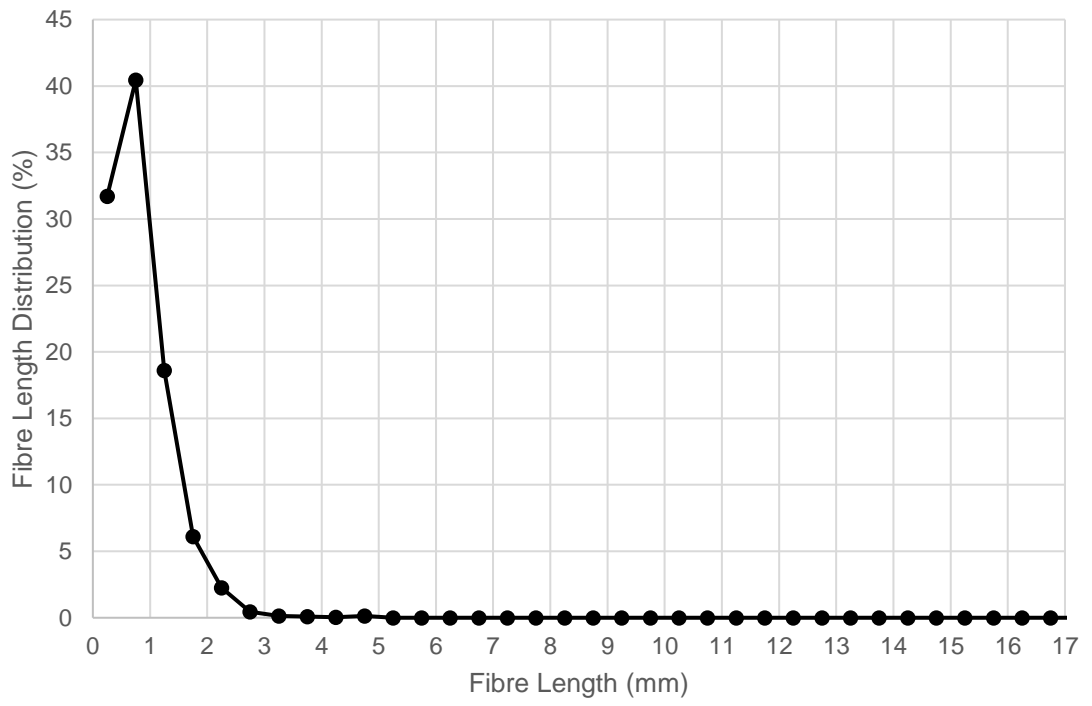
**Figure A1.32. - Sample: C3**



**Figure A1.33. - Sample: M1**



**Figure A1.34. - Sample: M2**



**Figure A1.35. - Sample: Sprue**



<b>Machine Settings</b>	<b>Arburg Allrounder 270C</b>
<b>Injection Time (secs)</b>	1.07
<b>Injection Speed (cm<sup>3</sup>/s)</b>	20
<b>Screw Speed (RPM)</b>	300
<b>Back Pressure (bar)</b>	2.5
<b>Packing Pressure (bar)</b>	27
<b>Packing Time (secs)</b>	5
<b>Melt Temperature (°C)</b>	220
<b>Mould Temperature (°C)</b>	20
<b>Cooling Time (secs)</b>	30

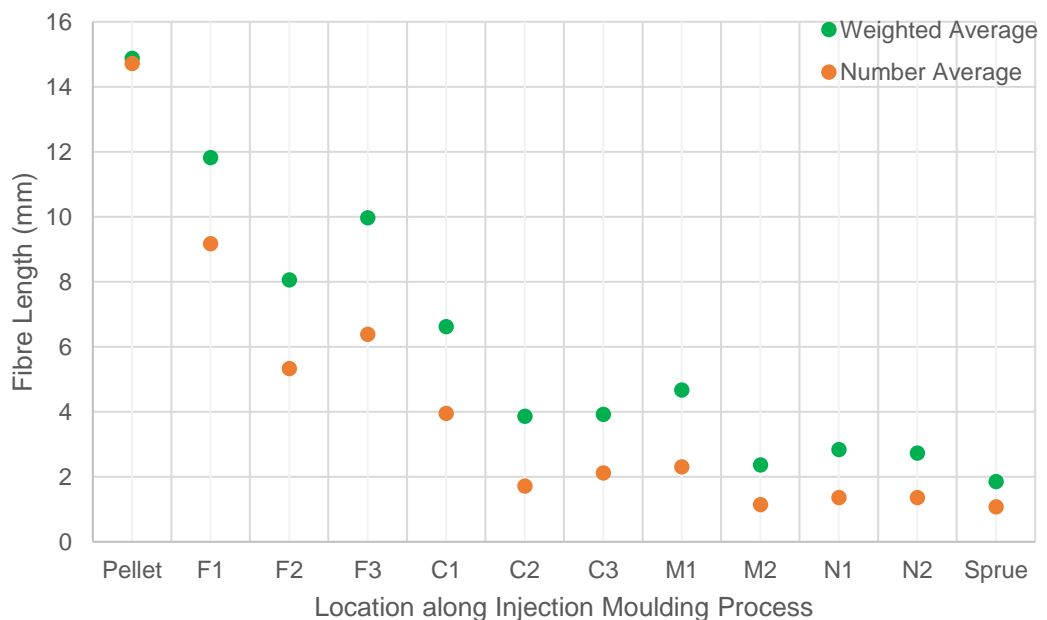
**Table A1.7. - Injection moulding settings for 20 mm screw pull out test -  
Low BP / High RPM. Material: 20YM240.**

<b>Machine Settings</b>	<b>Arburg Allrounder 270C</b>
<b>Injection Time (secs)</b>	1.07
<b>Injection Speed (cm<sup>3</sup>/s)</b>	20
<b>Screw Speed (RPM)</b>	300
<b>Back Pressure (bar)</b>	5
<b>Packing Pressure (bar)</b>	27
<b>Packing Time (secs)</b>	5
<b>Melt Temperature (°C)</b>	220
<b>Mould Temperature (°C)</b>	20
<b>Cooling Time (secs)</b>	30

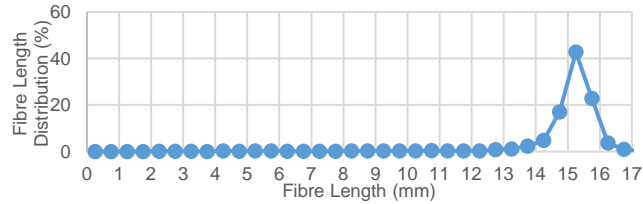
**Table A1.8. - Injection moulding settings for 20 mm screw pull out test -  
Medium BP / High RPM. Material: 20YM240.**

Sample	Average Fibre Length (mm)	Weighted Average Length (mm)	Maximum Fibre Length Measured (mm)	Minimum Fibre Length Measured (mm)
Pellet	14.72	14.87	16.91	2.02
F1	9.17	11.82	16.40	0.07
F2	5.33	8.06	15.28	0.08
F3	6.38	9.97	16.02	0.1
C1	3.95	6.62	15.11	0.07
C2	1.71	3.86	12.83	0.06
C3	2.12	3.92	10.60	0.1
M1	2.31	4.67	14.54	0.06
M2	1.14	2.36	10.16	0.04
N1	1.36	2.84	14.36	0.04
N2	1.36	2.73	14.64	0.04
Sprue	1.07	1.85	11.24	0.06

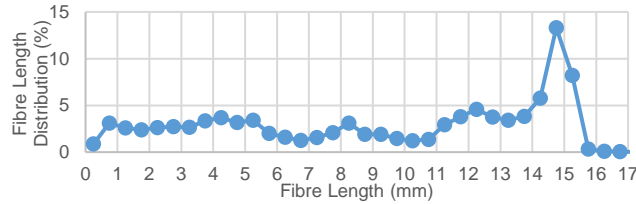
**Table A1.9. - 20 mm screw pull out test - Medium BP (5 bar) / High RPM (300 RPM). Material: 20YM240.**



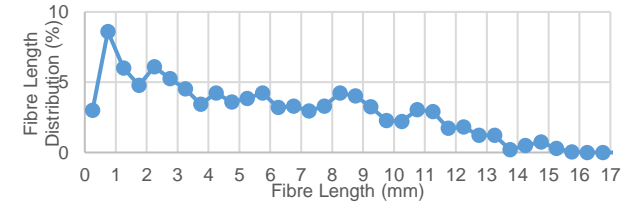
**Figure A1.36. - Number and Weighted average distribution of each 24 mm cut taken from various locations along the injection moulding process**



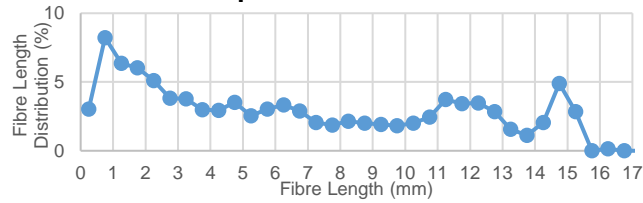
**Sample Location – Pellet**



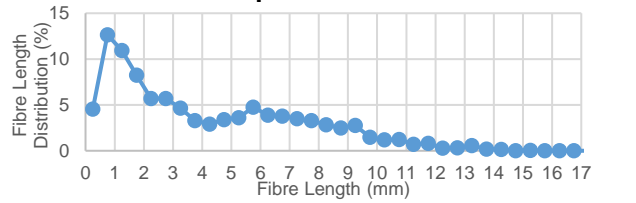
**Sample Location – F1**



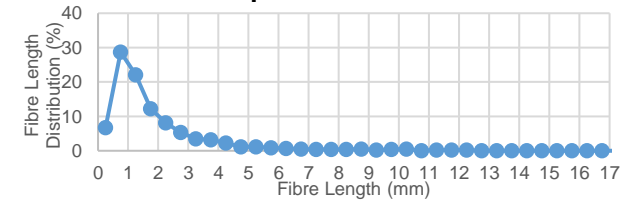
**Sample Location – F2**



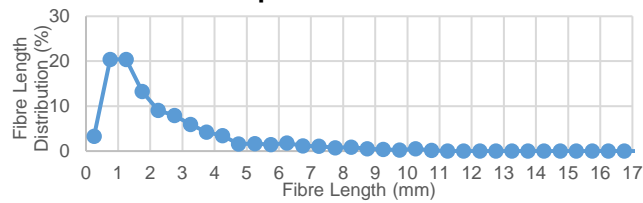
**Sample Location – F3**



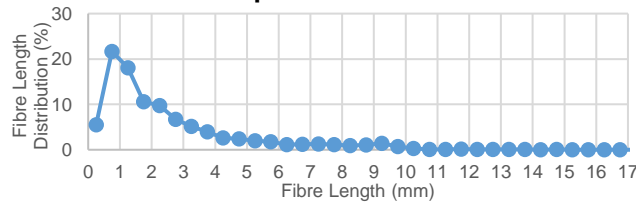
**Sample Location – C1**



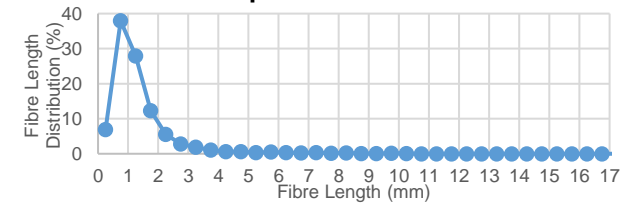
**Sample Location – C2**



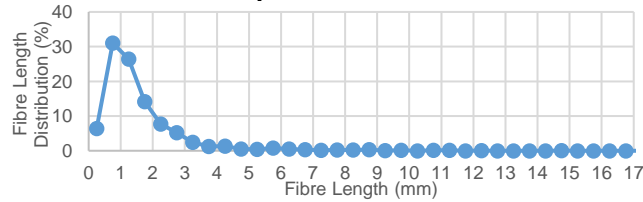
**Sample Location – C3**



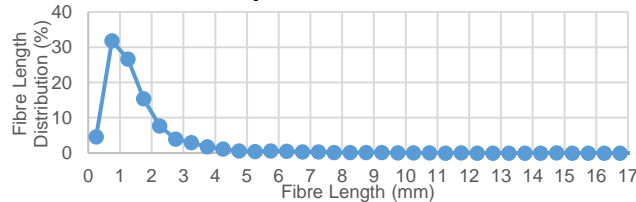
**Sample Location – M1**



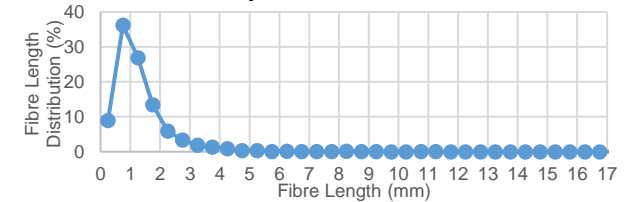
**Sample Location – M2**



**Sample Location – N1**

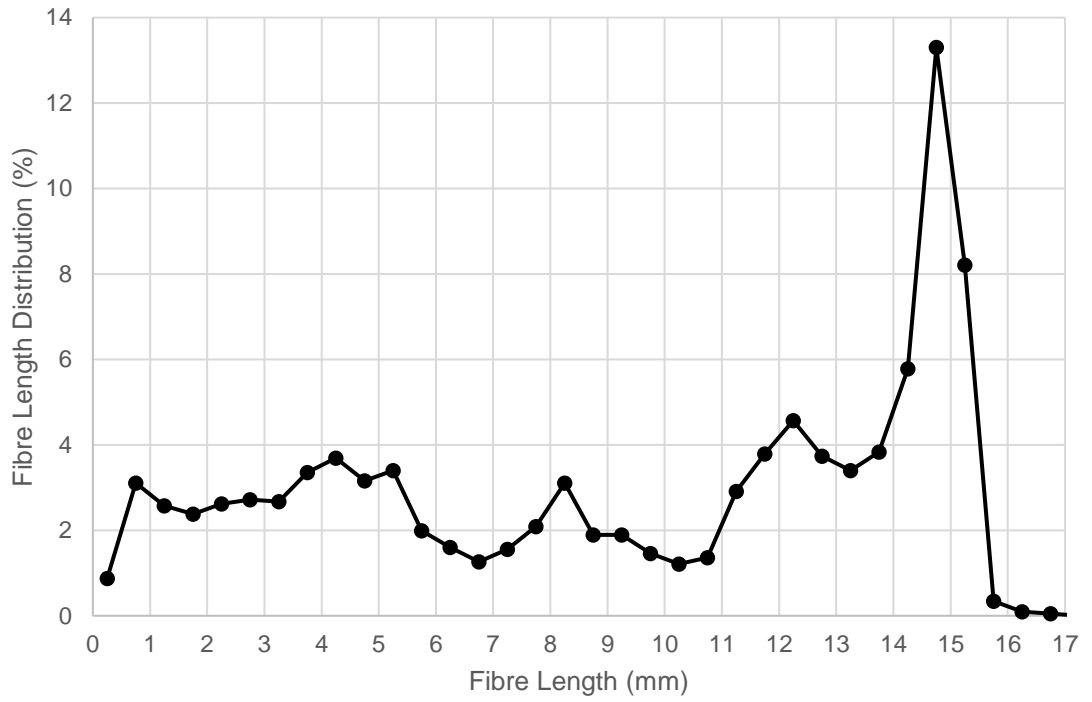


**Sample Location – N2**

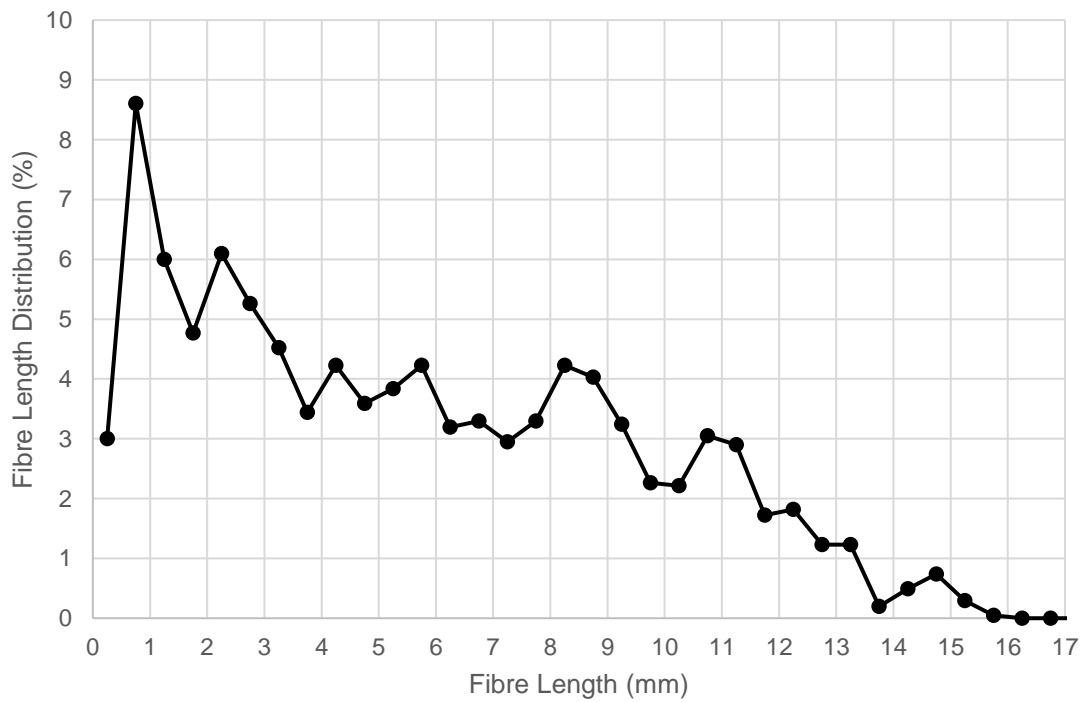


**Sample Location – Sprue**

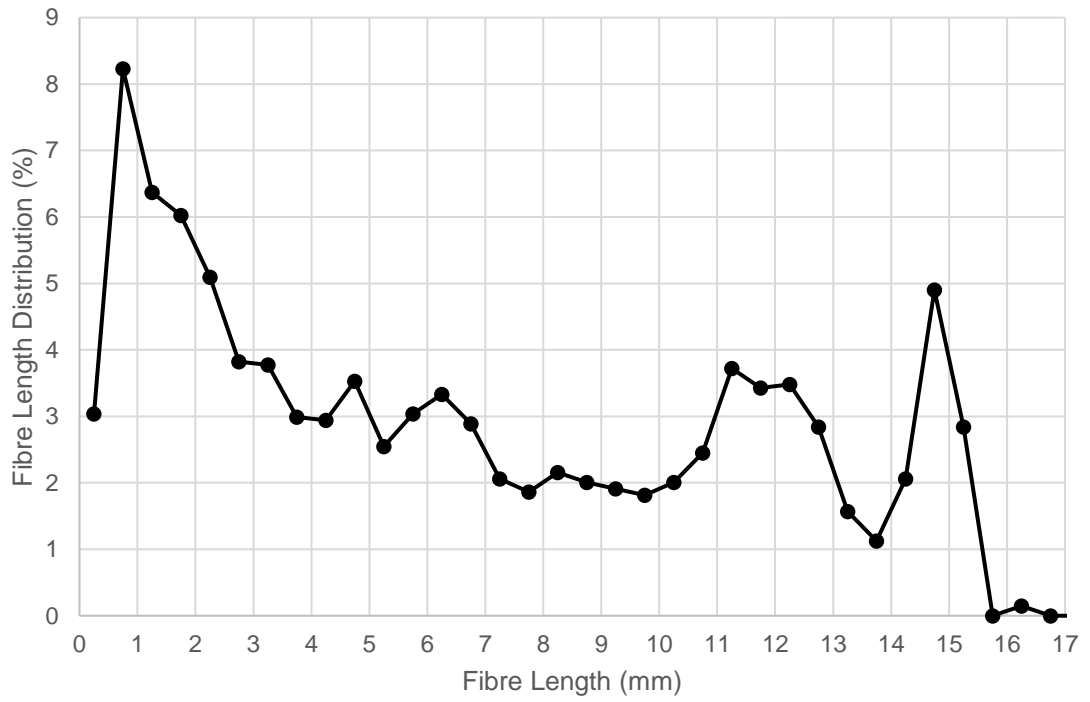
**Figure A1.37. - Summary of fibre length distribution results**



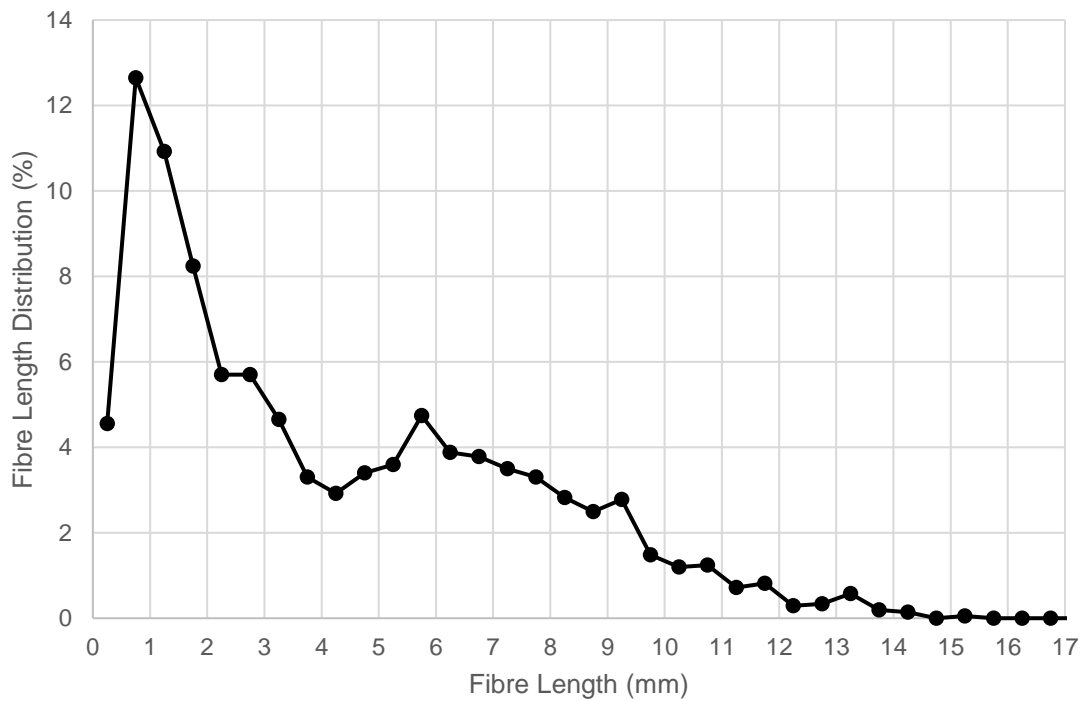
**Figure A1.38. - Sample: F1**



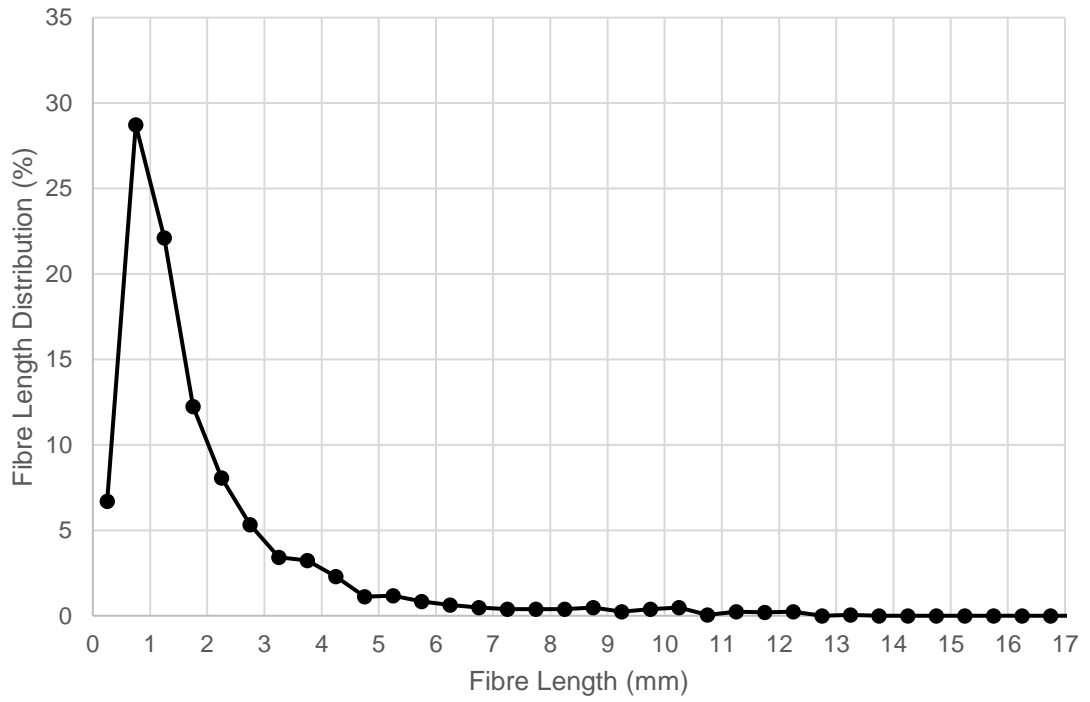
**Figure A1.39. - Sample: F2**



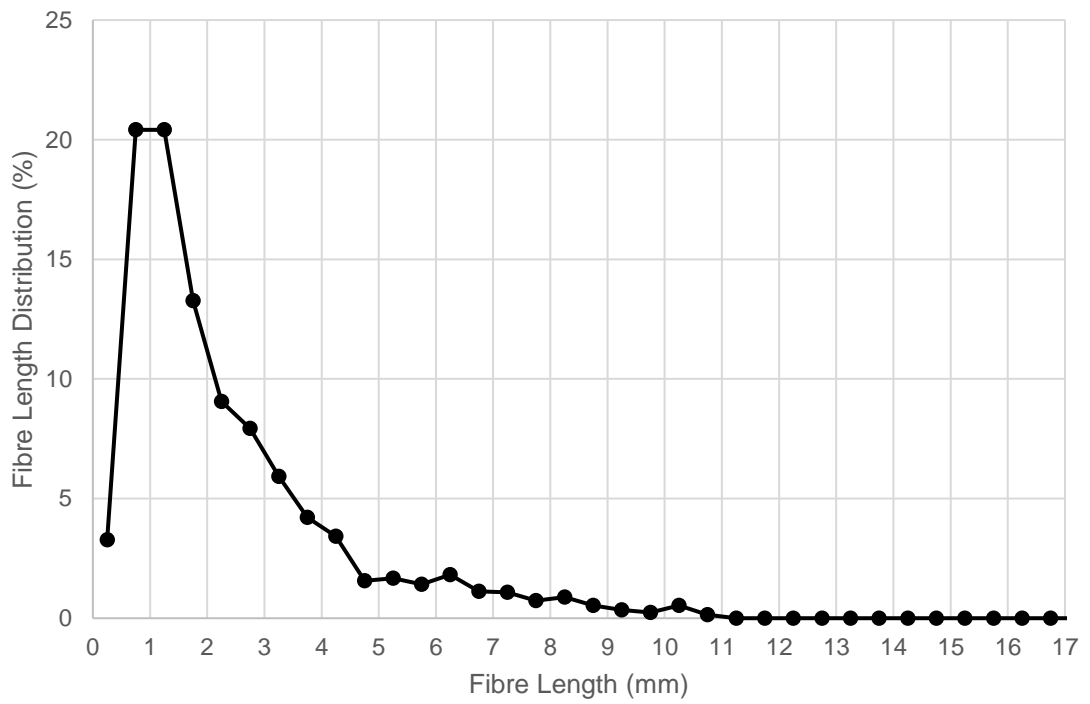
**Figure A1.40. - Sample: F3**



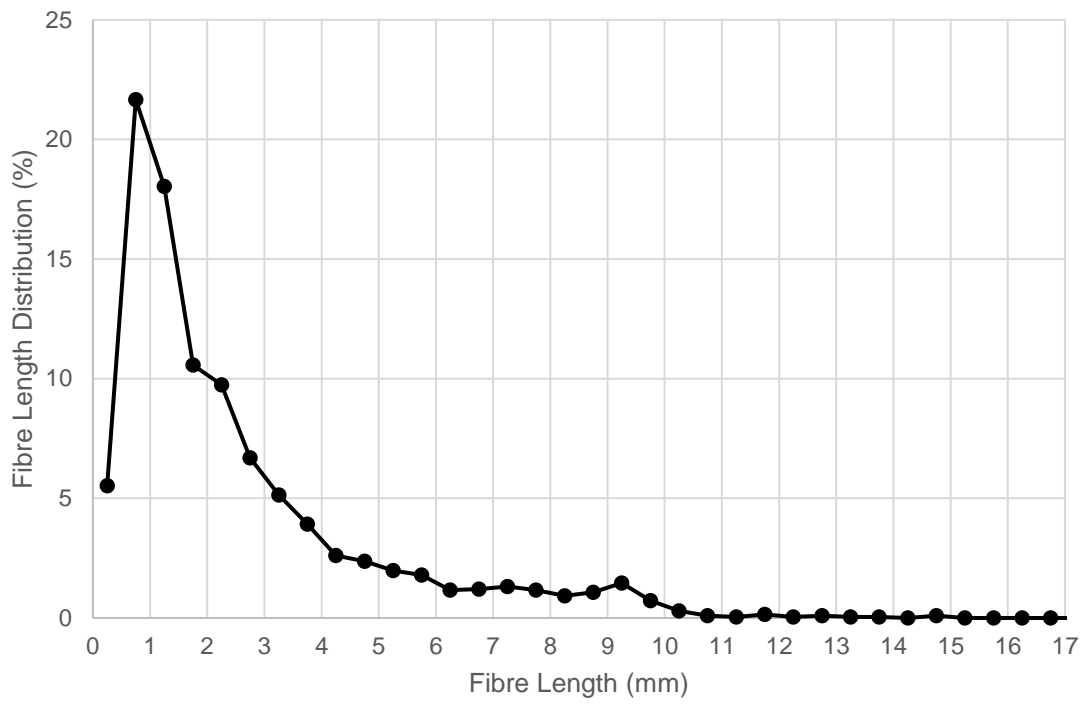
**Figure A1.41. - Sample: C1**



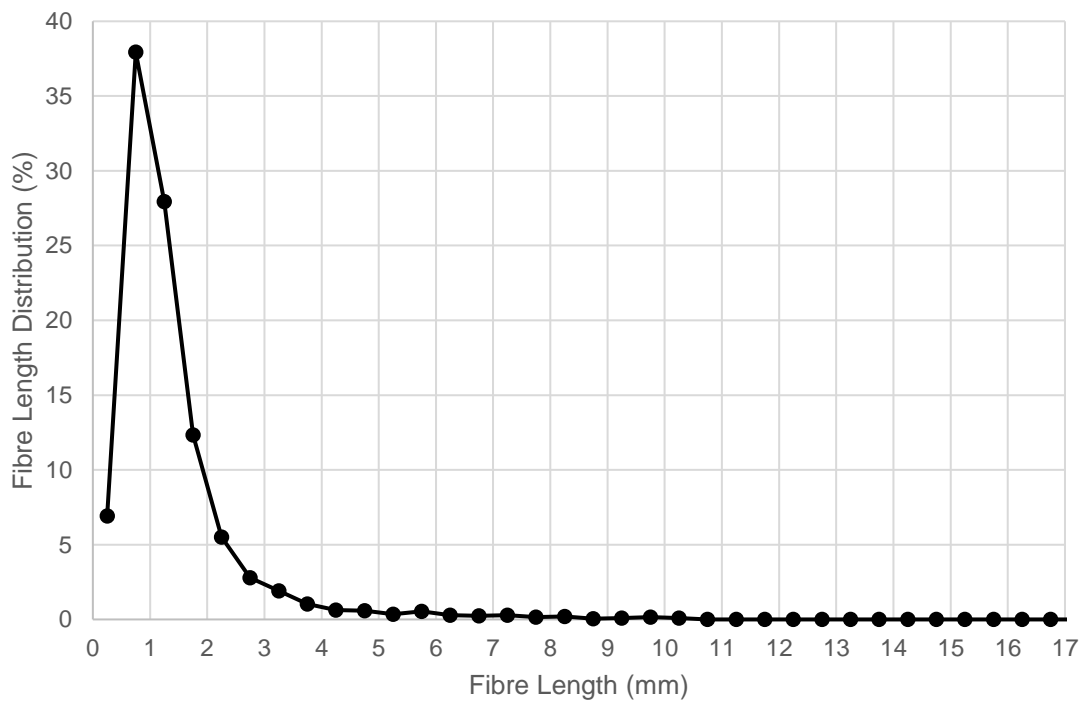
**Figure A1.42. - Sample: C2**



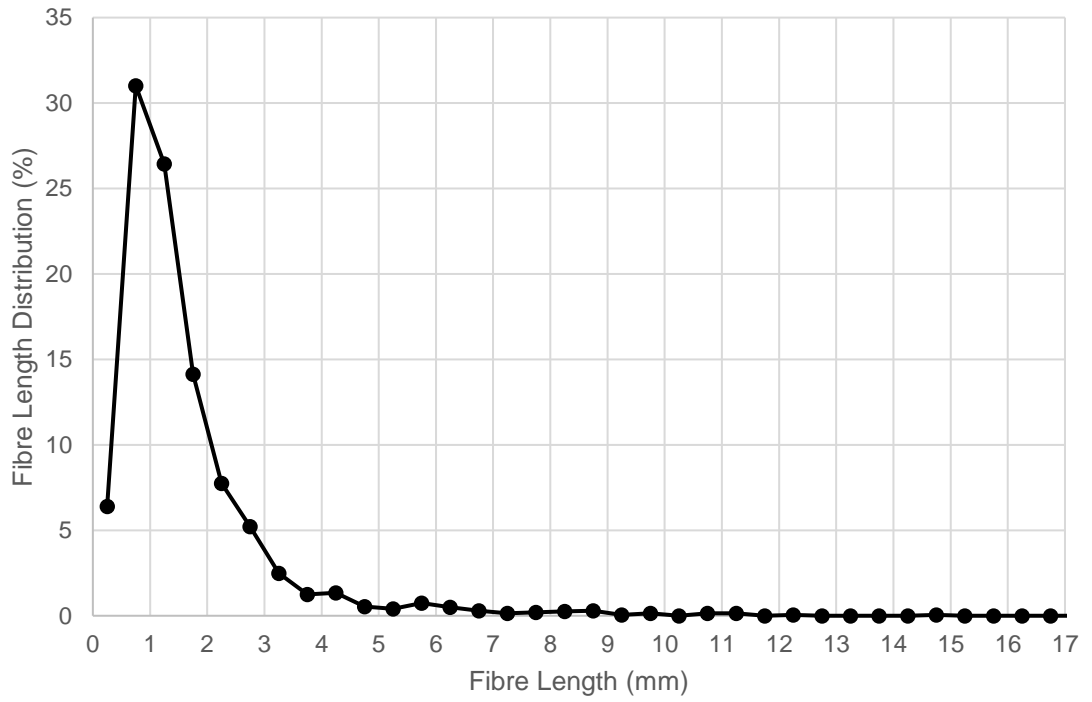
**Figure A1.43. - Sample: C3**



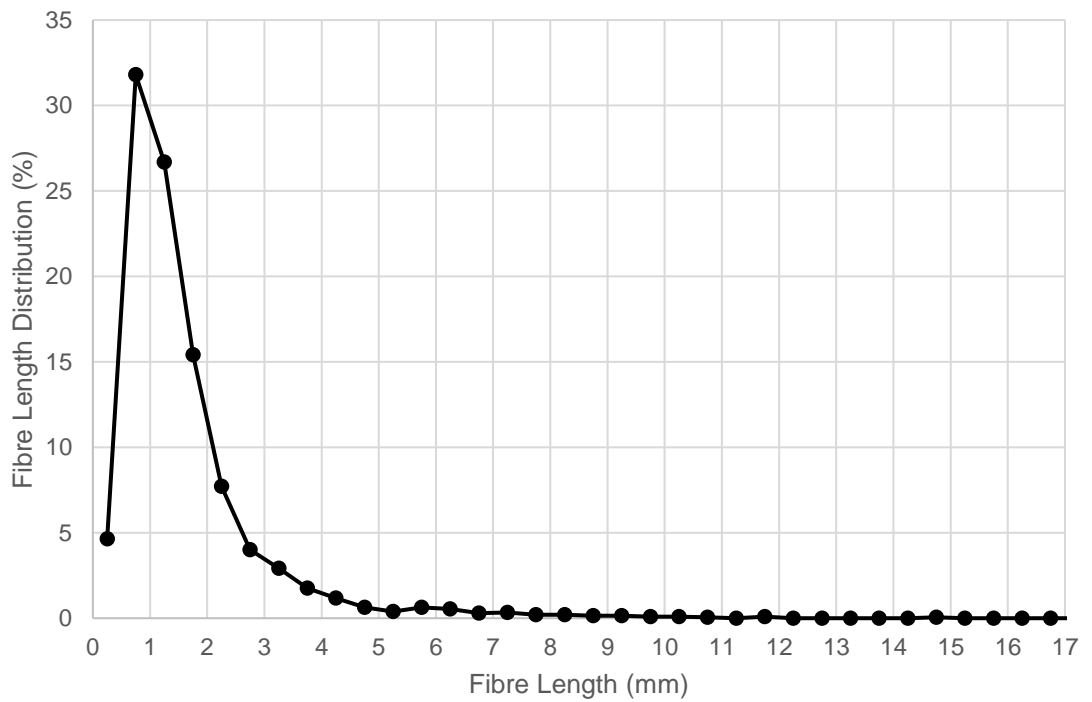
**Figure A1.44. - Sample: M1**



**Figure A1.45. - Sample: M2**

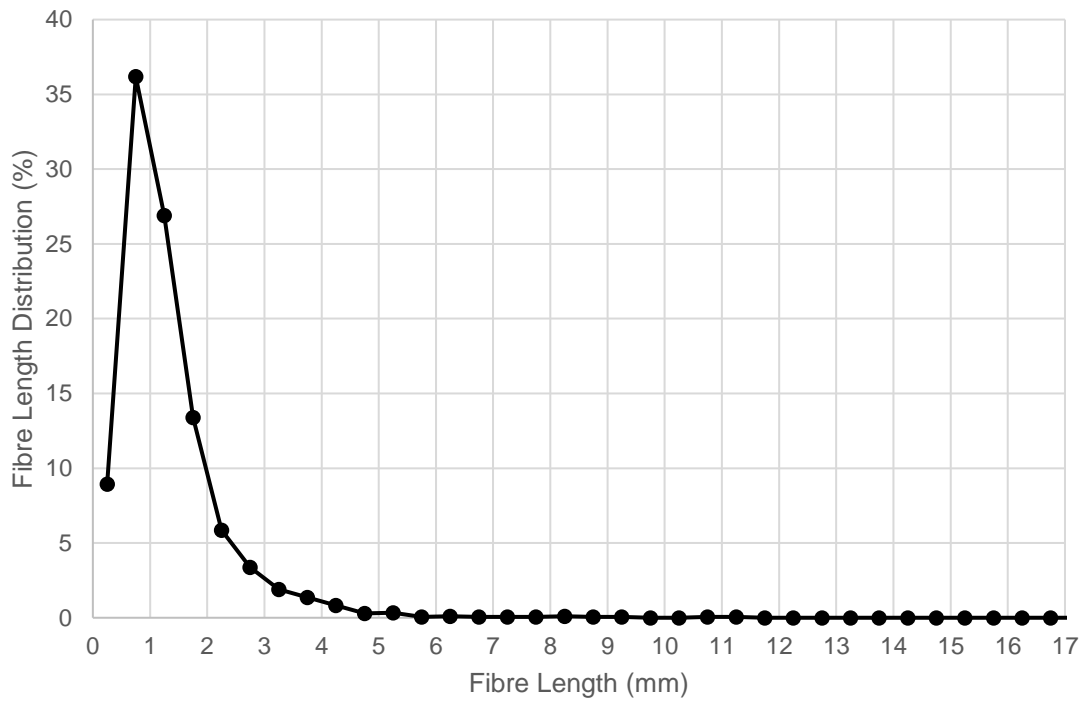


**Figure A1.46. - Sample: N1**



**Figure A1.47. - Sample: N2**





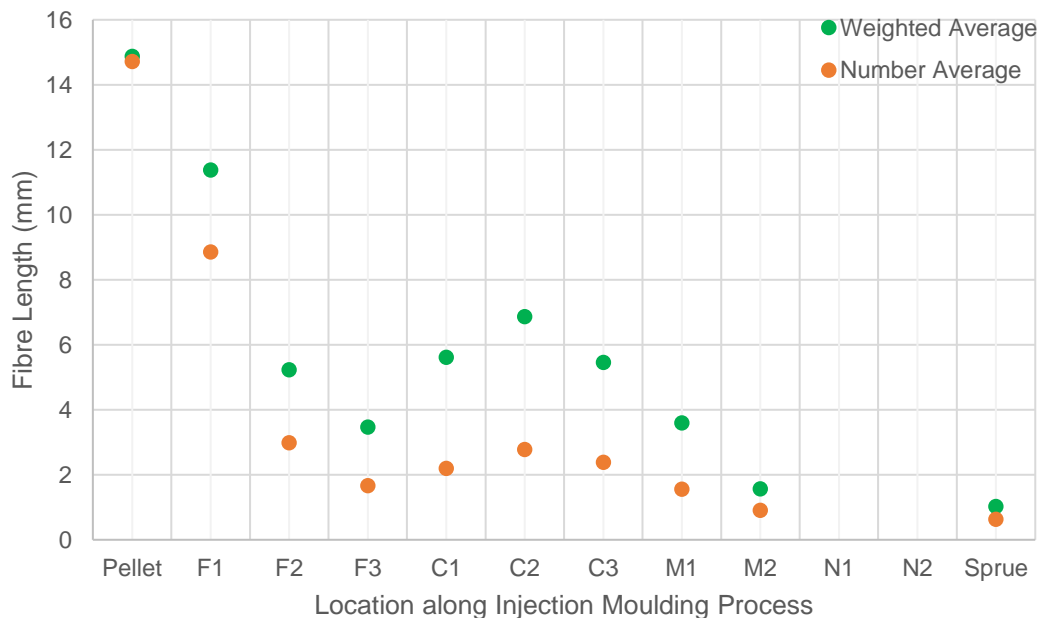
**Figure A1.48. - Sample: Sprue**

<b>Machine Settings</b>	<b>Arburg Allrounder 270C</b>
<b>Injection Time (secs)</b>	0.84
<b>Injection Speed (cm<sup>3</sup>/s)</b>	20
<b>Screw Speed (RPM)</b>	300
<b>Back Pressure (bar)</b>	7.5
<b>Packing Pressure (bar)</b>	27
<b>Packing Time (secs)</b>	5
<b>Melt Temperature (°C)</b>	220
<b>Mould Temperature (°C)</b>	20
<b>Cooling Time (secs)</b>	30

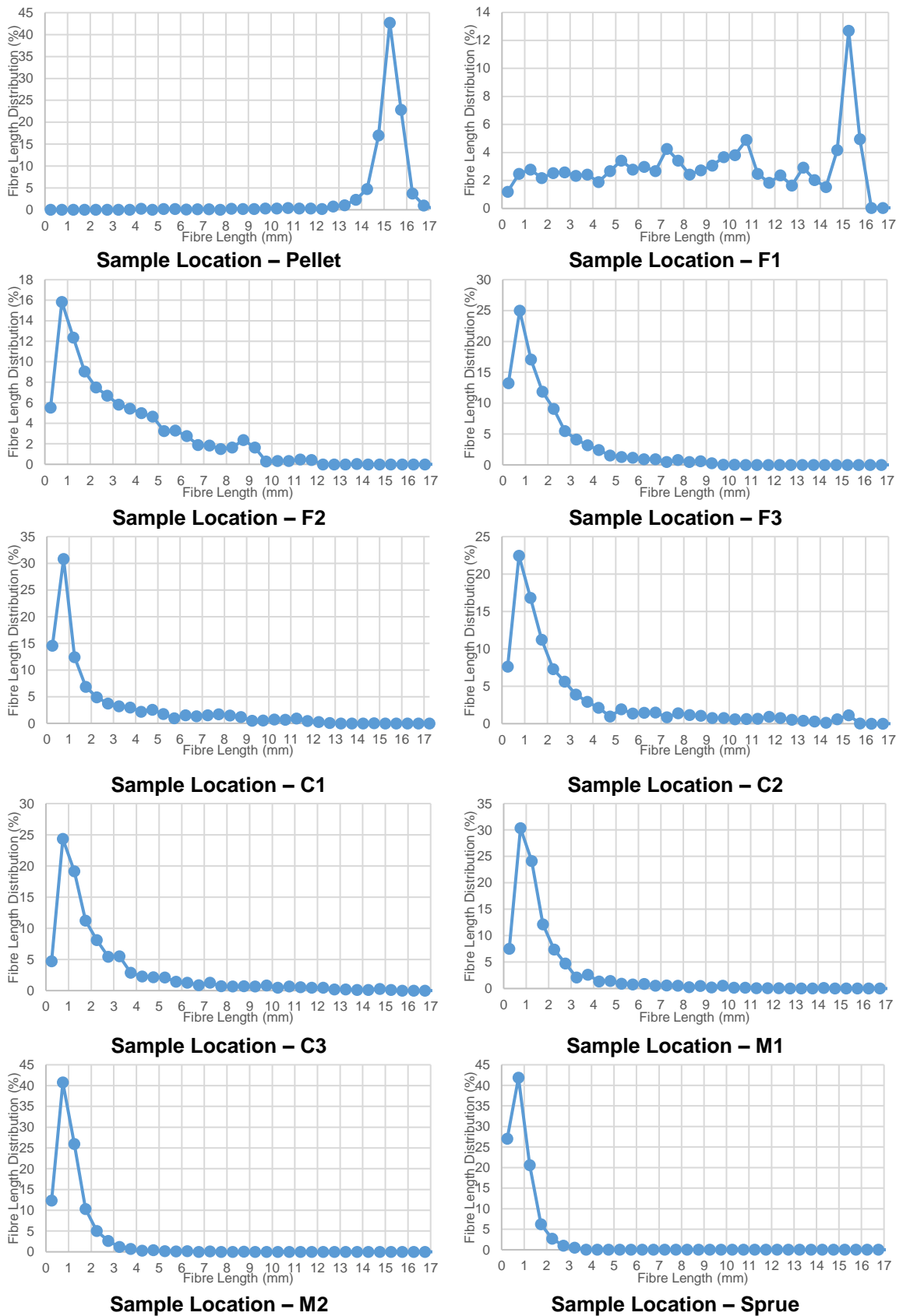
**Table A1.10. - Injection moulding settings for 20 mm screw pull out test - High BP / High RPM. Material: 20YM240.**

Sample	Average Fibre Length (mm)	Weighted Average Length (mm)	Maximum Fibre Length Measured (mm)	Minimum Fibre Length Measured (mm)
Pellet	14.72	14.87	16.91	2.02
F1	8.86	11.38	16.81	0.08
F2	2.99	5.23	13.46	0.05
F3	1.67	3.47	10.04	0.04
C1	2.20	5.62	14.55	0.06
C2	2.78	6.87	15.44	0.06
C3	2.38	5.46	14.86	0.06
M1	1.56	3.60	14.02	0.07
M2	0.91	1.57	8.67	0.07
N1	<i>n/a</i>	<i>n/a</i>	<i>n/a</i>	<i>n/a</i>
N2	<i>n/a</i>	<i>n/a</i>	<i>n/a</i>	<i>n/a</i>
Sprue	0.63	1.04	5.22	0.03

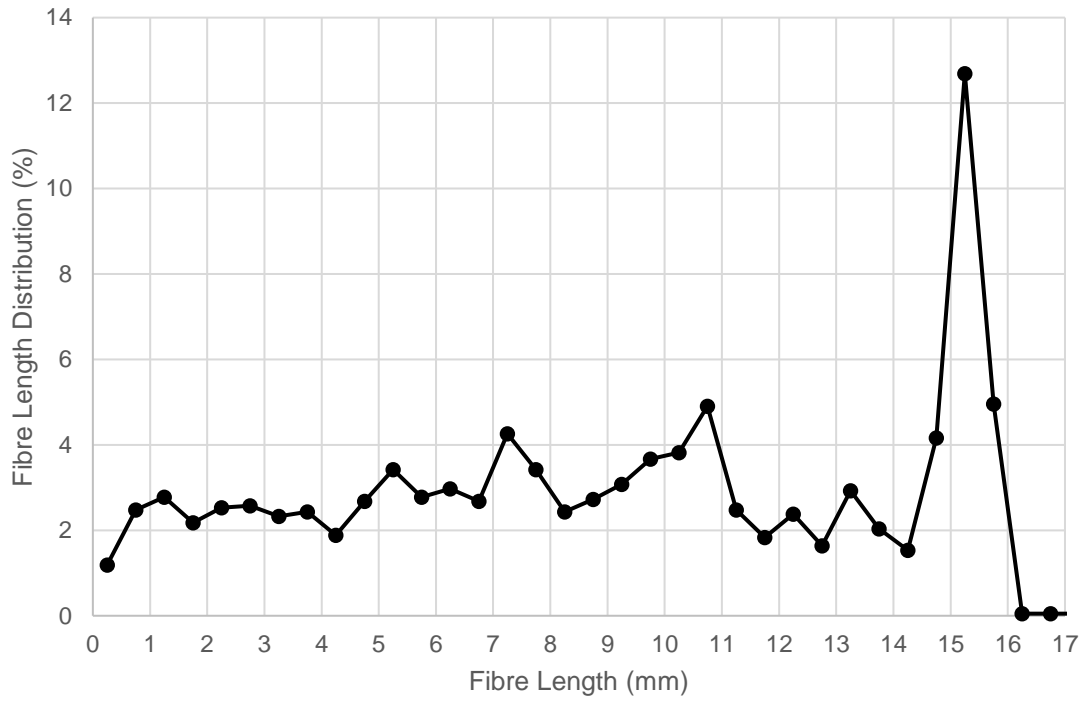
**Table A1.11. - 20 mm screw pull out test - High BP (7.5 bar) / High RPM (300 RPM). Material: 20YM240.**



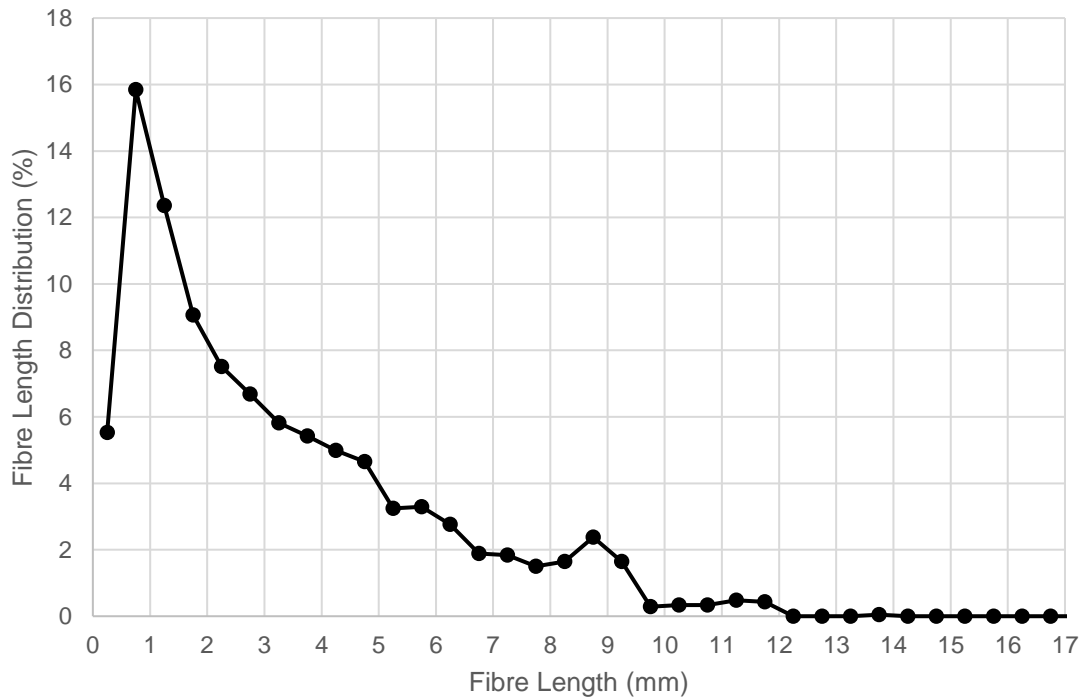
**Figure A1.49. - Number and weighted average distribution of each 24 mm cut taken from various locations along the injection moulding process.**



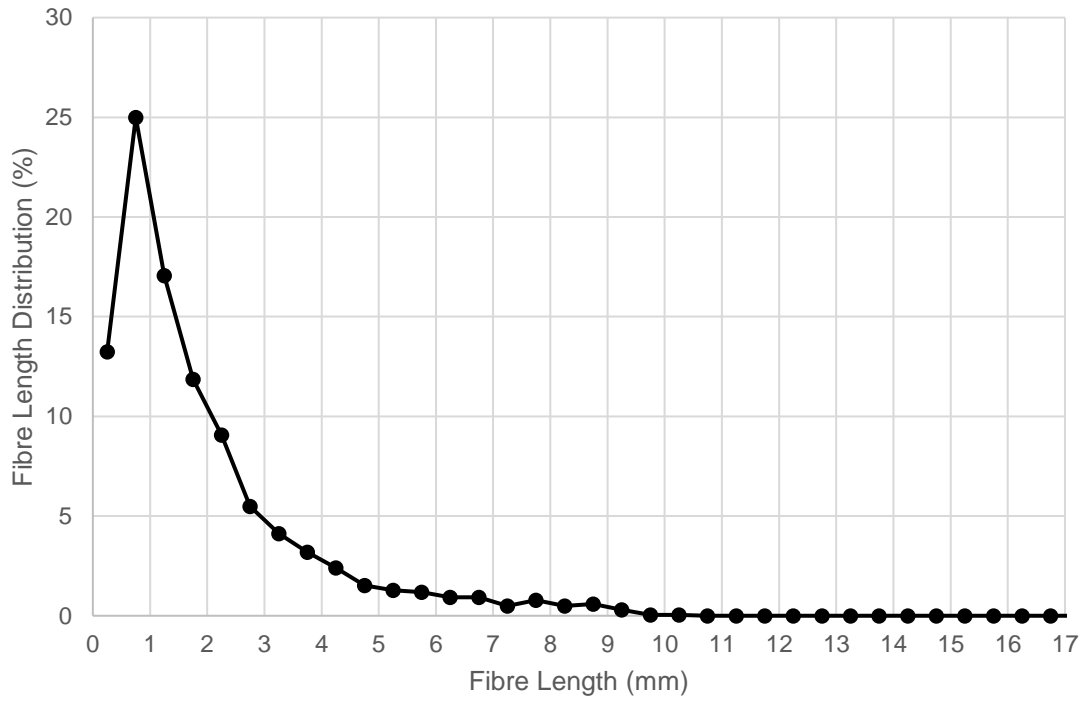
**Figure A1.50. - Summary of fibre length distribution results**



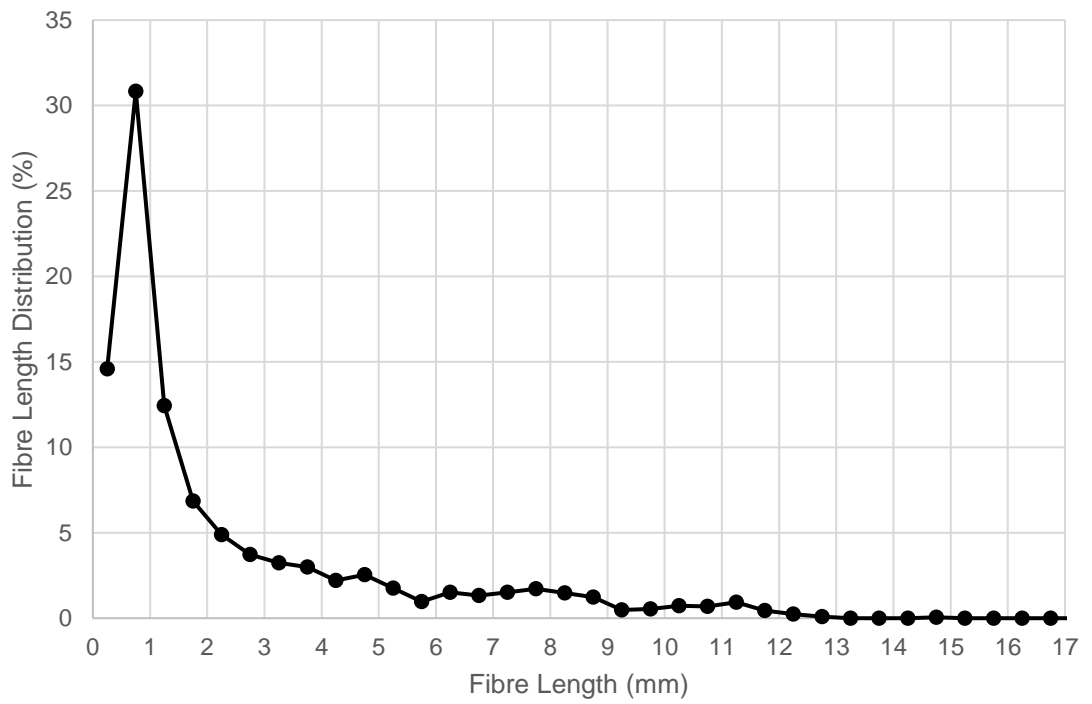
**Figure A1.51. - Sample: F1**



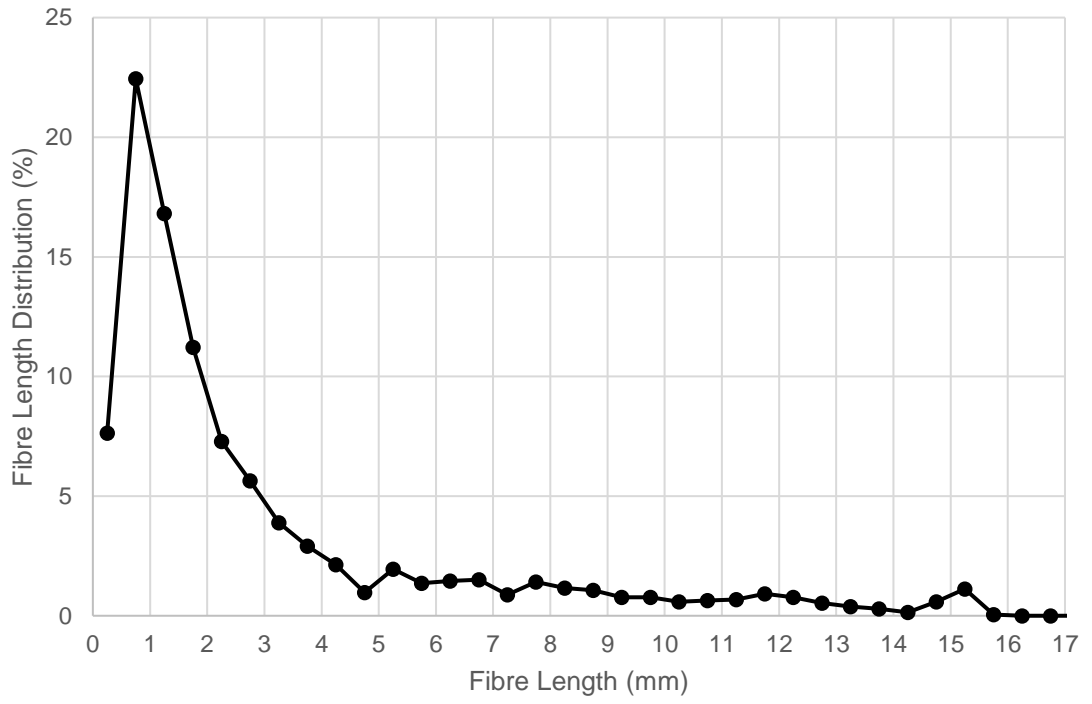
**Figure A1.52. - Sample: F2**



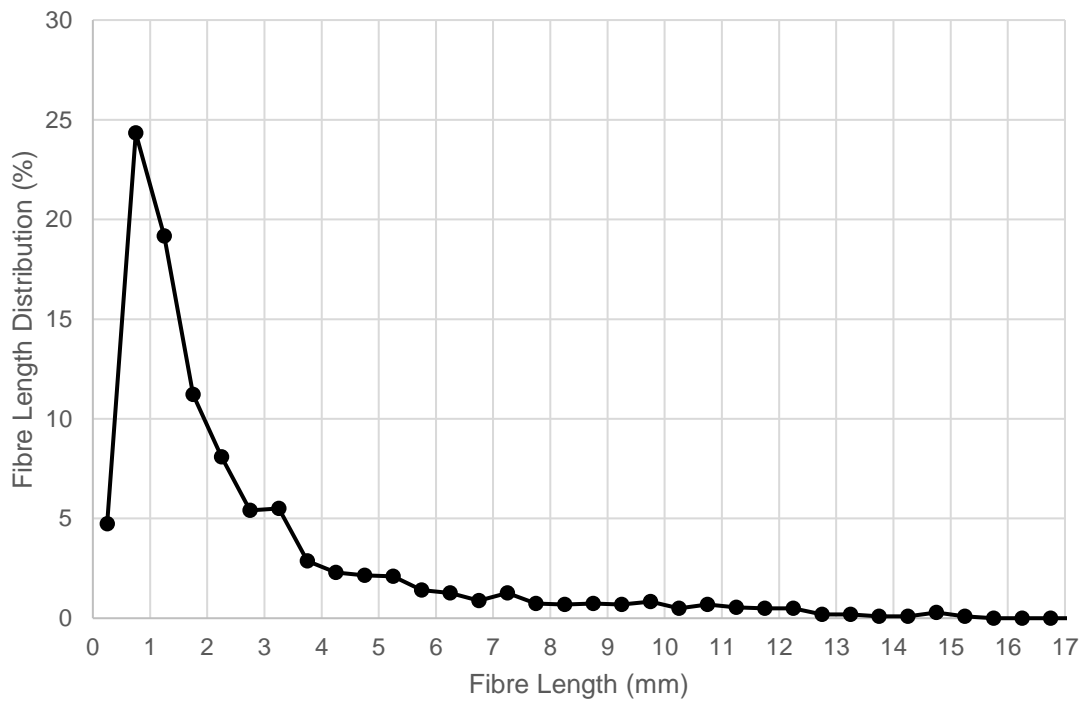
**Figure A1.53. - Sample: F3**



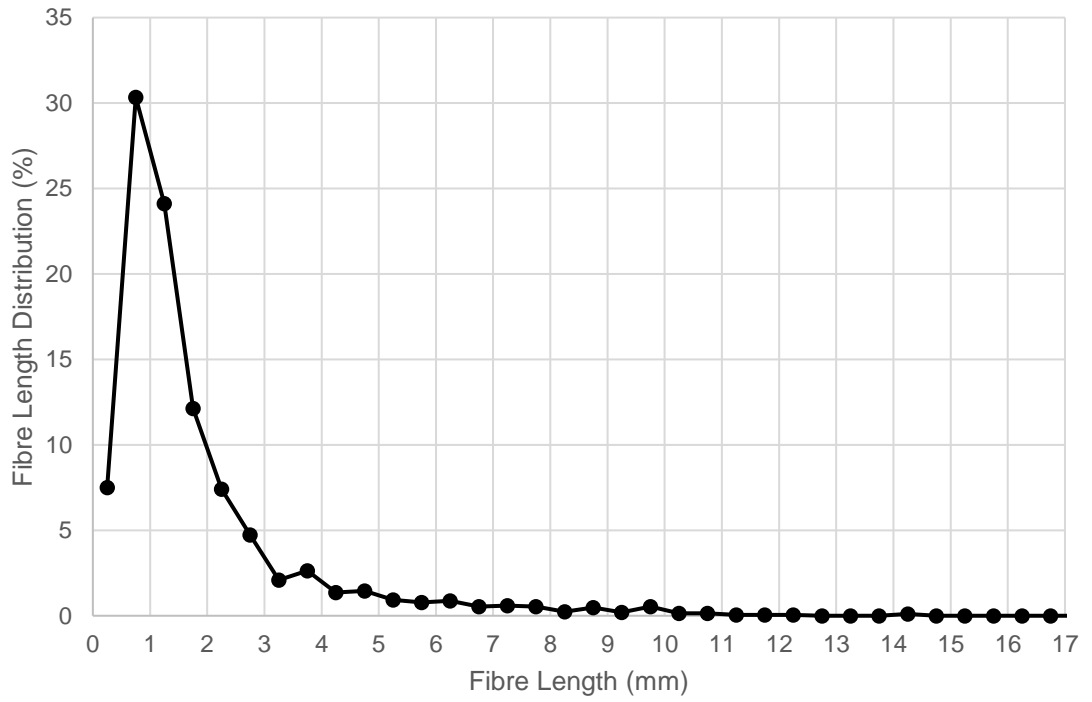
**Figure A1.54. - Sample: C1**



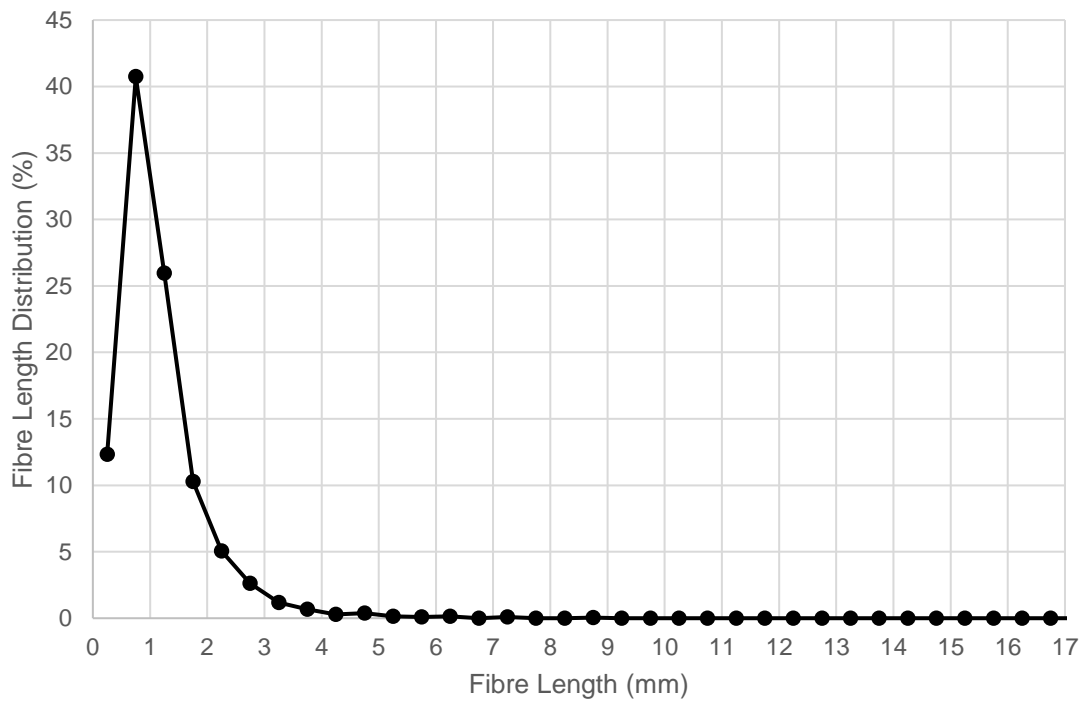
**Figure A1.55. - Sample: C2**



**Figure A1.56. - Sample: C3**

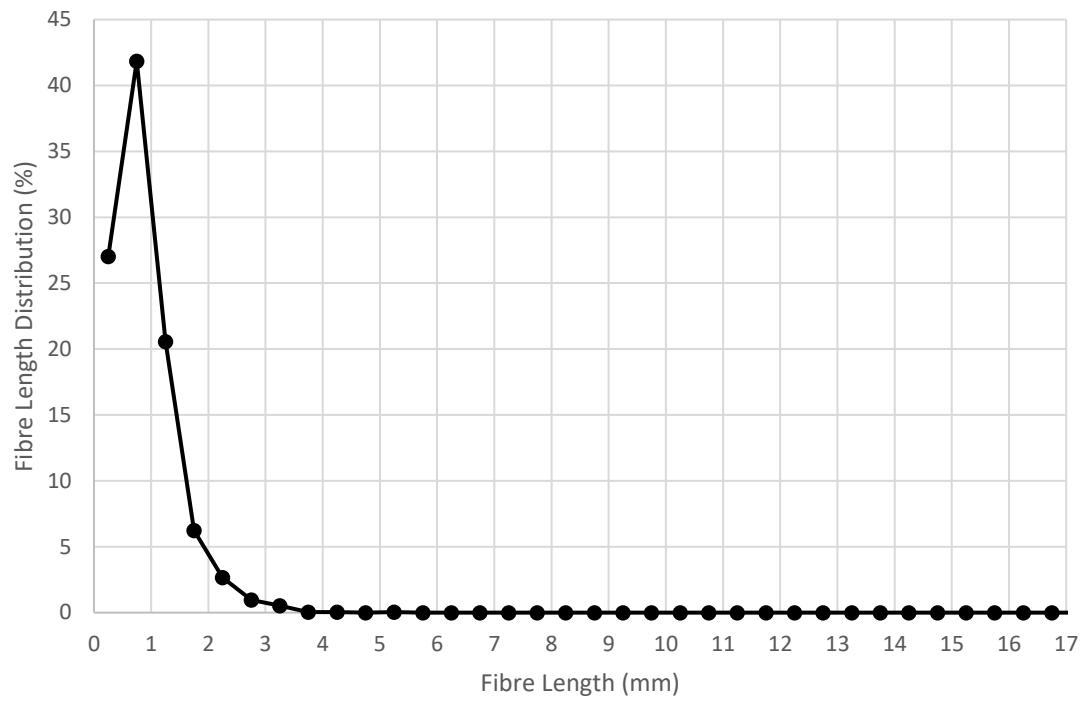


**Figure A1.57. - Sample: M1**



**Figure A1.58. - Sample: M2**





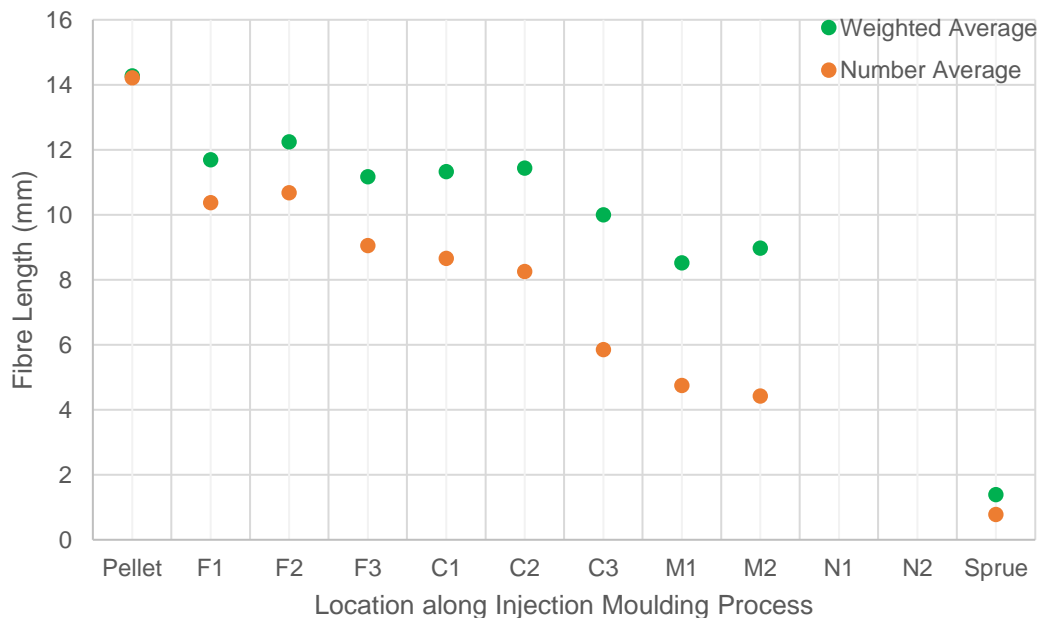
**Figure A1.59. - Sample: Sprue**

<b>Machine Settings</b>	<b>Arburg Allrounder 270C</b>
<b>Injection Time (secs)</b>	0.86
<b>Injection Speed (cm<sup>3</sup>/s)</b>	20
<b>Screw Speed (RPM)</b>	300
<b>Back Pressure (bar)</b>	2.5
<b>Packing Pressure (bar)</b>	27
<b>Packing Time (secs)</b>	5
<b>Melt Temperature (°C)</b>	220
<b>Mould Temperature (°C)</b>	20
<b>Cooling Time (secs)</b>	30

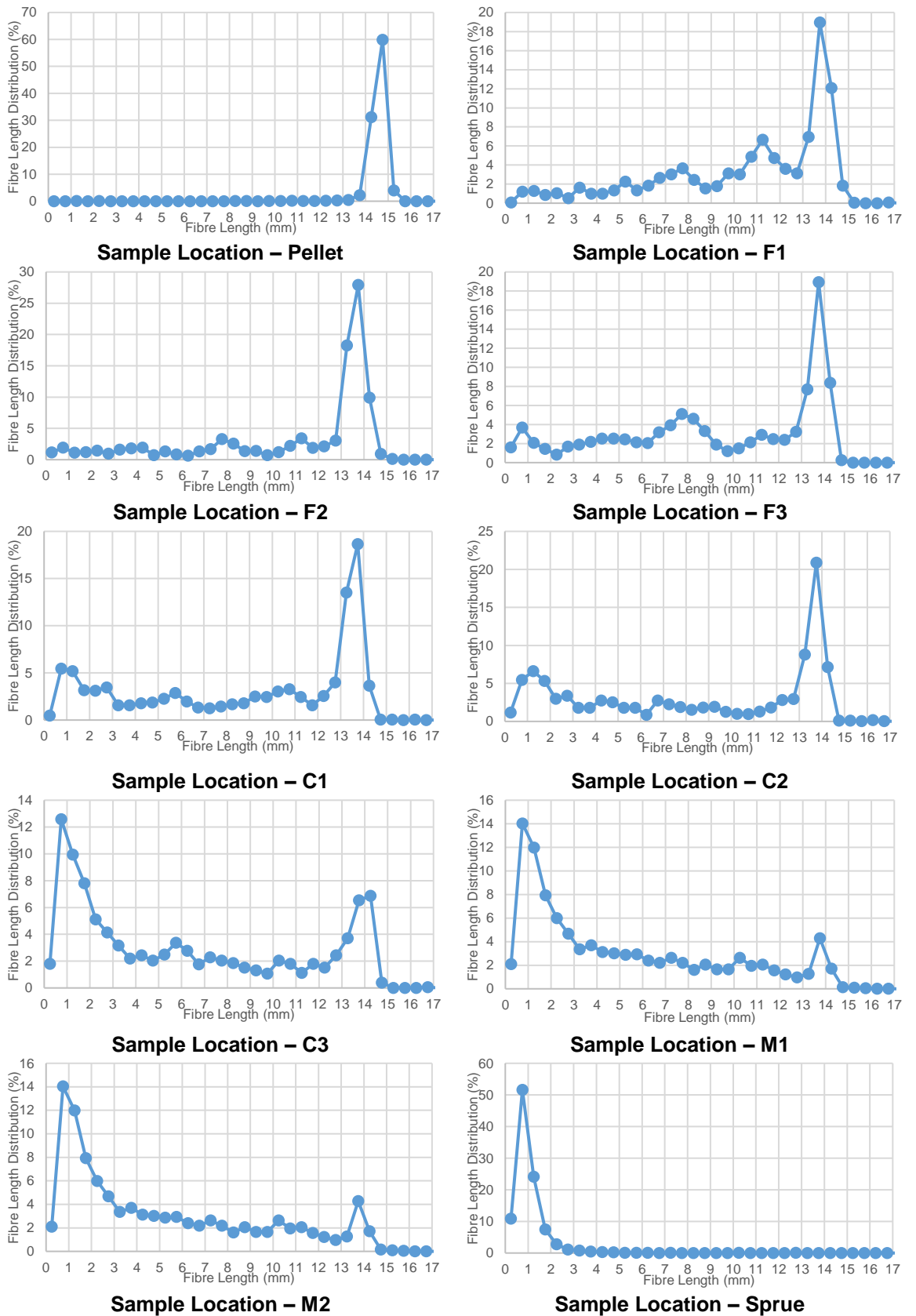
**Table A1.12. - Injection moulding settings for 20 mm screw pull out test -  
Low BP / High RPM. Material: 40YM243.**

Sample	Average Fibre Length (mm)	Weighted Average Length (mm)	Maximum Fibre Length Measured (mm)	Minimum Fibre Length Measured (mm)
Pellet	14.21	14.27	15.83	0.71
F1	10.37	11.69	16.34	0.18
F2	10.68	12.24	15.18	0.02
F3	9.05	11.17	14.66	0.08
C1	8.66	11.33	15.81	0.12
C2	8.26	11.44	16.32	0.12
C3	5.85	10.00	16.46	0.05
M1	4.75	8.52	15.74	0.11
M2	4.42	8.97	15.78	0.06
N1	<i>n/a</i>	<i>n/a</i>	<i>n/a</i>	<i>n/a</i>
N2	<i>n/a</i>	<i>n/a</i>	<i>n/a</i>	<i>n/a</i>
Sprue	0.78	1.39	12.33	0.06

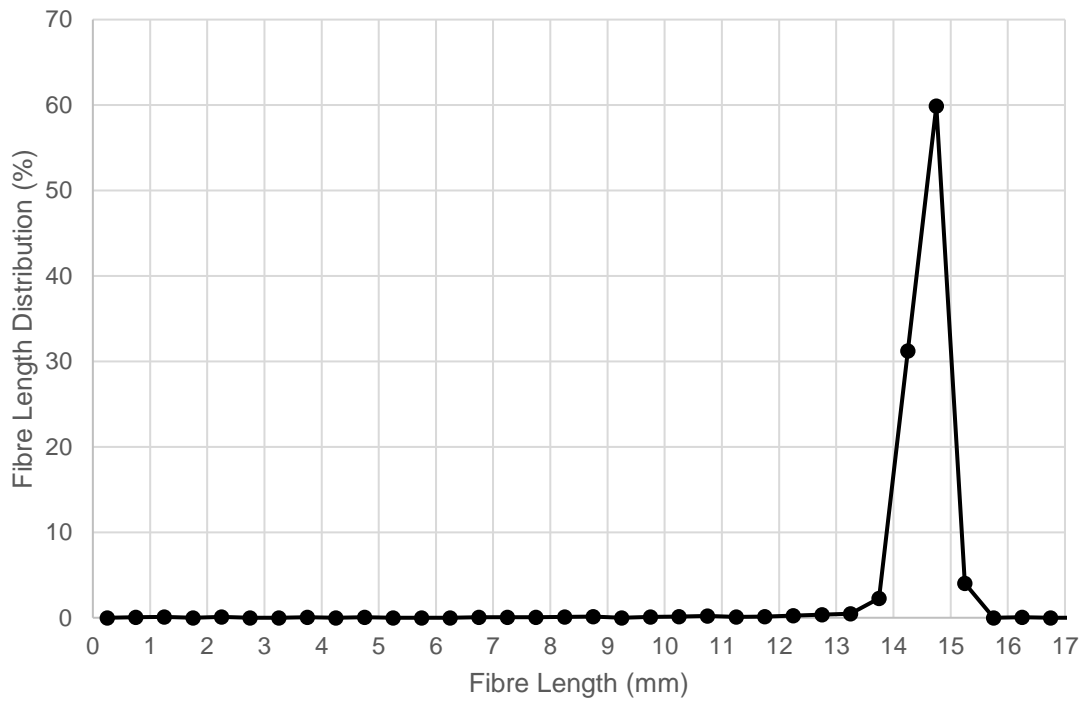
**Table A1.13. - 20 mm screw pull out test - Low BP (2.5 bar) / High RPM (300 RPM). Material: 40YM243.**



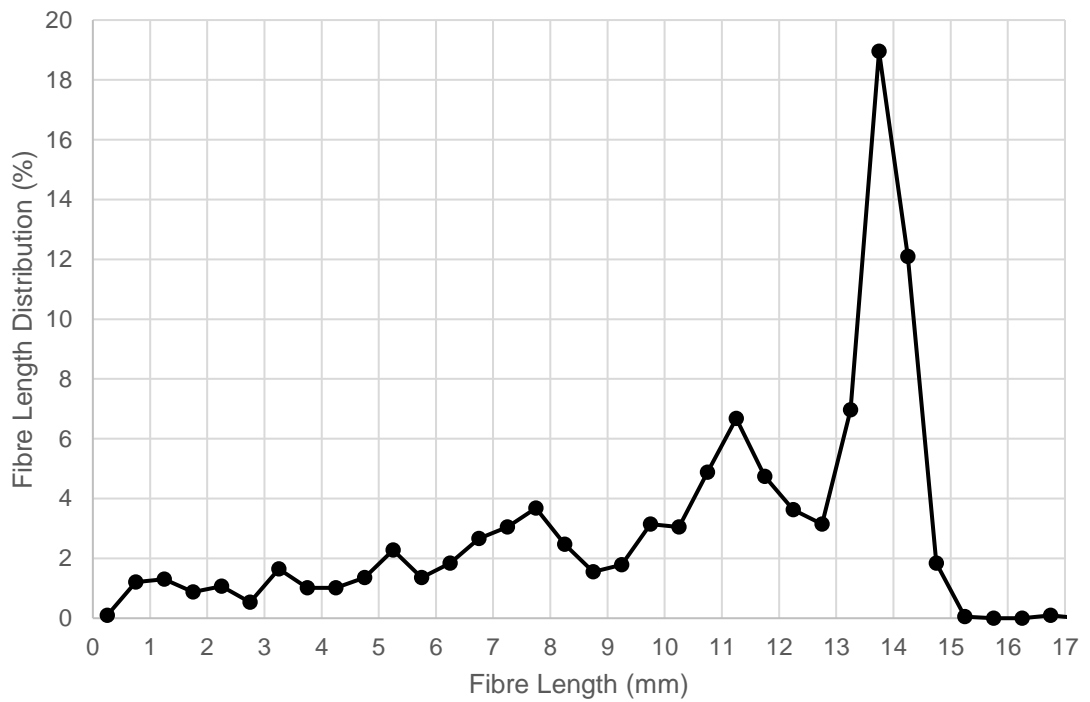
**Figure A1.60. - Number and weighted average distribution of each 24 mm cut taken from various locations along the injection moulding process**



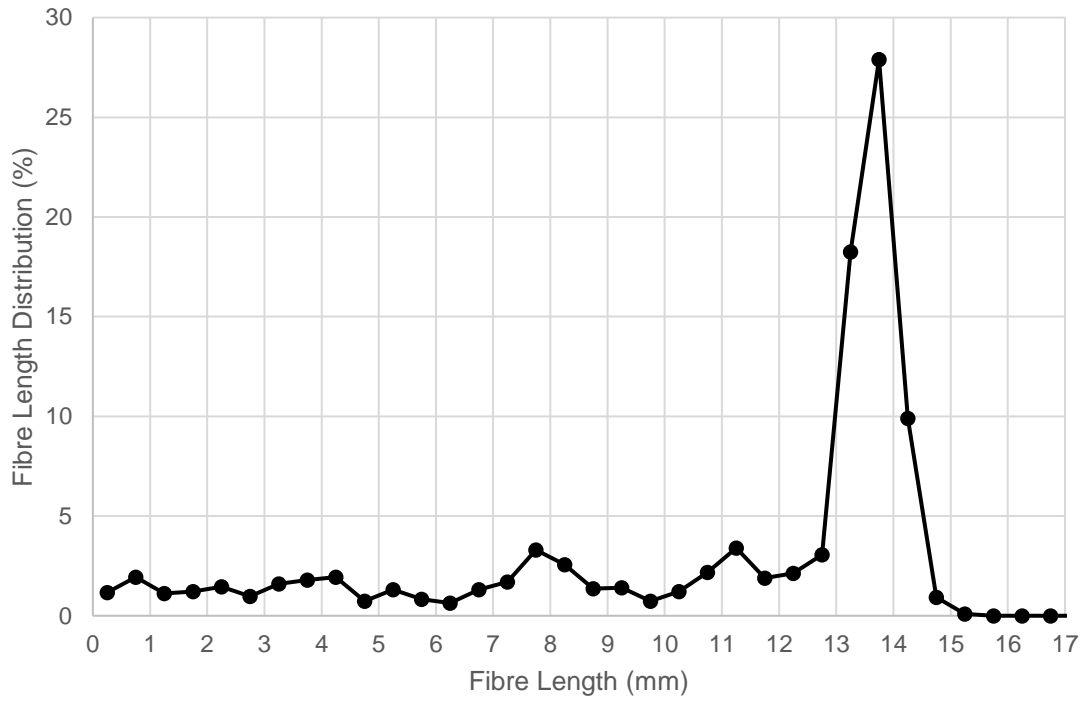
**Figure A1.61. - Summary of fibre length distribution results**



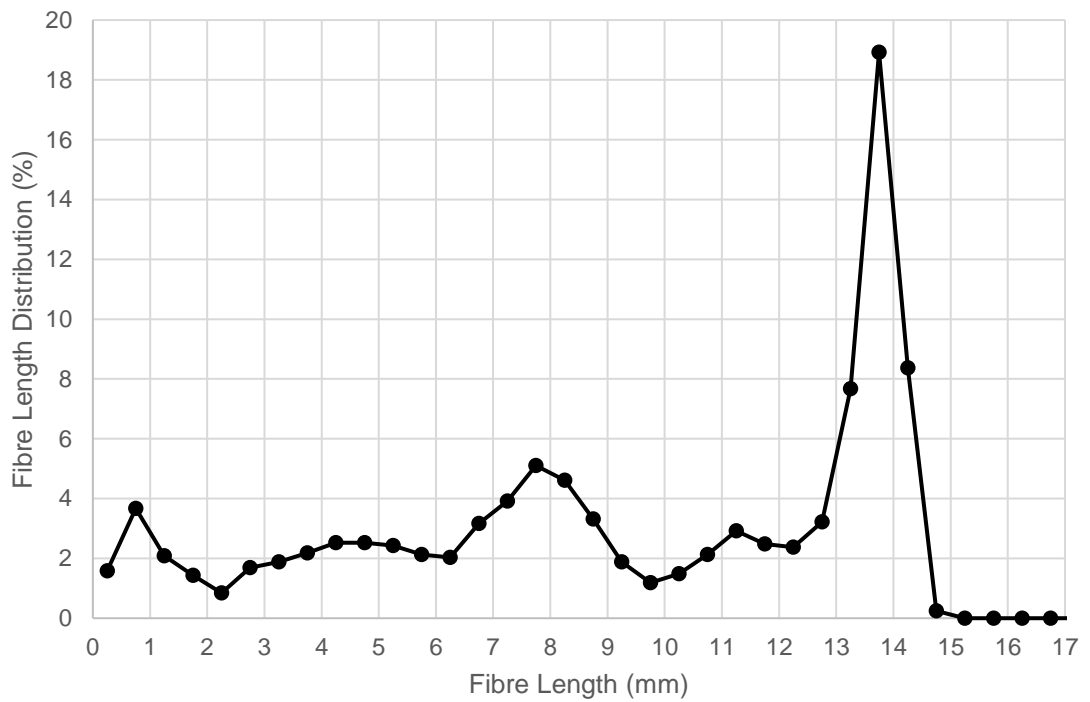
**Figure A1.62. - Sample: Pellet**



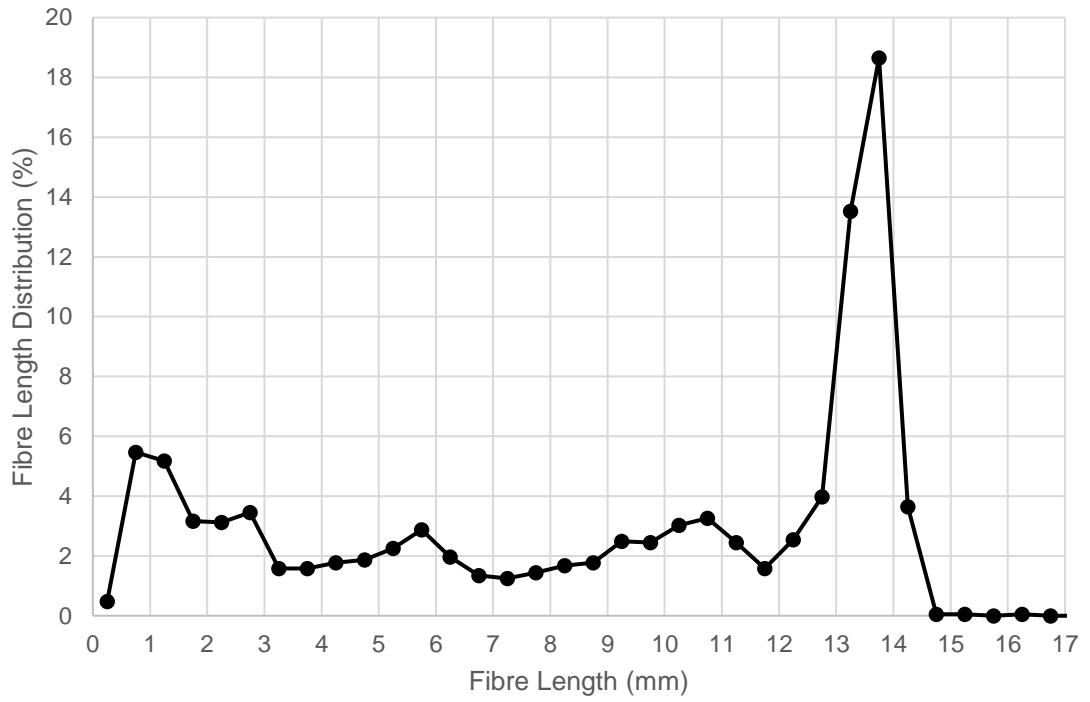
**Figure A1.63. - Sample: F1**



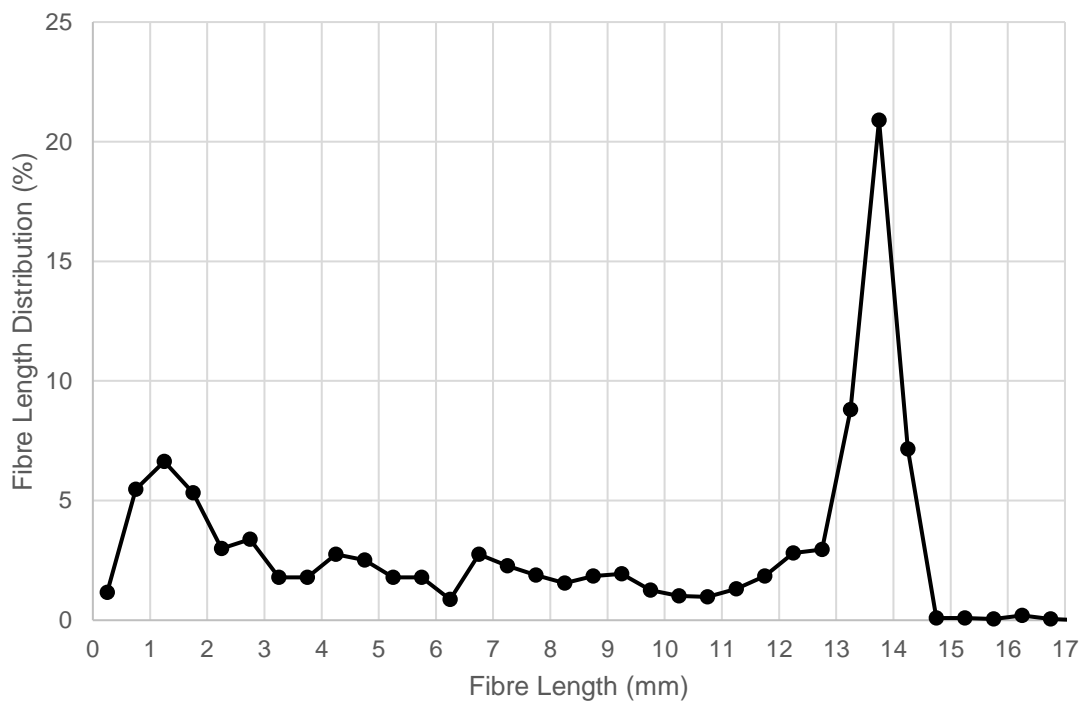
**Figure A1.64. - Sample: F2**



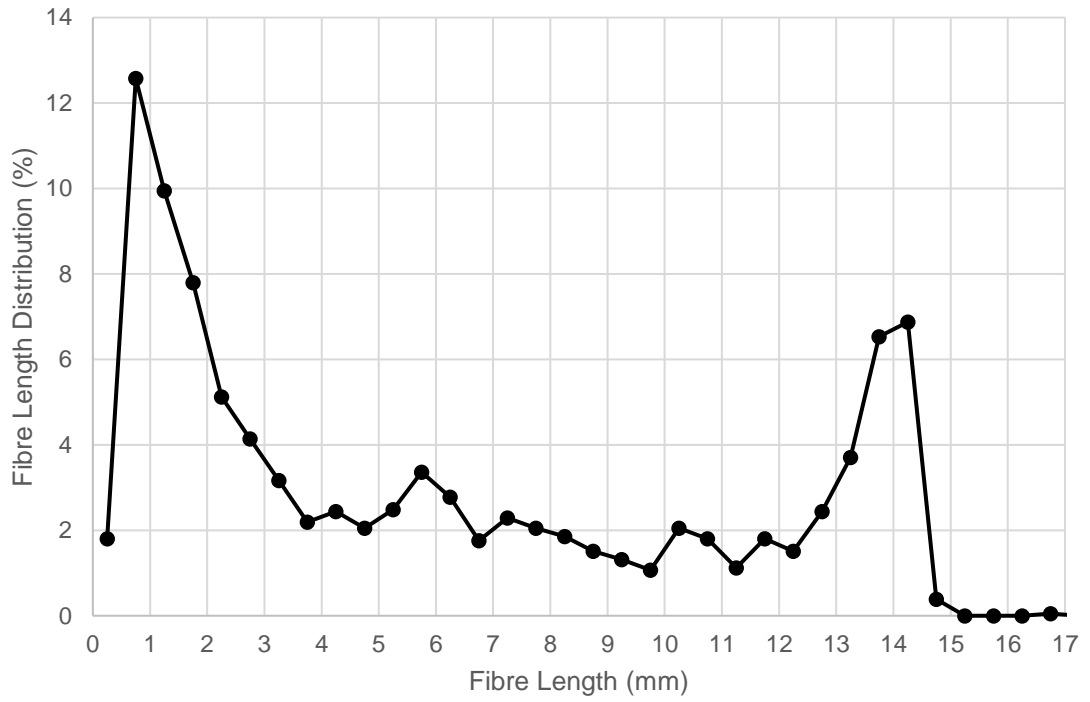
**Figure A1.65. - Sample: F3**



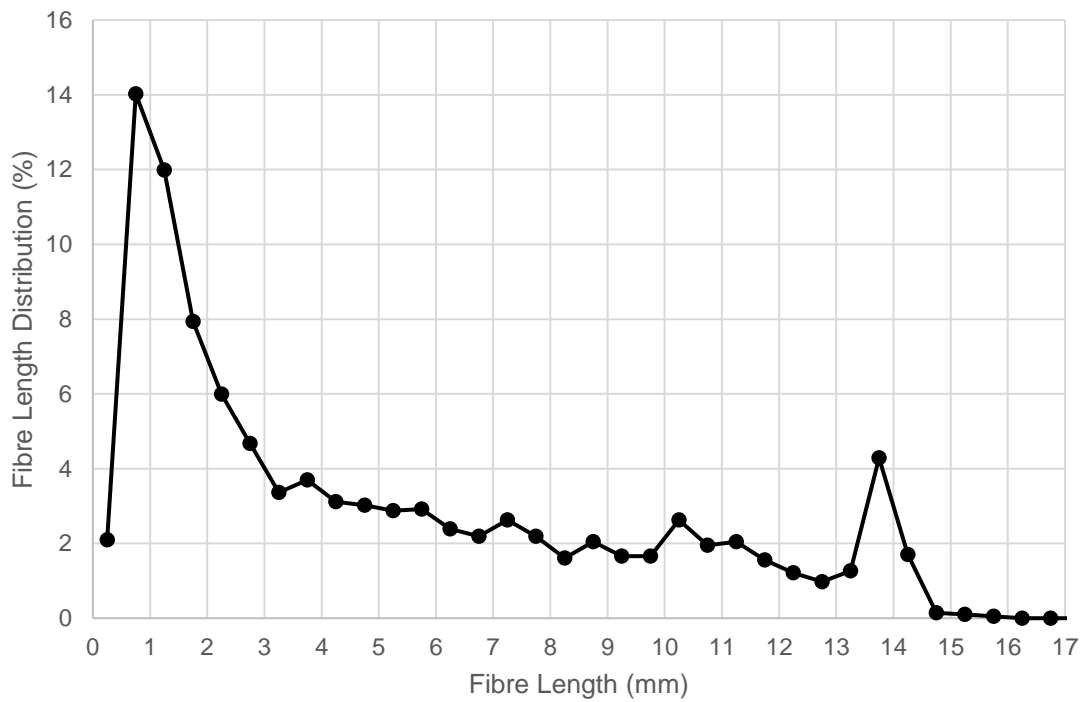
**Figure A1.66. - Sample: C1**



**Figure A1.67. - Sample: C2**

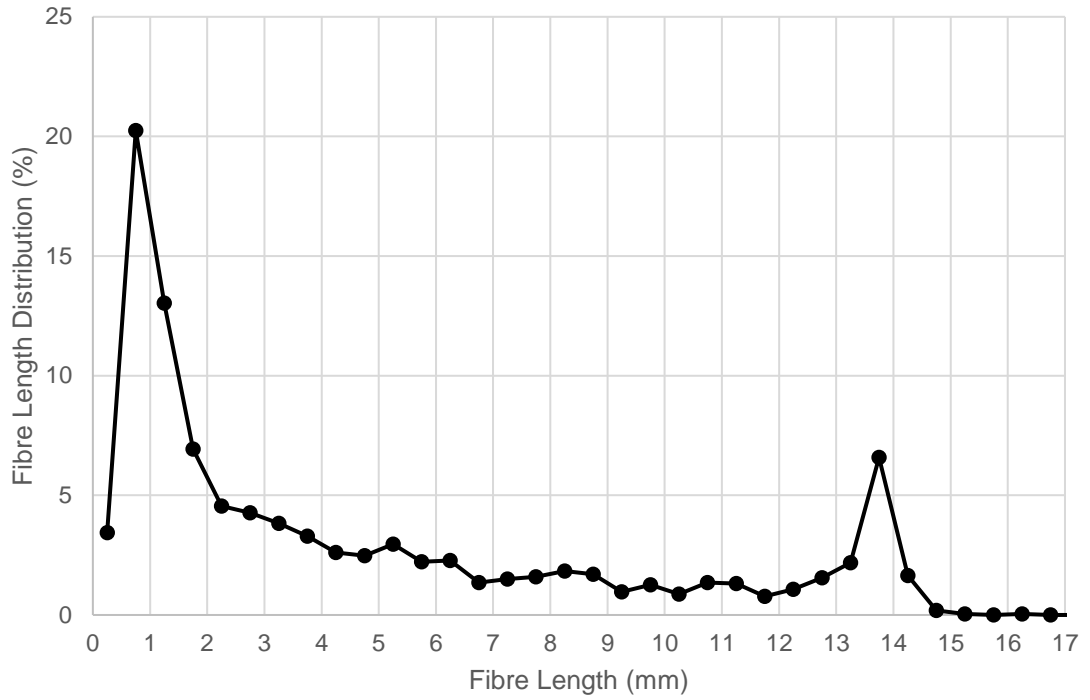


**Figure A1.68. - Sample: C3**

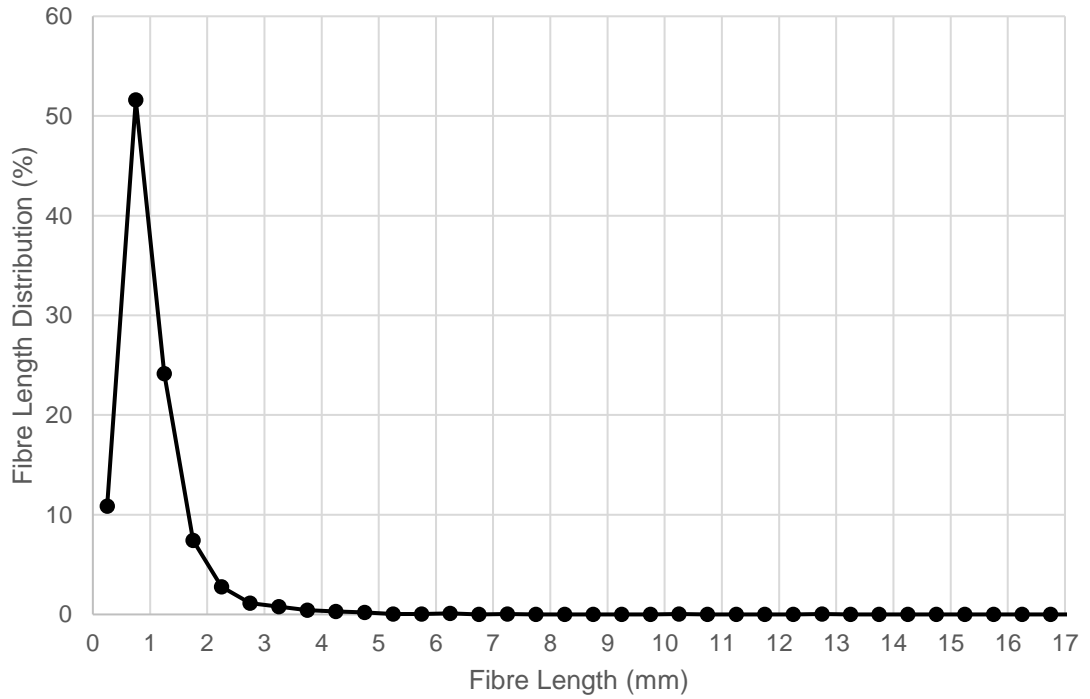


**Figure A1.69. - Sample: M1**





**Figure A1.70. - Sample: M2**



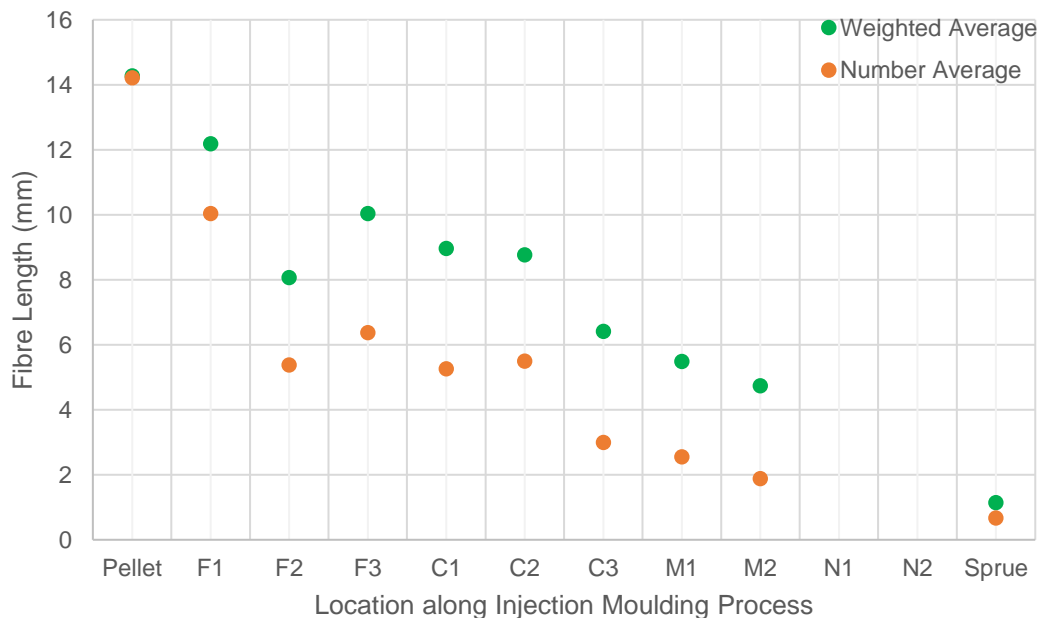
**Figure A1.71. - Sample: Sprue**

<b>Machine Settings</b>	<b>Arburg Allrounder 270C</b>
<b>Injection Time (secs)</b>	0.71
<b>Injection Speed (cm<sup>3</sup>/s)</b>	20
<b>Screw Speed (RPM)</b>	300
<b>Back Pressure (bar)</b>	5
<b>Packing Pressure (bar)</b>	27
<b>Packing Time (secs)</b>	5
<b>Melt Temperature (°C)</b>	220
<b>Mould Temperature (°C)</b>	20
<b>Cooling Time (secs)</b>	30

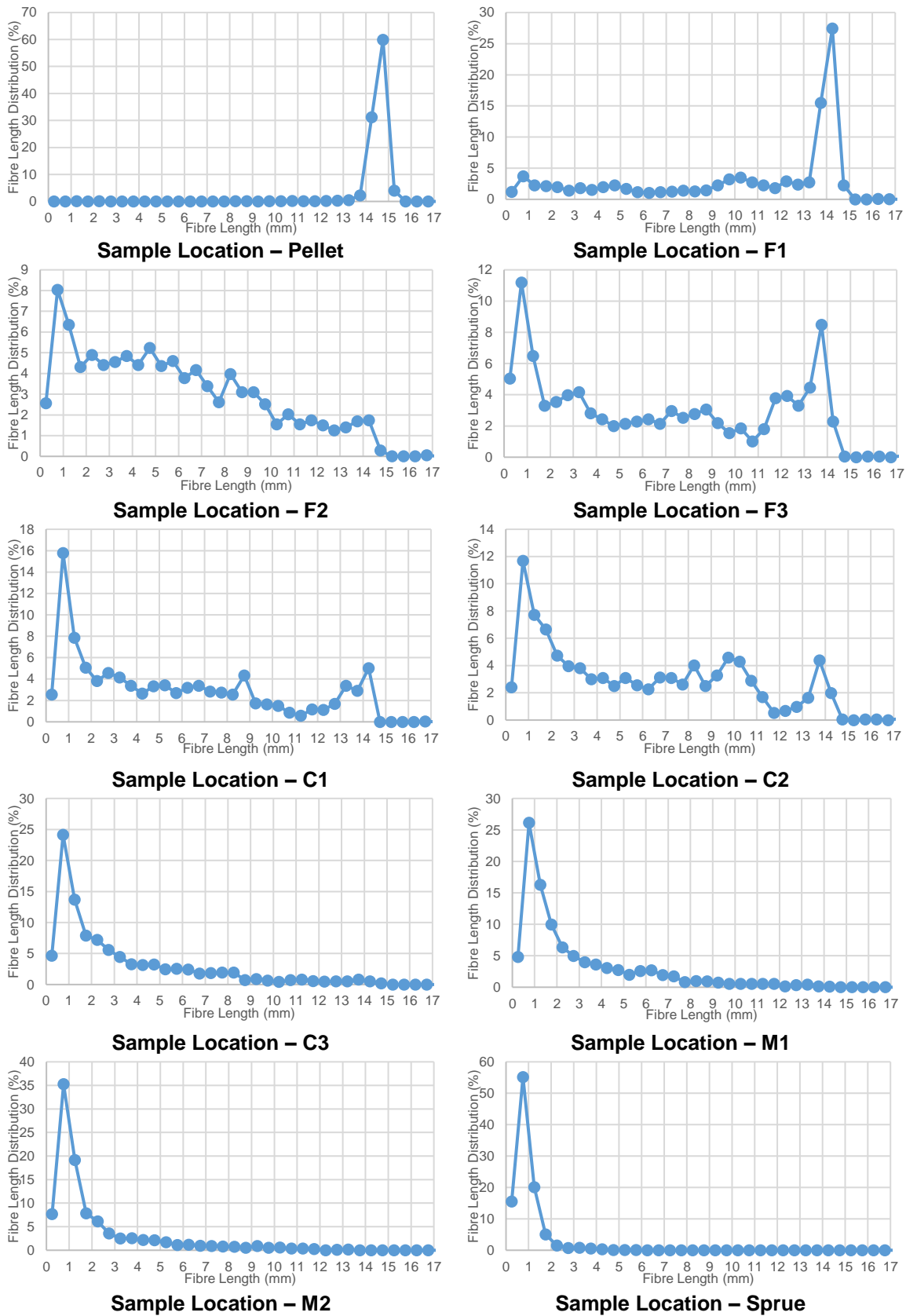
**Table A1.14. - Injection moulding settings for 20 mm screw pull out test -  
Medium BP / High RPM. Material: 40YM243.**

Sample	Average Fibre Length (mm)	Weighted Average Length (mm)	Maximum Fibre Length Measured (mm)	Minimum Fibre Length Measured (mm)
Pellet	14.21	14.27	15.83	0.71
F1	10.04	12.19	16.27	0.05
F2	5.38	8.07	16.28	0.09
F3	6.37	10.04	16.96	0.07
C1	5.26	8.96	16.75	0.10
C2	5.50	8.77	16.96	0.09
C3	3.00	6.41	14.44	0.09
M1	2.55	5.49	13.95	0.07
M2	1.88	4.74	13.18	0.08
N1	<i>n/a</i>	<i>n/a</i>	<i>n/a</i>	<i>n/a</i>
N2	<i>n/a</i>	<i>n/a</i>	<i>n/a</i>	<i>n/a</i>
Sprue	0.67	1.14	5.58	0.05

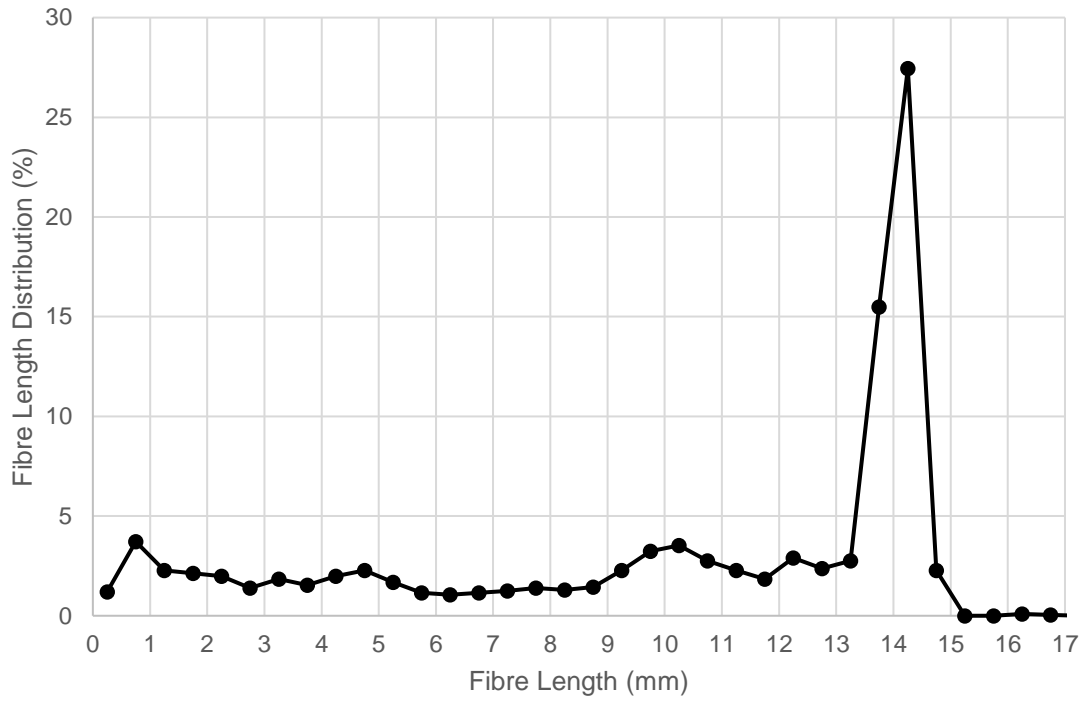
**Table A1.15. - 20 mm screw pull out test - Medium BP (5 bar) / High RPM (300 RPM). Material: 40YM243.**



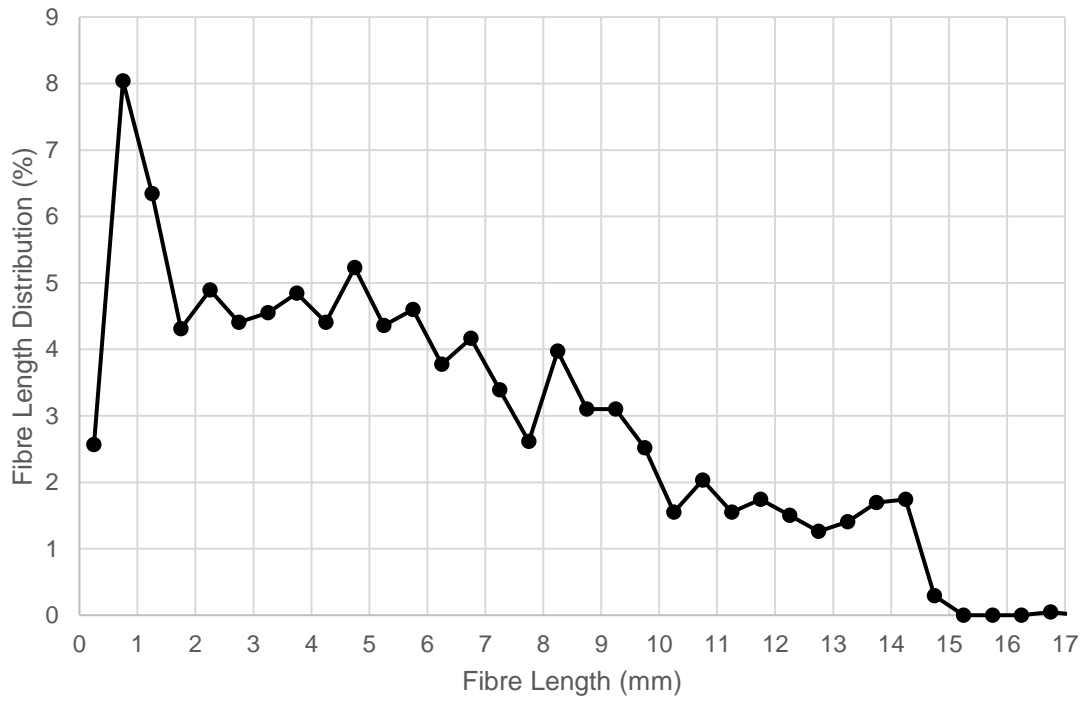
**Figure A1.72. - Number and weighted average distribution of each 24 mm cut taken from various locations along the injection moulding process**



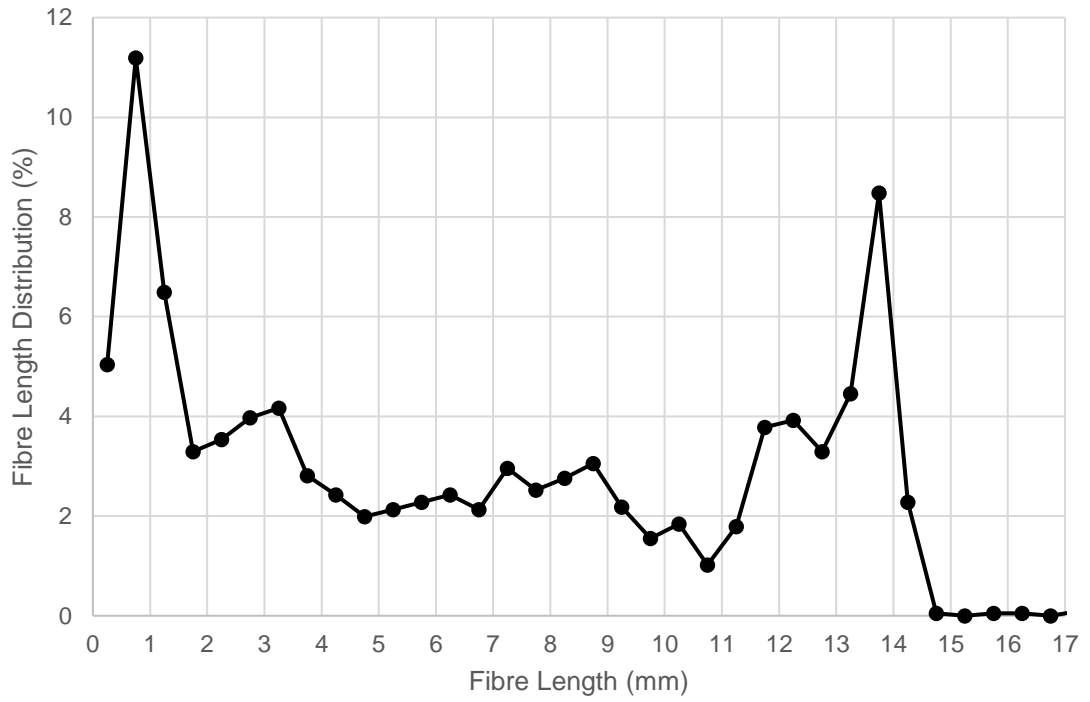
**Figure A1.73. - Summary of fibre length distribution results**



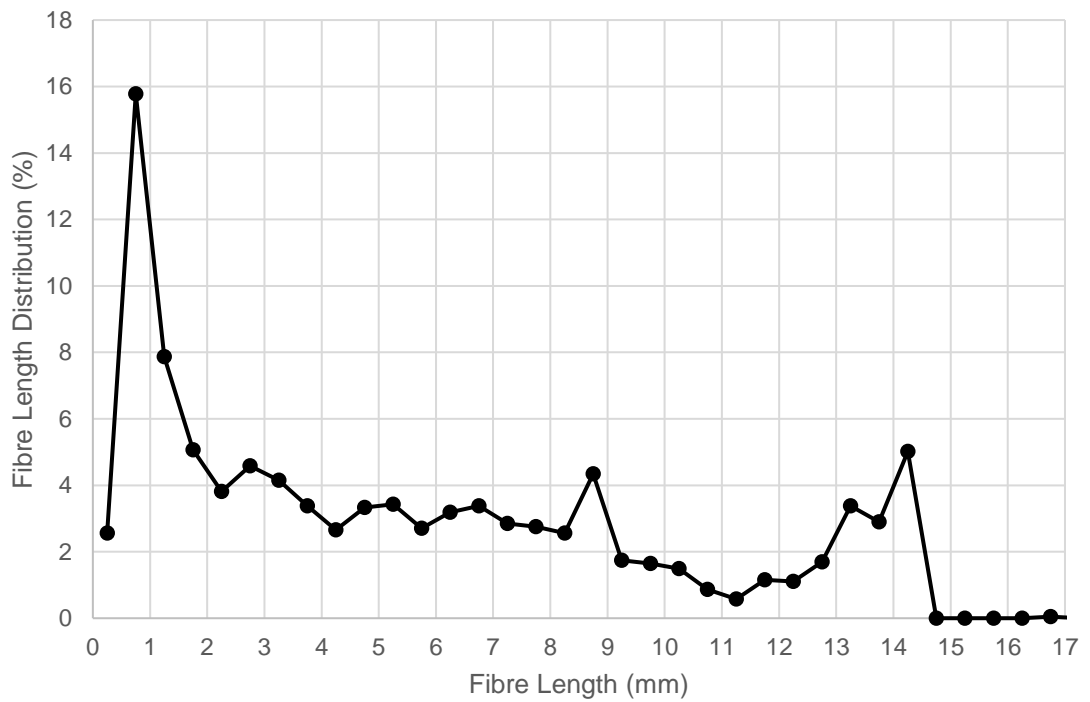
**Figure A1.74. - Sample: F1**



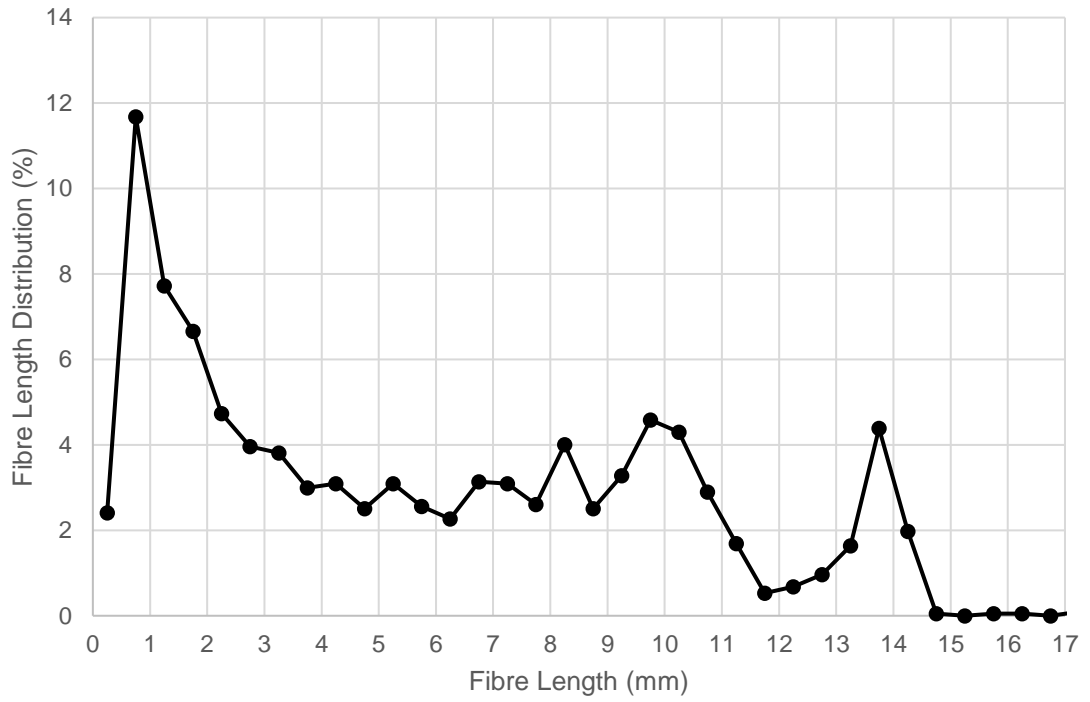
**Figure A1.75. - Sample: F2**



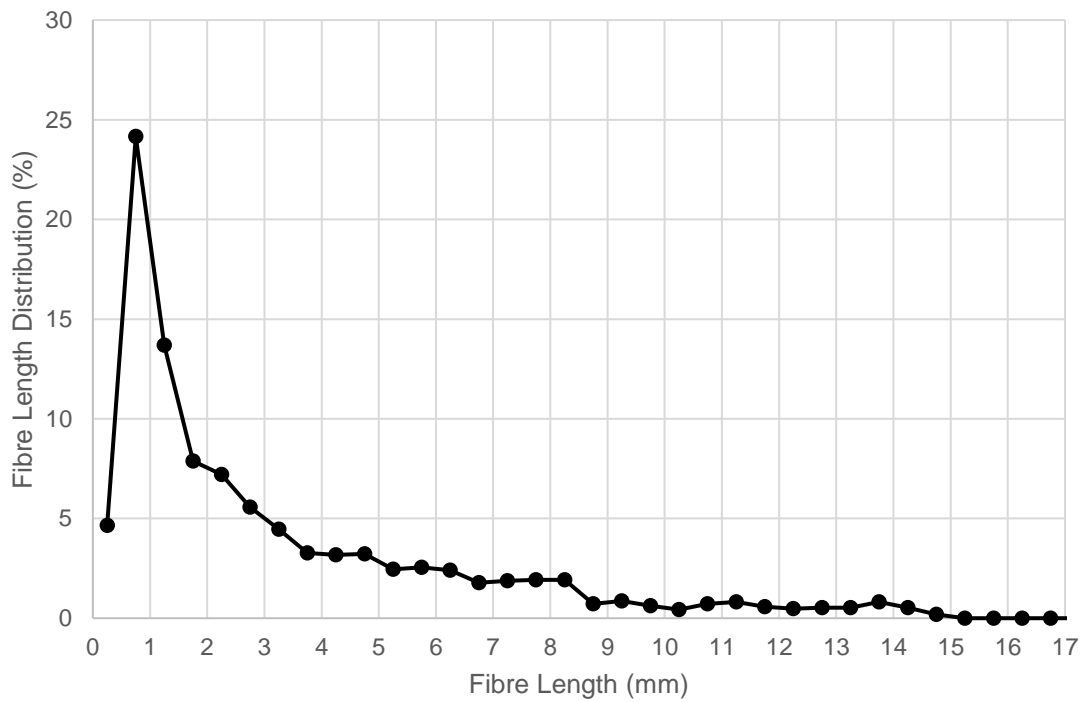
**Figure A1.76. - Sample: F3**



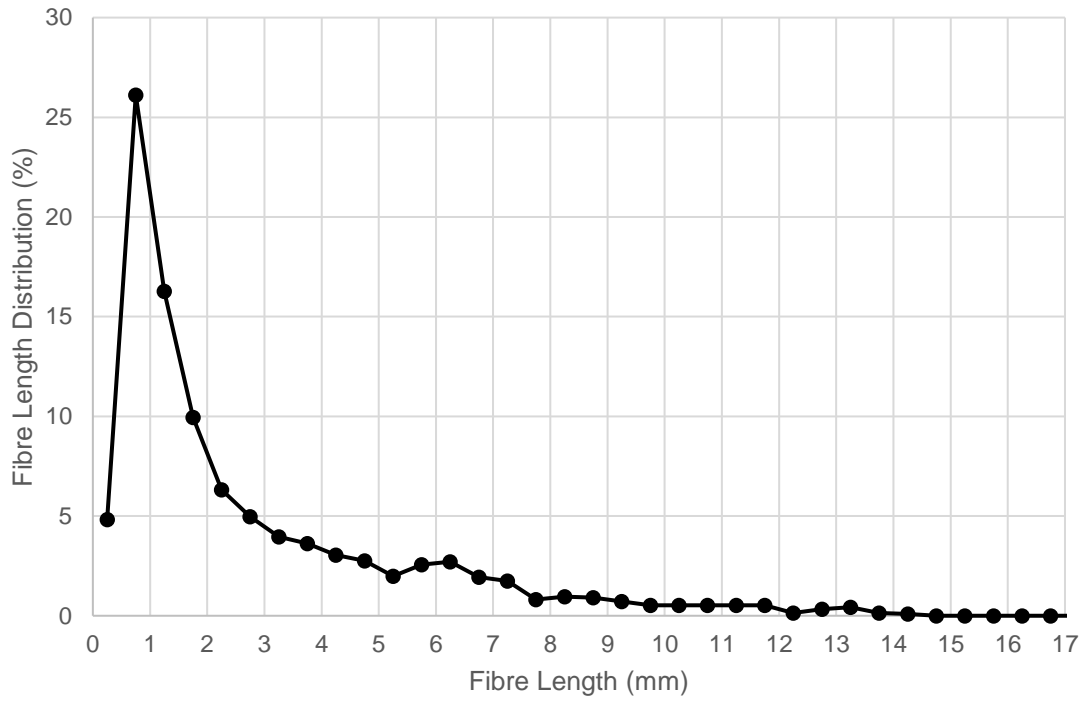
**Figure A1.77. - Sample: C1**



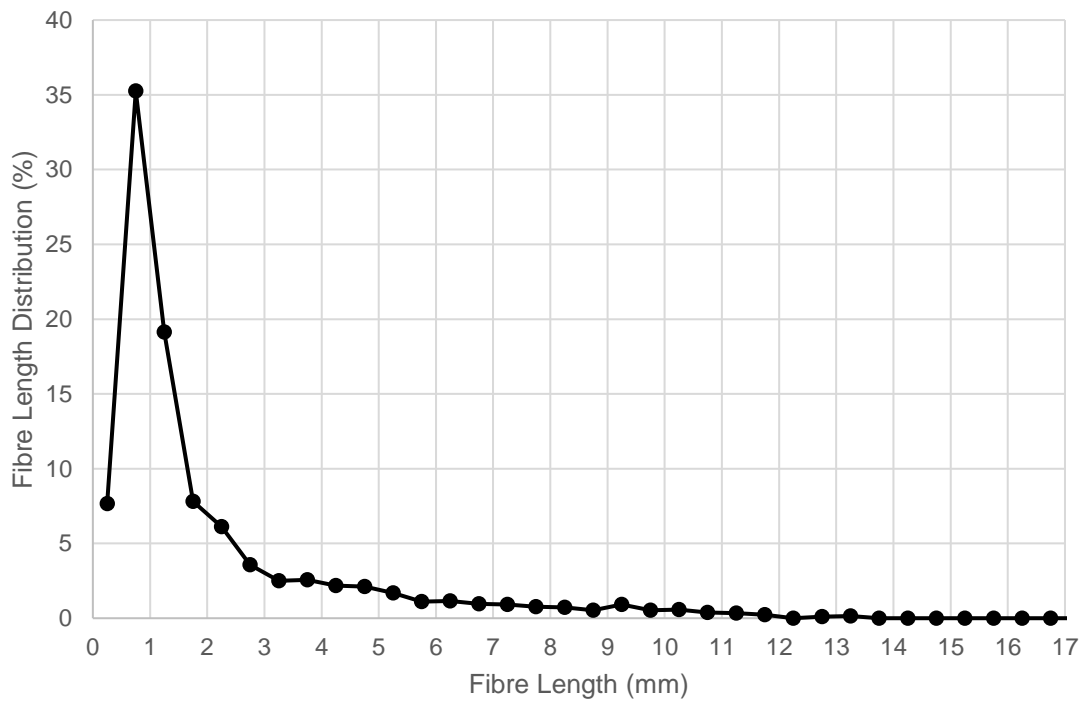
**Figure A1.78. - Sample: C2**



**Figure A1.79. - Sample: C3**

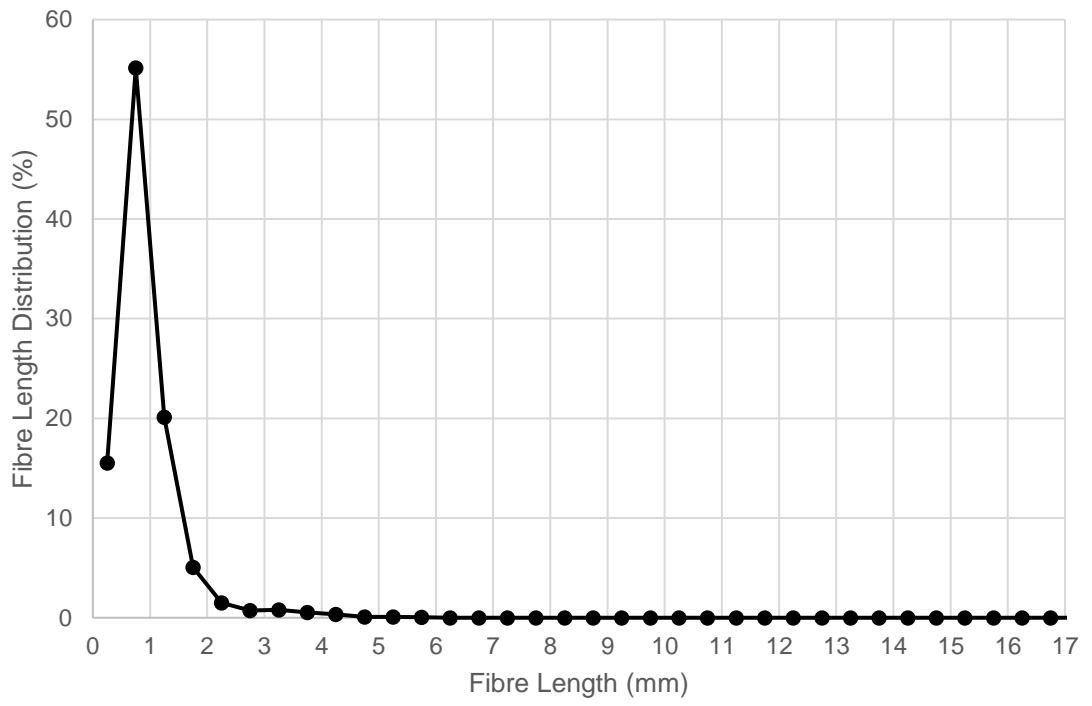


**Figure A1.80. - Sample: M1**



**Figure A1.81. - Sample: M2**





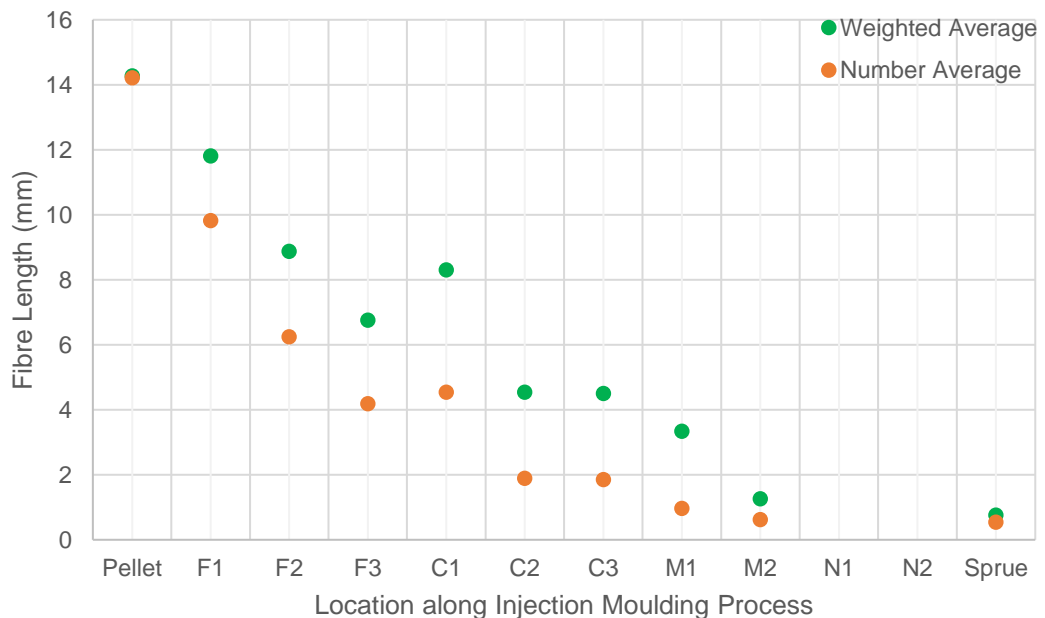
**Figure A1.82. - Sample: Sprue**

<b>Machine Settings</b>	<b>Arburg Allrounder 270C</b>
<b>Injection Time (secs)</b>	0.84
<b>Injection Speed (cm<sup>3</sup>/s)</b>	20
<b>Screw Speed (RPM)</b>	300
<b>Back Pressure (bar)</b>	7.5
<b>Packing Pressure (bar)</b>	27
<b>Packing Time (secs)</b>	5
<b>Melt Temperature (°C)</b>	220
<b>Mould Temperature (°C)</b>	20
<b>Cooling Time (secs)</b>	30

**Table A1.16. - Injection moulding settings for 20 mm screw pull out test - High BP / High RPM. Material: 40YM243.**

Sample	Average Fibre Length (mm)	Weighted Average Length (mm)	Maximum Fibre Length Measured (mm)	Minimum Fibre Length Measured (mm)
Pellet	14.21	14.27	15.83	0.71
F1	9.82	11.81	14.65	0.06
F2	6.25	8.88	16.54	0.07
F3	4.19	6.76	13.81	0.06
C1	4.54	8.30	16.68	0.07
C2	1.90	4.54	13.43	0.04
C3	1.85	4.50	13.28	0.06
M1	0.97	3.34	12.30	0.05
M2	0.62	1.26	7.19	0.04
N1	<i>n/a</i>	<i>n/a</i>	<i>n/a</i>	<i>n/a</i>
N2	<i>n/a</i>	<i>n/a</i>	<i>n/a</i>	<i>n/a</i>
Sprue	0.54	0.76	2.83	0.05

**Table A1.17. - 20 mm screw pull out test - High BP (7.5 bar) / High RPM (300 RPM). Material: 40YM243.**



**Figure A1.83. - Number and weighted average distribution of each 24 mm cut taken from various locations along the injection moulding process**

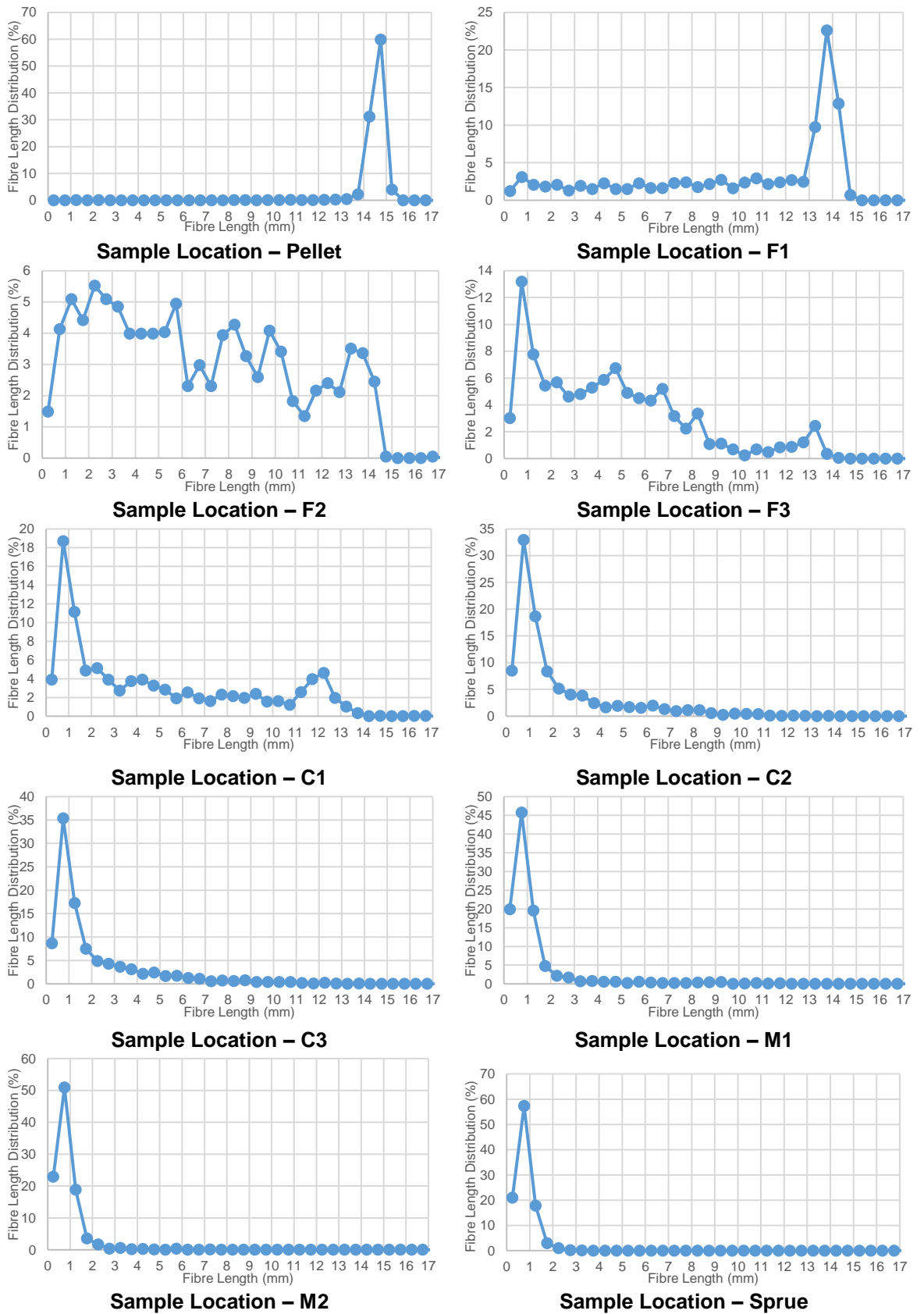
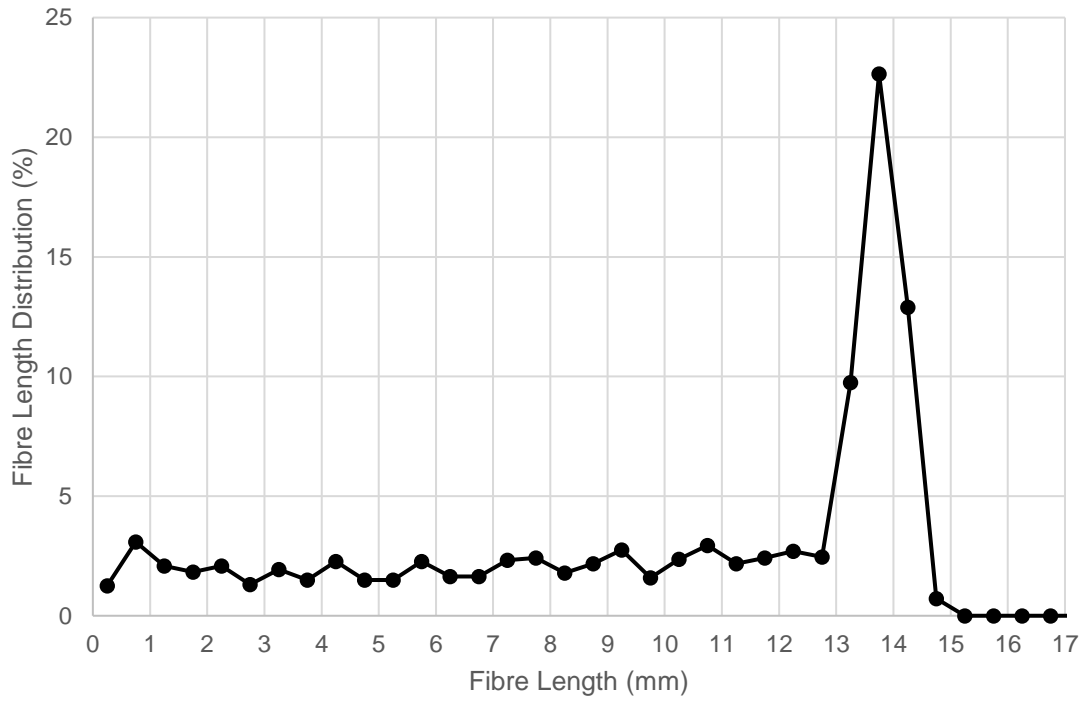
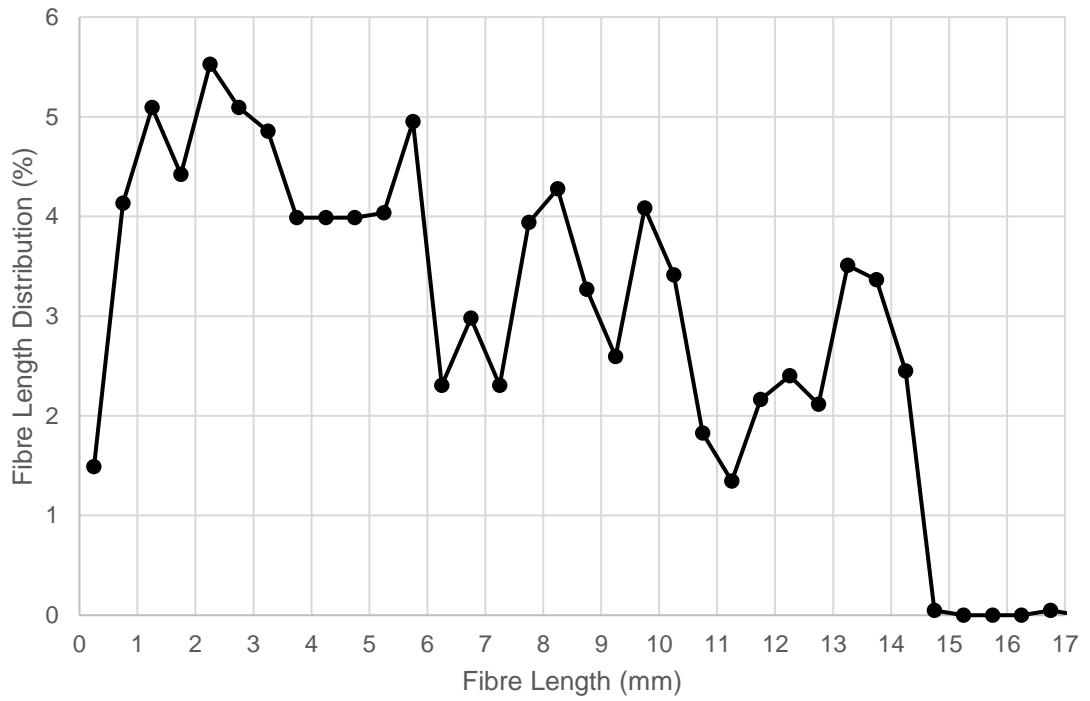


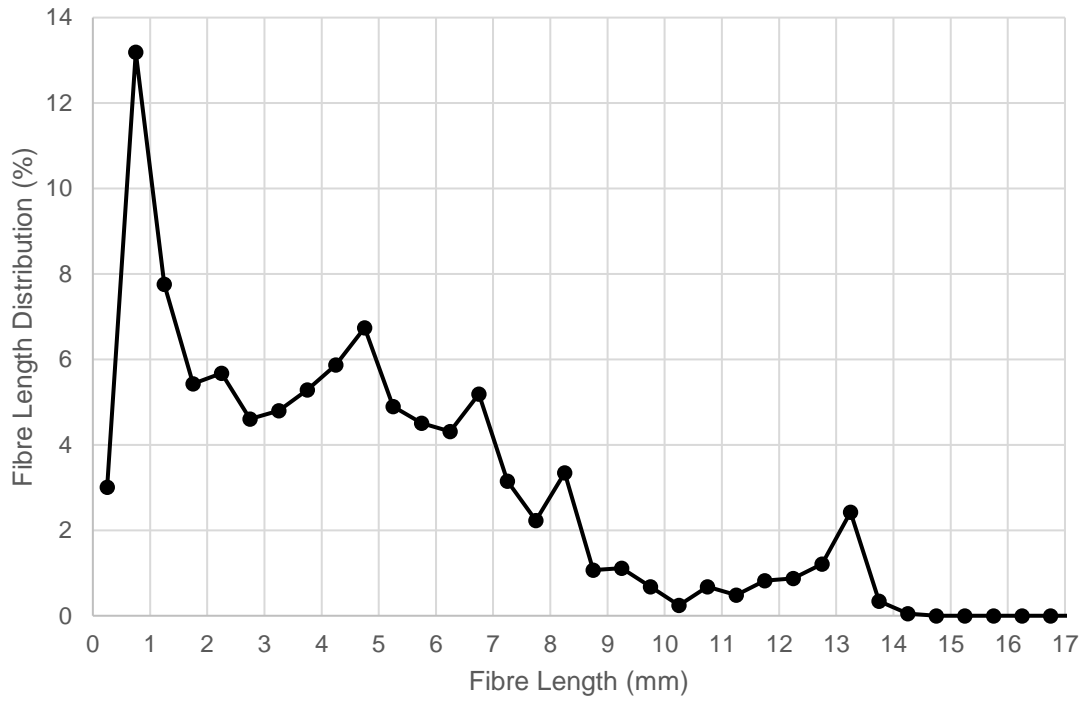
Figure A1.84. - Summary of fibre length distribution results



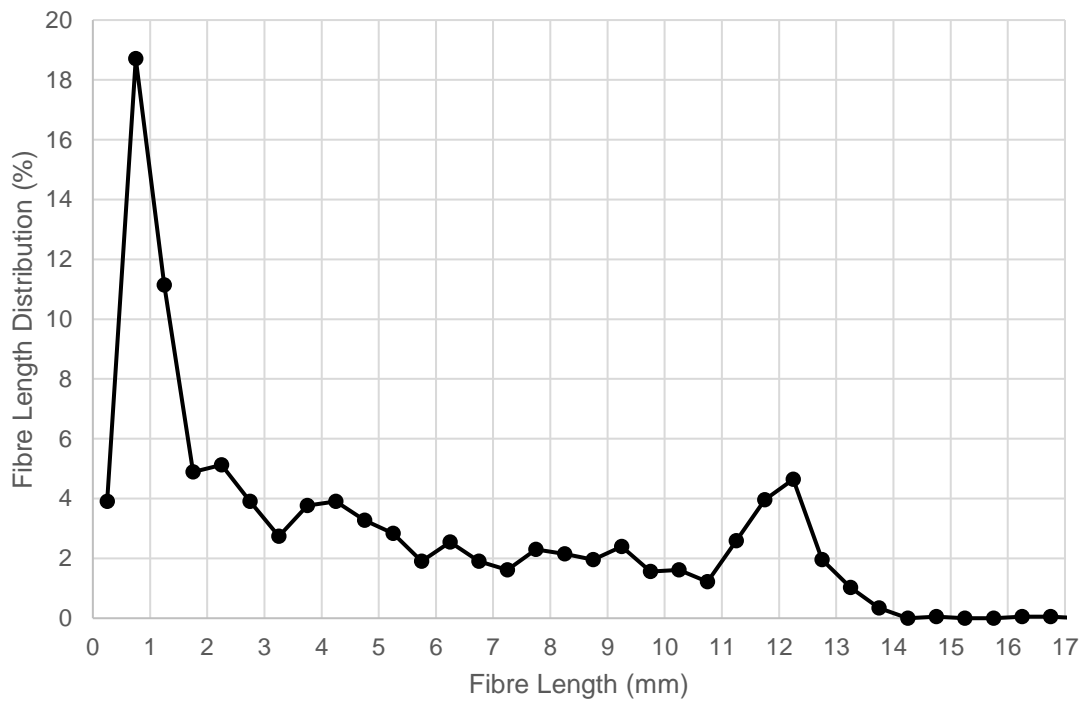
**Figure A1.85. - Sample: F1**



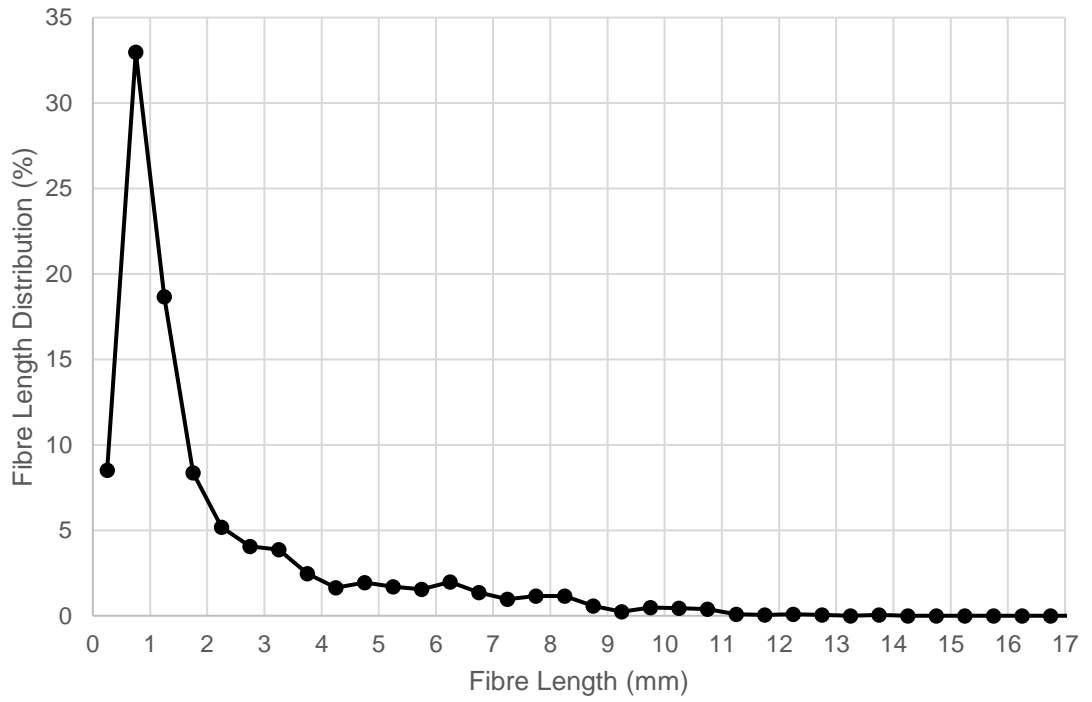
**Figure A1.86. - Sample: F2**



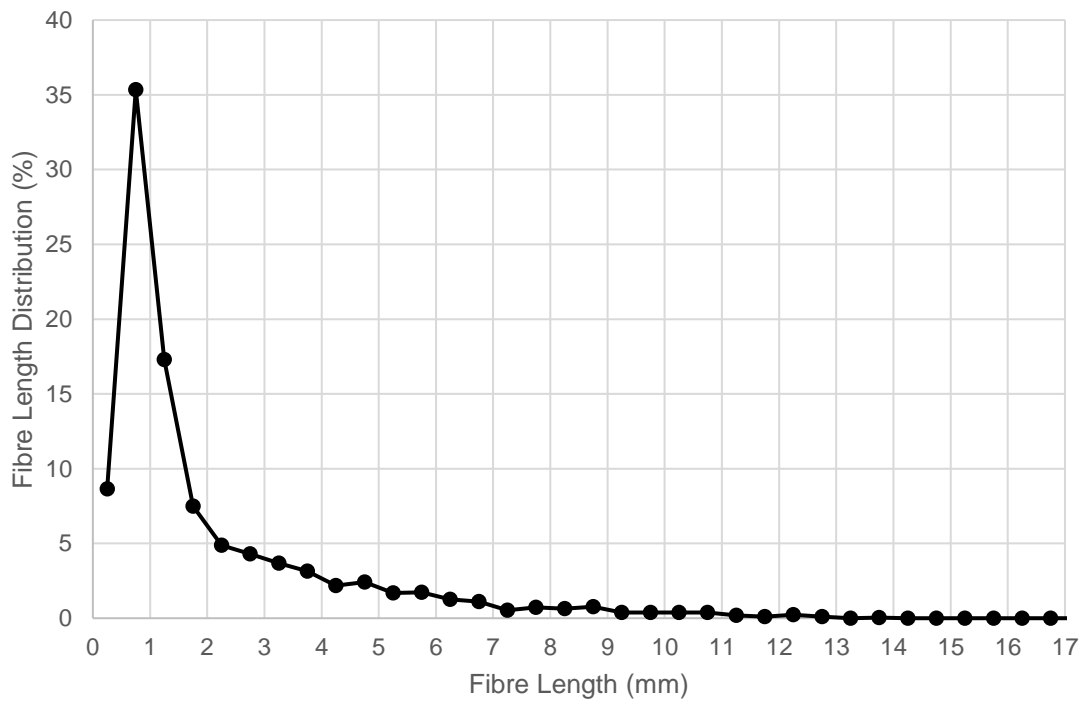
**Figure A1.87. - Sample: F3**



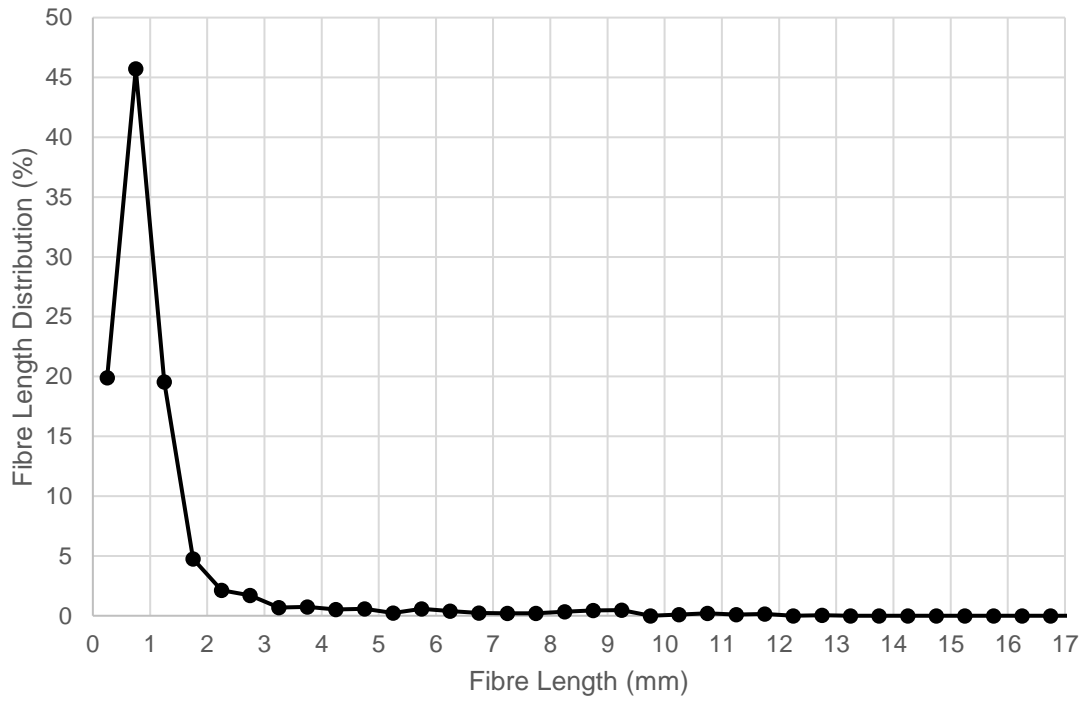
**Figure A1.88. - Sample: C1**



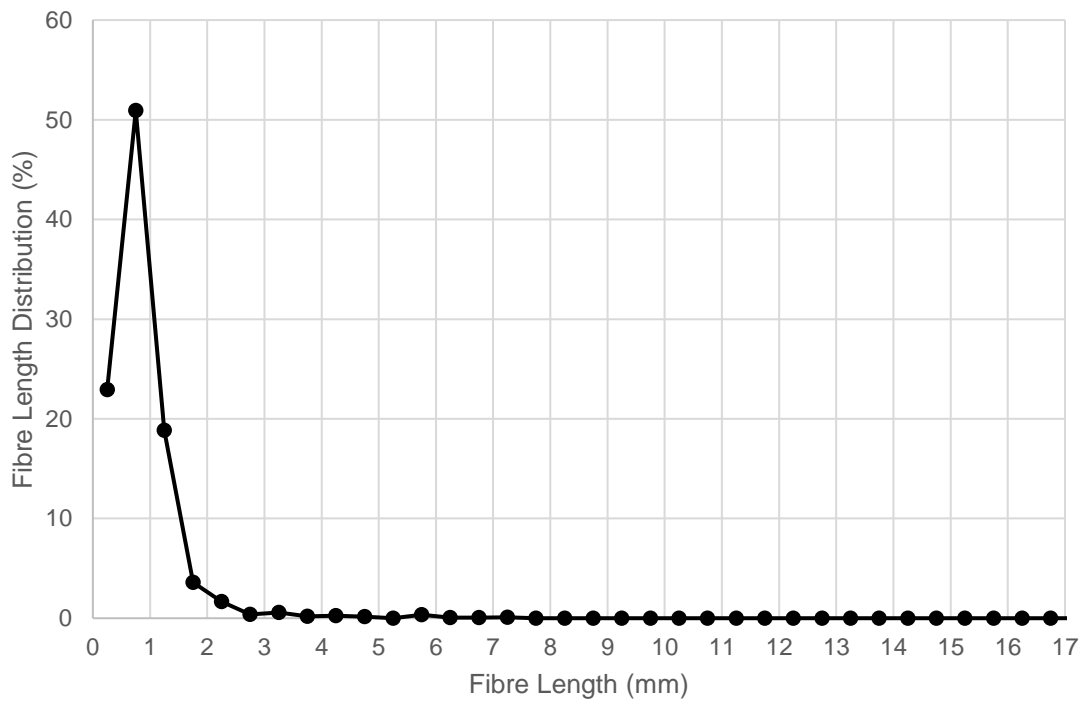
**Figure A1.89. - Sample: C2**



**Figure A1.90. - Sample: C3**

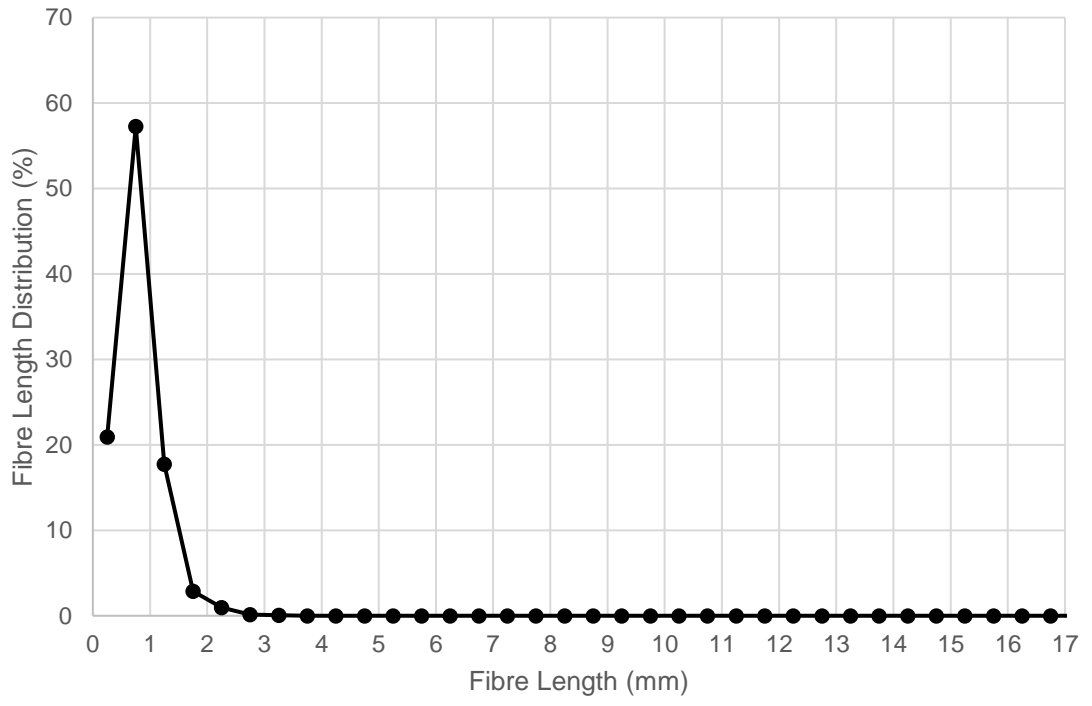


**Figure A1.91. - Sample: M1**



**Figure A1.92. - Sample: M2**





**Figure A1.93. - Sample: Sprue**

## Appendix 2: Compensation for Cut Sample Size

### Appendix 2.1. Manual Orientation Data Results

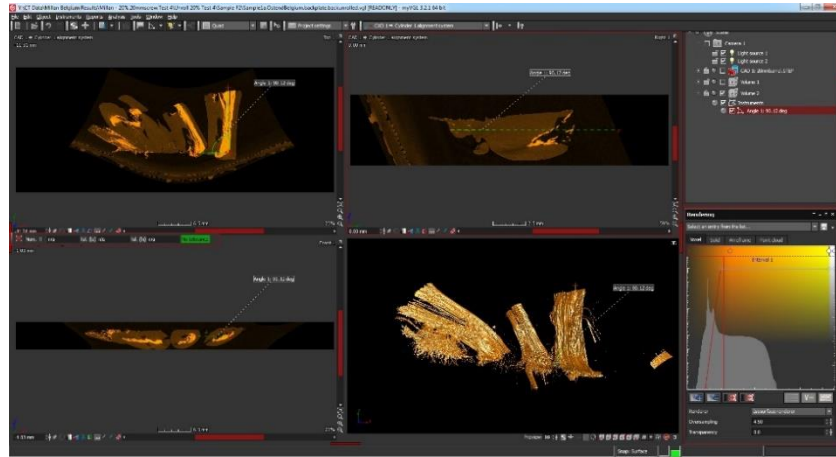


Figure A2.1. - Sample F2: Manual 2D correction angles

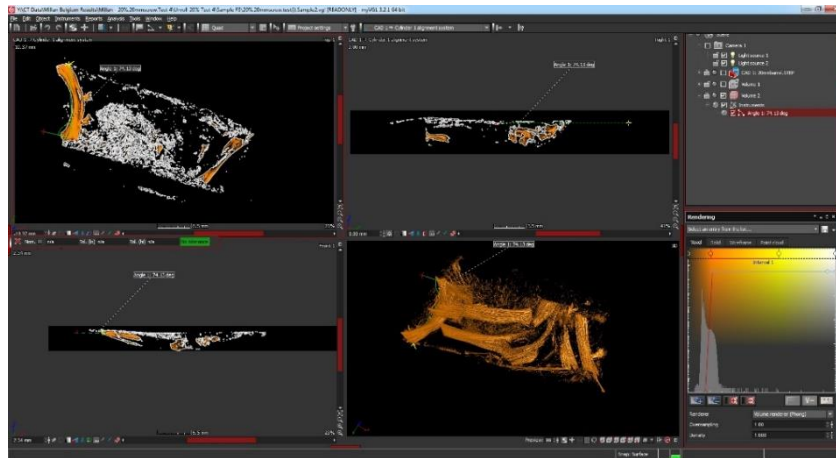


Figure A2.2. - Sample F3: Manual 2D correction angles

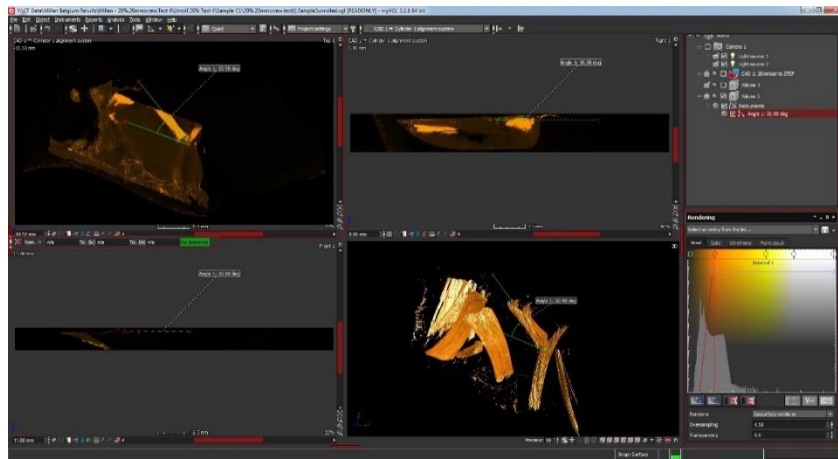


Figure A2.3 - Sample C1: Manual 2D correction angles

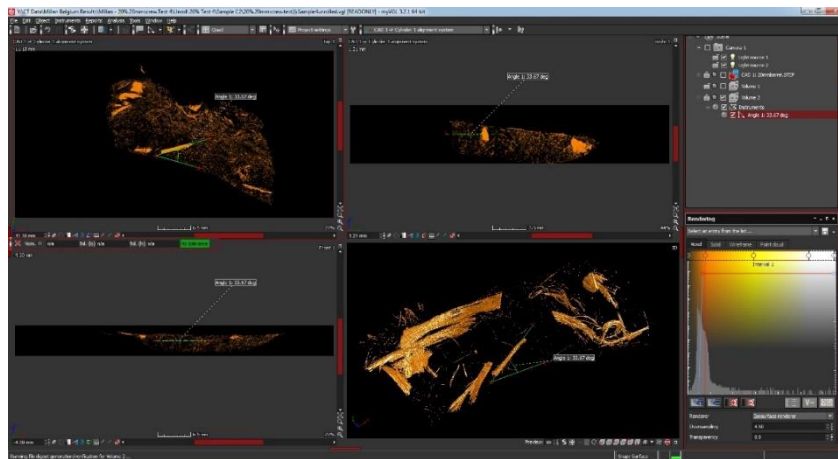


Figure A2.4 - Sample C2: Manual 2D correction angles

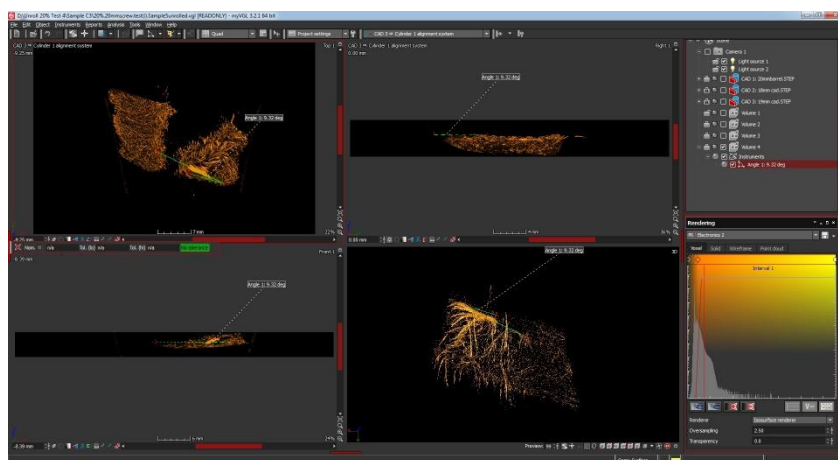


Figure A2.5 - Sample C3: Manual 2D correction angles

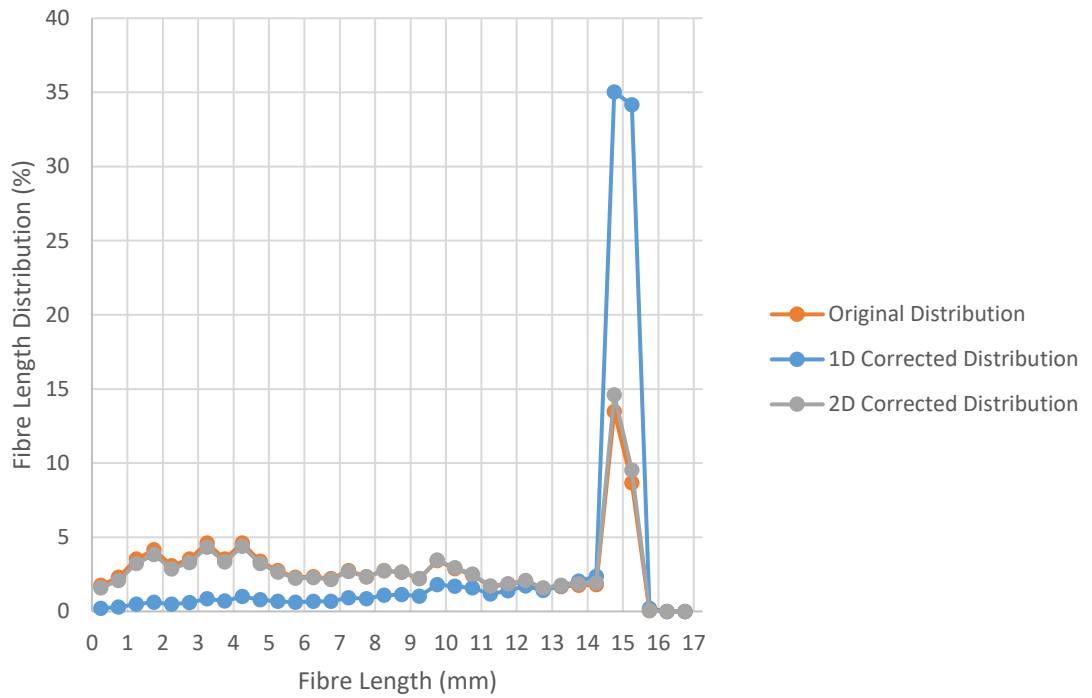


**Figure A2.6 - Sample M1: Manual 2D correction angles**

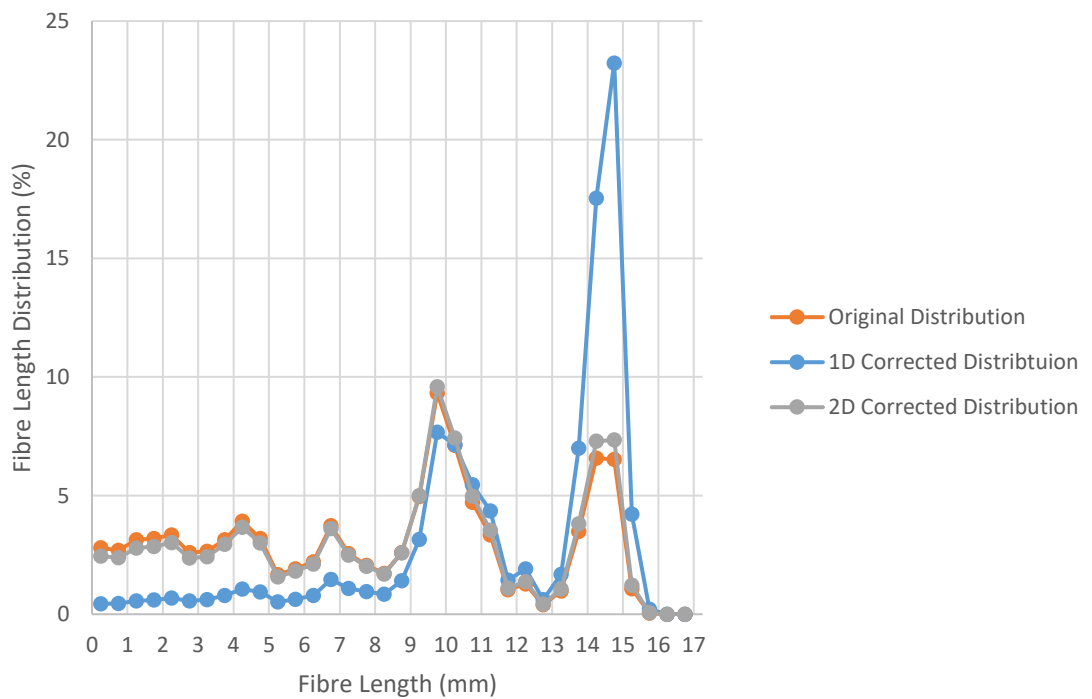


**Figure A2.7 - Sample M2: Manual 2D correction angles**

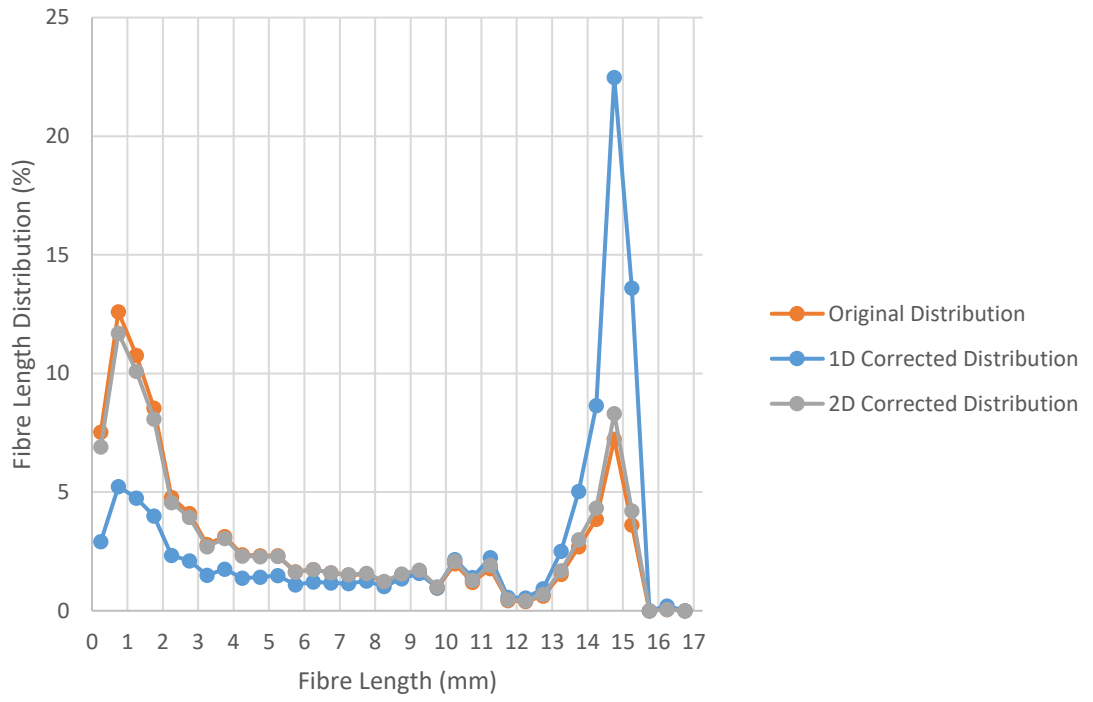
**Appendix 2.2.** Comparison of Original, 1D and 2D corrected fibre length distribution results for all other sample locations



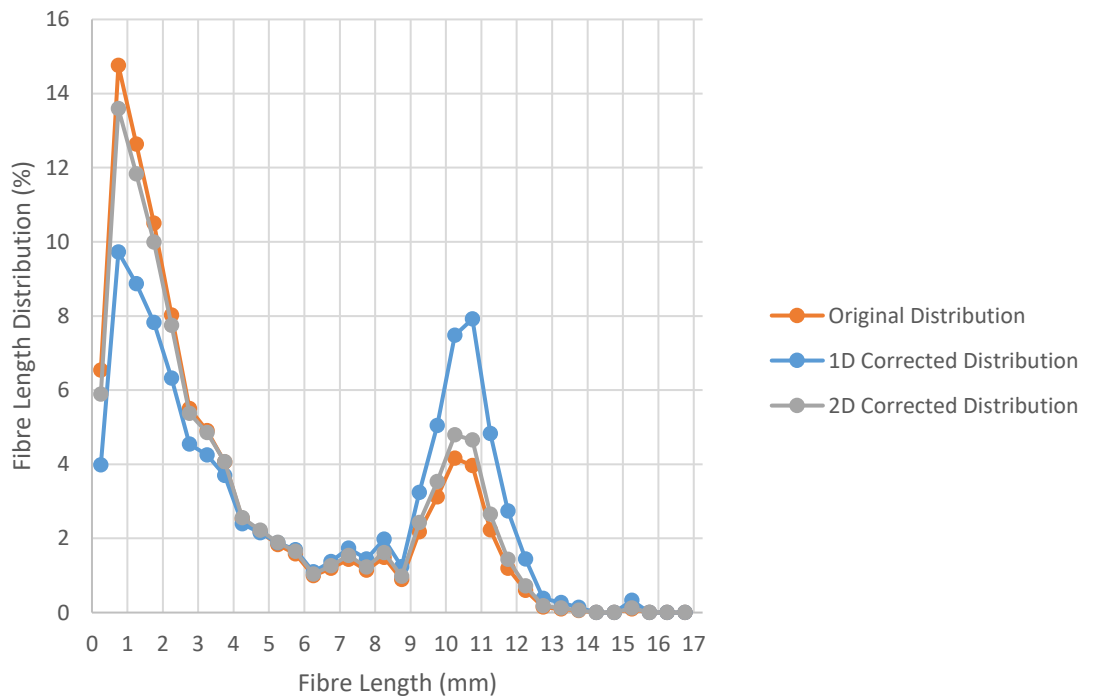
**Figure A2.9 - Sample F3**



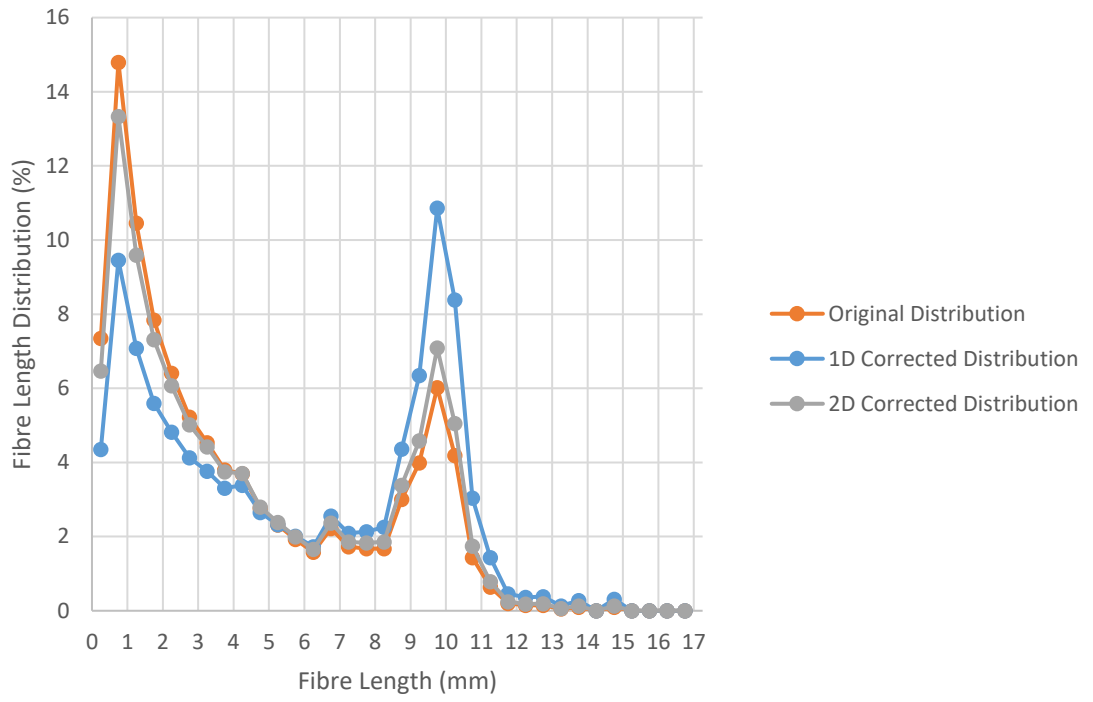
**Figure A2.10 - Sample C1**



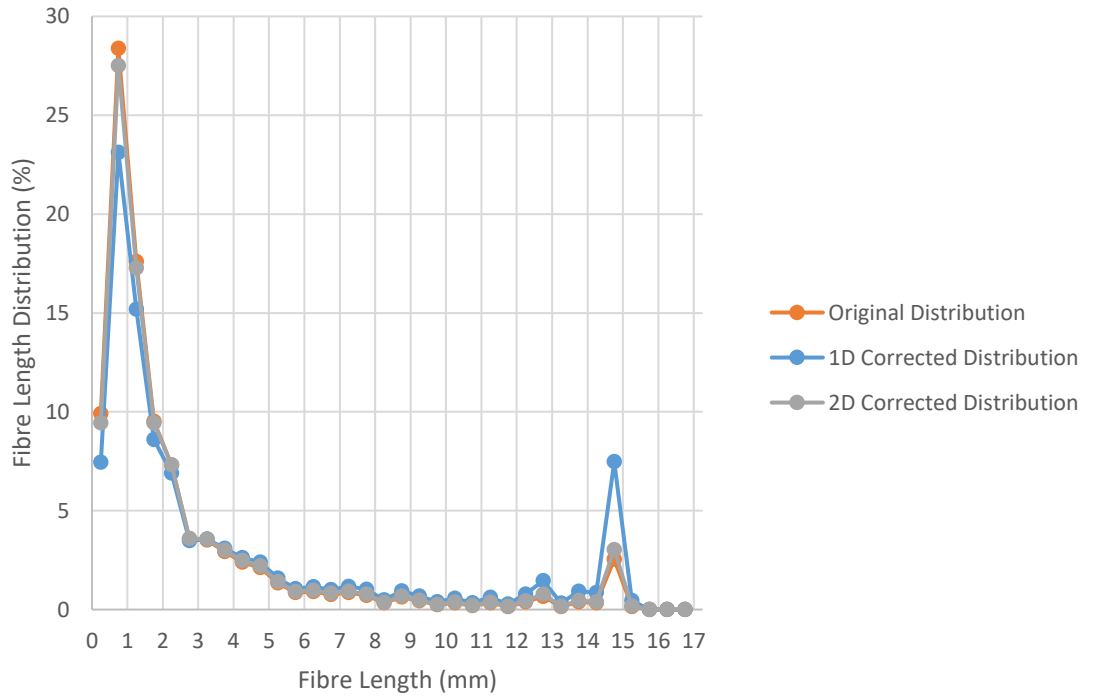
**Figure A2.11 - Sample C2**



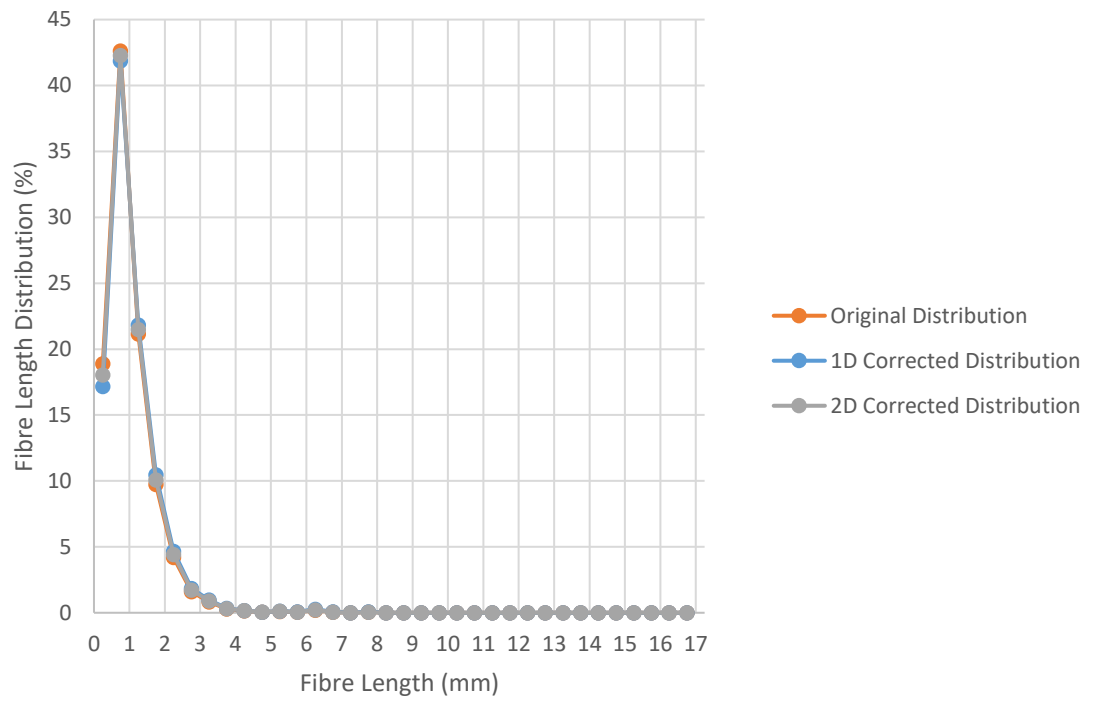
**Figure A2.12 - Sample C3**



**Figure A2.13 - Sample M1**



**Figure A2.14 - Sample M2**



**Figure A2.15 - Sample S1**